DX

189635

THE DEVELOPMENT OF NEW METHODS FOR THE ASSESSMENT OF OXYGEN RADICAL-MEDIATED OXIDATIVE DAMAGE TO BIOMOLECULES WITH SPECIAL REFERENCE TO LIPIDS.

ISMAIL YUSUF PATEL.

A thesis submitted in partial fulfilment of the requirements of the University of North London for the degree of Doctor of Philosophy.

THIS RESEARCH PROGRAMME WAS CARRIED OUT IN COLLABORATION WITH THE LONDON HOSPITAL MEDICAL COLLEGE.

DECEMBER 1994

ABSTRACT

The involvement of chemically-reactive oxygen radical species (RORS) in the pathogenesis of inflammatory joint diseases has been well documented. Much of the toxicity produced by increased superoxide ion ($O_2 \cdot^-$) and hydrogen peroxide (H_2O_2) generation has been attributed to the production of the highly reactive hydroxyl radical ($\cdot OH$) which is mediated by low-molecular-mass iron chelates such as iron-citrate complexes.

The $\cdot OH$ radical is extremely reactive and proving its formation *in vivo* is very difficult. Hence, assays for the assessment of $\cdot OH$ radical activity in the inflamed rheumatoid joint have involved identification and/or quantification of 'unnatural' chemical species produced by the attack of $\cdot OH$ radical on a range of endogenous or, alternatively, therapeutically-administered exogenous 'target' molecules.

This study involves:

(1) An investigation of the precise chemical nature of intermediates in and so called 'end-products' of the process of lipid peroxidation. Second-derivative (2D) electronic absorption spectrophotometry has been applied to the analysis of isomeric conjugated hydroperoxydienes, hydroxydienes and ketodienes and also to thiobarbituric acid-reactive material in synovial fluid (SF) obtained from patients with inflammatory joint diseases.

(2) A method for determining the extent of RORS-dependent peroxidation of polyunsaturated fatty acids (PUFAs) has been further developed for application to biological samples. This technique involves the conversion of conjugated hydroperoxydienes and compounds derived therefrom, i.e. oxodiene and hydroxydienes, to strongly chromophoric conjugated triene and tetraene species. The chromophore(s) produced are measured by their absorbance in the ultra-violet or near ultra-violet regions of spectra using 2D spectrophotometry.

(3) An evaluation of the chemical nature of non-transferrin-bound iron in inflammatory synovial fluid is investigated by high-resolution, high-field proton (^1H) nuclear magnetic resonance (NMR) spectroscopy, combined with the use of powerful iron(III) chelators (desferrioxamine and nitrilotriacetate), and the iron(III)-binding protein apotransferrin in order to 'speciate' catalytic, low-molecular-mass iron complexes present in inflammatory SF samples.

(4) The application of high field proton NMR spectroscopy to evaluate the abilities of the antioxidant thiol drug N-acetylcysteine and exogenous cysteine to protect metabolites present in intact inflammatory SF samples against oxidative damage arising from reactive oxygen radical species generated via gamma-radiolysis (5.00 kGy) in the presence of atmospheric oxygen.

Dedicated to my family.

Knowledge is like a garden,
if it is not cultivated,
then it cannot be harvested.
.....Guinean Proverb.

ACKNOWLEDGEMENTS

I would like to express my sincere gratitude to my supervisors, Dr. M. Grootveld and Dr. B. E. Davison, for their invaluable advise and support throughout the experimental work and preparation of this thesis. I thank Mr W. Dissanayake and Mr L. William for their technical support. I am also very grateful to the Royal London Hospital Medical College for financial support. I extend my thanks to Professor D. R. Blake and his research team at the Inflammation Research Group (Royal London Hospital Medical College) for providing the necessary biological samples, and the University of London Intercollegiate Research services (ULIRS) for the provision of NMR facilities.

Finally, I would like to extend a special thanks to all the members of my family, especially my brother Imtiyaz for his help in preparing this thesis, and also to Alex and Reetu for their whole-hearted support and patience.

CONTENTS

CHAPTER 1

INTRODUCTION

1.1 Reactive Oxygen Radical Species

Free radicals play a critical role in many diseases including cancer, rheumatoid arthritis, reperfusion injury (the sudden release of oxygen to organs after ischaemia, such as those occurring during a stroke or heart surgery) and lung disease[1-3]. Oxygen radicals are capable of reversibly or irreversibly damaging compounds of all biochemical classes, including nucleic acids, proteins, free amino acids, lipids, carbohydrates, and connective tissue macromolecules[4]. Table 1.1 lists some of the conditions in which the deleterious involvement of oxygen-derived free radical species has been implicated.

As early as the 1950's it was thought that the adverse production of reactive oxygen radical species (RORS) were responsible for the damaging effects of oxygen. However, early attempts to demonstrate this conclusively were hampered by the high intrinsic reactivity of these species which precluded their detection. The identification of superoxide dismutase in biological systems by McCord and Fridovich[5] however, led to a widespread acceptance of the importance of RORS in biological systems. The production of RORS is usually tightly controlled, but interest is now focused on the idea that many diseases may result from either the excessive or inappropriate production of RORS, or lack of the necessary control or defence mechanisms[6-8].

1.1.1 Free radicals

Free radicals are generally defined as chemical species with one or more unpaired electrons in their outer orbital. This is the major property which confers a high chemical reactivity on radical species. They can be formed by either of the following two processes (1) homolytic fission of a covalent bond between two atoms A and B which form the molecule AB (equation 1.1), and, (2) by electron transfer reactions (equation 1.2)[9].

$$A{:}B \rightarrow A^{\cdot} + B^{\cdot} \qquad (1.1)$$

$$(A{:})^{-} + B \rightarrow A^{\cdot} + B^{\cdot -} \qquad (1.2)$$

In writing a symbol for a free radical, a dot is generally included to represent the presence of the unpaired ('odd') electron (e.g. A·).

Free radical production is generated by many initiators including gamma-radiation, UV light and environmental pollutants. However, the most important source of these radical species *in vivo* is from univalent biochemical redox reactions involving oxygen (i.e. non-enzymatic electron transfer reactions, metal ion-catalysed reactions or enzyme-catalysed processes).

A major consequence of having one or more unpaired electrons in their outer orbital is that radical species have an increased reactivity with other molecules. This reactivity is determined by the ease with which a species can accept an electron (i.e. is reduced), or donate them (i.e. is oxidised). This is best illustrated by studies of the redox reactions of molecular oxygen, superoxide ($O_2^{\cdot -}$) and peroxide (O_2^{2-}) ions.

1.1.2 Oxygen-derived radical species and their biological reactivity

While oxygen is by definition essential for aerobic life, it is known to be toxic when supplied at concentrations greater than those present in the atmosphere[10]. Its toxicity can be related directly to its unique electronic configuration. Molecular oxygen is the most common of all biologically important free radical species. The term RORS not only covers oxygen-derived free radicals but also other products of oxygen metabolism, which may also be reactive and potentially damaging species.

Molecular oxygen (O_2) is a biradical, having two unpaired electrons, each one located in a separate orbital (i.e. electrons of opposite spin). As non-radical species possess paired electrons of opposite spin, one electron must spin invert before both electrons can be accepted. This process is feasible, but limits its reactivity with oxygen which preferentially accepts one electron at a time (univalent reduction)[11-12].

The univalent reduction of oxygen produces the superoxide anion radical ($O_2^{\cdot -}$). The anion is protonated to give the more reactive perhydroxyl radical ($HO_2^{\cdot}$) at acidic pH values

(pKa 4.7- 4.8). Due to its unique electronic configuration, $O_2^{\cdot -}$ is both a reducing agent and a nucleophile (i.e. seeking to react with an electropositive source). Superoxide can thus reduce iron(III) ions (equation 1.3), enabling resulting iron (III) species to participate in the Fenton reaction (equation 1.5).

$$O_2^{\cdot -} + Fe^{3+} \rightarrow Fe^{2+} + O_2 \qquad (1.3)$$

The divalent reduction of O_2 (or the univalent reduction of $O_2^{\cdot -}$) yields a non radical species O_2^{2-} (equation 1.4) which is protonated at physiological pH values (pKa 10.2) to yield hydrogen peroxide (H_2O_2), a long lived and membrane permeable species.

$$e^- + O_2^{\cdot -} + 2H^+ \rightarrow H_2O_2 \qquad (1.4)$$

Homolytic fission of the O-O bond of the H_2O_2 molecule produces the hydroxyl radical ($\cdot$OH). This homolytic process requires an energy input which may be provided by heat, ionising radiation, or the simple addition of a metal ion catalyst in an appropriate oxidation state. Since many transition metal ions are able to accept or donate single electrons they are thus important catalysts for free radical reactions. In a transition metal ion-free system, H_2O_2 is of limited toxicity, but in the presence of iron(II) and copper(I) ions it is reduced giving rise to the production of $\cdot$OH radical (equation 1.5). This reaction is known as the Fenton reaction, or an iron-catalysed Haber-Weiss reaction. The reaction of an iron(II) salt with H_2O_2 to produce a whole range of reactive intermediates was first described by Fenton in 1894.

$$Fe^{2+} + H_2O_2 \rightarrow \cdot OH + Fe^{3+} + OH^- \qquad (1.5)$$

Proteins such as transferrin (the extracellular transport protein) or ferritin (the intracellular storage protein) which compartmentalise iron in the stable iron(III) form, are considered as antioxidants that limit oxidative damage by virtue of their abilities to complex this redox-active metal ion.

Alternatives to the production of highly reactive $\cdot$OH radical via the Fenton reaction have also been proposed. Walling *et. al.* [13] suggested the ferryl ion, (FeO^{2+}), (with the iron

having an oxidation state of +4), as a major contributor to oxidative damage in biological systems. To date, however, there is no clear evidence for the generation of FeO^{2+} outside a haem ring and haem-associated ferryl ion has been proposed to account for the ability of mixture of myoglobin or haemoglobin with H_2O_2 to accelerate the lipid peroxidation process.

In contrast to H_2O_2, the ·OH radical is extremely reactive with a half life of less than 10^{-9} seconds and has therefore very limited diffusion capacity. The ·OH radical will react with almost every molecule present in living systems. These reactions include the modification of carbohydrates, production of strand breakage's and base hydroxylation in deoxyribonucleic acid (DNA), initiation of lipid peroxidation and the induction of irreversible damage to proteins[8,14]. Its reactivity relates to three main classes of reaction (1-3 below)[10].

1) HYDROGEN ABSTRACTION.

The ·OH radical removes a hydrogen atom from a molecule to form water, leaving a further free radical species (equation 1.6).

$$\mathbf{LH + \cdot OH \rightarrow HOH + L\cdot} \qquad \mathbf{(1.6)}$$

(where LH may be a polyunsaturated fatty acid)

2) ELECTRON TRANSFER.

OH readily accepts an electron from another atom or molecule, generating a secondary radical species, e.g. its interaction with thiols (equation 1.7).

$$\mathbf{RS^- + \cdot OH \rightarrow RS\cdot + OH^-} \qquad \mathbf{(1.7)}$$

3) ADDITION.

·OH radical can add to aromatic compounds such as the amino acids, phenylalanine and histidine, or the purine and pyrimidine base moieties of DNA, generating hydroxylated derivatives of these compounds (e.g., equation 1.8).

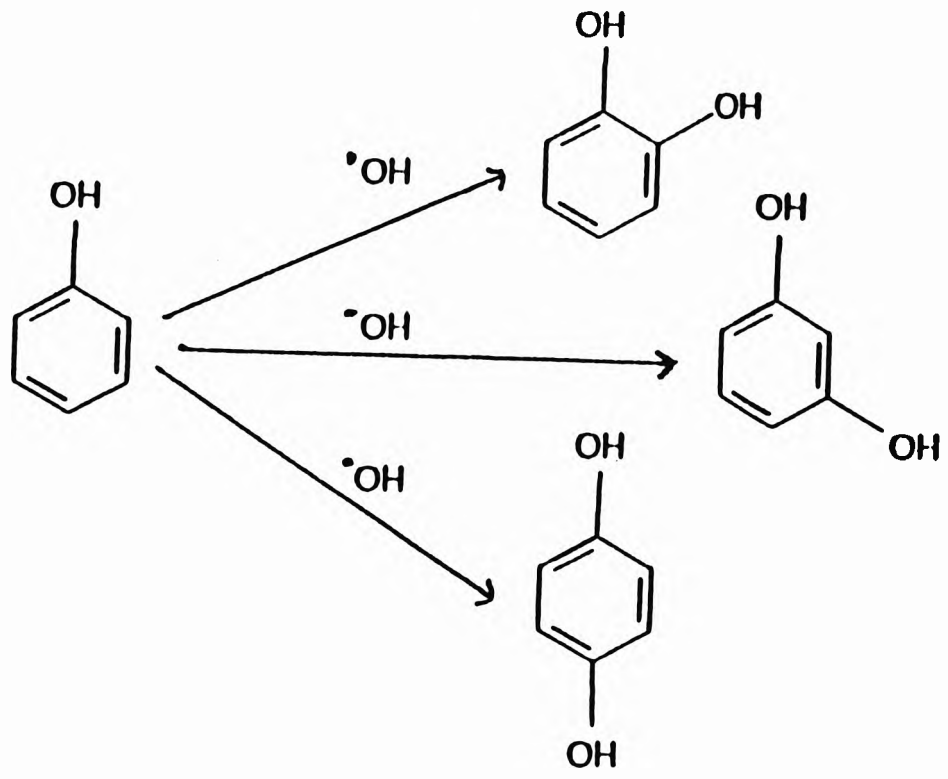

(1.8)

For all of these reaction systems, the induction of autocatalytic (self-propagating) chain reactions can occur under certain biological and experimental conditions, e.g., the process of lipid peroxidation[15-16].

Table 1.1: Some clinical conditions in which the involvement of oxygen radicals have been suggested.[19]

Inflammatory-immune injury	Glomerulonephritis (idiopathic membranous), Vasculitis(hepatitis B virus, drugs) Auto immune diseases Rheumatoid arthritis
Heart and cardiovascular system	Alcohol cardiomyopathy Keshan disease (Se deficiency) Atherosclerosis Adriamycin cardiotoxicity
Ischemia-reflow states	Stroke/myocardial infarction Organ transplantation
Kidney	Auto immune nephritic syndromes Aminoglycoside nephrotoxicity Heavy metal nephrotoxicity
Lung	Bronchopulmonory dysplasia Oxidant pollutants (O_3) Mineral dust pneumoconosis Bleomycin toxicity SO_2 toxicity Acute respiratory distress syndrome Cigarette-smoke effect Emphysema Hyperoxia
Red blood cells	Malaria Phenylhydrazine Primaquine, related drugs Lead poisoning Sickle cell anaemia Favism Fanconi's Anaemia
Brain	Neurotoxins Hyperbaric oxygen Vitamin E defiency Senile demantia Parkinson's disease Hypertensive cerebrovascular injury Neuronal ceroid lipofuscinoses Allergic encephalomyelitis and other demyelinating diseases

	Aluminium overload Potentiation of traumatic injury
Eye	Cataractogenosis Ocular haemorrhage Degenerative retinal damage Retinopathy of prematurity Photic retinopathy
Gastrointestinal tract	Endotoxin liver injury Halogenated hydrocarbon liver injury (e.g. CCL_4) Diabetogenic action of alloxan Free-fatty-acid-induced pancreatitis NSAID-induced lesions Oral iron poisoning
Iron overloaded	Idiopathic haemochromatosis Bantu tribe iron pot beer drinkers Thalassaemia and other chronic anaemias treated with multiple blood transfusions Nutritional deficiencies (Kwashiorkov)
Skin	Hypericin other photosensitizers Contact dermatitis Solar radiation Thermal injury Porphyria
Ageing	Disorders of 'premature ageing'
Radiation Injury	
Alcoholism	
Drug- and toxin-induced reactions	

1.2 Protection Against Free Radical Damage In Biological Systems

Many defence mechanisms within the organism have evolved to limit the levels of reactive oxygen species and the damage they induce. Free radical scavengers occur both intra- and extracellularly. Amongst these defence systems are SOD, catalase and gluthathione peroxidase, as well as antioxidants such as reduced vitamin C, beta-carotene, tocopherols, urate, and the proteins transferrin, lactoferrin, caeruloplasmin, and albumin[7,9,17-18]. In view of the finite time between the generation of a radical species and its destruction via an endogenous defence mechanism, low levels of reactive oxygen species can exist for periods sufficient to induce damage to cellular macromolecules[19].

1.2.1 Enzymatic protection

1.2.1.1 Superoxide dismutase (SOD)

Within cells, antioxidant defence is provided largely by specific enzymes such as SOD. SOD is a specific scavenger of superoxide radicals and is therefore thought to have a role in preventing the generation of more reactive radical species. Despite an intensive research, no other substrates on which SOD enzymes act catalytically have been discovered[9,19]. There are two types of SOD enzymes, one containing copper and zinc ions and the other manganese and zinc ions, the latter being located in mitochondria. This enzyme catalyses the conversion of superoxide radicals to oxygen and H_2O_2 (equation 1.9). Both the Cu/Zn and Mn/Zn SODs catalyse this reaction.

$$2O_2^{\cdot -} + 2H^+ \rightarrow H_2O_2 + O_2 \qquad (1.9)$$

McCord and others have reported that the reactive hydroxyl radical may be produced from the metal ion-catalysed reaction between $O_2^{\cdot -}$ and H_2O_2 in the absence of SOD (equations 1.10 and 1.11)[9,7,20].

$$O_2^- + Fe^{3+} \rightarrow Fe^{2+} + O_2 \qquad (1.10)$$

$$Fe^{2+} + H_2O_2 \rightarrow Fe^{3+} + OH^- + \cdot OH \qquad (1.11)$$

Fenton reaction

The net overall reaction is referred to as the iron-catalysed Haber-Weiss reaction (equation 1.12) :

$$O_2^{\cdot -} + H_2O_2 \rightarrow O_2 + OH^- + {\cdot}OH \qquad (1.12)$$

Although superoxide production by cells during normal metabolism is high *in vivo*, the intracellular $O_2^{\cdot -}$ concentration is kept extremely low (calculated to be 10^{-11}M)[7]. These low levels are maintained both by spontaneous dismutation of the superoxide ion to H_2O_2 and, more importantly, its catalytic transformation by the two SOD enzymes (equation 1.9). Extracellular levels of these enzymes are very low, but SOD activity is high in tissue with high oxygen utilisation e.g. the liver. The 'acute-phase' protein, caeruloplasmin, also appears to have some superoxide-scavenging ability but its effectiveness in removing $O_2^{\cdot -}$ is only 1/3000 that of SOD[3,21]. SOD is, however, an intracellular enzyme with little or no enzymatic activity outside cellular compartments.

According to the 'superoxide theory of oxygen toxicity', superoxide formation is a major factor in oxygen toxicity and SOD enzymes are considered to constitute an essential defence against oxygen toxicity. At present, many research workers believe that superoxide is the only substrate for the catalytic action of SOD.

SOD and synthetic compounds with SOD-mimetic activity are of increasing interest to the pharmaceutical industry in view of their potential therapeutic use as antioxidant drugs to reduce tissue damage arising from re-oxygenation subsequent to local oxygen deprivation. The administration of SOD has potential benefits to patients following heart attacks, during cardiac surgery and organ transplant, and also in the healing of wounds and burns.

1.2.1.2 Catalase and peroxidase

Intracellular H_2O_2 levels are maintained at 10^{-9}-10^{-7} M by the selenium-dependent glutathione peroxidase enzyme system which catalyses the oxidation of reduced glutathione (GSH) to oxidised glutathione (GSSG) at the expense of H_2O_2 (equation 1.13). H_2O_2 can

react rapidly with Fe(II) to yield the highly toxic ·OH radical. It is therefore biologically advantageous for cells to control the amount of H_2O_2 that is allowed to accumulate.

$$H_2O_2 + 2GSH \rightarrow GSSG + 2H_2O \qquad (1.13)$$

Glutathione peroxidase is abundant in the heart, lungs, brain, liver and erythrocytes, and is located in the cytosol and mitochondria. Glutathione peroxidase is also responsible for de-toxifying organic hydroperoxides such as fatty acid and steroid hydroperoxides arising from episodes of oxidative stress.

Catalase is a haem-containing enzyme which controls the intracellular concentration of H_2O_2 by promoting the reaction depicted in equation 1.14.

$$2H_2O_2 \rightarrow 2H_2O + O_2 \qquad (1.14)$$

Catalase is found in the most aerobic cells in the cytosol, mitochondria and other sub-cellular organelles, such as peroxisomes. It is also abundant in liver and erythrocytes.

The extracellular levels of both of the above enzymes are very low. The high reactivity of ·OH hinders its enzymatic removal and defence mechanisms against this radical involve the prevention of its generation, or its scavenging by appropriate low-molecular-mass antioxidants.

1.2.2 Non-enzymatic free radical scavengers

Enzymes such as catalase and gluthathione peroxidase offer only a limited, directed protection against the damaging effects of the highly reactive ·OH radical. However, a variety of low-molecular-mass free radical scavengers (antioxidants) exist which can react directly with free radicals and convert them to less harmful, more stable derivatives.

1.2.2.1 Vitamin C (Ascorbic acid, AA)

AA is an essential dietary vitamin which humans, other primates, guinea-pigs and the fruit-eating bat cannot synthesise, a phenomenon attributable to the absence of the enzyme l-

gulonolactone oxidase. AA has a role in iron metabolism, especially with respect to its transport and mobilisation. Dietary deficiency of AA causes scurvy.

AA also acts as a water-soluble antioxidant and a powerful reducing agent (electron donor). At high concentrations, AA reacts rapidly with $O_2^{\cdot -}$ and even more rapidly with ·OH radical to form, via a semidehydroascorbate intermediate, its metabolite, dehydroascorbic acid (DHA) (equation 1.15).

$$AA + 2H^+ + 2O_2^{\cdot -} \rightarrow 2H_2O_2 + DHA \qquad (1.15)$$

However, at low concentrations and in presence of catalytic metal ions, its metal-reducing capacity (like that of $O_2^{\cdot -}$) may stimulate ·OH generation via the Fenton reaction, and accelerate lipid peroxidation (equation 1.16).

$$Fe^{3+} + AA \rightarrow Fe^{2+} + DHA \qquad (1.16)$$

AA is normally maintained at high concentrations in cytosol and sera (40-80 μM). The concentration of AA has been reported to be low in patients with RA. The concentration of AA is also reduced in other disease states, e.g., diabetes mellitus, cancer and alcoholic liver disease, and also in some elderly populations[19].

1.2.2.2 Vitamin E (α-tocopherol) and other non-enzymatic antioxidants

Vitamin E is a lipid-soluble antioxidant which can react with $O_2^{\cdot -}$, ·OH radical and, more specifically, with lipid hydroperoxides. Its lipid-soluble nature allows it to concentrate preferentially within the phospholipid bilayer of cell membranes and in blood plasma it is associated with lipoproteins such as low-density-lipoprotein.

Vitamin E acts as a free radical scavenger which protects against lipid peroxidation, and reacts with lipid peroxyl radicals to form vitamin E radicals that are insufficiently reactive to abstract H· from membrane lipids. It thus intercepts the chain reaction of lipid peroxidation by acting as a chain terminator. The vitamin E radical is converted back to vitamin E by ascorbate, thus providing a further important role for ascorbate as an antioxidant.

Transition metal ions such as those of copper and iron can also be classified as radicals since they contain unpaired electrons and can react with H_2O_2 to generate the highly reactive ·OH radical. Transition metal ions are also essential components of various enzymatic and non-enzymatic proteins, e.g. SOD (Cu), cytochrome oxidase (Cu), caeruloplasmin (Cu), cytochromes (Fe), ferritin (Fe) and lactoferrin (Fe). Some of these proteins actually serve, under certain conditions, to limit oxidative processes. Removal of free transition metal ions reduces the chance of random ·OH generation, although the possibility of 'site-specific' catalysis at metal ion binding sites remains.

Free iron concentrations, intra- and extracellularly, are kept low by binding iron to the iron storage and transport proteins ferritin, transferrin and lactoferrin. Thus, by ensuring the absence of low-molecular-mass iron ions from normal human plasma at physiological pH, plasma transferrin may act as an antioxidant in addition to its iron transport role. The iron-binding protein lactoferrin , released by activated neutrophils, may also function as an antioxidant by binding iron and preventing it from participating in radical reactions.

Caeruloplasmin, a copper-containing protein, is also a major serum antioxidant capable of inhibiting lipid peroxidation at a concentration of 10 mg dm^{-3} [19]. Non-caeruloplasmin-bound copper ions in blood serum are bound mainly to serum albumin, and traces bound to amino acids such as histidine may also be present. However, complexation of Cu(II) to these species does not prevent its interaction with superoxide and hydrogen peroxide to generate ·OH radical in a 'site-specific' manner [19].

Uric acid, albumin, haptoglobin, and haemopexin have also been shown to inhibit various radical reactions, generally by sequestering metal ions. Caeruloplasmin, an important extracellular antioxidant, oxidises Fe^{2+} to Fe^{3+}, which swiftly binds to transferrin, as indeed will any Fe(III) mobilised from serum ferritin.

1.3 Iron in Biological Systems

1.3.1 Iron distribution

Many transition elements are of biological importance and Table 1.2 list some of the essential transition metal ions required by humans[19]. The most important feature of such metals is their variable oxidation states which enable them to participate in and be effective catalysts of many redox reactions. They are utilised for this purpose at the active sites of many enzymes which catalyse such reactions.

Iron is essential in the human diet and is the most abundant transition metal in humans. An adult human contains approximately 4.5 g of iron, of which about 65% is present in haemoglobin, a further 10% in myoglobin, with much smaller quantities associated with various iron-containing enzymes and the transport-protein transferrin. The remainder is present in the intracellular storage proteins ferritin and haemosiderin[19]. The average daily iron intake is about 1 mg, but the amount absorbed is equal only to its losses. Slight disturbances in this quantity leads to 'iron overload' or 'iron-deficiency'[7].

Iron is more readily absorbed in the ferrous state (Fe(II)). However, most of the dietary iron is in the ferric form (Fe(III)), which requires dissolution and reduction before it can be absorbed. The hydrochloric acid in the stomach achieves solubilization, and dietary vitamin C (ascorbic acid, a reducing agent) and other reducing substances in the diet facilitate the conversion of ferric to ferrous ions and assist in its absorption. Iron taken up by the gut enters the plasma-protein transferrin, which functions as a carrier molecule. Transferrin is a glycoprotein of molecular mass 80 kDaltons, and each molecule has two separate binding sites to which Fe(III) attaches extremely tightly.

Iron from transferrin enters iron-requiring cells in a vacuole. The contents of the vacuole are then acidified to facilitate the release of iron, which then binds to various cellular constituents such as citrate and ATP. The iron-free transferrin (apotransferrin) is then ejected from the cell. Any iron not required by cells is stored in the protein ferritin.

Ferritin is a large 24 sub-unit protein and its function appears to involve the prevention of an excessive intracellular accumulation of non-protein-bound iron. The ferritin molecule can contain as many as 4,000 atoms of iron. It consists of a protein shell (apoferritin) enclosing iron, which exists in the Fe(III) form. It is rarely saturated with iron *in vivo*. Iron enters ferritin as Fe(II), which becomes oxidised by the protein to Fe(III) and deposited in the interior. Iron can also be removed from ferritin as Fe(II) by the action of number of biological reducing agents such as ascorbate, cysteine and reduced flavins.

1.3.2 Iron and free radical reactions

Normally, the transferrin present in blood plasma is only about 30% saturated with iron, which binds with a very high affinity at pH 7.4, so that the amount of 'free' iron complexes available in the blood plasma would be expected to be virtually zero, a result confirmed by experiment[26]. The normal plasma iron level is about 23 μmol dm^{-3} in males and 19 μmol dm^{-3} in females[23]. Iron bound to the two specific binding sites of transferrin is either inactive, or only weakly active, in accelerating lipid peroxidation and ·OH radical production at pH 7.4[24]. Once the pH falls below 6, iron becomes easily detachable from transferrin. Hypoxic tissues and exercising muscle may also reflect this level of acidosis. Thus, iron mobilisation from transferrin might occur under certain physiological conditions[25].

Haemoglobin is another potential source of 'catalytic' iron in the blood. Whole erythrocytes have antioxidant properties since they are rich in SOD, catalase, and gluthathione, and they can act as 'sinks' of $O_2\cdot^-$ and H_2O_2[24]. Haemoglobin has often been reported to stimulate peroxidation of membrane lipids and sometimes to accelerate the deleterious generation of ·OH radical. H_2O_2 and lipid peroxides can cause iron release from haemoglobin and this 'released' iron may be responsible for haemoglobin-stimulated radical reactions[26]. The ferritin molecule can also lose iron via the actions of $O_2\cdot^-$ radical, H_2O_2 and organic peroxides[26]. This 'released' iron accounts for ferritin-stimulated radical reactions.

The mobile intracellular iron 'pool' is a further candidate for accelerating oxygen radical reactions. Until recently, the chemical nature of this 'free' iron pool was unknown.

This 'free' iron can readily promote the deleterious generation of ·OH radical from $O_2^{\cdot -}$ and H_2O_2. The iron-catalysed Haber-Weiss reaction can give significant fluxes of ·OH. However, this reaction does not generally take place in the presence of physiological iron chelators such as transferrin, lactoferrin or ferritin, unless they are fully saturated since they compartmentalise iron in the stable and inaccessible ferric state.

Table 1.2 : Biological importance of some d-block elements[19].

Metal	Biochemical significance
Copper (Cu)	Essential in human diet. Required for enzymes such as SOD, cytrochrome oxidase, lysine oxidase, dopamine hydroxylase and caeruloplasmin. About 80 mg Cu in adult human body. Concentrated in liver and brain. Overall blood content in males 0.106 mg/100 ml.
Zinc (Zn)	Non-transition element, fixed valency of 2. Essential in human diet; found in RNA polymerase, carbonic anhydrase, and SOD. Plasma zinc approx. 0.112 mg/100 ml.
Chromium (Cr)	Probably essential in diet, involved in regulation of glucose metabolism. Normal serum Cr is 1-5 ng/ml.
Manganese (Mn)	Essential in animal, probably in man as well (normal blood level 9 μ g/ml.). Needed for mitochondrial SOD, also activates a number of hydrolase and carboxylase enzymes.
Iron (Fe)	Essential in human diet: deficency causes simple anaemia. Most abundant transition metal in humans. Normal serum iron in males approx. 0.127 mg/100 ml. mostly bound to protein transferrin. Needed for haemoglobin, myoglobin, cytochromes, several enzymes and non-haem-iron proteins.
Nickel (Ni)	Probably essential in animals, requirement in man not yet established. Found in urease in plant cells and in several bacterial enzymes, such as hydrogenase and carbon monoxide hydrogenase.
Cobalt (Co)	Essential as a component of Vitamin B_{12} but little else is known.
Molybdenum (Mo)	Essential in trace amounts for some flavin metalloenzymes, such as xanthine oxidase, sulphite oxidase, nitrogenase and nitrate reductase.

1.4 Rheumatoid Arthritis

Rheumatoid arthritis is a common and debilitating disease classically involving the peripheral synovial joint in a symmetrical fashion. Its usual characteristics consist of persistent inflammation involving the synovial membrane and surrounding structures.

Normally, the acute inflammatory response is beneficial to the organism in that it deals with unwanted and potentially dangerous foreign particles such as bacteria. Inflammation is usually a self-limiting event, but anything causing the abnormal activation of phagocytes has the potential to provoke a devastating response.

RA is a slowly progressing degenerative disease of connective tissues, particularly of the diarthrodial joints. The disease begins with inflammation of synovial connective tissue, followed by fibrinoid deposition, derangement of the articular cartilage and osteoelastic change in the articulating region of the bone. Inflammation is a defensive reaction to injury and arises from associated cell damage. Agencies and means of provoking the response include mechanical trauma (especially crushing), radiation (thermal, UV, radioactivity), chemical and biochemical damage (metabolic inhibitors, anoxia), invading organisms (viruses, bacteria, parasites) and finally antibody-antigen reactions.

In RA, the synovium of the joint becomes swollen and damaged, and there is an increased deposition of iron proteins, ferritin and haemosiderin therein. The disease often proceeds to erosion of the joint cartilage. Production of synovial fluid, the natural joint lubricant, is increased but its lubricating capacity is greatly diminished. This decrease in lubrication is attributable to a decreased viscosity which is due to de-polymerisation of the high-molecular-mass polysaccharide hyaluronic acid (Figure 1.17). The cartilage wear particles, produced by increased friction in the joints, can activate neutrophils and perpetuate the disease process.

The blood serum and joint fluid of rheumatoid patients often contains an antibody (rheumatoid factor) that binds to immunoglobin G. Autoantibodies are present in inflammatory bowel diseases such as Crohn's disease and ulcerative colitis. The former is a

recurrent inflammation that can involve ulceration of the whole digestive tract, although it is often most severe in the lower part of the ileum, and in the colon and rectum. In ulcerative colitis, however, the ulceration and inflammation affects the colon and rectum only.

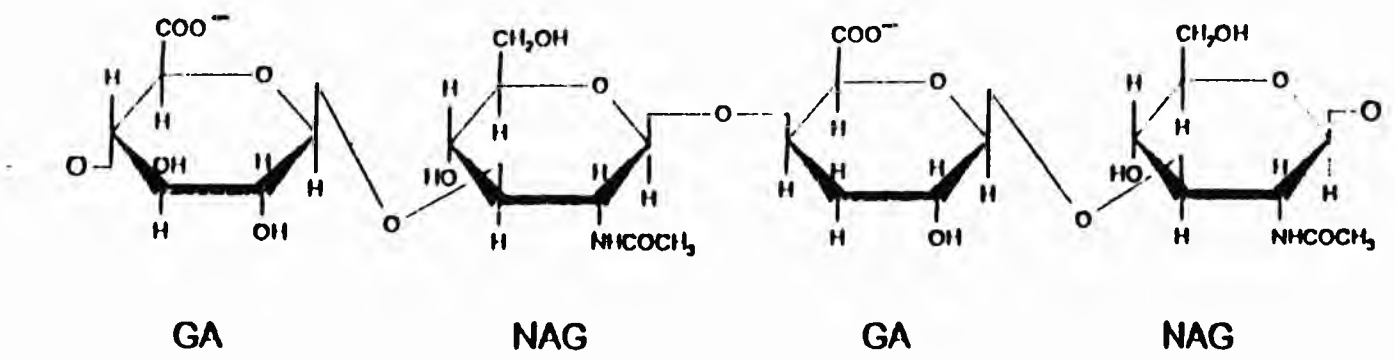

Figure 1.17. Structure of hyaluronic acid. Hyaluronic acid is a long polymer formed by joining together alternatively two different sugars: glucuronic acid (GA) and N-acetylglucosamine (NAG). The negative charge on the carboxyl group of GA at physiological pH gives rise to a subunit repulsion, so that the molecule extends out in solution. Hence solutions of hyaluronic acid are extremely viscous.

1.4.1 Hypoxic reperfusion injury

Hypoxic reperfusion injury in relation to rheumatoid arthritis is a relatively new concept. McCord originally documented hypoxic reperfusion injury to heart injury and the gut[20]. A transient ischaemic episode followed by reperfusion injury results in the production of RORS, which may be responsible for tissue damage, and therefore inflammation. There are several physiological and biochemical features present in the inflamed rheumatoid joint that provide a potential environment for hypoxic reperfusion injury[29-31]. Jayson and Dixon found that the resting pressure of SF in the normal human joint was at or below atmospheric pressure, whereas patients with RA and inflammatory joint effusions had significantly higher resting pressures than the control group[32].

Previous work has established the existence of a pathophysiological environment within the inflamed human joint, capable of sustaining hypoxic-reperfusion events. Hypoxic-

reperfusion injury is an established mechanism involving the production of RORS with subsequent tissue damage in many organ systems. This process, previously described in detail by McCord[20], involves the restoration of the blood supply to tissue subsequent to a transient ischaemic event, giving rise to RORS production via the uncoupling of certain intracellular redox enzyme systems, leading to tissue damage.

In normal synovial capillaries the hydrostatic pressure is about 30 mm Hg and can increase to 60 mm Hg in inflamed tissue. It is therefore clear that in rheumatoid arthritis the potential exists for temporary occlusion of the synovial capillary bed during exercise of the inflamed joint, giving rise to the production of a transient hypoxic environment[31].

In order to investigate this phenomenon further, Merry *et. al.*[28] applied the technique of laser doppler flowmetry to assess the synovial microvascular perfusion in the knees of both normal subjects and rheumatoid arthritis patients. They found that in the normal knee the capillary flow-rate was 5-10 perfusion units (PU) and was unaffected by exercise. In rheumatoid arthritis patients, however, the resting capillary flow-rates ranged from 100-600 PU, and fell dramatically during quadriceps exercise to levels ranging from 0-10 PU, an effect that lasted longer than the exercise period and which was followed by a reactive hyperaemia. These findings demonstrated that during exercise, inflamed joints with effusions will have temporary periods of capillary shutdown. Subsequent to exercise, there is also an increased oxygen supply to the synovium[28].

During a hypoxic-reperfusion event, exercise causes intra-articular pressure (IAP) to rise well above capillary perfusion pressure, resulting in occlusion of the synovial capillary bed and hypoxia. On cessation of exercise IAP falls and reperfusion occurs. In a normal joint there is no such exercise-promoted rise in IAP, no occlusion of synovial capillaries, and hence no oxidative damage to biomolecules. It is therefore proposed that exercise-promoted hypoxic-reperfusion injury explains the peculiar persistence of inflammatory synovitis[11,28].

It has been suggested that during temporary ischaemia the mitochondrial oxidative pathway is halted, a process attributable to a diminished oxygen tension, and the cellular

ATP production can become dependent upon anaerobic glycolysis. This is an inefficient means of ATP production from glucose. During ischaemia, ATP metabolism produces raised levels of adenosine and its breakdown products include hypoxanthine which acts as a substrate for xanthine oxidase (Figure 1.2)[33].

Upon reperfusion, generation of O_2 is dramatically increased when the oxygen supply is restored. Superoxide radical is then converted spontaneously to H_2O_2 by the enzyme superoxide dismutase (SOD). Indeed, SOD and other scavengers of oxygen radicals have been observed to suppress inflammation in some animal model systems. Temporary intestinal ischaemia in cats has been reported to be reduced by pre-treatment with SOD. Temporary myocardial ischaemia has also been reported to be inhibited by both SOD, catalase and mannitol[11]. Ischaemia also releases iron from its storage protein, ferritin, and this release of iron together with the generation of $O_2^{\cdot -}$ and H_2O_2 leads to the production of the reactive ·OH radical via the Fenton reaction[29]. Hydroxyl radical generated in this manner has the ability to initiate the process of lipid peroxidation. Superoxide and H_2O_2 have been reported to be removed using specific enzymes, such as SOD and glutathione peroxidase, either by administration of these enzymes or by increasing their *in vivo* activities[34]. SOD is reported to be effective in protecting against reperfusion damage after ischemia in several systems, although it cannot protect against damage induced by the ischaemia itself.

Like most extracellular fluids of the body, synovial fluid contains little, if any, SOD or catalase activities, and hence $O_2^{\cdot -}$ and H_2O_2 generated during the respiratory burst can generate ·OH in the presence of 'catalytic' iron complexes. Hydroxyl radical is known to attack and degrade hyaluronic acid, which would account for the decrease in viscosity of rheumatoid SF relative to that of the normal joint. Greenwald *et. al.*[35], have shown that radical-generating systems such as activated neutrophils, or a mixture of xanthine and xanthine oxidase, can degrade hyaluronic acid in an *in vitro* model system in a manner similar to that observed *in vivo*[35]. It is well established that ·OH radical is the most toxic of the oxygen radical species, and its formation is dependent on the presence of transition metal

ion catalysts. Halliwell *et.al.*[25] and Greenwald *et. al.*[35] have shown that micromolar concentrations of non-protein-bound iron salts capable of generating ·OH radical are present in human rheumatoid synovial fluid.

Halliwell and Gutteridge have developed an assay to detect this 'free' iron (i.e. iron ions not bound to transferrin, lactoferrin, ferritin or haem)[19]. The assay makes use of the iron-chelating capacity of the anti-tumour, antibiotic bleomycin which, when iron-loaded, degrades DNA to release TBA reactive compounds (predominantly malondialdehyde). Approximately 5-10% of synovial fluid iron is present in this 'catalytic' form, the levels of which correlate with the extent of lipid peroxidation found in the joint and clinical indices of inflammation. Transferrin is present in rheumatoid synovial fluid and appears to have adequate iron-binding capacity. It has been speculated that transferrin in inflammatory synovial fluids of lowered pH value does not retain its iron as avidly as that of normal serum, and that 'free' iron can participate in Fenton type reactions to generate the highly reactive hydroxyl radical[11].

Utilising a variety of techniques, including that of electron spin resonance spectroscopy coupled with spin-trapping techniques, the production of radicals by synovial tissue has been demonstrated, with an accelerated production following reperfusion injury. In this study, indirect assays of oxidative damage to lipids following exercise of the inflamed joint have been conducted using second-derivative (2D) electronic absorption spectrophotometry.

Figure 1.2 Generation of free radicals during ischaemia with reperfusion damage[33].

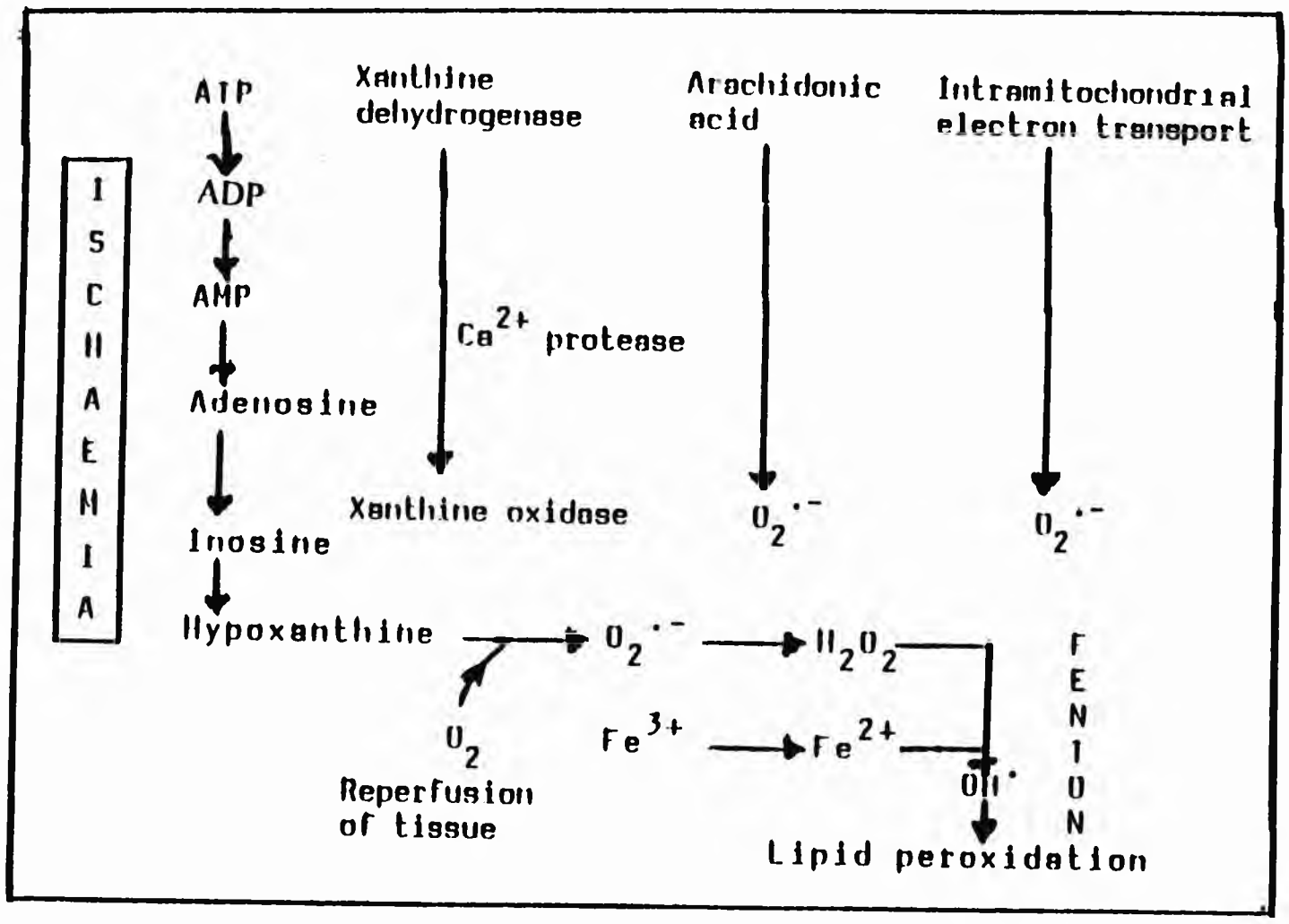

1.5 Aims of this Project

The involvement of chemically-reactive oxygen radical species (RORS) in the pathogenesis of inflammatory joint diseases has been well documented[1-3]. Much of the toxicity produced by increased superoxide ion ($O_2^{\cdot -}$) and hydrogen peroxide (H_2O_2) generation has been attributed to the production of the highly reactive hydroxyl radical (·OH) the generation of which is mediated by low-molecular-mass iron chelates such as iron-citrate complexes.

The ·OH radical is extremely reactive and proving its formation *in vivo* is very difficult. Hence, assays for the assessment of ·OH radical activity in the inflamed rheumatoid joint requires the application of indirect analytical techniques. The aim of this project is to investigate the production of RORS in inflammatory diseases by establishing the possibility of a Fenton type reaction system generating ·OH *in vivo* and to develop identification of potential assays for the measurement of free radical activity in patients with inflammatory diseases and then to determine the chemical nature of transferrin-bound-iron responsible for participating in Fenton-type reaction in inflammatory synovial fluid samples. Also to evaluate the ability of antioxidant drugs to protect biomolecules present in intact synovial fluid samples against oxidative damage arising from RORS.

The project involves the identification of 'unnatural' chemical species (*i.e.* those not usually formed by normal metabolic processes) produced by the attack of ·OH radical on a range of endogenous or, alternatively, therapeutically-administered exogenous 'target' molecules. For example, a series of these 'unnatural' products arising from the attack of ·OH on lipids, ascorbate, or other such biomolecules which are readily detectable in biological fluids such as blood plasma or knee-joint synovial fluid may serve as 'marker' of oxidative damage therein.

A variety of analytical techniques and procedures are employed, and their potential for the assessment of free radical activity in patients with inflammatory joint diseases is discussed.

CHAPTER 2

EXPERIMENTAL AND INSTRUMENTATION

2.1 Ultraviolet/Visible Spectrophotometry

2.1.1 Brief Theory

The ultraviolet and visible spectra of organic compounds are associated with the transitions between electronic energy levels[37-39]. Absorption of energy is quantised and the total energy of a molecule is given by,

$$E_{total} = E_{elect} + E_{vib} + E_{rot} + E_{trans}$$

where E_{total} = total electronic energy of a molecule

E_{elect} = the electronic energy of a molecule

E_{vib} = energy of the molecule due to interatomic vibrations

E_{rot} = energy associated with rotation of a molecule.

E_{trans} = energy associated with transition of a molecule.

The energy of electronic excitation is related to wavelength by the equation,

$$E = h\nu = hc/\lambda$$

where E = energy in joules

ν = frequency in Hz

h = Planck's constant (6.62×10^{-34} Js)

λ = wavelength in m

c = speed of light in a vacuum (2.998×10^{8} ms^{-1})

The transitions are generally between a bonding or lone-pair orbital and an unfilled non-bonding or anti-bonding orbital. The wavelength of the absorption is then a measure of the separation of energy levels of the orbitals concerned. The highest energy separation is found when electrons in σ-bonds are excited, giving rise to absorption in the 120-200 nm range. However, this range, known as the vacuum ultraviolet, is both difficult to measure and is relatively uninformative. Above 200 nm, however, excitation of electrons from p-, d- and π-orbitals, and particularly π-conjugated systems give rise to readily measurable and informative spectra.

Electronic transitions, however, occur in different manners. A transition in which a bonding σ-electron is excited to an anti-bonding σ-orbital is referred to as a $\sigma \rightarrow \sigma^*$ transition. Similarly, $\pi \rightarrow \pi^*$ represents the transition of a bonding π-electron to an anti-bonding π-orbital. An $n \rightarrow \pi^*$ transition represents the transition of one electron of a lone pair i.e., a non-bonding pair of electrons, to an anti-bonding π-orbital. This type of transition occurs with compounds containing double bonds involving hetero-atoms, e.g., >C=O, >C=S, >C=N-, etc. and may be represented as follows:

$$>C\text{—}O, \quad \leftarrow > \quad >C{=}O, \quad \rightarrow > \quad >C{=}O,$$
$$(\pi \rightarrow \pi^*) \qquad\qquad (n \rightarrow \pi^*)$$

A schematic representation of energy levels is shown below.

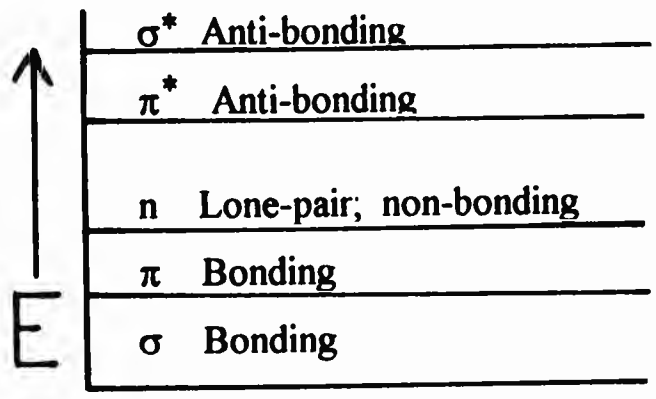

The transitions are brought about by the absorption of different amount of energy. The order of energy difference is; $\sigma \rightarrow \sigma^* > n \rightarrow \sigma^* > \pi \rightarrow \pi^* > n \rightarrow \pi^*$

$\pi \rightarrow \pi^*$ transitions are the least energetic and appear at longer wavelengths where they can be conveniently measured. They are characteristic of conjugated systems. Conjugation of double bonds lowers the energy required for the transition and the more extended the conjugation in a molecule the longer the wavelength of absorption. In a transition to a higher electronic level, a molecule can go from any of a number of occupied sub-levels corresponding to various vibrational and rotational states, to any of a number of empty sub-levels, and hence ultraviolet absorption bands are broad.

2.1.2 Derivative spectrophotometry

Derivative spectroscopy is an analytical technique of great utility for obtaining both qualitative and quantitative information from spectral curves composed of unresolved absorption bands. In general, the derivatisation procedure discriminates against broad absorption bands whilst emphasising sharper features of the spectrum to an extent that increases with increasing derivative order[40].

In derivative spectroscopy, the first or higher derivative of spectral intensity or absorbance with respect to wavelength is recorded versus wavelength (Figure 2.1), enhancing the detectability of minor spectral features such as a weakly-intense shoulder.

In 2D spectroscopy, the minima in the spectrum corresponds to the maximum absorbance in the conventional zero-order (absorption) spectrum. A new generation of UV-visible spectrophotometers equipped with appropriate differentiation units permits the precise recording of derivative spectra of variable order. The first-derivative of a zero-order spectrum measures the change in slope with wavelength, and the second-derivative spectrum measures the change in slope of the first-derivative spectral components with wavelength.

The 2D spectroscopy was developed in order to resolve in and clearly identify the conjugated diene species products produced from lipid peroxidation process. Previous studies on lipid peroxidation products measures absorbance reading between 220-280 nm however direct measurement of absorbance at a specified wavelength in this region is of limited practical utility since the absorption maxima of the conjugated diene species appear as a poorly defined shoulder superimposed on a high absorbance of other endogenous components present in the lipid/chloroform extacts. These overlapping absorption maxima are readily ressolved by the recording and subsequent examination of the corresponding 2D spectra of these samples.

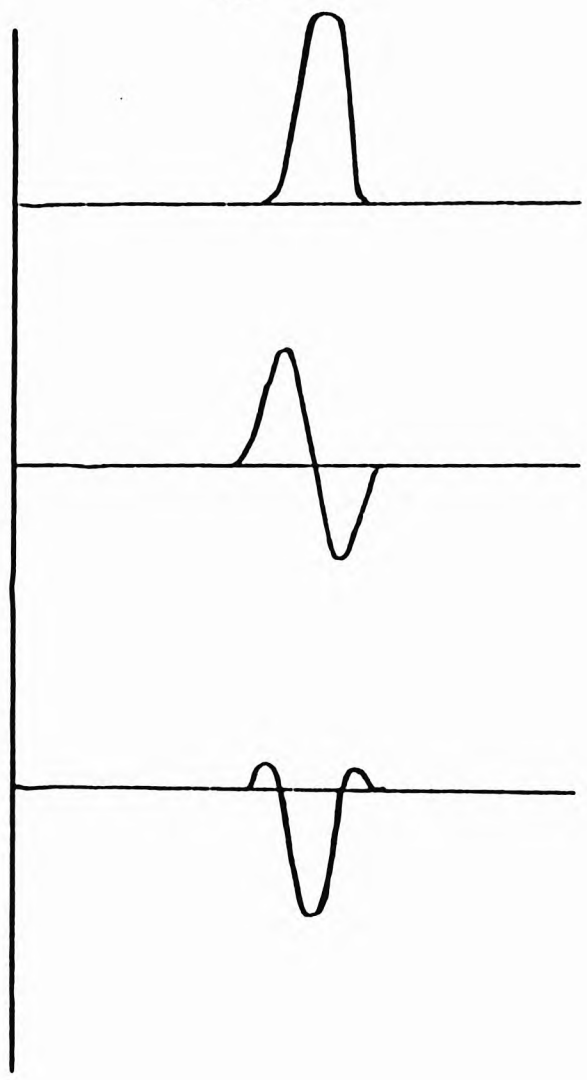
Zero-order
(absorption) spectrum
First-derivative spectrum
Second-derivative spectrum

Figure 2.1

2.2 Proton Nuclear Magnetic Resonance Spectroscopy

Like ultraviolet/visible spectroscopy, nuclear magnetic resonance spectroscopy (NMR) deals with the measurement of energy gaps between the states of different energy. However, unlike u.v/visible spectroscopy, NMR spectroscopy requires the presence of an external magnetic field and concerns nuclei rather than electrons[37-39]. With the aid of NMR spectroscopy it is possible to define the chemical environment of practically all commonly occurring functional groups.

2.2.1 Brief theory

Atomic nuclei have charge (i.e. they contain protons) and nuclei of certain atoms have spin. A spinning charge of a nuclei is equivalent to a current in a conductor loop; therefore, nuclei with non-zero spin will generate a magnetic field (magnetic moment). Consequently, they behave as tiny bar magnets and can interact with an externally applied magnetic field, Ho. In the absence of a magnetic field the nuclear spin of magnetic nuclei are oriented randomly and the energy states are degenerate. In the presence of a magnetic field, alignment of nuclei occur (with the field more stable), and energy must be absorbed to 'flip' the tiny proton magnet over to the less stable alignment, against the field. The energy needed to flip the proton over is dependent on the strength of the external field ; the stronger the field, the greater the tendency to remain lined up with it. The external field (electromagnetic radiation) of an appropriate frequency, ν is given by the LARMOR EQUATION (figure 2.2),

$$\nu = \zeta Ho/2\pi \qquad (2.2)$$

where ν = frequency, in Hz

Ho = strength of magnetic field, in gauss

ζ = nuclear constant (the gyromagnetic ratio for the proton is 26,750.)

In NMR spectroscopy the radiofrequency is normally kept constant and the strength of the magnetic field is varied till the energy required to flip the proton matches the energy of the radiation. Hence, absorption occurs and a signal is observed. However, the frequency at which a proton absorbs depends on the magnetic field which that proton 'feels', and this

'effective' field strength is not the same as the 'applied' field strength. The effective field strength at each proton depends on the environment of that proton, the electron density at the proton and the presence of nearby protons. Each set of equivalent protons has a slightly different environment from each other set of protons, and therefore requires a slightly different applied field strength to produce the same effective field strength (i.e. the particular field strength at which absorption takes place).

At a given radiofrequency, all protons absorb at the same effective field strength, but they absorb at different applied field strengths. In an NMR spectrum, it is this applied field strength that is measured, and against which the absorption is plotted.

More recently, the development of high-field NMR spectroscopy to study the chemical composition of biological systems has become fairly widespread[41-43]. NMR spectroscopy is a non-destructive, non-invasive and highly sensitive technique. In biological systems, the great majority of the compounds of interest contain hydrogen nuclei. This abundance of hydrogen-containing compounds together with the greater inherent sensitivity of ^1H NMR spectroscopy has led to its widespread use.

^1H NMR spectra of biological samples such as intact blood plasma usually contain broad overlapping resonances attributable to relatively immobile macromolecular species such as protiens. Application of the Hahn spin-echo technique suppresses these broad resonances leaving an NMR spectrum that has well resolved resonances arising from relatively mobile low-molecular-mass components.

2.2.2 The Proton Hahn spin-echo sequence

The spin-echo experiment was originally developed by Hahn for the measurement of spin-spin relaxation times and self diffusion coefficients[45].

The Hahn spin-echo sequence consists of a 90° pulse, a delay interval of length T_2, a 180° pulse, and a second delay of length T_2. The behaviour of the nuclear magnetization in the rotating co-ordinate system is represented in Figure 2.3[46].

Following the 90° pulse, the magnetisation in the $x'y'$ plane fans out due to loss of phase coherence from spin-spin relaxation and inhomogenity in Ho. Inhomogenity in Ho contributes to the fanning out because nuclei in some parts of the sample precess more rapidly than the average, while the others precess more slowly. After the time delay T_2, the 180° pulse is applied.

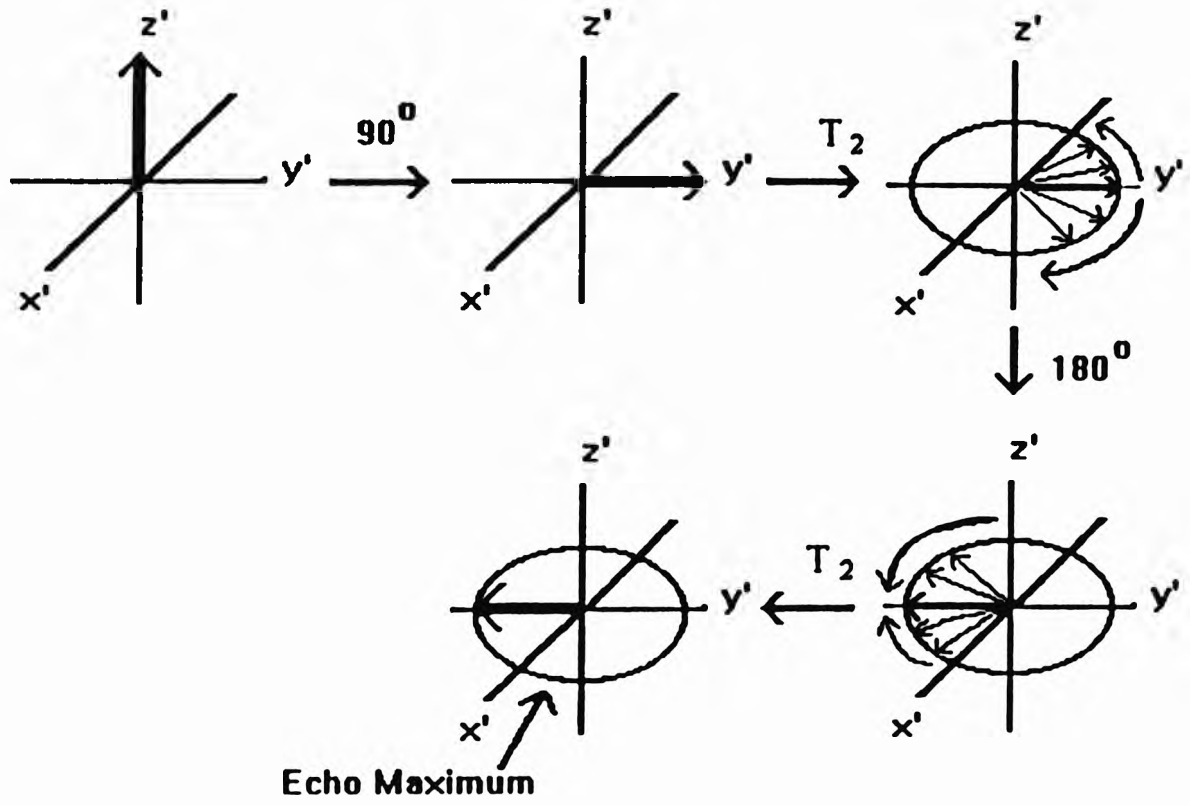

Figure 2.3 Nuclear magnetization in the rotating co-ordinate system

This rotates the magnetization vectors by 180° about the y' axis. The individual vectors precess at the same rate as before so that those precessing more rapidly now catch up with the average, and those precessing more slowly fall back to the average, and the echo results along the y' axis. Using this technique the effects due to Ho are eliminated. The spin-echo sequence is commonly written as $D[90°x\text{-}t\text{-}180°y\text{-}t\text{-}collect]_n$.

Proton NMR spectra of large molecules and of mixtures often consist of a multitude of overlapping signals. The spin-echo sequence increases the resolution on the basis of small

differences in the relaxation time (T_2) of different compounds. For example, in a high-molecular-mass macromolecule the T_2 values for its ^1H resonance are in general quite short compared to those of smaller, more mobile molecules. Thus, by making T_2 long enough in the spin-echo sequence, signals arising from large overlapping molecules are eliminated leaving a well-resolved spectrum.

Simplification of ^1H NMR spectra of biological materials in this manner was first reported by Daniels *et. al.*[47]. A major attraction of this technique is that little or no pre-treatment of the sample is required. In this study high-field proton Hahn spin-echo NMR spectroscopy is employed to detect abnormal components present in biofluid samples that may be derived from the adverse generation of reactive oxygen-radical species.

2.3 Reagents Used

Glacial acetic acid	ALDRICH
NaOH	ALDRICH
$NaBH_4$	ALDRICH
NaCl	ALDRICH
Sodium sulphate	ALDRICH
EDTA	BDH
H_2O_2	BDH
Fe_2SO_4	BDH
Conc. H_2SO_4	BDH
Iron(III) chloride	BDH
Chloroform	BDH (Spectroscopy grade)
Methanol	BDH (" ")
Cyclohexane	BDH (" ")
Ethanol	BDH (" ")
Hexane	BDH (" ")
TBA	SIGMA
Linoleic acid	SIGMA
Linolenic acid	SIGMA
Prostaglandin E_2	SIGMA
Methyl linoleate	SIGMA
Methyl linoleneate	SIGMA
N-acetyl-L-cysteine	SIGMA
L-cysteine	SIGMA
L-cystine	SIGMA
Iron(III) monocitrate	SIGMA
Disodium nitrilotriacetate	SIGMA
Ferrozine	SIGMA
Apotransferrin	SIGMA

All other reagents employed were of the highest possible grade and obtained from commercially available source.

2.4 Second-derivative Spectrophotometric Analysis of Different Classes of Conjugated Diene Species and Thiobarbituric Acid-Reactive Material in Biological Samples

cis-Linoleic and linolenic acid (10 µl) were sonicated in HPLC-grade water (2.00 ml) immediately before use. Peroxidation of these commercially-available PUFAs was initiated as follows: to the above suspensions was added EDTA (5.75×10^{-3} mol dm^{-3}), H_2O_2 (1.14×10^{-2} mol dm^{-3}) and Fe(II) (5.75×10^{-3} mol dm^{-3}) in the given order (final concentrations are given in brackets).

This system can initiate the peroxidation of PUFAs by generating the highly reactive ·OH radical (via the Fenton reaction, equation. 2.1) and/or propagate the process by interaction of iron(II) or iron(III) ions with pre-formed lipid hydroperoxides (equations 2.2 and 2.3).

$$Fe(II) + H_2O_2 \rightarrow Fe(III) + \cdot OH + OH^- \quad (2.1)$$

$$Fe(II) + LOOH \rightarrow Fe(III) + LO\cdot + OH^- \quad (2.2)$$

$$Fe(III) + LOOH \rightarrow Fe(II) + LOO\cdot + H^+ \quad (2.3)$$

The above mixtures were incubated at 37°C for 5 min. In some reaction systems EDTA was omitted. Autoxidation experiments were conducted on commercial PUFAs by placing samples in open glass test tubes and allowing them to autoxidise in the air at ambient temperature. Samples were taken at various time intervals and analysed for diene conjugates and TBA reactivity as described in this section.

2.4.1 Preparation of extracts : synovial fluid

Knee-joint synovial fluid was drawn into heparinized tubes for genuine therapeutic purposes from patients with moderately severe rheumatoid arthritis (RA) according to the criteria of the American Rheumatism Association. The samples were centrifuged immediately to remove particulate matter and then either analysed within a few hours after collection or stored at -20°C for a maximum duration of 8 days.

Synovial fluid samples were thawed at room temperature and the supernatant used for analysis. In a typical experiment, 250 µl of synovial fluid was added to 3.00 ml of chloroform/methanol (2:1 v/v) and lipid/chloroform extracts were obtained by vortex mixing for 3 min, followed by centrifugation at 1200 g for 10 min with subsequent removal of precipitated protein. The chloroform phase was removed from the aqueous phase using a glass Pasteur pipette and placed in glass test tubes with ground glass stoppers and the solvent removed at ambient temperature under nitrogen gas. The extracts were then reconstituted in 4.00 ml of spectroscopic-grade cyclohexane (a solvent that is transparent in the wavelength region of interest : lower wavelength limit 210 nm), and the resulting solution diluted 1:10 in the same solvent for 2D spectrophotometric analysis of isomeric conjugated diene species.

2.4.2 Determination of diene-conjugated lipid hydroperoxides

Cyclohexane-reconstituted lipid/chloroform extracts of synovial fluid samples were analysed for conjugate diene signals using a Philips PU 8740 spectrophotometer. The extracts were scanned over the wavelength range 200-400 nm and their zero-order (absorbance), first- and second-derivative spectra were recorded using a scan rate of 50 nm/min. All measurements were performed against a computer-memorised solvent blank.

2.4.3 Thiobarbituric acid reactivity

Analysis and interpretation of TBA-reactive material in synovial fluid samples was performed using an adaptation of the method of Stocks *et. al.*[48] A typical experiment involved the addition of 50 µl of synovial fluid to 3.00 ml of glacial acetic acid, and the mixture heated at 95°C for 30 min with 1.00 ml of a 1% (w/v) solution of TBA in 0.05 mol dm^{-3} NaOH. The resulting mixture was then cooled and centrifuged. Zero-order, first- and second-derivative electronic absorption spectra of the supernatant were recorded in the 350-700 nm wavelength region using a Philips PU 8740 spectrophotometer.

2.4.4 Application of spectrophotometric analysis to the assessment of lipid-derived conjugated diene species in the inflamed rheumatoid joint during exercise.

Knee-joint synovial fluid was drawn into heparinized tubes from patients with moderate to severe rheumatoid arthritis. A pre-exercise aliquot of synovial fluid was aspirated. In one group of patients, the knee was then exercised for 2 min by isometric quadriceps contraction, and samples of SF were taken at 2 min intervals post-exercise (n=5). In a second (control) group of patients, the exercise period was omitted and synovial fluid samples were aspirated at 2 min intervals (n=4). A third group of patients were exercised by walking a total distance of 300 yards and SF samples both pre- and post-exercise were similarly obtained (n=6).

2.5 Extension To The Conjugated Diene Method

2.5.1 Preparation of reagents

2.5.1.1 Reducing agent : Sodium borohydride solution

Sodium borohydride solutions were prepared daily by dissolving 0.2 g of solid reagent in 25 ml of spectroscopic grade ethanol to give a 0.2 M $NaBH_4$ solution.

2.5.1.2 Dehydrating reagent : alcoholic sulphuric acid

Concentrated H_2SO_4 was added to spectroscopic grade ethanol to yield a 10% (w/v) solution.

2.5.2 Peroxidation of methyl linoleate or linolenate

Methyl esters of linoleic acid or linolenic acid (10 µl) were sonicated in HPLC-grade water (2.00 ml) immediately before use. Peroxidation of these commercially-available polyunsaturated fatty acids was initiated by adding to the above suspension EDTA (1 mM), H_2O_2 (3.3 mM) and Fe(II) (1 mM) in the given order (final concentrations are given in brackets). In the control sample the addition of EDTA, H_2O_2 and Fe(II) was omitted.

Autoxidation experiments on model polyunsaturated fatty acid methyl esters were conducted by allowing them to autoxidise in the air at ambient temperature for a 72 hr period. These samples were analysed for conjugated hydroperoxydienes, oxodienes and hydroxydienes as described in section 2.5.8.

2.5.3 Biological samples

Colonic mucosal biopsies were collected during diagnostic colonscopy of patients with ulcerative colitis (UC) and immediately frozen at -70°C prior to analysis.

Control subjects included patients with normal mucosal appearance who were undergoing routine investigation for lower gastrointestinal symptoms or follow-up for cancer. Characteristics of the subjects are outlined below (Table 2.1).

Table 2.1

	Control	Inactive UC	active UC
Number	13	25	9
Age (range)	63(18-79)	45(22-65)	50(29-64)
Sex - male:female	6:7	12:13	6:3

2.5.4 Peroxidation of colorectal biopsies

Peroxidation of colectral biopsies was performed by incubating them at 37°C for 1 hr in 1 ml of phosphate-buffered saline, to which EDTA, H_2O_2 and Fe(II) were added, in that order, to achieve the final concentrations given above. At the end of the incubation period, biopsies were processed and analysed immediately, as described below. Controls were paired biopsies taken from the same site and patient which remained frozen until processing and analysis in parallel with the tissue samples subjected to the peroxidising system.

2.5.5 Preparation of prostaglandin E_2

PGE_2 (1 mg) was dissolved in 60 µl of chloroform/methanol solution. 15 µl (0.25 mg) of this solution was then added to 3 ml of the chloroform/methanol mix and the samples processed in the same manner as linoleate and linolenate and the rectal biopsies (as outlined below). This concentration is approximately that produced by a biopsy of a patient with active UC in 24 hr (22 ng/mg tissue)[86].

2.5.6 Preparation of extracts

Tissue biopsies were thawed at room temperature and were blot dried and weighed as soon as they had defrosted. In a typical experiment, samples (average weight 5-10 mg) were added to 3 ml of the chloroform/methanol mix (2:1-v/v) and lipid/chloroform extracts were obtained by vortex mixing for 5 min followed by rotary mixing for a further 1 hr The biopsies were then removed and the solvent removed at ambient temperature under nitrogen gas. The lipid/chloroform extracts were then reconstituted in 2.00 ml of ethanol.

2.5.7 Reduction and dehydration

To the ethanol-reconstituted extracts was added 2 ml of the $NaBH_4$ solution and the mixture was heated at 40°C for 30 min. The sample was then allowed to cool to room temperature followed by slow addition of alcoholic H_2SO_4 (2 ml) and the sample heated for a further 30 min at 60°C. The sample was then analysed for conjugated trienes and tetraenes.

The model PUFA esters methyl linoleate and methyl linolenate were reduced and dehydrated in a similar manner.

2.5.8 INSTRUMENTATION : Second-derivative spectrophotometry

1. *In vitro* studies: Samples were analysed for conjugated triene and tetraene signals using a Shimadzu UV-2100 UV-visible spectrophotometer. Samples were scanned over the wavelength range 250-360 nm at medium scan speed with an ethanol blank and 2D spectra calculated using $\Delta\lambda$ (nm) = 5.

2. Lipid peroxidation product measurement in colonic samples: analysis of all samples was performed on a Philips PU 8740 spectrometer. The extracts were scanned over a wavelength range of 200-400 nm and spectra recorded using a scan-rate of 50 nm/min. All measurements were performed against a computer-memorised solvent blank.

2.5.9 Statistics

The Wilcoxon test was used to assess the effect of the peroxidising system on the detection of lipid peroxide in colonic tissue samples. Differences amongst groups (control, active and inactive UC) were analysed using analysis of variance on log_{10}- transformed 2D minima using Fisher's population limited standard deviation (PLSD) to assess the differences between groups.

2.6 Molecular Nature of Catalytic, Non-Transferrin-Bound-Iron in SF from Patients with Inflammatory Joint Diseases: A High Field NMR Study

2.6.1 Preparation of reagents

Disodium nitrilotriacetate, 3-(2-pyridyl)-5,6-bis(4-phenylsulphonic acid)-1,2,4-triazine (ferrozine, monosodium salt) and iron-free transferrin (apotransferrin) were used without further purification. Iron(III)-monocitrate was checked for purity prior to use by electronic absorption spectrophotometry[114]. Its spectrum indicated that basic and polymeric iron(III)-citrate species were absent from the sample supplied.

The 400 MHz single-pulse ^{1}H NMR spectrum of a 4.07 g dm^{-3} aqueous solution of apotransferrin containing 22% (v/v) $^{2}H_2O$ and treated with 1.56 x 10^{-3} mol dm^{-3} trisodium citrate contained relatively broad, weakly-intense signals located at 1.93, 2.04, and 2.08 ppm (singlets), 3.14 ppm (apparent doublet), and 3.265 and 3.66 ppm (singlets) in addition to the citrate resonances centred at 2.65 ppm. The singlet resonance at 1.93 ppm is attributable to an acetate impurity, and those at 3.265 and 3.66 ppm (with relative intensities of 1 and 2 respectively) are assignable to the acetate and ethylenic protons respectively of EDTA, a chelator presumably employed by the manufacturer to remove iron(III) from the protein.

2.6.2 Synovial fluid and serum samples

Knee-joint synovial fluid samples were drawn into clear sterile plastic or heparinized tubes for therapeutic purposes from rheumatoid (n=19) or osteoarthritic patients (n=5) with inflamed knees. These samples were centrifuged immediately to remove cell and debris (2,500 r.p.m. for 15 min) and the supernatants were either analysed within a few hours after collection, or stored at -70°C for a maximum duration of 14 days. Incubation of a 2.00 x 10^{-3} mol dm^{-3} aqueous citrate solution (pH 7.00) in the heparinized tubes, or those containing no preservative for a period of 14 days at ambient temperature gave a negative spectrophotometric test for iron with the ferrozine reagent in the presence of 1.00 x 10^{-4} mol dm^{-3} ascorbate as reductant, demonstrating no detectable iron ion contamination of the

heparin preservative and no leaching of iron (as Fe(II) or Fe(III)) from the internal surfaces of the tubes utilised.

Samples of human blood serum (prepared by allowing freshly drawn non-heparinized blood to clot) and heparinized plasma obtained from rheumatoid patients and healthy adult volunteers were centrifuged, stored and analysed as described above. For some rheumatoid patients, matched serum and synovial fluid samples were obtained at the same times of collection.

2.6.3 NMR Measurements

Proton NMR measurements were carried out on a JOEL JNM-GSX 500 (University of London Intercollegiate Research Services (ULIRS), Biomedical NMR Centre, Birkbeck College, London.) or Bruker WH 400 (ULIRS, Queen Mary and Westfield College, London.) spectrometers operating in quadrature detection mode at 500 or 400 MHz respectively for ^{1}H. The Bruker WH 400 spectrometer was equipped with a Bruker Aspect 3000 data system. All spectra were recorded at a probe temperature of 293 K.

Typically, 0.60 ml of the supernatant obtained from centrifuged synovial fluid or serum samples (either freshly collected or stored at -70, -20 or 4°C for variable periods of time) were placed in 5mm diameter NMR tubes, and 0.07 ml of $^{2}H_2O$ was added to provide a field frequency lock. High-field ^{1}H NMR spectra of synovial fluid and serum supernatants were obtained using the JOEL JNM-GSX 500 spectrometer. The broad protein resonances were suppressed by the Hahn spin-echo sequence (D[90°x-t-180°y-t-collect])[45], which was repeated 128-848 times with t=60 ms. The spectral width for Hahn spin-echo spectra was 5,100 Hz. The intense water signal was suppressed either by continuous secondary irradiation at the water frequency or by pre-saturation via gated decoupling during the delay between pulses. Chemical shifts were referenced to external sodium 3-(trimethylsilyl) propane-1-sulphonate (TSP, δ=0.00 ppm). The methyl group resonances of alanine (1.487 ppm), lactate (1.330 ppm) or valine (1.050 ppm) served as secondary internal references.

Storage of a 2.00 x 10^{-3} mol. dm^{-3} solution of citrate in ^2H_2O in several of the NMR tubes employed for 12 days gave a negative ferrozine test in the presence of 1.00 x 10^{-4} mol dm^{-3} ascorbate and did not induce any increase in the citrate proton resonance line-widths throughout this period.

One dimensional single-pulse spectra of synovial fluid ultrafiltrates were acquired using a Bruker WH 400 spectrometer. Each spectrum corresponded to 77-128 free induction decays (FIDS), using 6,688 data points, 30-40° pulses and a 3 s pulse repetition rate. The large water signal was suppressed by presaturation via gated decoupling during the delay between pulses. Spectra were referenced to internal TSP with the alanine, lactate or valine methyl group signals acting as secondary internal references as above. Where appropriate, quantitative measurements on these ultrafiltrates were conducted by adding a fixed microlitre volume of a standard solution of TSP in ^2H_2O (5.46 x 10^{-2} mol dm^{-3}) to the samples prepared as described above.

Line-widths ($\Delta\nu_{1/2}$) of the citrate proton resonances in ^1H Hahn spin-echo NMR spectra of rheumatoid or osteoarthritic synovial fluid were measured by counting the number of data points between the half-heights of each of the four peaks present in this metabolite's characteristic AB coupling pattern, and converting these values to Hz (0.18 or 0.37 Hz per data point).

2.6.4 Kinetic measurements

The rate of transfer of iron(III) from citrate to desferrioxamine was followed spectrophotometrically in 0.10 mol dm^{-3} $NaNO_3$ at pH 8.00 at 25.0 °C.

2.7 The Role of N-Acetylcysteine in Protecting Synovial Fluid Biomolecules against Radiolytically-Mediated Oxidative Damage: A High Field Proton NMR Study

2.7.1 Preparation of samples - inflammatory knee-joint synovial fluid

Knee-joint synovial fluid samples were drawn into clear sterile plastic tubes for therapeutic purposes from the total of 10 rheumatoid arthritis patients (American Rheumatism Association criteria) with inflamed knees and associated effusions. These samples were centrifuged immediately to remove cells and debris (2,500 r.p.m. for 20 min) and the supernatants either analysed within a few hours after collection, or stored at 4°C for a duration of 18 hr.

Synovial fluid supernatants (0.60 ml, n=5) were each treated with μl liquots of an aqueous stock solution of N-acetyl-L-cysteine to yield 1.00 and 3.00 x 10^{-3} mol dm^{-3} concentrations of added thiol. Similarly, 0.60 ml portions of further synovial fluid supernatant samples (n=5) were each treated with μl aliquots of an aqueous L-cysteine stock solution to give final added thiol concentrations of 1.00, 2.00 and 5.00 x 10^{-3} mol dm^{-3}. These samples were equilibrated at 4°C for a period of 18 hr prior to gamma-radiolysis and ^1H NMR analysis. Corresponding control samples containing no added N-acetyl-L-cysteine or L-cysteine were also stored in this manner.

2.7.2 Gamma-radiolysis of synovial fluids and aqueous thiol solutions

Synovial fluid samples were subjected to gamma-radiolysis in the presence of atmospheric O_2 using a ^{60}Co source (Department of Immunology, The Royal London Hospital Medical College) at a total dose level of 5.00 kGy (dose rate 288.6 Gy hr^{-1}). Corresponding synovial fluids 'spiked' with increasing concentrations of N-acetyl-L-cysteine or L-cysteine, together with phosphate-buffered 2.00 x 10^{-2} mol dm^{-3} aqueous solutions of N-acetyl-L-cysteine and L-cysteine (pH 7.00) were similarly irradiated.

Under these experimental conditions, the major primary radiolytic products of water are ·OH (G=2.7), $e^-_{(aq.)}$ (G=2.7) and H· (G=0.5), (equation 2.4), where the G value denotes the 10^{-6} mol dm^{-3} concentration of product generated per 10 Gy dosage. In the presence of atmospheric O_2, radiolytically-generated aquated electrons ($e^-_{(aq.)}$) are converted to $O_2^{\cdot -}$ (equation 2.5).

$$H_2O \rightarrow \cdot OH, e^-_{(aq.)}, H\cdot, H_2, H_2O_2, H_3O^+ \qquad (2.4)$$

$$e^-_{(aq.)} + O_2 \rightarrow O_2^{\cdot -} \qquad (2.5)$$

2.7.3 NMR measurements

Proton NMR measurements on control and thiol-treated synovial fluid samples prior and subsequent to gamma-radiolysis were conducted on a JOEL JNM-GSX 500 (University of London Intercollegiate Research Services (ULIRS), Biomedical NMR Centre, Birkbeck College, London) spectrometer operating in quadrature detection mode at 500 MHz for ^1H. All spectra were recorded at a probe temperature of 293 K.

Typically, 0.60 ml of sample was placed in a 5-mm diameter NMR tube and 0.07 ml of ^2H_2O was added to provide a field frequency lock. The broad protein resonances were suppressed by the Hahn spin-echo sequence (D[90°x-t-180°y-t-collect]), which was repeated 128 times with t=60 ms. The spectral width for these Hahn spin-echo spectra was 5,100 Hz. The intense water signal was suppressed by pre-saturation via gated decoupling during the delay between pulses. Chemical shifts were referenced to external sodium 3-trimethylsilyl-(2,2,3,3-$^2H_4$)-propane-1-sulphonate (TSP, δ = 0.00 ppm). The methyl group resonances of alanine (1.487 ppm), lactate (1.330 ppm) or valine (1.050 ppm) served as secondary internal references in biofluid spectra.

One dimensional, single-pulse ^1H NMR spectra of control and gamma-irradiated L-cysteine solutions (containing 10.4% (v/v) added ^2H_2O) were also obtained on the JOEL JNM-GSX 500 spectrometer using a pulse angle of 30-40° and a total delay between pulses of 3 s to allow full spin-lattice (T_1) relaxation of the protons in the samples investigated.

Each spectrum corresponded to 49 free induction decays (FIDs) using 32,768 data points. The intense water signal was suppressed by pre-saturation via gated decoupling during the delay between pulses. Spectra were referenced to external TSP. ^2H_2O (0.07 ml) was added to 0.60 ml aliquots of control and gamma-irradiated N-acetyl-L-cysteine solutions and single-pulse ^1H NMR spectra of these samples were acquired using a Bruker WH 400 spectrometer (ULIRS facility, Queen Mary and Westfield College, London). Each spectrum corresponded to 65 FIDs using 6,557 data points, 30-40° pulses and a 3 s pulse repetition rate. The large water signal was suppressed as described above. Spectra were recorded at ambient probe temperature (293 K) and also referenced to external TSP.

CHAPTER 3

LIPID PEROXIDATION

3.1 Introduction

3.1.1 Lipid peroxidation

The involvement of chemically-reactive oxygen radical species in the pathogenesis of inflammatory joint diseases has been well documented. Much of the toxicity produced by increased $O_2^{\cdot -}$ and H_2O_2 has been attributed to the production of the highly reactive ·OH radical[1-3].

Radical species are extremely difficult to measure directly in biological materials and particularly *in vivo*. Direct measurements rely on complex methods such as electron spin resonance spectroscopy or native chemiluminesence[9]. In view of the high cost, these techniques are not usually available in many laboratories.

PUFAs, DNA and carbohydrates are all susceptible to free radical attack, particularly by ·OH radical. The products of these reactions are becoming better characterised and are now widely used as evidence for free radical-mediated oxidative damage occurring *in vivo*.

In rheumatoid arthritis, the excess production of ·OH radical via the Fe^{2+}-mediated Fenton reaction, postulated to occur in the synovium leads to the denaturation of hyaluronic acid, a high-molecular-mass polysaccharide which usually maintains the viscosity of synovial fluid. This gives rise to exaggerated erosion of cartilage in the inflamed rheumatoid joint. PUFAs are particularly vulnerable to free radical attack. This oxidative damage is termed lipid peroxidation, and it causes a reduction in membrane fluidity and permeability[10].

Perhaps one of the most promising techniques for the assessment of oxygen radical activity in patients with inflammatory joint diseases is the identification of intermediates in and so-called 'end-products' of the process of lipid peroxidation. Lipid peroxidation has been broadly defined as the 'oxidative deterioration of polyunsaturated lipids', i.e. lipids that contain two or more carbon-carbon double bonds.

3.1.1.1 Chemistry of lipid peroxidation

PUFAs are particularly sensitive to oxidative damage due to the facile abstraction of an allylic hydrogen atom from their *bis*-allylic methylene (-CH=CH-CH_2-CH=CH-) groups by radical species of sufficient reactivity (Figure 3.1)[19]. The reaction of ·OH radical with PUFAs is illustrated in figure 3.1.

The ·OH radical readily initiates this oxidative degradation by combining with the abstracted hydrogen atom (H·) to form water. The carbon-centred radical is stabilised by a molecular rearrangement and interacts with dioxygen to yield a diene peroxyl radical (ROO·) which in turn can abstract a hydrogen atom from an adjacent PUFA (propagation) to form a conjugated lipid hydroperoxide. This attack generates a further lipid radical, leading to a self-perpetuating, autocatalytic chain reaction. The primary products formed by the autoxidation of PUFAs are *cis,trans (c,t)*- and *trans,trans (t,t)*- diene hydroperoxides, as illustrated in Figure 3.2 for linoleic acid[54].

Despite the relative stability of conjugated diene lipid hydroperoxide species at biologically-relevant temperatures, their degradation to a wide variety of further lipid peroxidation 'end-products' is catalysed by traces of redox-active transition metal-ions (i.e. those of iron and copper)[55]. These secondary and tertiary end-products consist of saturated and unsaturated aldehydes, di- and epoxyaldehydes, lactones, furans, ketones, oxo- and hydroxy-acids, and saturated and unsaturated hydrocarbons[56].

Identification and quantification of one or more of these end-products resulting from the ·OH radical-mediated peroxidation of polyunsaturated lipids can be utilised to form the basis of a series of potential methods for the assessment of reactive oxygen radical activity in the inflamed rheumatoid joint. Moreover, the autocatalytic, self-perpetuating nature of the process allows the employment of analytical techniques of lowered sensitivity[57]. In view of its autocatalytic nature, only a small quantity of ·OH radical or alternative RORS is required to trigger the process.

Figure 3.1

THE AUTOXIDATION OF PUFA BY FREE RADICAL CHAIN MECHANISM INVOLVING THREE STAGES

INITIATION :

Unsaturated lipid containing 18:2

$+ \cdot OH \longrightarrow$

resonance hybrid

$+ H_2O$

PROPAGATION :

$$R^{\cdot} + O_2 \longrightarrow ROO^{\cdot}$$

$$ROO^{\cdot} + RH \longrightarrow ROOH + R^{\cdot}$$

TERMINATION :

$$R^{\cdot} + R^{\cdot} \longrightarrow R_2$$

$$R^{\cdot} + {}^{\cdot}O_2R \longrightarrow RO_2R$$

$$ROO^{\cdot} + {}^{\cdot}O_2R \longrightarrow RO_2R + O_2$$

Figure 3.2

PEROXIDATION OF LINOLEIC ACID WITH THE FORMATION OF *cis,trans* AND *trans, trans* DIENE CONJUGATES[37].

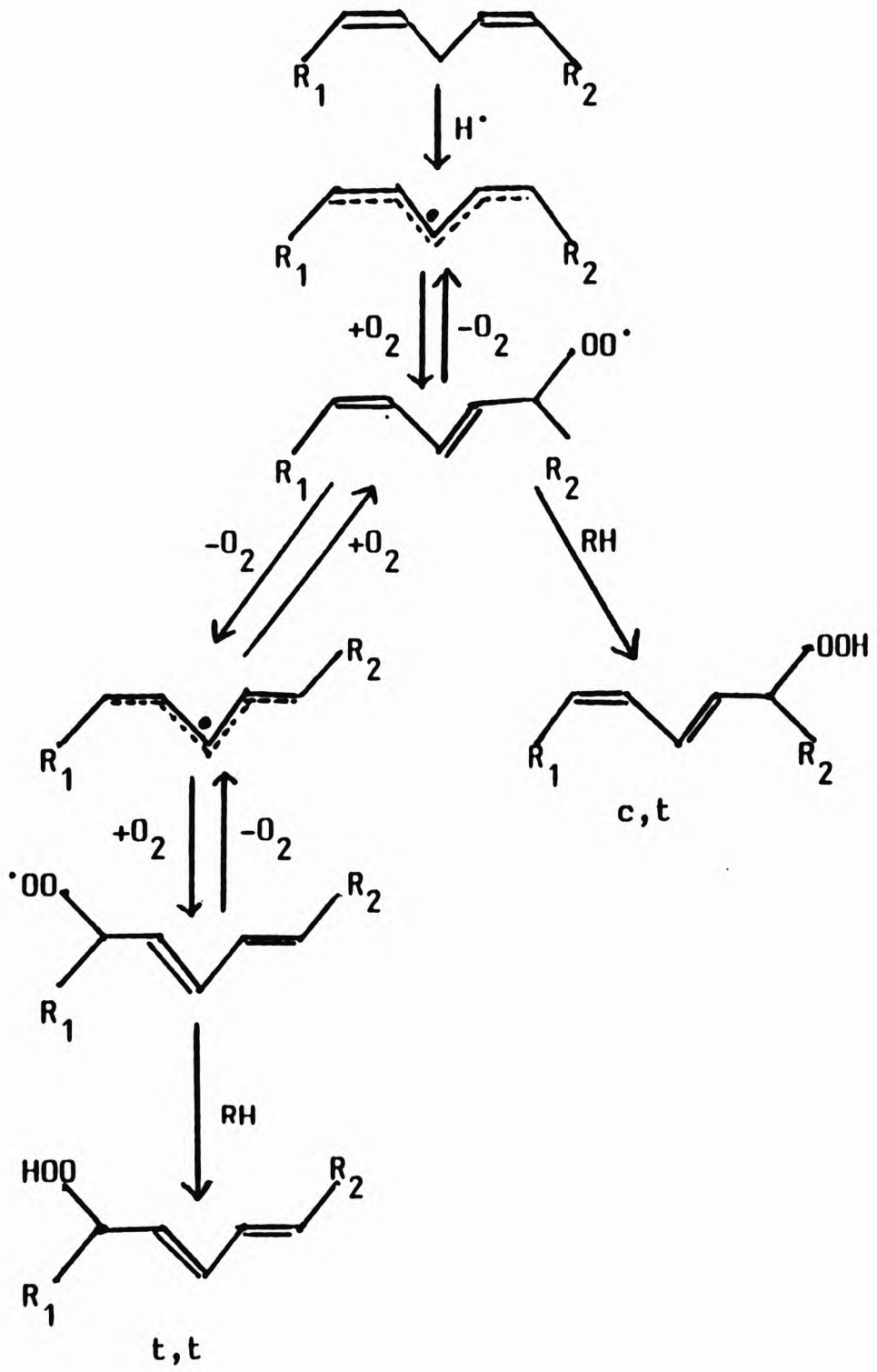

$R_1 = C_5H_{11}$

$R = (CH_2)_7COOH$

3.1.1.2 Measurement of lipid peroxidation

The peroxidation-mediated rearrangement of double bonds present in PUFAs leads to a mixture of conjugated diene species. A new procedure for monitoring the course of free radical damage to PUFAs is the identification and quantification of such conjugated diene adducts (including diene hydroperoxides) in appropriate extracts of human body fluids or tissues. These species, and the conjugated ketodienes arising from their degradation, have UV maxima at various wavelengths in the 230-280 nm range[58-60].

However, although lipids and their corresponding peroxidation products are readily isolated from biological materials by a simple chloroform extraction procedure, direct measurement of absorbance at a specified wavelength in this region of the spectrum is of limited practical utility since the absorption maxima of the conjugated diene species appear as a poorly defined shoulder superimposed on the high absorbance of other endogenous components present in the lipid/chloroform extracts. The method is extremely useful in studies upon pure lipids, since it measures an early stage of the peroxidation process, but it often cannot be used directly on biological materials since many other UV-absorbing artefacts are present. These artefacts give rise to high background absorbance values that hamper spectrophotometric measurements[19]. Conjugated diene absorption maxima can be resolved and clearly identified by monitoring minima present in corresponding second-derivative (2D) spectra of the extracts (absorption maxima in zero-order spectra appear as absorption minima in the 2D spectrum).

Corongiu *et. al.*[61] have previously applied 2D spectrophotometry to monitor the time-dependent production of *c,t*- (λ_{max} 242 nm) and *t,t*- (λ_{max}232 nm) diene conjugates of microsomal PUFAs following exposure of rats to carbon tetrachloride (CCl_4). Previous studies using chemical model systems have established that autoxidation of linolenic or arachidonic acid results in the production of *c,t*- and *t,t*- conjugated diene hydroperoxides that have λ_{max} values of 236 and 232.5 nm respectively[62-63].

3.1.2 The thiobarbituric acid test

The reaction of thiobarbituric acid (TBA) with aerobically incubated tissue homogenate to give a distinct red chromogen was first described by Kohn and Liversedge in 1944. The compound reacting with TBA was shown to be a 3-carbon atom molecule derived from the lipid component of tissue. The TBA test has been frequently used as an indicator of lipid peroxidation in biological matrices[64]. During lipid peroxidation, the primary products generated are a complex mixture of peroxides, which are then further degraded to produce a range of products including carbonyl compounds e.g. malondialdehyde (MDA) (Figure 3.3)[65-66].

The TBA test involves the reaction of aldehydes in the sample with TBA under acidic conditions (equation 3.1), to produce a distinct pink colour which has generally been attributed to the chromophoric 2:1 TBA-MDA adduct, a species that absorbs light at a wavelength of 532 nm ($E=1.59 \times 10^5\ M^{-1}\ cm^{-1}$)[67].

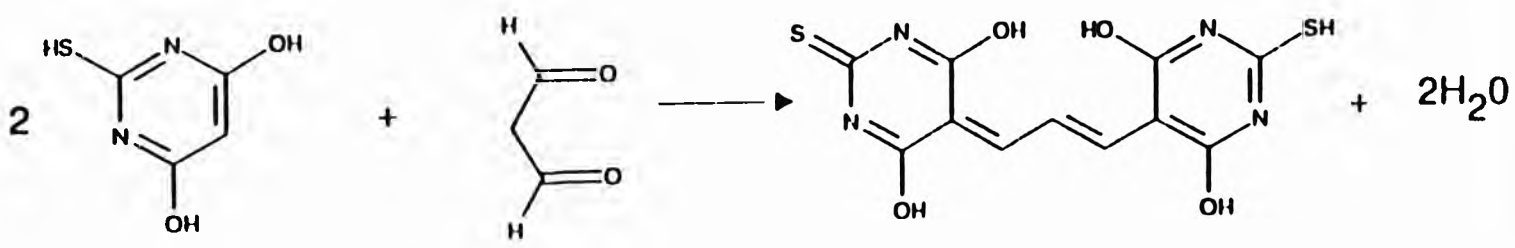

Although the 2:1 TBA-MDA adduct is considered to be the major contributor to the chromogen, it is now clear that a number of other endogenous species, i.e. unsaturated carbonyl compounds, biliverdin and other aldehydes also give products that absorb at, or at wavelengths close to 532 nm on heating with TBA[68]. Exposure of several carbohydrates

and amino acids to ·OH radical also produces TBA-reactive materials. It is also important to note that since only a small amount (ca. 1-2%) of the lipid peroxidation end-products is actually MDA, a large quantity of the chromogen produced in the TBA test is derived from the decomposition of lipid hydroperoxides during the stringent acid/heating stage of the assay. Hence, although the TBA test is a simple and relatively sensitive analytical method for the assessment of reactive oxygen radical-induced oxidative damage to PUFAs, it has a low specificity and cannot be utilised as a reliable marker of lipid peroxidation since it has a very low specificity.

This study describes the application of 2D electronic absorption spectrophotometry to the analysis of isomeric conjugated diene species and TBA-reactive material present in the synovial fluid of arthritic patients, a potential probe for the measurement of RORS generated during hypoxic-reperfusion injury occurring in the inflamed rheumatoid joint. The 2D spectrophotometric technique has not previously been applied to the TBA test and serves to overcome its inherent lack of specificity, allowing the direct determination of MDA derived from lipid hydroperoxides[69].

Figure 3.3

FORMATION OF MALONDIALDEHYDE FROM A TRIENE SYSTEM.

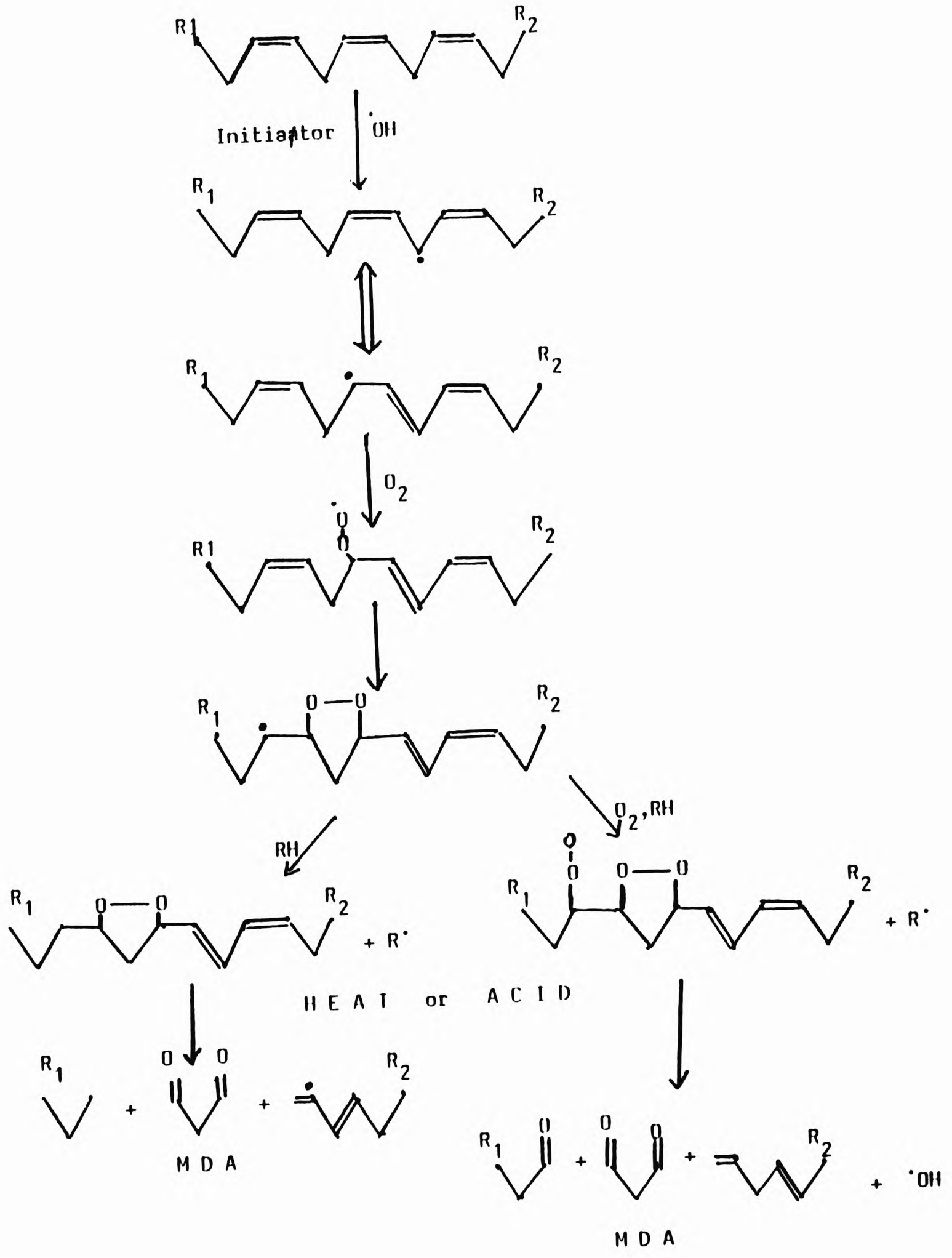

3.2 Results

3.2.1 Peroxidation of commercially-available fatty acids

3.2.1.1 Detection of conjugated dienes

Figure 3.4 shows the resulting zero-order and corresponding 2D absorption spectra of samples of linoleic acid which were obtained (i) after being allowed to autoxidise at ambient temperature for a period of 24 hr, and (ii) after incubation at ambient temperature for 24 hr. following exposure to an Fe(II)/EDTA/H_2O_2 system. The development of a number of over-lapping absorption bands in the 220-255 nm region of the zero-order spectra of both samples indicates the formation of two or more classes of conjugated diene lipid hydroperoxide species. The increased absorbance of the Fe(II)/EDTA/H_2O_2-treated sample in this wavelength region demonstrates the ability of this system to trigger and consequently enhance the lipid peroxidation process.

As expected, the intensity of the overlapping conjugated diene absorption band is greater in the sample exposed to the catalytic Fenton system. These overlapping absorption maxima are readily resolved by the recording and subsequent examination of the corresponding 2D spectra of these samples. The 2D spectra shown in Figure 3.4 exhibit minima located at 226, 234 and 243 nm, which correspond to conjugated diene absorption maxima in the zero-order spectra. The 2D minima located at 234 and 243 nm are conceivably attributable to *t,t*- and *c,t*-conjugated diene species respectively (e.g. hydroperoxydienes and/or hydroxydienes).

A corresponding spectrophotometric analysis of the diene-conjugated species derived from both autoxidised and Fe(II)/EDTA/H_2O_2-peroxidised linolenic acid yielded similar results.

Figure 3.5 shows zero-order and corresponding 2D absorption spectra of linolenic acid subjected to autoxidation in air at ambient temperature or following exposure to the catalytic Fe(II)/EDTA/H_2O_2 system obtained 24 hr after incubation at ambient temperature. The 2D spectra shown in Figure 3.5 exhibit minima located at 229, 237 and 245 nm, which

correspond to conjugated diene absorption maxima in zero-order spectra. The 2D minima located at 237 and 245 nm are conceivably attributable to *t,t*- and *c,t*- conjugated diene species respectively.

A comparison of these data with those obtained in Figure 3.4 demonstrates that linolenic acid is peroxidised at a faster rate than linoleic acid, a reflection of a higher degree of unsaturation in the former PUFA. The relative rates of peroxidation of oleic, linoleic and linolenic acids which have 1, 2 and 3 double bonds respectively have been shown to be in the ratio 1:12:25[50] .

Corongiu *et. al.*[61] found that the autoxidation of arachidonic acid in air gave rise to two conjugated diene signals at 232 and 242 nm which were also identified in a 2D spectrum under similar experimental conditions. Although the origin of the 2D signal located at 226 nm is at present unclear, it may be attributable to a further isomeric conjugated diene species. The difference in the 2D absorption spectra observed in this study and those of Corongiu *et. al.*[61] are likely be due to the higher resolution of overlapping conjugated diene absorption bands obtained here, revealing a series of isomers formed in this chemical model system. However, the difference in the chemical nature of the substrates employed may also account for these differences in part or in whole. For example, it has been reported that methyl linoleate hydroxydiene has a $\lambda_{max.}$ value of 233 nm ($E = 2.74 \times 10^4\ M^{-1}cm^{-1}$), whereas methyl linolenate hydroxydiene has one located at 235 nm ($E = 2.44 \times 10^4\ M^{-1}\ cm^{-1}$)[70].

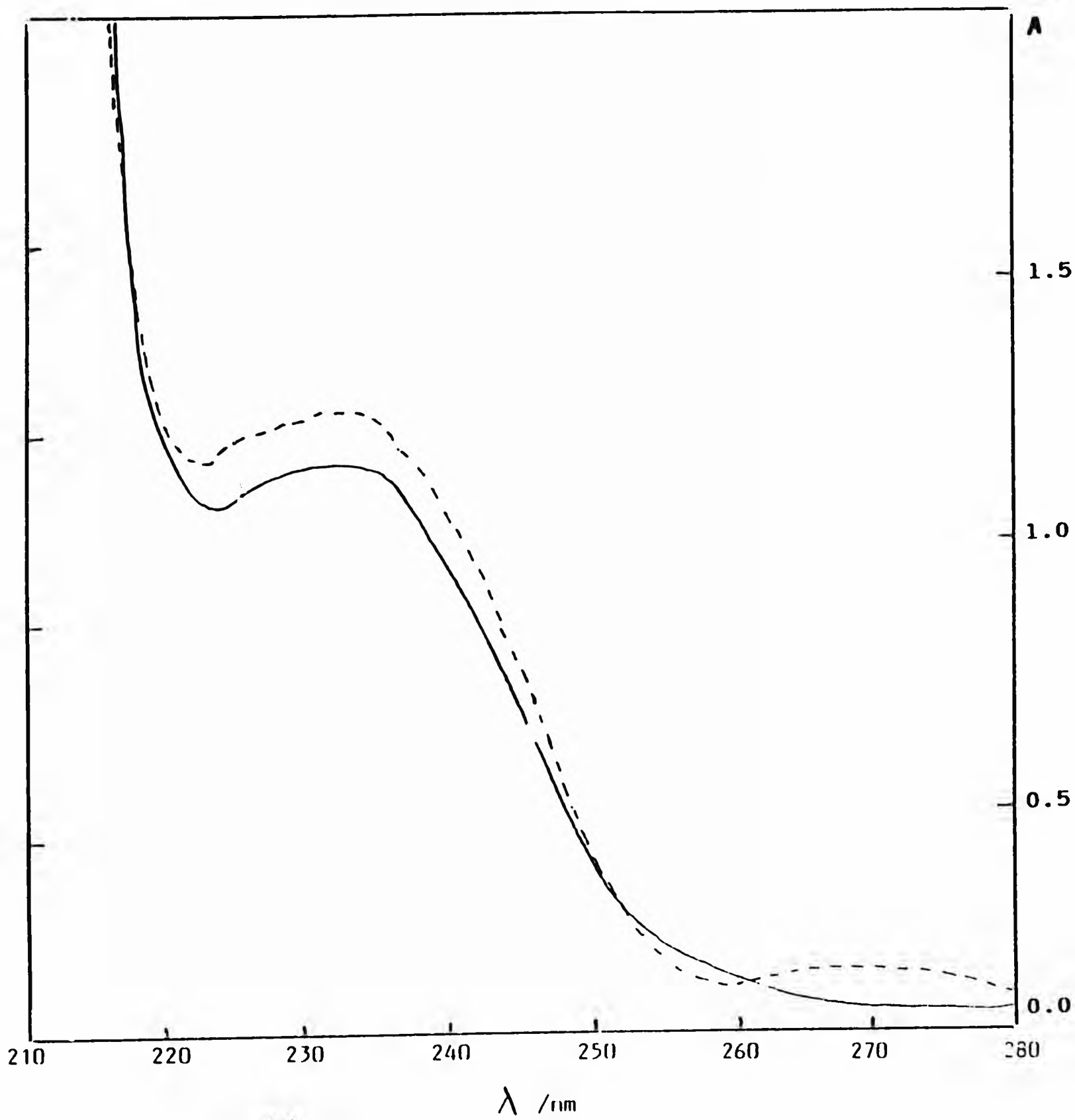

FIGURE 3.4 (a)

Zero-order electronic absorption spectra of cyclohexane-reconstituted chloroform extracts of linoleic acid obtained subsequent to autoxidation in air at ambient temperature (——) or exposure to a catalytic Fe(II)/EDTA/H_2O_2 system (------) for a time period of 24 hr.

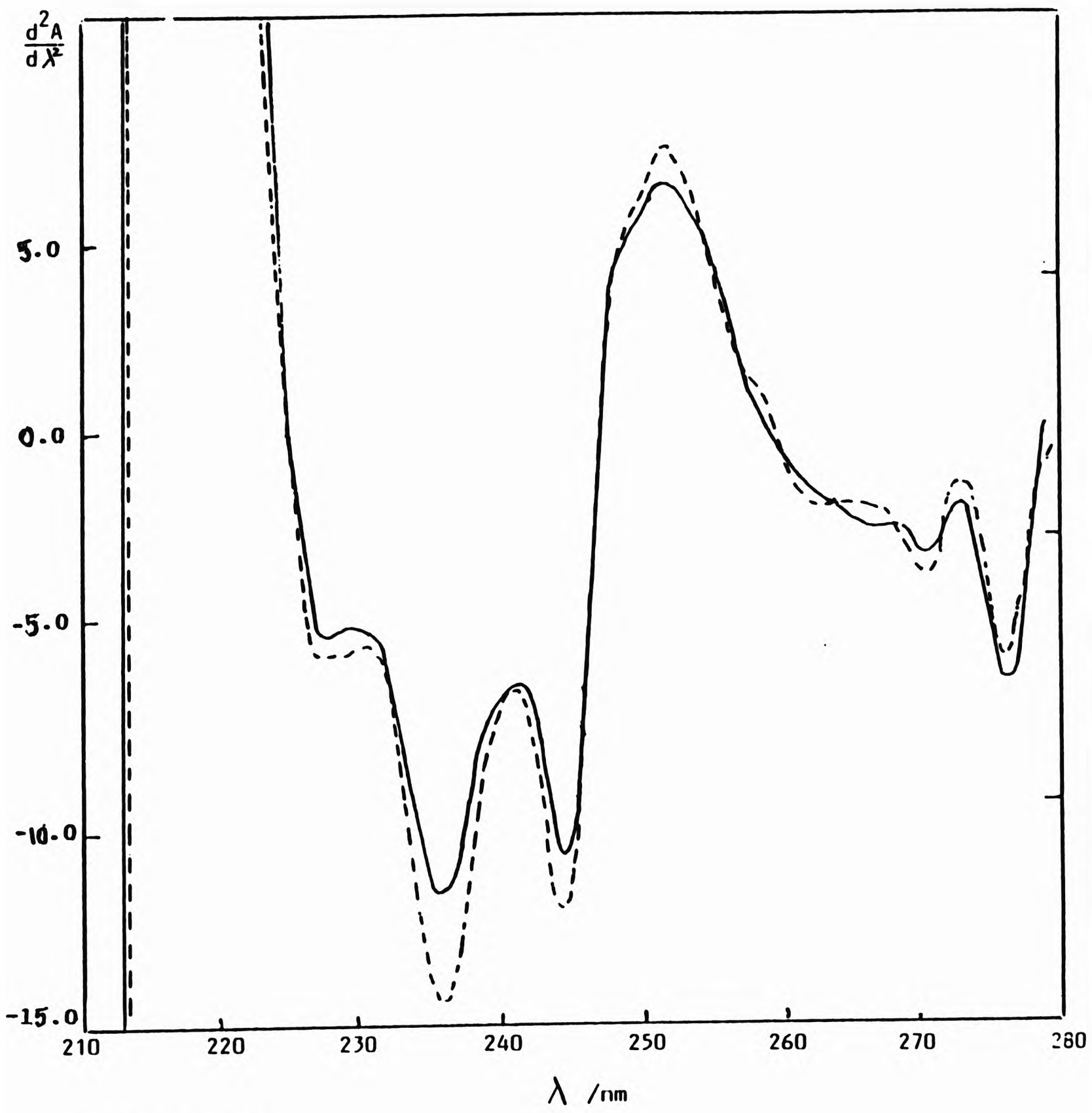

FIGURE 3.4 (b)

Second derivative (2D) electronic absorption spectra of cyclohexane-reconstituted chloroform extracts of linoleic acid obtained subsequent to autoxidation in air at ambient temperature (——) or exposure to a catalytic Fe(II)/EDTA/H_2O_2 system (------) for a time period of 24 hr.

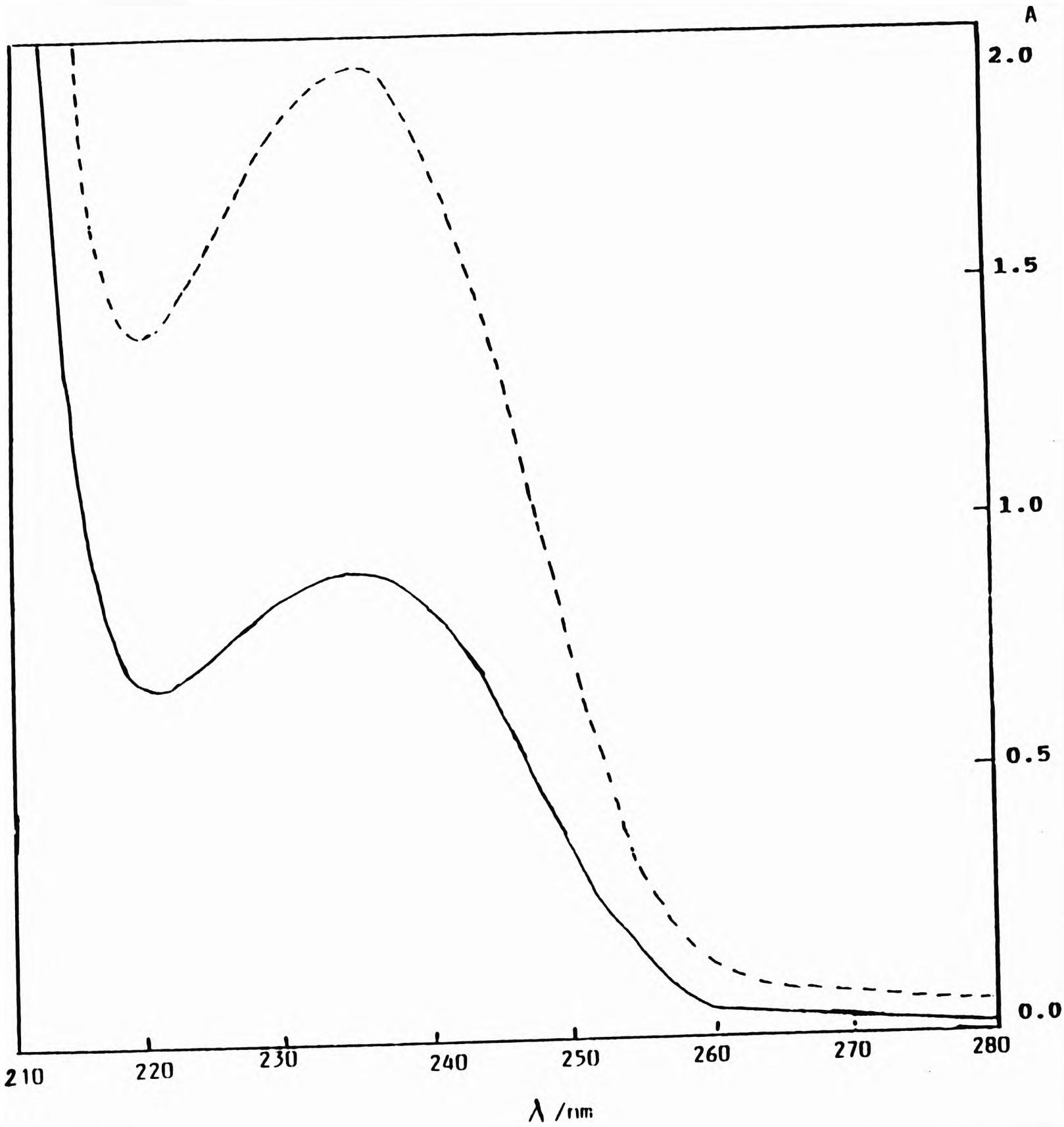

FIGURE 3.5 (a)

Zero-order electronic absorption spectra of cyclohexane-reconstituted chloroform extracts of linolenic acid obtained subsequent to autoxidation in air at ambient temperature (——) or exposure to a catalytic Fe(II)/EDTA/H_2O_2 system (------) for a time period of 24 hr.

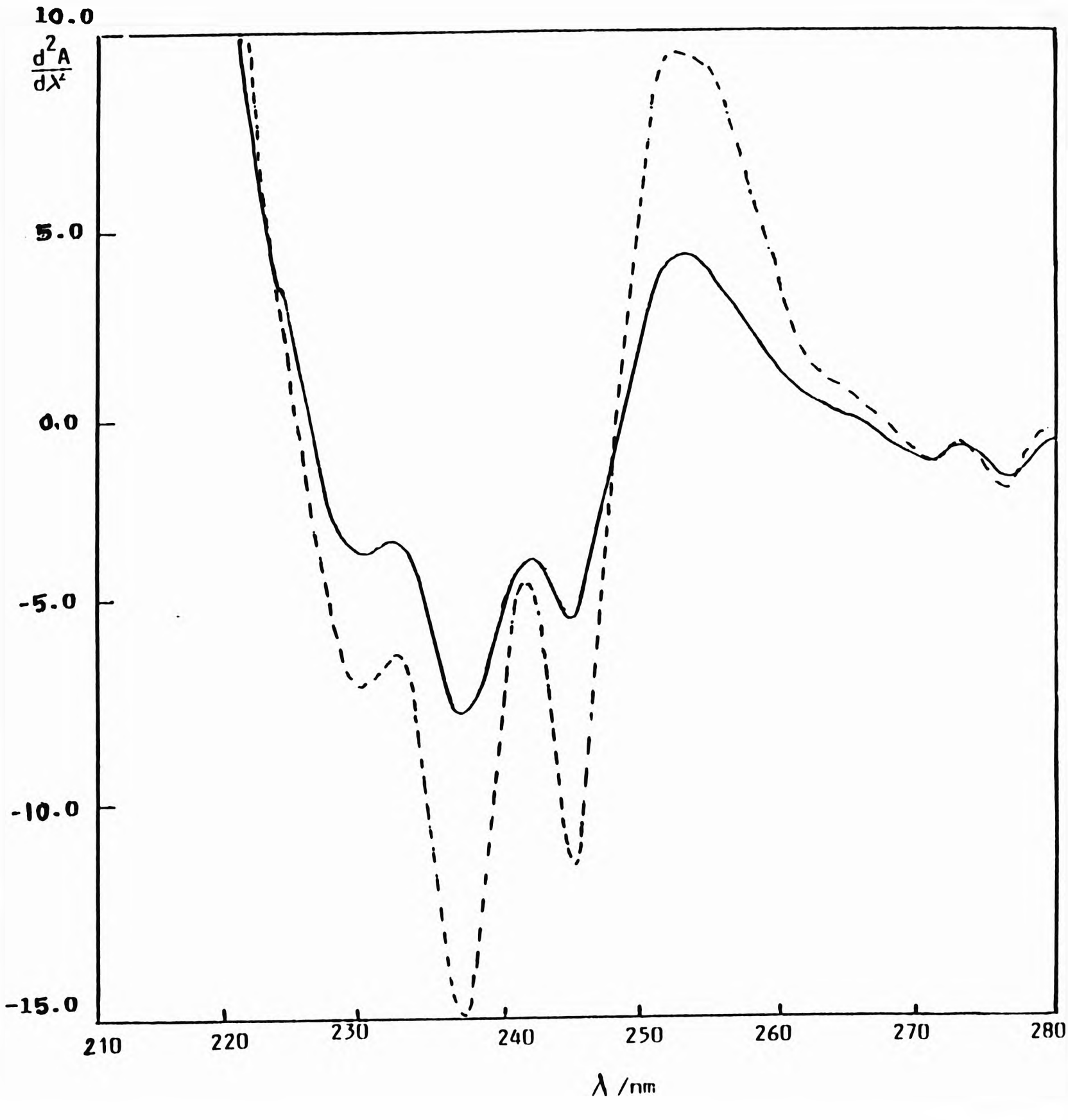

FIGURE 3.5 (b)

Second derivative (2D) electronic absorption spectra of cyclohexane-reconstituted chloroform extracts of linolenic acid obtained subsequent to autoxidation in air at ambient temperature (——) or exposure to a catalytic Fe(II)/EDTA/H_2O_2 system (------) for a time period of 24 hr.

3.2.1.2 Application of the thiobarbituric acid method to determine peroxidised fatty acids

The TBA-reactivity of peroxidised PUFAs was also evaluated by spectrophotometric analysis of chemical model systems. Figure 3.6 exhibits zero-order and corresponding 2D electronic absorption spectra which were obtained after allowing both control and Fe(II)/EDTA/H_2O_2-treated samples of linoleic acid to react with TBA under acidic conditions. The 2D spectrum of the sample exposed to the Fe(II)/EDTA/H_2O_2 system exhibits relatively intense maxima centred at 453, 490 and 532 nm, whereas the control sample shows only very weak absorption at 453 nm. Although the lower-energy absorption band located at 532 nm in the former spectrum can be assigned to the TBA-MDA adduct (the MDA is largely derived from the breakdown of isomeric linoleic acid hydroperoxides during the stringent acid./heating stage of the assay), the origin of the 453 and 490 nm bands is unknown. However, they are likely to arise from the reaction of an alternative secondary oxidation product with TBA.

Zero-order and corresponding 2D electronic absorption spectra resulting from the reaction of control and Fe(II)/EDTA/H_2O_2-treated samples of linolenic acid with TBA are shown in Figure 3.7. The 2D spectrum of the peroxidised sample exhibits maxima located at 454, 492 and 532 nm. Comparison of the spectrum resulting from the Fe(II)/EDTA/H_2O_2-induced peroxidation of linolenic acid with that obtained from peroxidised linoleic acid (Figure 3.6) reveals striking differences. Firstly, for linolenic acid the 2D absorption band at 532 nm (attributable to the TBA-MDA adduct) is of far greater intensity than that at 492 nm, whereas for linoleic acid, the absorption band at 532 nm is less intense than the one centred at 490 nm. Secondly, the peroxidised sample of linolenic acid exhibits a much higher absorbance at 532 nm than that of linoleic acid, reflecting the higher concentration of lipid peroxides and free MDA produced from linolenic acid, a probable consequence of its relatively rapid peroxidation rate.

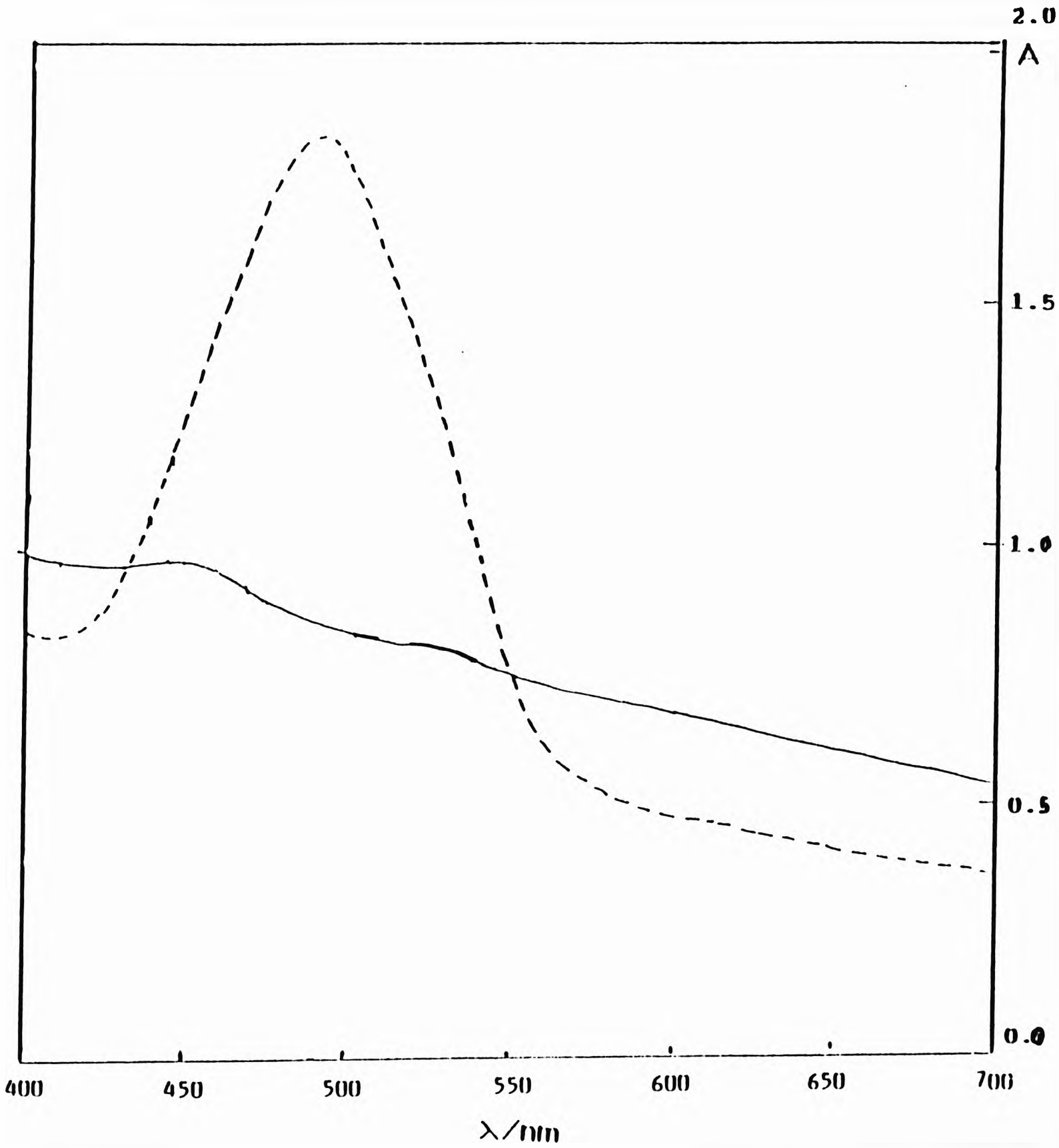

FIGURE 3.6 (a)

Zero-order electronic absorption spectra obtained after allowing both control(———) and Fe(II)/EDTA/H_2O_2- treated (-----) samples of linoleic acid to react with TBA under acidic conditions.

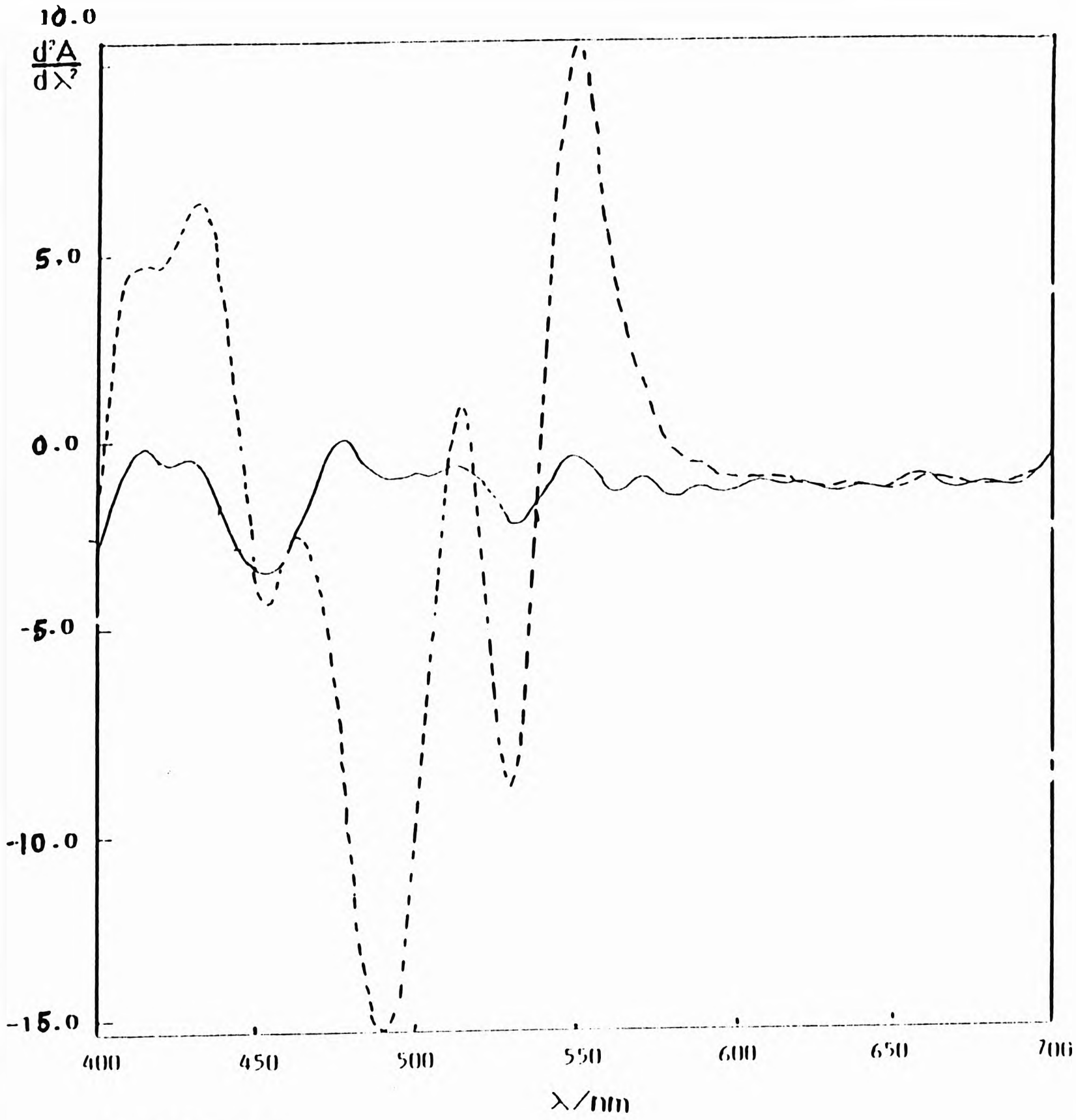

FIGURE 3.6 (b)

Second derivative (2D) electronic absorption spectra obtained after allowing both control(-) and Fe(II)/EDTA/H_2O_2- treated (-----) samples of linoleic acid to react with TBA under acidic conditions.

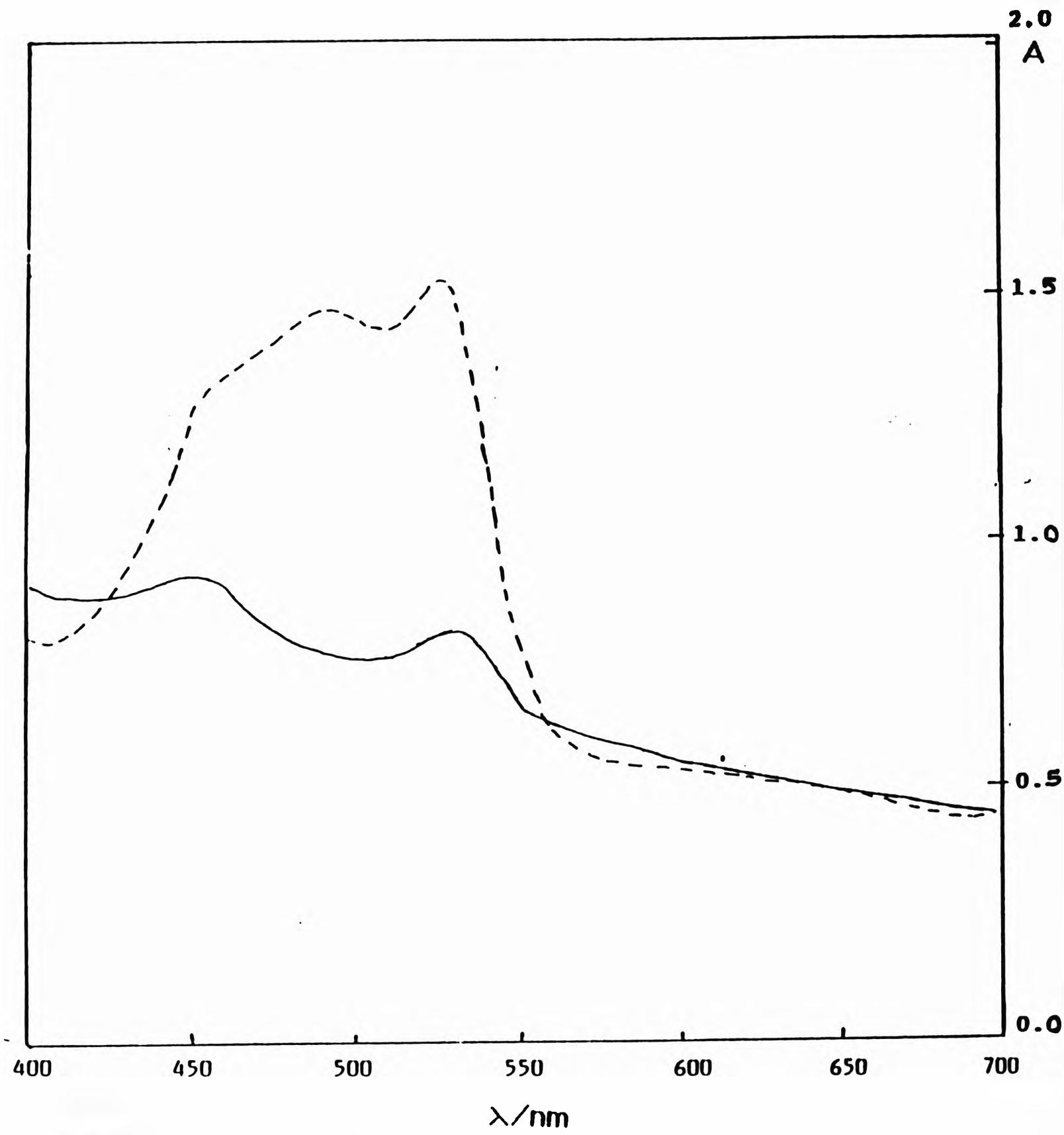

FIGURE 3.7 (a)

Zero-order electronic absorption spectra obtained after allowing both control (———) and Fe(II)/EDTA/H_2O_2- treated (-----) samples of linolenic acid to react with TBA under acidic conditions.

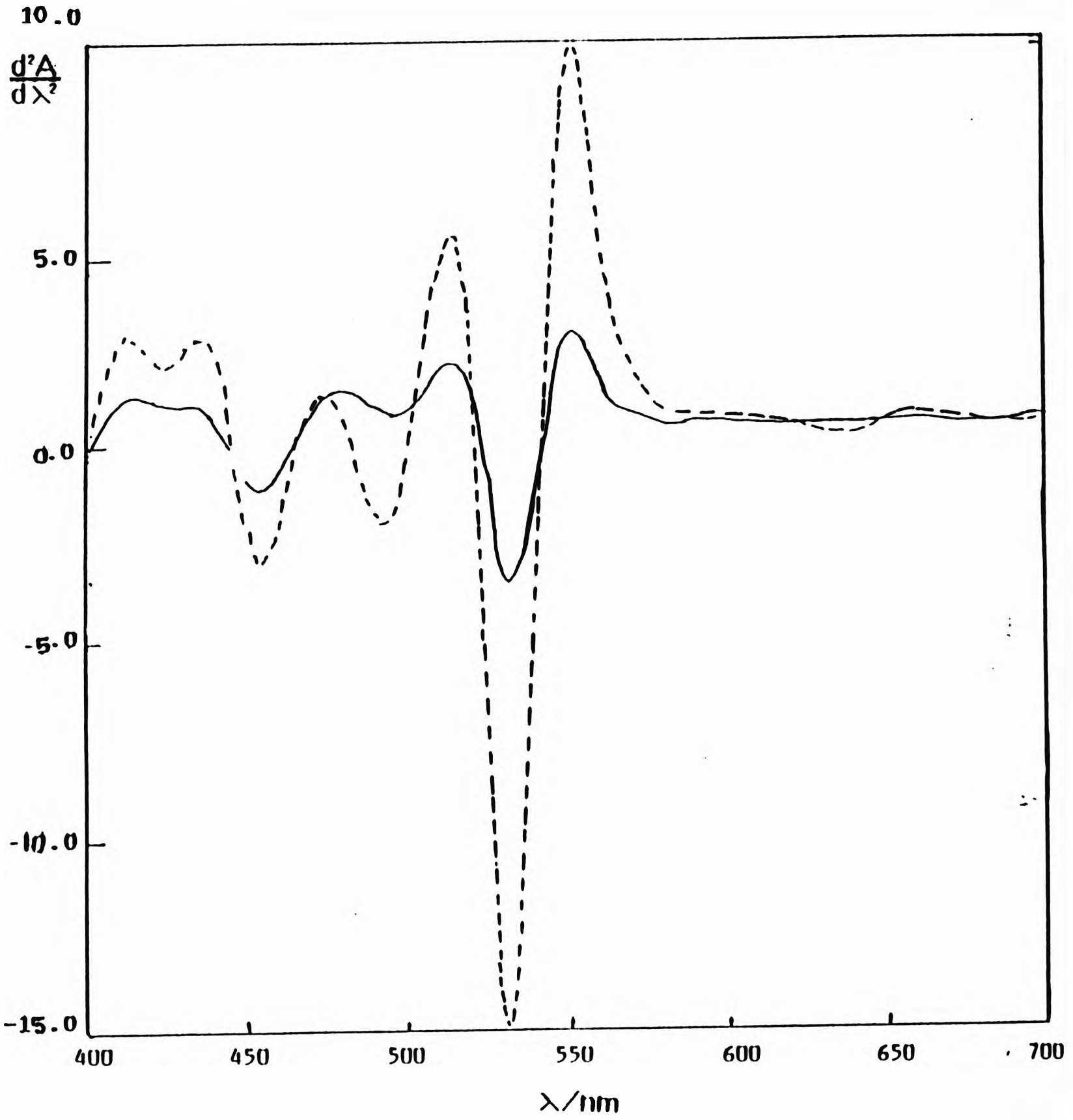

FIGURE 3.7 (b)

Second derivative (2D) electronic absorption spectra obtained after allowing both control (—) and Fe(II)/EDTA/H_2O_2- treated (-----) samples of linolenic acid to react with TBA under acidic conditions.

3.2.2 Production of different classes of conjugated diene species following exercise of the inflamed human knee

Although both zero-order and 2D electronic absorption spectra of PUFAs and their corresponding peroxidation end-products extracted from rheumatoid synovial fluid samples prior to any exercise period varied markedly 'between patients' (presumably a consequence of variable oxidative damage to PUFAs and variable levels of octadeca-9*cis*,11*trans*-dienoate) differences 'within patients' were demonstrable between samples obtained pre- and post-exercise from participants subjected to exercise by either isometric quadriceps contraction or a 300 yard walk. Figure 3.8 exhibits examples of zero-order and corresponding 2D absorption spectra of cyclohexane-reconstituted lipid/chloroform extracts of synovial fluid obtained from patients who were (a) unexercised, (b) exercised by isometric quadriceps contraction for a period of 2 min. and (c) exercised by walking a standard distance of 300 yards. The overlapping absorption bands observed in the 220-230 nm region of the zero-order spectra are clearly resolved in the corresponding 2D spectra. 2D signals (minima) located at ca. 226, 231, 239 and 245 nm, characteristic of conjugated diene species derived from peroxidised PUFAs (illustrated for linoleic acid in Figure 3.4), are present in all spectra recorded. The minima located at 231 and 239 nm are conceivably attributable to *t,t*- and *c,t*- conjugated diene species respectively. Although 'spiking' the cyclohexane-reconstituted synovial fluid extracts with samples of peroxidised linoleic acid confirmed the identities of these two signals, it is possible that the minimum located at 239 nm may be attributable to octadeca-9*cis*,11*trans*-dienoate, the concentration of which is also expected to increase on exposure to a hypoxia/reperfusion-mediated oxygen radical flux, in view of the large quantities of protein present in synovial fluid samples. (i.e. extracts treated in this way showed a significant increase in the magnitude of each of these four 2D signals). Treatment of synovial fluid samples with the Fe(II)/EDTA/H_2O_2 system also gave rise to a marked increase in the amplitude of these four 2D signals.

Subsequent to either of the two exercise regimens, the magnitude of these 2D signals increased in four of the six patients studied, indicating an increase in the concentration of

conjugated diene species culminating from the generation of RORS (i.e. ·OH radical) in the inflamed rheumatoid joint during hypoxic reperfusion injury. Figure 3.8(b) and (c) show typical examples of exercise-dependent increases in the intensity of these 2D signals. Clear differences between synovial fluid extracts obtained pre- and post-exercise are also apparent in the zero-order spectra. Figure 3.9(a) shows a typical plots of the absorbance at 231 nm. and its corresponding 2D signal versus time for synovial fluid samples obtained pre- and post-exercise from a rheumatoid patient. In the 4 exercised patients studied, there is an increase in the intensity of this signal followed by a decrease with time. The greatest increase appears to take place during the 4-6 min. post-exercise time period. a possible consequence of the relatively slow, autocatalytic nature of the lipid peroxidation process. The 2 unexercised patients, however, exhibited no corresponding time-dependent change (Figure 3.9(b)).

However, it should be noted that despite these modifications in the 2D spectra which occur subsequent to exercise, the absorbance at 234 nm (A_{234} , obtained from the zero-order spectra), previously widely utilised as a measure of diene conjugation in peroxidised lipids extracted from biological matrices such as synovial fluid[59,60,71], did not generally increase during the post-exercise period. Indeed, in several of the patients studied, A_{234} was found to decrease following exercise, as illustrated in Figure 3.10(a). This apparent paradox is readily resolved by a consideration of the potentially large number of chloroform-extractable endogenous components other than conjugated diene lipid-derived species which also absorb in this region of the spectrum, placing a major constraint on its applicability. However, as shown in Figure 3.10(b), the 2D spectrophotometric approach suffers from fewer restrictions and hence is recommended as a rapid, convenient and relatively selective method for the assessment of conjugated diene formation during the initial phases of the lipid peroxidation process. As expected, plots of A_{234} versus post-exercise time exhibit a rather high level of non-experimental 'scatter' reflecting a composite of the variation in the concentration of a wide range of the UV-absorbing species present in the extracts. Hence,

direct measurement of absorbance at or near 234 nm in extracts obtained from biological fluids appears to be erroneous.

The 2D signal located at ca. 262 nm, which increases in magnitude significantly following either of the two exercise protocols utilised in patients (e.g. Figure 3.8(b) and (c)), is conceivably attributable to one or more ketodiene species arising from the further degradation of lipid hydroperoxides. Indeed, the direct measurement of absorbance at 268 nm (A_{268}) has been recommended as a method for the assessment of secondary oxidative damage to lipids[70].

A time series of synovial fluid samples obtained from a total of 15 rheumatoid patients who were (i) unexercised (n=4), (ii) exercised for a period of 2 min. by isometric quadriceps contraction (n=5) and (iii) exercised by walking a standard distance of 300 yards (n=6), were analysed for conjugated diene species using this spectrophotometric method. The modifications observed in the 2D spectra of their cyclohexane-reconstituted lipid/chloroform extracts following either exercise period were reproducible for each exercised patient studied. In the 4 unexercised patients, no corresponding time-dependent qualitative changes in the 2D spectra were observed.

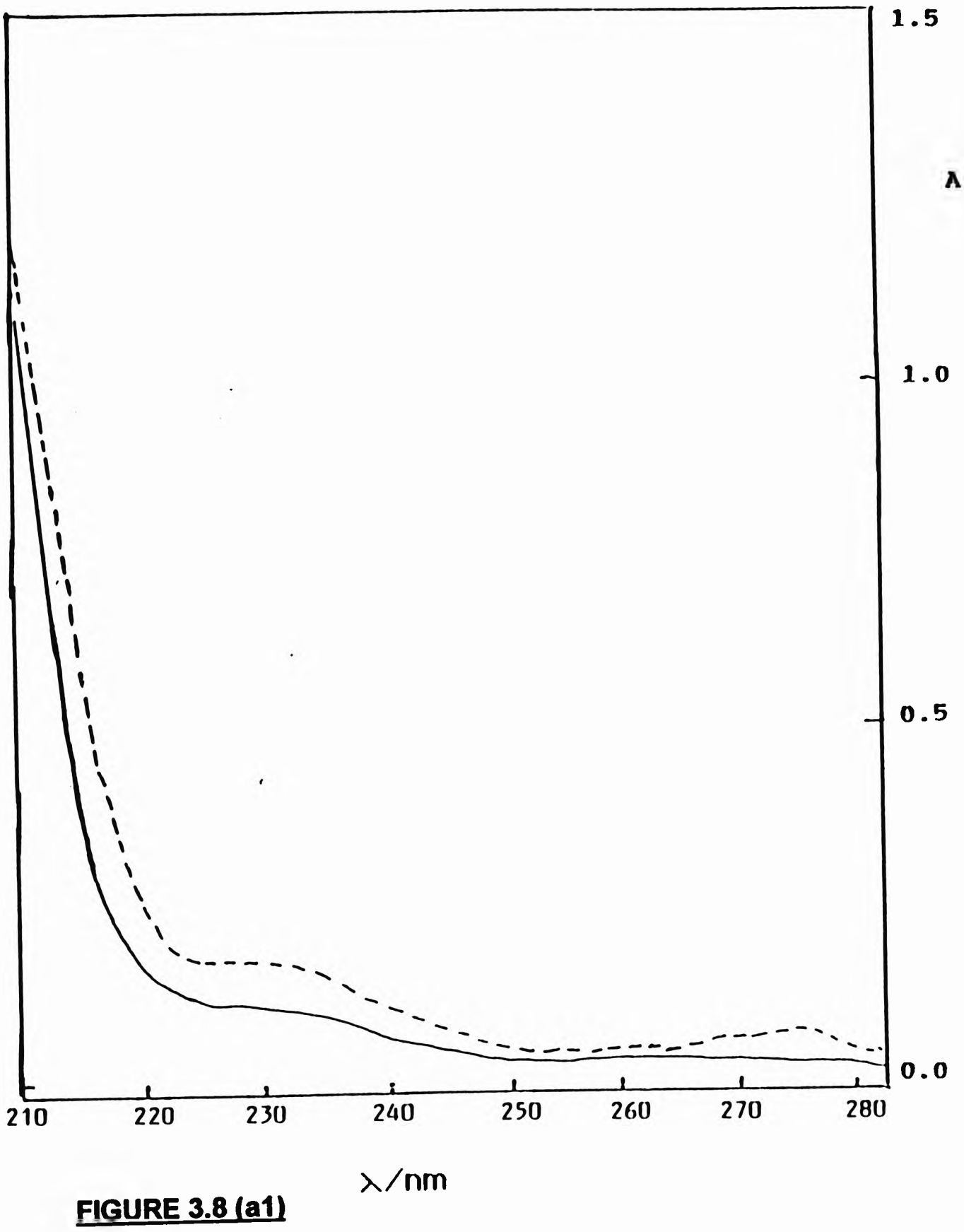

FIGURE 3.8 (a1)

Zero-order electronic absorption spectra of cyclohexane-reconstituted lipid/chloroform extracts of synovial fluid obtained from a rheumatoid patient who was unexercised with a 10 min. period between sample aspirated ((——), 0 min; (-----), 10 min.)

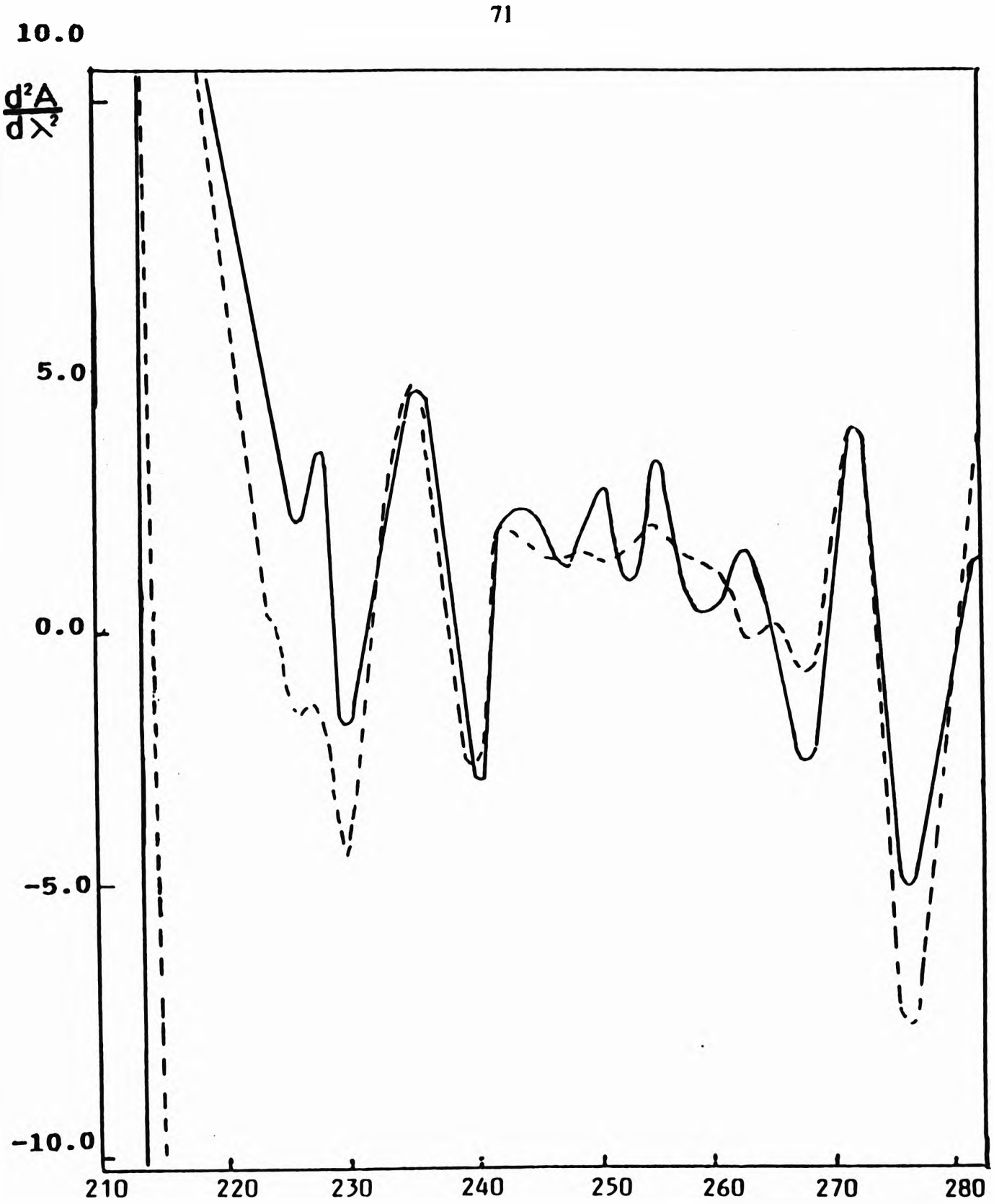

FIGURE 3.8 (a2)

Second derivative (2D) electronic absorption spectra of cyclohexane-reconstituted lipid/chloroform extracts of synovial fluid obtained from a rheumatoid patient who was unexercised with a 10 min. period between sample aspirated ((——), 0 min; (-----), 10 min.)

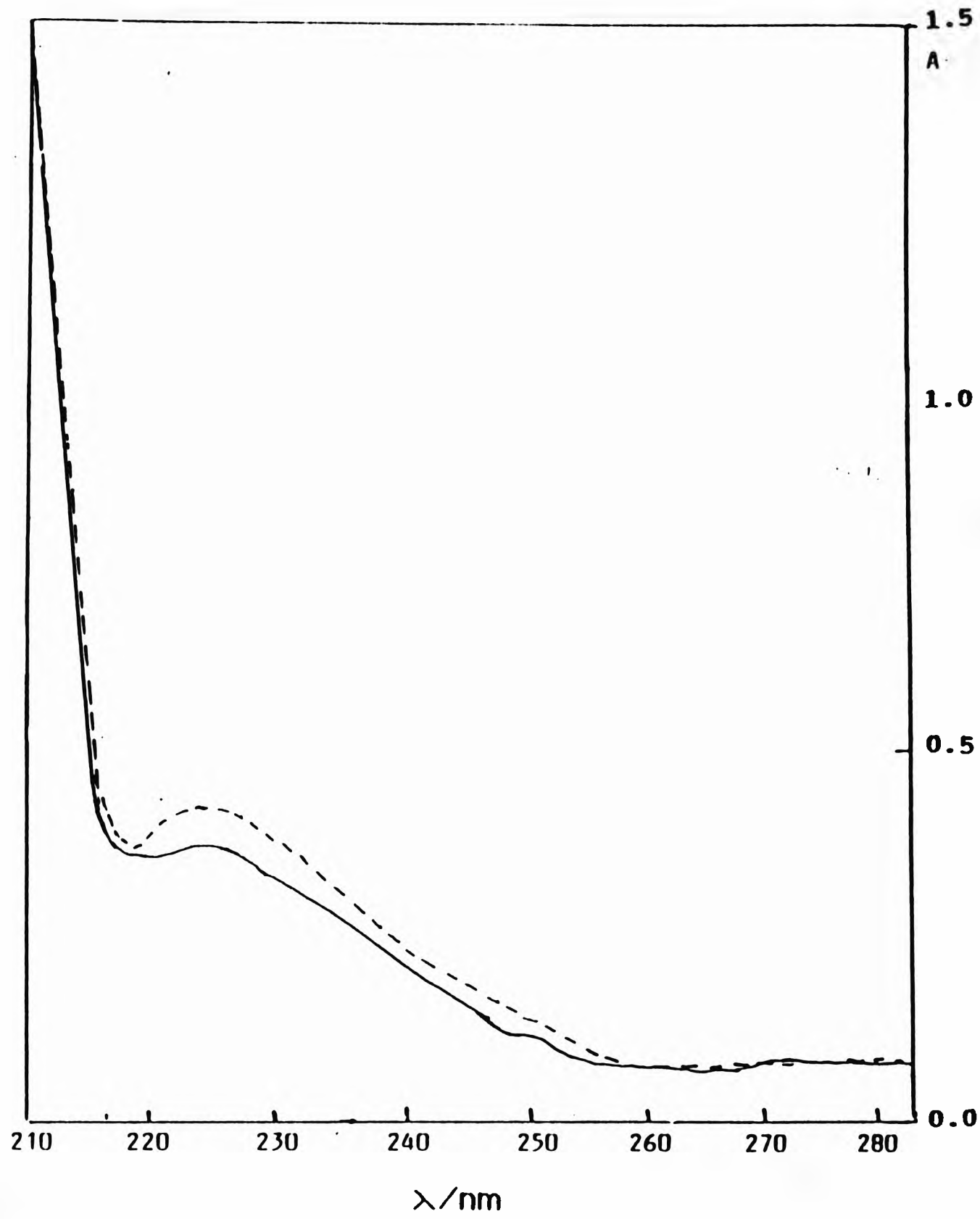

FIGURE 3.8 (b1)

Zero-order electronic absorption spectra of cyclohexane-reconstituted lipid/chloroform extracts of synovial fluid obtained from a patient who were exercised by isometric quadriceps contractions for a period of 2 min.
((——), 2 min. pre-exercise; (-----) 8 min. post-exercise).

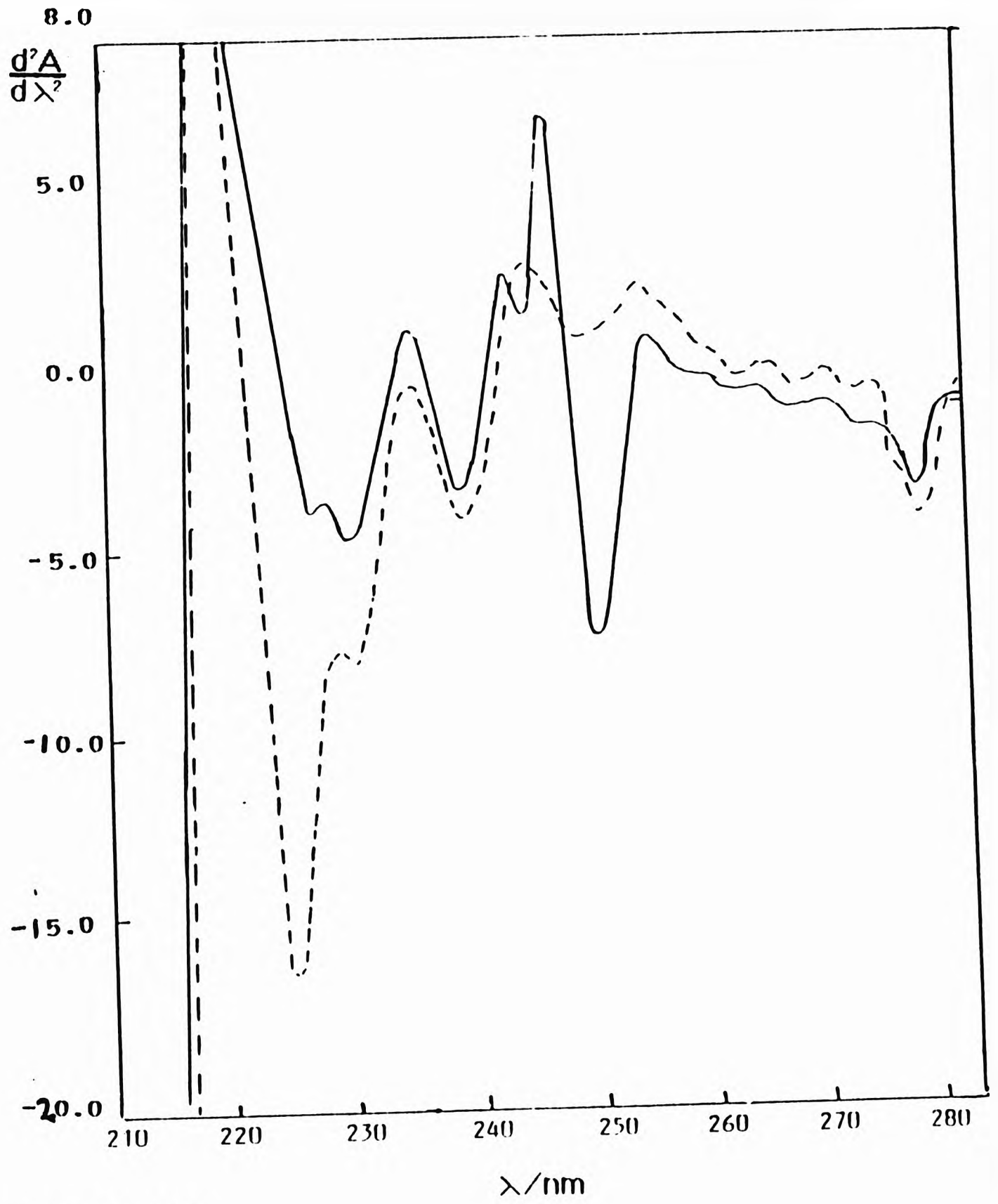

FIGURE 3.8 (b2)

Second derivative (2D) electronic absorption spectra of cyclohexane-reconstituted lipid/chloroform extracts of synovial fluid obtained from a patient who were exercised by isometric quadriceps contractions for a period of 2 min.
((——), 2 min. pre-exercise; (-----) 8 min. post-exercise).

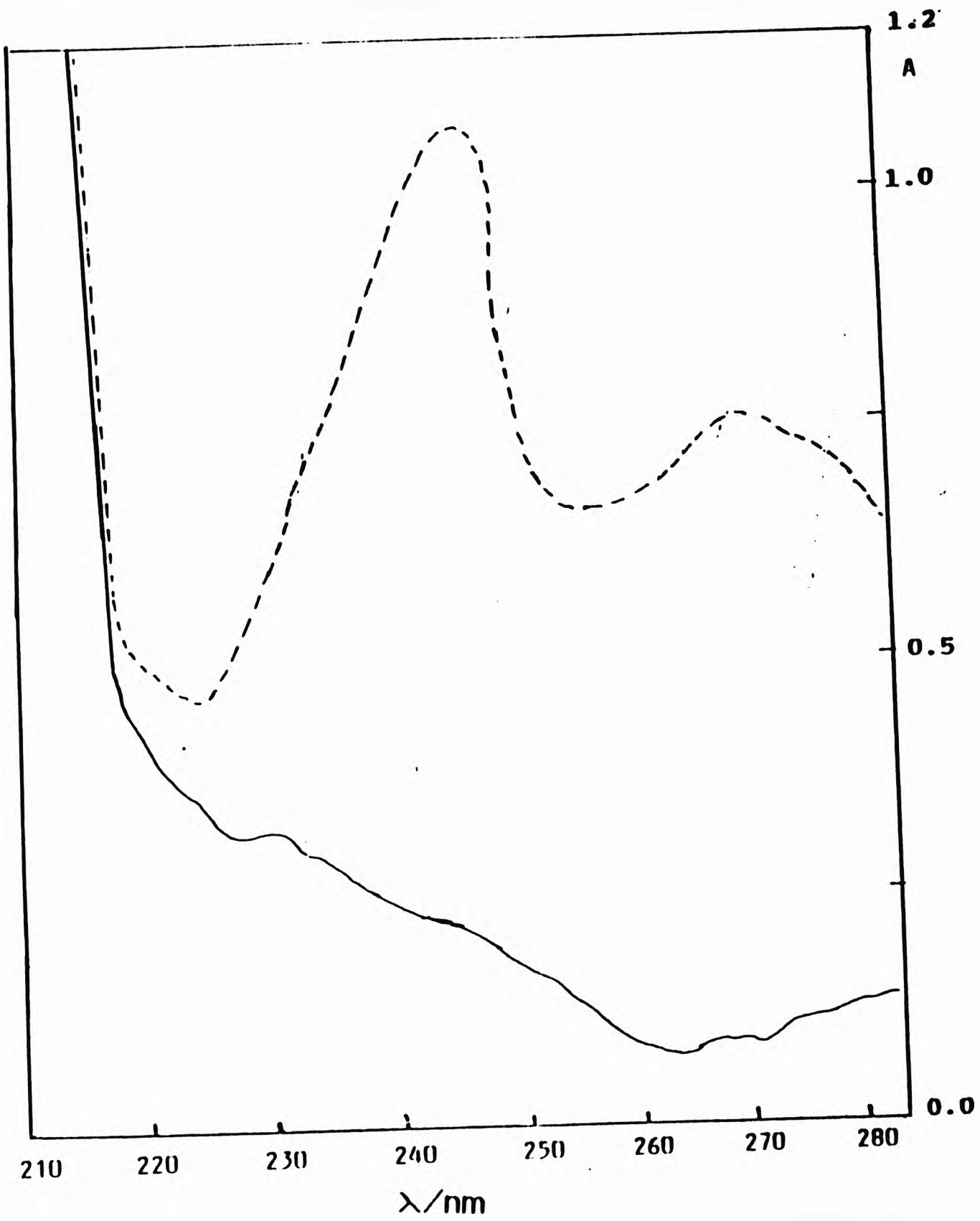

FIGURE 3.8 (c1)

Zero-order electronic absorption spectra of cyclohexane-reconstituted lipid/chloroform extracts of synovial fluid obtained from a patient who were exercised by walking a standard distance of 300 yards. ((——), 2 min. pre-exercise; (-----), 6 min. post-exercise).

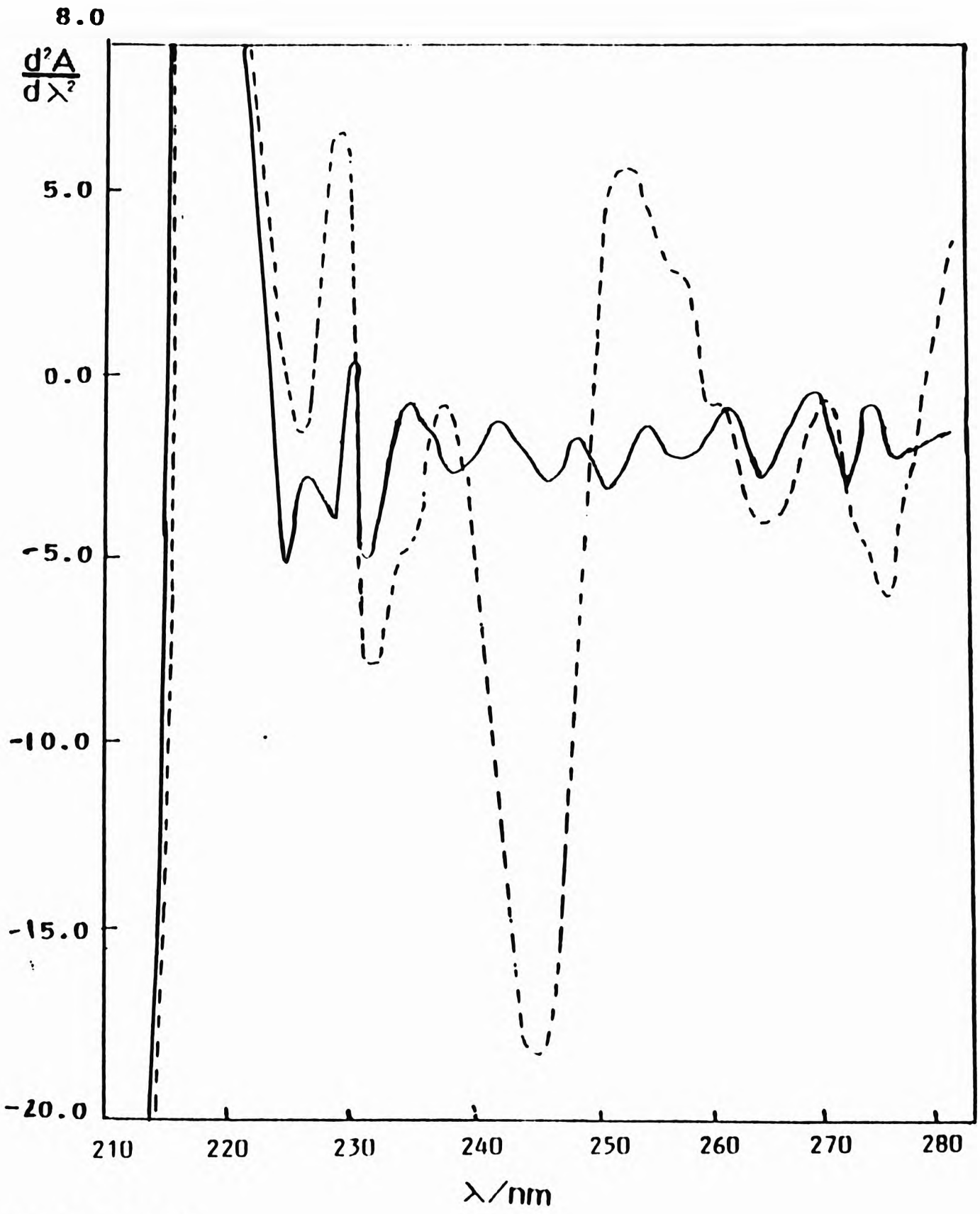

FIGURE 3.8 (c2)

Second derivative (2D) electronic absorption spectra of cyclohexane-reconstituted lipid/chloroform extracts of synovial fluid obtained from a patient who were exercised by walking a standard distance of 300 yards. ((——), 2 min. pre-exercise; (-----), 6 min. post-exercise).

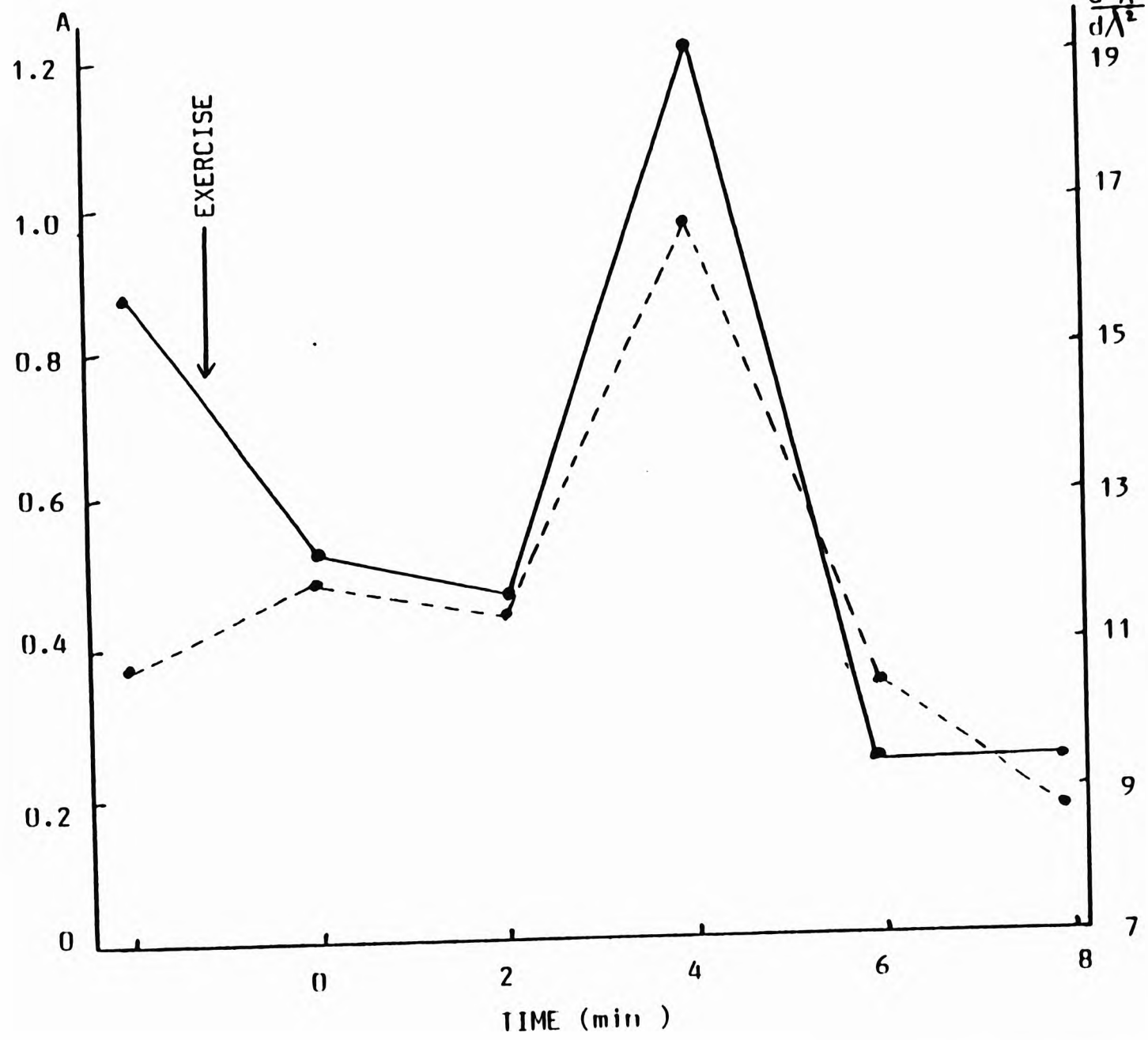

FIGURE 3.9 (a)

Plot of absorbance (——) and its corresponding 2D (-----) signal at 231 nm versus time for synovial fluid samples obtained from pre- and post-exercise from a rheumatoid patient.

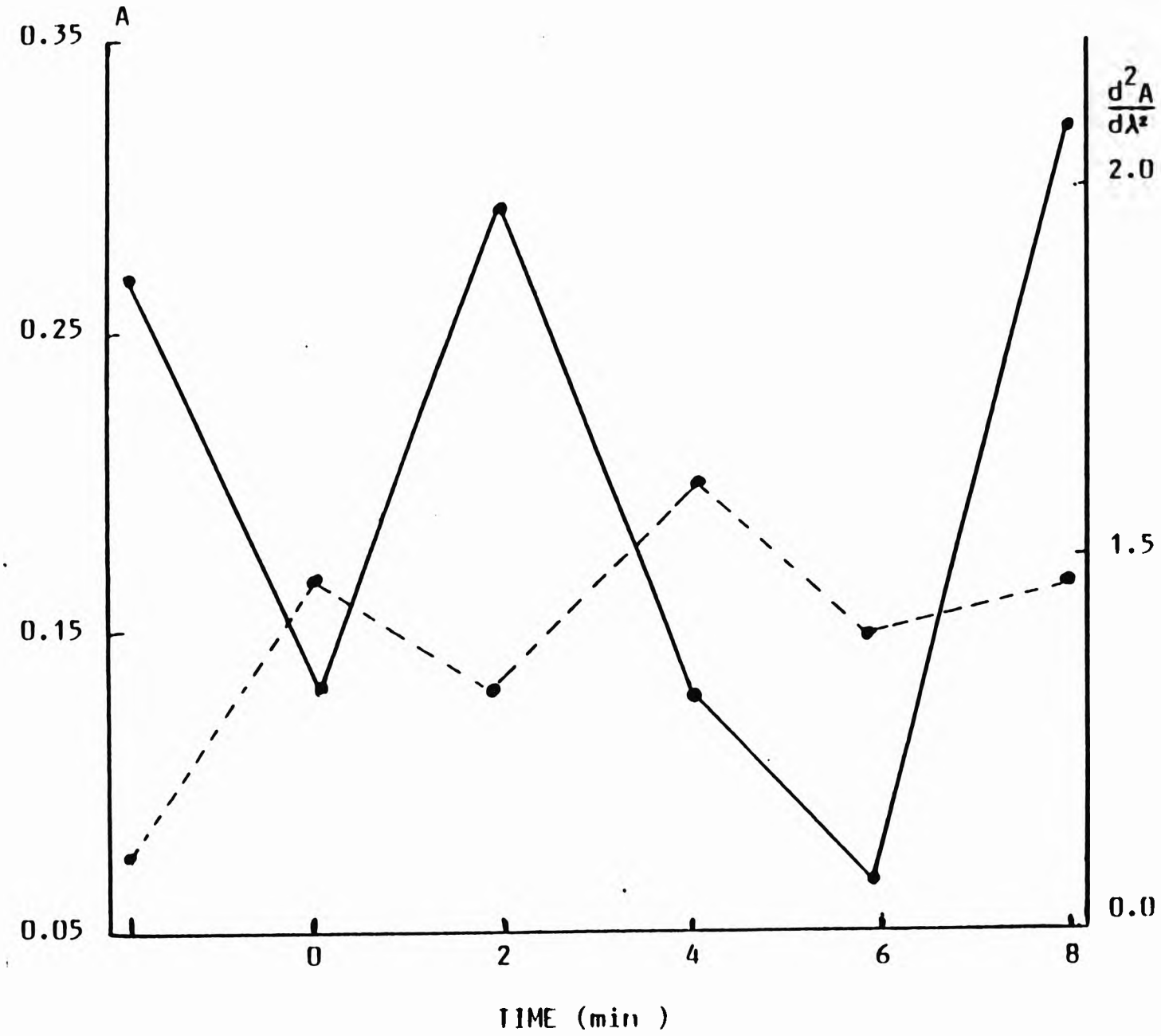

FIGURE 3.9 (b)

Plot of absorbance (——) and its corresponding 2D (-----) signal at 231 nm versus time for synovial fluid samples obtained from an unexercised patient.

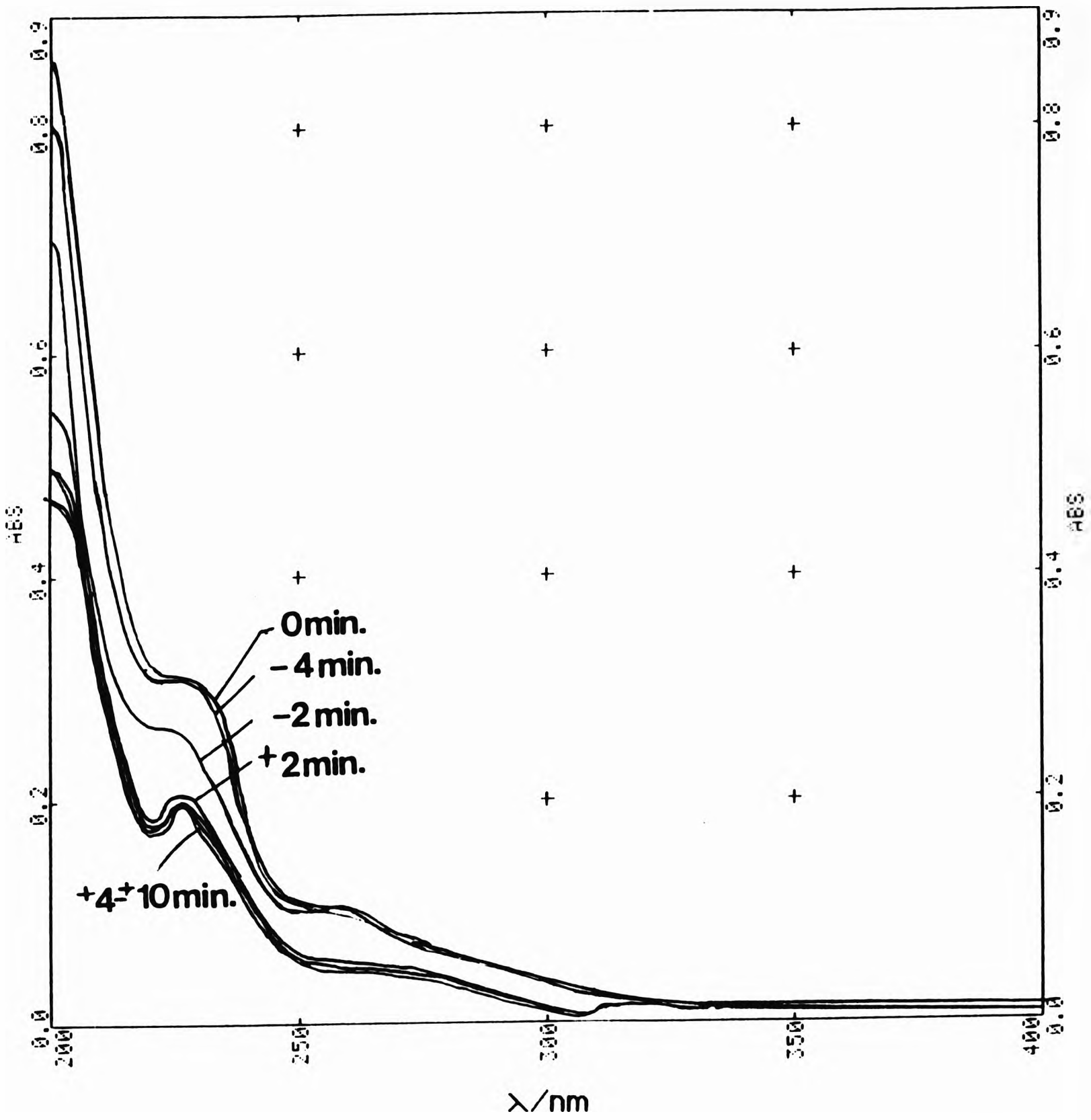

FIGURE 3.10 (a)

Zero-order absorption spectra of cyclohexane-reconstituted lipid/chloroform extracts of synovial fluid samples obtained from a inflamed knee at various time points pre- and post-exercise. Exercise was conducted by isometric quadriceps contraction for a period of 2 min.

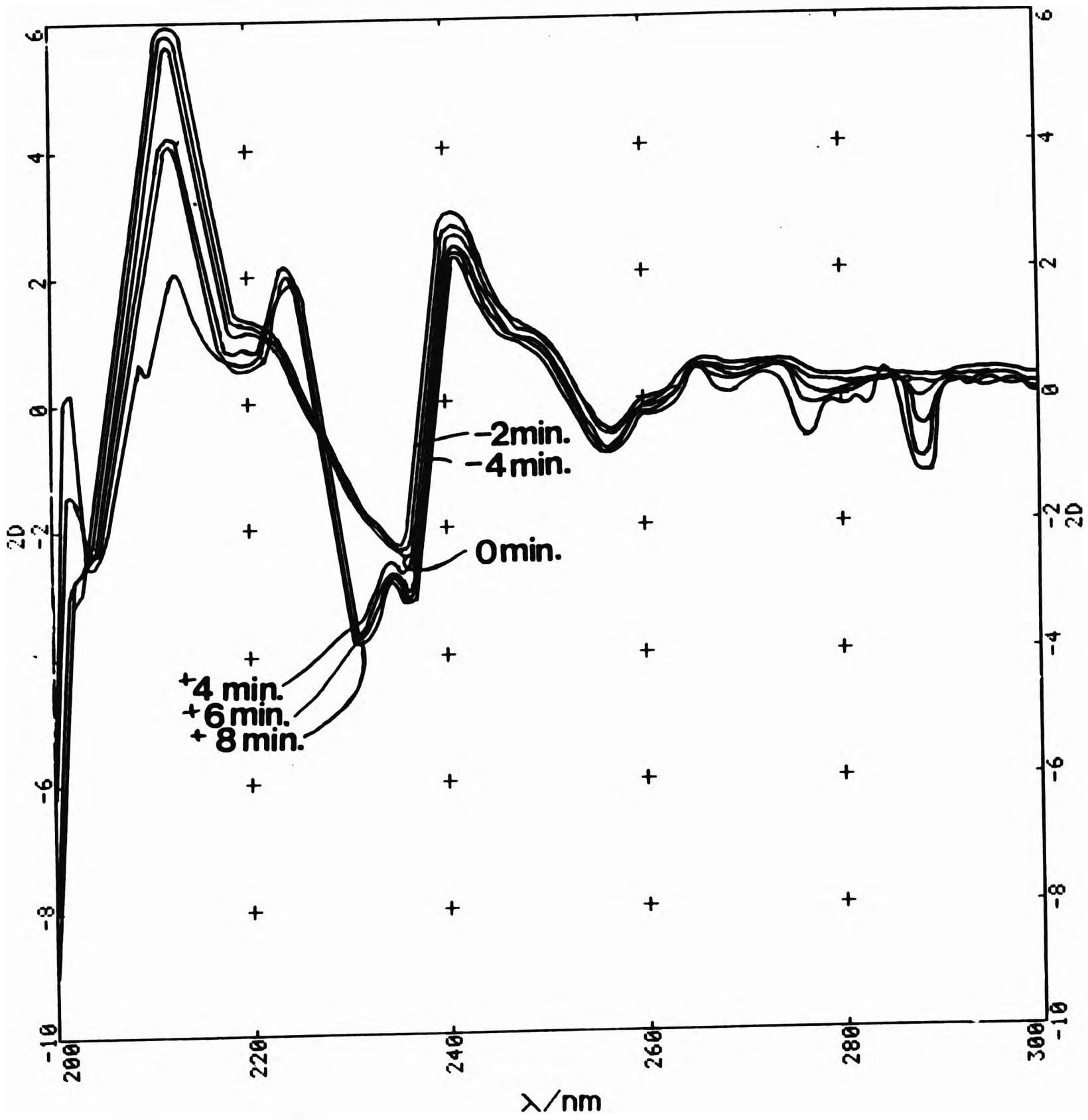

FIGURE 3.10(b)

Second derivative (2D) electronic absorption spectra of cyclohexane-reconstituted lipid./chloroform extracts of synovial fluid obtained from an inflamed knee at various time points pre- and post-exercise. Exercise was conducted by isometric quadriceps contraction for a period of 2 min.

3.2.3 2D spectrophotometric analysis of TBA-reactive material in synovial fluid: specific determination of MDA as a measure of oxidative damage to lipids during hypoxic reperfusion injury

The 2D spectrophotometric technique was employed to resolve overlapping absorption maxima present in visible spectra obtained from the reaction of synovial fluid samples with TBA. This methodology enables the specific determination of MDA, facilitating the assessment of free radical-mediated oxidative damage to lipids in the inflamed rheumatoid joint during hypoxic reperfusion injury. A total of 6 rheumatoid arthritis patients with inflamed knees were recruited to this study. 4 patients were exercised by walking a standard distance of 300 yards, and in the remaining 2 the exercise protocol was omitted.

Typical zero-order and corresponding 2D visible absorption spectra obtained from the reaction of synovial fluid with TBA is shown in Figure 3.11. The resulting 2D spectra from all patients studied exhibit minima located at 448, 503, 532, 560 and 579 nm. In addition, all synovial fluid samples obtained from one of the patients exhibited a relatively intense maximum at 520 nm. The probable, and in some cases, known, identities of these 2D signals are summarised in the Table 3.1. The signal located at 532 nm is solely attributable to the 2:1 TBA:MDA adduct. This was confirmed by 'spiking' unreacted synovial fluid samples with 1,1,3,3-tetramethoxypropane. Indeed, reaction of 1,1,3,3- tetramethoxypropane (which is readily hydrolysed to MDA during the acid/heating stage of the assay) gave a 2D spectrum with minima located at 492 and 532 nm (Figure 3.12).

Table 3.1

2D absorption Minima	Identity of TBA-reactive component
448 nm (s)	Alternative secondary or tertiary aldehyde peroxidation product(s) arising from the breakdown of lipid hydroperoxide or an oxidation product derived from sialic acid, glucose and/or hyaluronate.
503 nm (v)	Product derived from the attack of ·OH radical on oxysugars (specifically glucose) or MDA
520 nm (s)	Possibly a further component derived from oxidative damage to glucose or hyaluronate.
532 nm (s)	MDA
560 nm (s)	Possibly biliverdin derived from the oxidation of bilirubin during the acid/heating stage of the assay.
579 nm (w)	unknown

[where (s), (w) and (v) denote the intensity of the signals : (s),strong; (w), weak; and (v),variable.]

By conducting the TBA reaction in an acetic acid rather than a trichloroacetic acid medium, further interferences derived from β-formylpyruvic acid, an oxidation product of sialic acid, are negligible when measuring of MDA by this method[72]. However, reaction of sialic acid with TBA in an acetic acid medium has been shown to give a weak absorption band at ca. 450 nm[73]. It has also been reported that acetaldehyde (CH_3CHO) in the presence of iron(III) ions[74], or sucrose and fructose pyrolysis products[75] yields a TBA chromophore with intense absorption at 532 nm which appears to be identical with that obtained using pure MDA. Moreover, it is well known that under the highly acidic conditions employed for this test and, in the presence of catalytic, redox-active transition metal-ions (e.g. iron(III)), bilirubin is autoxidised to biliverdin at a rapid rate. Reaction of biliverdin with TBA gives rise to zero-order absorption maxima centred at 465, 530 and 560 nm[64].

Additionally, ·OH radical damage to 2-deoxy sugars such as 2-deoxyribose gives an intense absorption peak at 532 nm attributable to the TBA:MDA adduct and the attack of ·OH radical on oxysugars such as glucose and lactose, or hyaluronate, gives rise to TBA-reactive materials which exhibit 2D absorption minima located at 454, 496, 503, 524 and 555 nm[76]. The 2D spectrum obtained from the reaction of synovial fluid with TBA exhibits a signal at 503 nm, the intensity of which varied considerably 'between patients'. However, the zero-order absorption spectrum resulting from the reaction of an authentic MDA standard sample with TBA has a shoulder at the same wavelength (Figure 3.12). If the synovial fluid 2D signal were solely attributable to the TBA-MDA adduct, then we should expect a close correlation between the magnitude of this signal and that of the more intense, lower energy one at 532 nm. However, no such correlation was observed and therefore it is likely that it is largely attributable to a TBA-reactive component derived from the attack of ·OH radical on glucose or hyaluronate.

It should also be noted that both iron(III) and copper(II) ions form complexes with TBA that have zero-order absorption maxima located at 380 and 400 nm respectively[77].

Figure 3.13 shows plots of the intensity of the 2D 2:1 TBA-MDA adduct signal at 532 nm versus time for synovial fluid samples obtained from both exercised and unexercised patients. In the 4 exercised patients studied, this signal generally shows a small but significant increase in magnitude with time. The greatest increase appears to take place during the 6-8 min. post-exercise time period, a possible consequence of the relatively slow, autocatalytic nature of the lipid peroxidation process. The 2 unexercised patients, however, exhibited no corresponding time-dependent changes. For all of the patients studied, facile plots of absorbance at 532 nm (A_{532}, obtained from the corresponding zero-order spectra) versus time (figure 3.14) exhibited a very high degree of non-experimental 'scatter' a reflection of the pooled variation in the concentrations of a relatively wide range of TBA-reactive materials (Table 3.1).

It should also be noted that a significant proportion of MDA measured in knee-joint synovial fluid samples using 2D spectrophotometry could also be attributable to prostaglandin endoperoxides, which decompose to form MDA under the experimental condition of the TBA test[78].

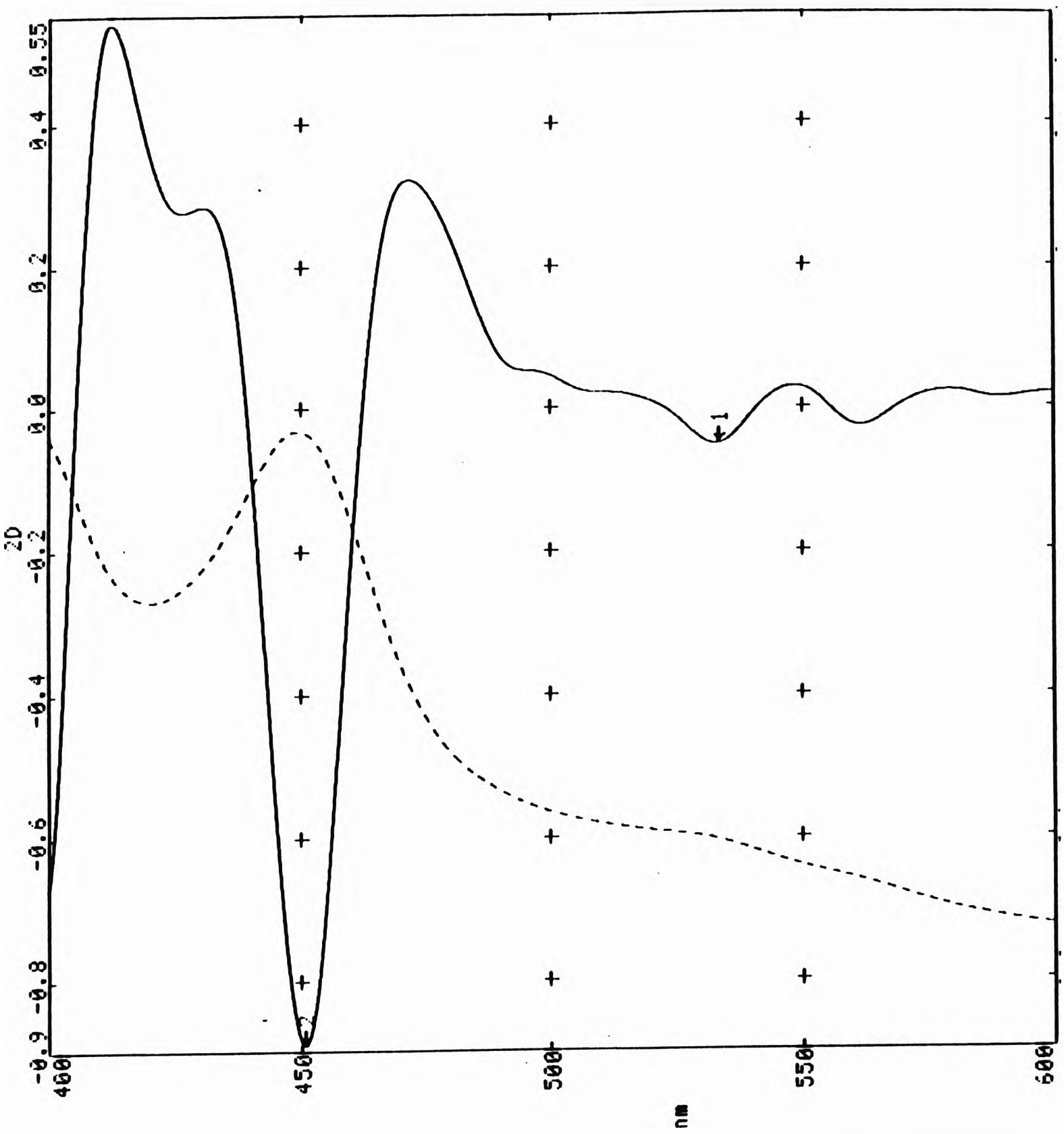

FIGURE 3.11

Zero-order and corresponding second derivative (2D) electronic absorption spectra obtained from the reaction of synovial fluid with TBA.

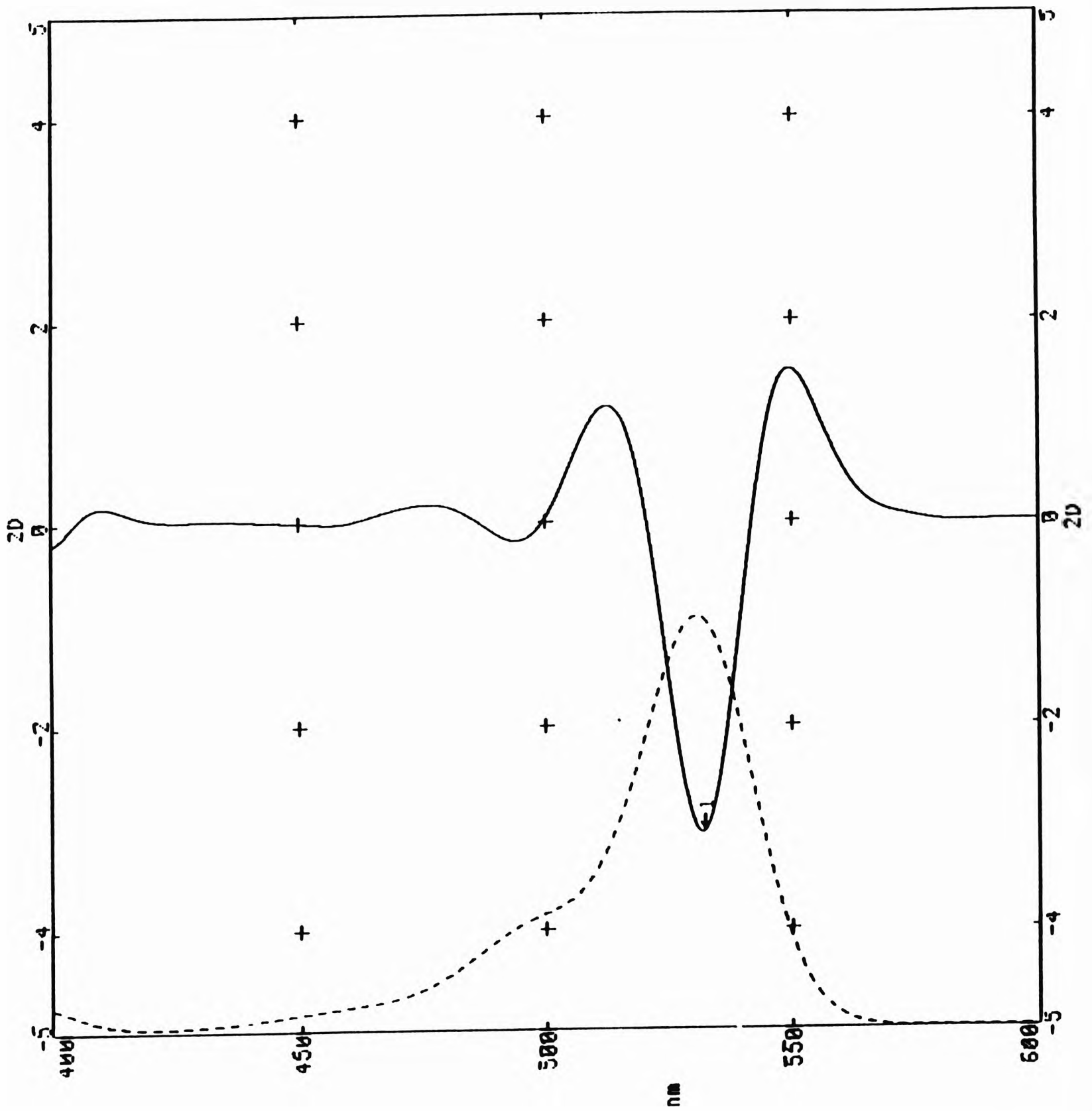

FIGURE 3.12

Zero-order and corresponding second derivative (2D) electronic absorption spectra of 1,1,3,3-tetramethoxypropane with TBA.

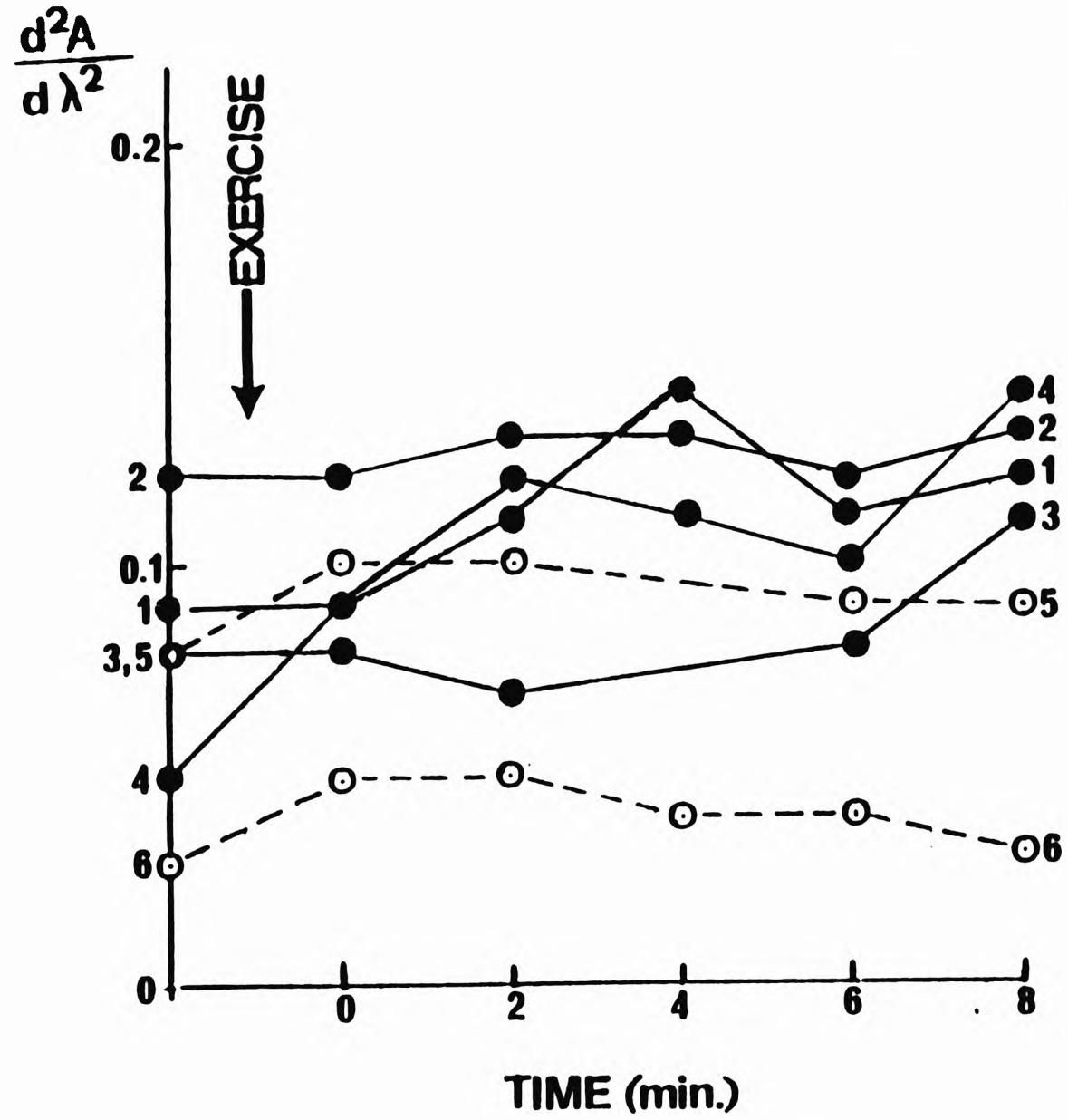

FIGURE 3.13

Plot of the intensity of the 2D 2:1 TBA-MDA adduct signal at 532 nm versus time for synovial fluid samples obtained from both exercised (—) and unexercised (-----) patients.

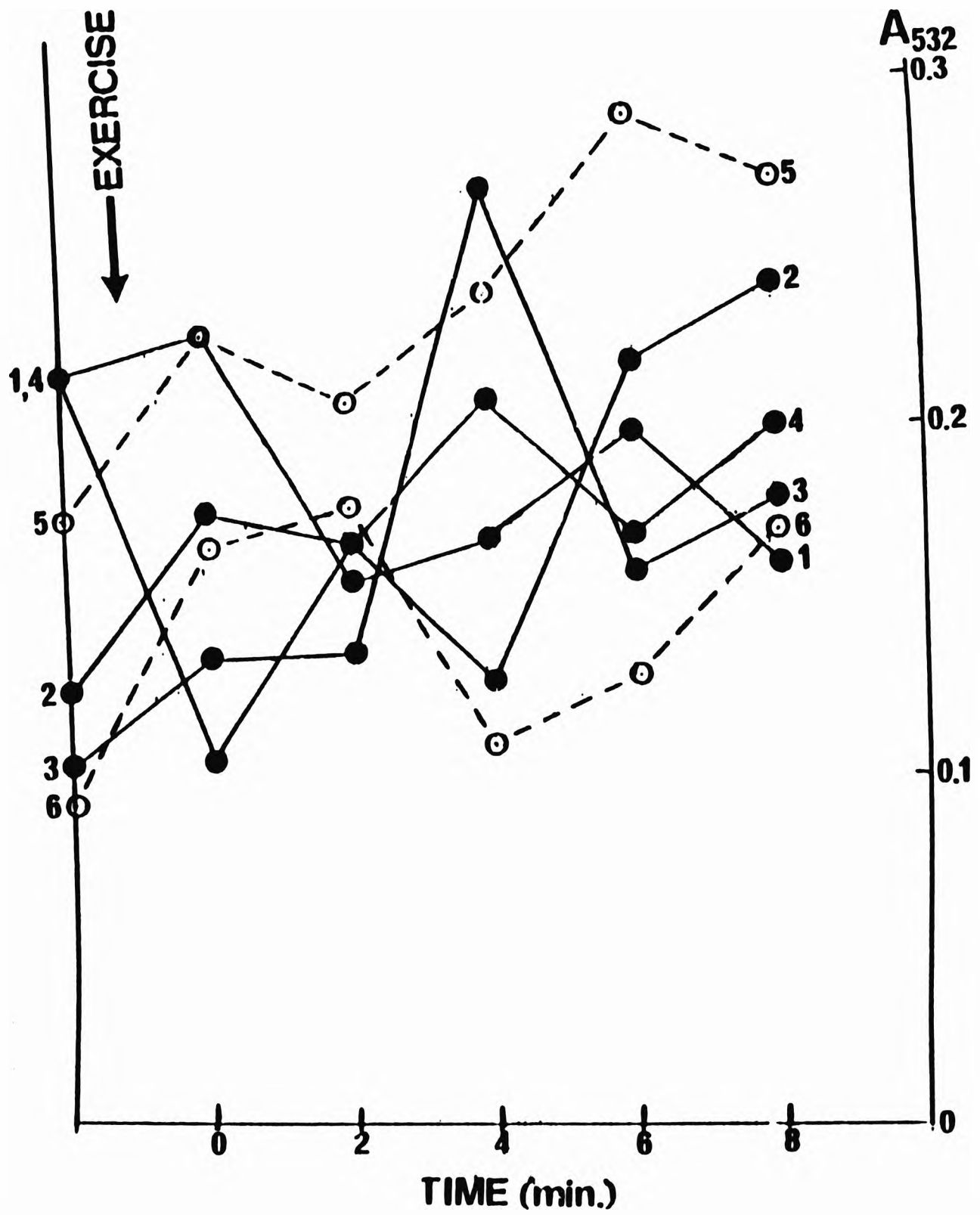

FIGURE 3.14

Plot of absorbance of the 2D 2:1 TBA-MDA adduct signal at 532 nm versus time for synovial fluid samples obtained from both exercised (—) and unexercised (-----) patients.

3.3 Conclusion and Discussion

3.3.1 Conjugated dienes method

The autocatalytic, self-perpetuating nature of the lipid peroxidation process leads to an overall amplification in the measurable concentrations of its end-products produced during exercise of the inflamed rheumatoid joint.

The specific determination of isomeric conjugated diene lipid hydroperoxydienes and hydroxydienes, together with conjugated ketodienes arising from their degradation by 2D spectrophotometry is a method which shows much promise for the assessment of primary and secondary oxidative damage to lipids in biological fluids or isolated tissue samples obtained from patients with inflammatory joint diseases. Unlike previously employed spectrophotometric methods for monitoring diene conjugate formation, the analytical system employed here is rapid, sensitive and relatively free from a myriad of bioavailable interferences. Moreover, it has the potential to provide detailed information regarding the thermodynamic equilibria, kinetics and mechanisms of available pathways for the interaction of reactive oxygen radical species with PUFAs *in vivo*.

It is likely that the hydrogen atom donating-ability of SF influences the *c,t-/t,t-* lipid hydroperoxide product ratio. Interaction of sufficiently reactive radical species such as ·OH with linoleic acid gives rise a pentadienyl radical which then rapidly reacts with dioxygen to produce a hydroperoxyl radical precursor of the *c,t-* lipid hydroperoxide isomer (Figure 3.2). However depletion of the hydrogen atom-donating ability of the reaction environment gives rise to the production of *t,t-* products via an alternative pathway involving a second pentadienyl radical which is formed by the loss of dioxygen from a conformer of the *c,t-* lipid hydroperoxide precursor. Hence, a high level of hydrogen atom-donating ability in biological matrices favours the production of *c,t-* isomers[54,61]. For linolenic acid, the Fe(II)/EDTA/H_2O_2-stimulated peroxidation can also give rise to conjugated diene hydroperoxyepidioxides via a mechanism involving ring closure. These species are formed

under reaction conditions in which the hydrogen atom-donating ability of the reaction environment has declined, subsequent to the initial formation of *c,t*-monohydroperoxides[79].

It is also interesting to speculate on the effect of intra-articular hyperoxia in the inflamed rheumatoid joint on the *c,t-/t,t-* diene conjugate product ratio. The production of *c,t-* isomers appears to be favoured by a hypoxic environment. However, on consideration of the complex series of equilibria involved (Figure 3.2), it is difficult to predict its influence on the formation of the *t,t-* isomer with any certainty.

3.3.2 Thiobarbituric acid method

The determination of MDA by the application of 2D spectrophotometry to the analysis of TBA-reactive materials present in synovial fluid is also a very promising method for the assessment of oxidative damage to lipids in the inflamed rheumatoid joint during hypoxic reperfusion injury. Although the selectivity of the widely used TBA test can be further increased by the high performance liquid chromatographic (HPLC) separation of the 2:1 TBA-MDA adduct followed by spectrophotometric detection at 546 nm[80], or alternatively by exploiting the adducts fluorescence properties[64], these methods are relatively tedious and require elaborate technical instrumentation. Several alternative spectrophotometric procedures which apparently correct for errors caused by the *in situ* generation of interfering compounds during the acid/heating stage of the assay have also been reported[72,81], but these methods do not have the ability to 'speciate' alternative TBA-reactive material as in the method described here.

Reaction of one or more alternative secondary oxidation products (derived from the transition metal-ion catalysed decomposition of lipid hydroperoxides) with TBA may account for the intense signal at *ca.* 450 nm observed in both zero-order and 2D spectra after subjecting peroxidised PUFAs or rheumatoid SF to the TBA test. Although alka-2,4-dienals and to somewhat lesser extent, alk-2-enals produce pink chromogens which absorb at *ca.* 530 nm, it has been demonstrated that aldehydes in general produce yellow-coloured pigments which absorb at ca. 450 nm[82]. Indeed, the range of carbonyl components derived

from the autoxidation of linoleic acid has been found to include the aldehydes pentanal and hexanal as well as the ketones propan-2-one and pentan-2-one[83].

CHAPTER 4

FURTHER EXTENSION TO THE CONJUGATED DIENE METHOD

4.1 Introduction

4.1.1 Inflammatory bowel diseases

The term inflammatory bowel disease (IBD) incorporates two chronic inflammatory disease of the gastrointestinal tract; Crohn's disease and ulcerative colitis. Despite intensive research, the cause of these disease remains unknown[84]. Both disease states show similar symptoms, namely weight loss, diarrhoea, haemorrhage and abdominal pain, and it is not always possible to distinguish between the two types. Pathologically, ulcerative colitis is a diffusely distributed mucosal disease, whereas Crohn's disease is a patchy disease involving all layers of the bowel wall.

Several lines of evidence suggest that an infection triggers a cascade of events leading to inflammation. Several inflammatory mediators are involved in IBD, in particular prostaglandin E_2 (PGE_2), leukotrienes and platelet activating factor (PAF)[86]. Recent evidence suggests that RORS may also be important[87-88]. This chapter investigates the possible role of RORS in patient with ulcerative colitis.

4.1.1.1 Evidence for the involvement of RORS in IBD

RORS are produced in the gastrointestinal tract of both healthy and diseased subjects. Phagocytic cells (neutrophils, monocytes and macrophages) all undergo the respiratory burst in response to a variety of stimuli producing the toxic RORS ($O_2^{\cdot-}$, H_2O_2 and $\cdot OH$). The most likely source of RORS in IBD is from the reaction involving xanthine oxidase which then produces RORS in response to ischeamic-reperfusion and inflammatory cells[11,85].

Recent evidence suggests the involvement of RORS in the pathogenesis of IBD is rather indirect, an assumption based on reports showing increased levels of RORS in isolated intestinal phagocytes and peripheral blood monocytes and neutrophils[11,89]. The plasma levels of vitamin A, vitamin C, β-carotene and serum zinc were found to be lowered in patients with active ulcerative colitis, suggesting RORS may have a role in the

pathogenesis of IBD[90]. Moreover, studies in patients with IBD have detected lower levels of SOD in blood neutrophils and lower levels of glutathione peroxidase in monocytes[90-91]. Low levels of SOD and glutathione are also found in the mucosa of patients with active IBD[91-93].

As mentioned earlier, RORS are extremely reactive species and will damage all biological molecules including DNA, lipids, polysaccharides and proteins. However, as yet there is no direct evidence of such processes occurring *in vivo* in patients with IBD. Ahnfelt-Rhone and his colleagues[94] measured the concentration of lipid peroxidase using the TBA test and found increased levels in patients with IBD, the levels correlating with the extent of the disease. However, the TBA test used is relatively non- specific and does not differentiate between the lipid peroxides produced from either enzymic and non-enzymic processes.

Thus, it seems likely that RORS has an important role in the pathophysiology of IBD. The aim of this study is to apply the extended conjugated dienes method to investigate the involvement of RORS in normal subjects and in pateints with:

(1) ulceritive colitis and

(2) rheumatoid arthiritis.

4.1.2 Further application of 2D spectrophotometry to the assessment of reactive oxygen radical-dependent peroxidation of PUFAs in biological materials. Extension To The Conjugated Dienes Method

In chapter 3, a method for determining the isomeric *cis,trans-* and *trans,trans-* conjugated hydroperoxydienes, hydroxydienes and conjugated oxodienes arising from their degradation is described. However, this method is somewhat limited in the information that it provides. For example, it does not distinguish between the different types of unsaturated fatty acid undergoing oxidation.

Moreover, it is also important to note that greater than 90% of conjugated diene species in freshly obtained human body fluids or tissue is accounted for by the presence of a single non-peroxidised fatty acid residue, octadeca-9 *cis*,11 *trans*-dienoic acid (18:2[9,11])[59,95] which is a simple isomer of linoleic acid. Intriguingly, this component can be generated *in vitro* by the exposure of linoleic acid to an oxygen radical generating source in the presence of albumin[60,96], indicating that protein plays an important role in re-directing peroxidation pathways which proceed via mechanisms involving reversal of the interaction of dioxygen with lipid-derived carbon-centred radicals, or alternatively, reduction of the carbon-centred radical. Operation of the latter mechanism may be dependent on the availability of electron-donating protein thiols such as the cysteine-34 residue of human serum albumin.

The presence of conjugated diene species in biological material is further complicated by the observation that anaerobic micro-organisms present in the rumen of cattle have the ability to effect the enzymic conversion of linoleic acid to octadeca-9 *cis*, 11 *trans*-dienoic acid[97]. This transformation probably accounts for the high level of conjugated diene species in milk. In addition, micro-organisms that are constituents of the normal flora of the mouth, nose and vagina can also effect the production of non-peroxidised conjugated diene isomers.

Fishwick and Swoboda have previously described an alternative analytical system which they employed to monitor the potentially deleterious autoxidation of PUFAs present in foodstuffs[98]. Their 'extended conjugable oxidation products' assay involved (1) reduction of conjugated hydroperoxydienes and oxodienes to their corresponding hydroxydienes with sodium borohydride ($NaBH_4$) and (2) dehydration of the resulting hydroxydienes to strongly chromophoric triene- and tetraene-containing species by a relatively concentrated solution of sulphuric acid in ethanol. The dienoic fatty acid oxidation products (e.g., 9-OOH-10(*t*),12(*c*)-octadecadienoic acid) yields a conjugated triene chromophore, and trienoic fatty acid oxidation products (e.g., 9-OOH-10(*t*),12(*c*),15(*c*)-octadecatrienoic acid) form a tetraene chromophore. The basis of this method was developed by Frankel in 1962 (Figure 4.1)[99]. By using this extended (reduction/dehydration) technique the absorption maxima (and 2D minima) due to conjugated hydroperoxides and conjugated oxodienes are shifted to the near-uv and visible regions of the spectrum and hence overcomes any problems with interferences, such as octadeca-9 *cis*,11 *trans*-dienoic acid which absorbs in the UV region (at ca. 240 nm) and is not transformable to a conjugated triene species by the above chemical modifications.

In this study, the above method has been further extended by employing 2D spectrophotometry. In addition, this analytical system has been applied to the assessment of ROR-mediated oxidative damage to PUFAs in: (1) knee joint SF obtained from pateints with inflammatory joint dieseases and (2) human colon tissue obtained from subjects with ulcerative colitis[100] .

To date, the only measurement performed on rectal biopsies of patients with ulcerative colitis was that by Ahnfelt-Ronne *et. al.*[94] They demonstrated an increase in lipid peroxidation in patients with active disease in human colonic samples, which returned to control levels after treatment. However, the technique they used was the thiobarbituric acid test (TBA), which is a non-specific assay subject to major interferences from substances such as prostaglandins[101]. Indeed, on reviewing the methods available for measuring lipid

peroxidation. Halliwell and Gutteridge[19] suggest that the methods of choice for the investigation of lipid peroxide in human material should be conversion of components to volatile derivatives, which can be readily separated and identified by gas chromatography coupled with mass spectrometry.

The aim of this work was to re-evaluate the findings of Ahnfelt-Ronne *et. al.*[94] which demonstrated increased lipid peroxidation in colorectal mucosal biopsies from patients with ulcerative colitis[94]. In order to do this, the technique developed by Fishwick and Swoboda[98] was chosen as one which was relatively specific, but widely applicable.

Figure 4.1 : Formation of triene containing structures from hydroperoxydienes and oxodienes

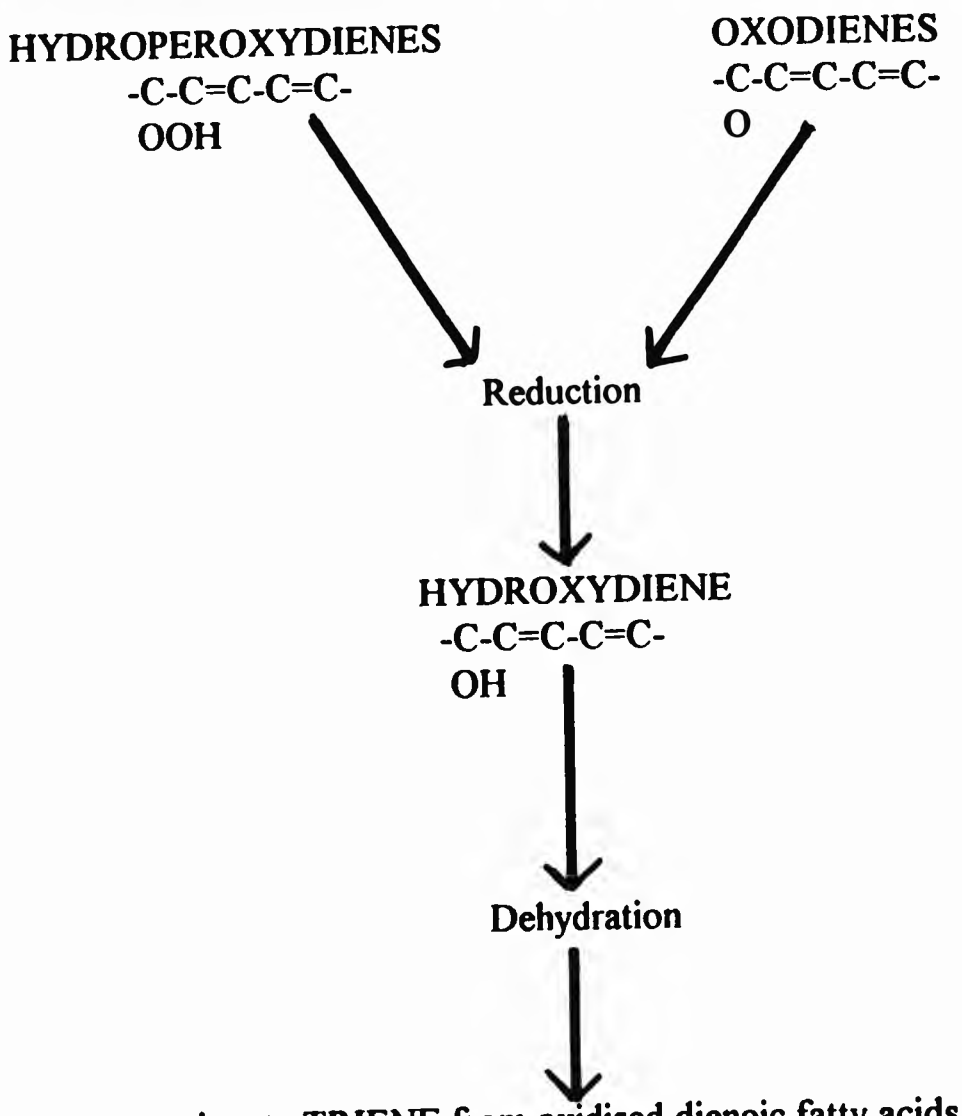

4.2 Results

4.2.1 *In vitro* peroxidation of methyl linoleate and linolenate

Figures 4.2(a) and (b) show zero-order and corresponding 2D absorption spectra of cyclohexane-reconstituted chloroform extracts of autoxidised and Fe(II)/EDTA/H_2O_2-treated methyl linoleate and methyl linolenate respectively. The development of a number of overlapping absorption bands in the 220-280 nm region of the zero-order spectra of these samples indicates the formation of three or more classes of conjugated diene species. These overlapping absorption maxima are readily resolved by the application of 2D spectrophotometry. The 2D spectra shown in Figure 4.2(a) exhibit minima located at 229, 236 and 245 nm, which correspond to conjugated diene absorption maxima in the zero-order spectrum. The 2D minima at 229 and 236 nm are conceivably attributable to *t,t*- and *c,t*-conjugated hydroperoxydienes (and/or hydroxydienes) respectively (Table 4.1). Additionally, the 2D signals centred at 270 and 276 nm are probably attributable to isomeric (*c,t*- *t,t*-)oxodiene species derived from the further oxidation of *c,t*- and *t,t*- isomers of the methyl ester of 9-OOH-10,12 octadecadienoic acid. However, the origin of the 2D signal located at 245 nm is at present unclear, but it is probably attributable to a *c,t*- isomer of an alternative conjugated diene species.

The corresponding 2D spectra of autoxidised and Fe(II)/EDTA/H_2O_2-treated methyl linolenate contain minima at 231, 238.5 and 248 nm which also correspond to conjugated diene absorption maxima in the zero-order spectrum (Figure 4.2(b)). The 2D signals located at 231 and 238.5 are attributable to *t,t*- and *c,t*- conjugated diene species respectively (Table 4.1). The conjugated oxodiene component signal at 271 nm in this spectrum is of much greater intensity than that present in the spectrum obtained from peroxidised methyl linoleate, demonstrating an increased production of this species from peroxidised methyl linolenate, which may be attributable to the faster peroxidation rate of the (latter) more unsaturated fatty acid[50].

Figure 4.3 shows the resulting zero-order and 2D absorption spectra of autoxidised and Fe(II)/EDTA/H_2O_2-treated methyl linoleate following sequential chemical modification with (1) $NaBH_4$ and (2) alcoholic H_2SO_4. Derivatisation of this model compound in this manner gave rise to product(s) with characteristics typical of conjugated triene chromophores, i.e., with 2D absorption minima located at 258, 269.5 and 281 nm (Table 4.2)[98]. It is conceivable that the products are a mixture of 8,10,12- and 9,11,13-octadecatrienoate chromophores. The $NaBH_4$ reduction step gave rise to the complete disappearance of the 2D signals centred at 270 and 276 nm, confirming that they are attributable to conjugated oxodiene species. In addition, a relatively intense 2D absorption minimum at 309.5 nm is also present in the spectrum.

Figure 4.4 exhibits the resulting zero-order and corresponding 2D spectra of autoxidised and Fe(II)/EDTA/H_2O_2-treated methyl linolenate. Reduction of the hydroperoxydiene and oxodiene components derived from its peroxidation followed by dehydration of the resulting hydroxydiene species gave rise to products with an electronic absorption spectrum typical of conjugated tetraene chromophores with 2D absorption minima located at 278, 289, 303 and 317.5 nm (Table 4.2)[98]. The resulting spectrum also suggests the presence of relatively small quantities of conjugated triene species, as is evident from the presence of weakly-intense 2D signals at 257.5, 267.5 and 278 nm. As expected, the reduction step was accompanied by a loss of the conjugated oxodiene signal at 271 nm. It has previously been reported that the acid-catalysed dehydration of conjugated hydroxydienes resulting from the reduction of peroxidised linolenic acid gave rise to 9,11,13,15-octadecatetraenoic acid[98], but no attempts to establish the stereochemistry of the product(s) have been made here due to their apparent susceptibility to polymerisation during purification. This acid-catalysed dehydration reaction has been proposed to proceed by a mechanism involving proton elimination to form a common carbonium ion intermediate[102]. The presence of only small amounts of conjugated triene species in the system indicates that the dehydration process predominantly involves proton abstraction from the central

methylene ($-CH_2-$) group rather than from a $-CH_2-$ group located directly adjacent to the conjugated diene system.

Table 4.1

2D ABSORPTION MINIMA		
Methyl Linoleate	Methyl linolenate	Identity of signals
229 (m)	231 (m)	*t*-conjugated hydroperoxydienes (and/or hydroxydienes)
236 (s)	238.5 (s)	*c-t*-conjugated hydroperoxydienes (and/or hydroxydienes)
245 (m)	248 (m)	unknown : probably due to *c-t*-isomer of alternative conjugated diene
270 (w)	272 (s)	probably attributable to oxodiene species from further oxidation of methyl esters of PUFA.

Where (w), (m) and (s) represents intensity of the minima, w = weak, m = medium, and s =strong.

Table 4.2

2D Absorption spectra wavelength minima (after reduction and dehydration to corresponding trienes and tetraenes).

SAMPLE	WAVELENGTH (nm)			
Peroxidised methyl linoleate	258.0	269.5	281.0	309.5
Peroxidised methyl linolenate	278.0	289.0	303.0	317.5
Prostaglandin E_2	260.0	267.0	272.0	284.0
Colonic biopsies	258.0	268.5	274.0	281.0
	289.5	305.0	315.0	

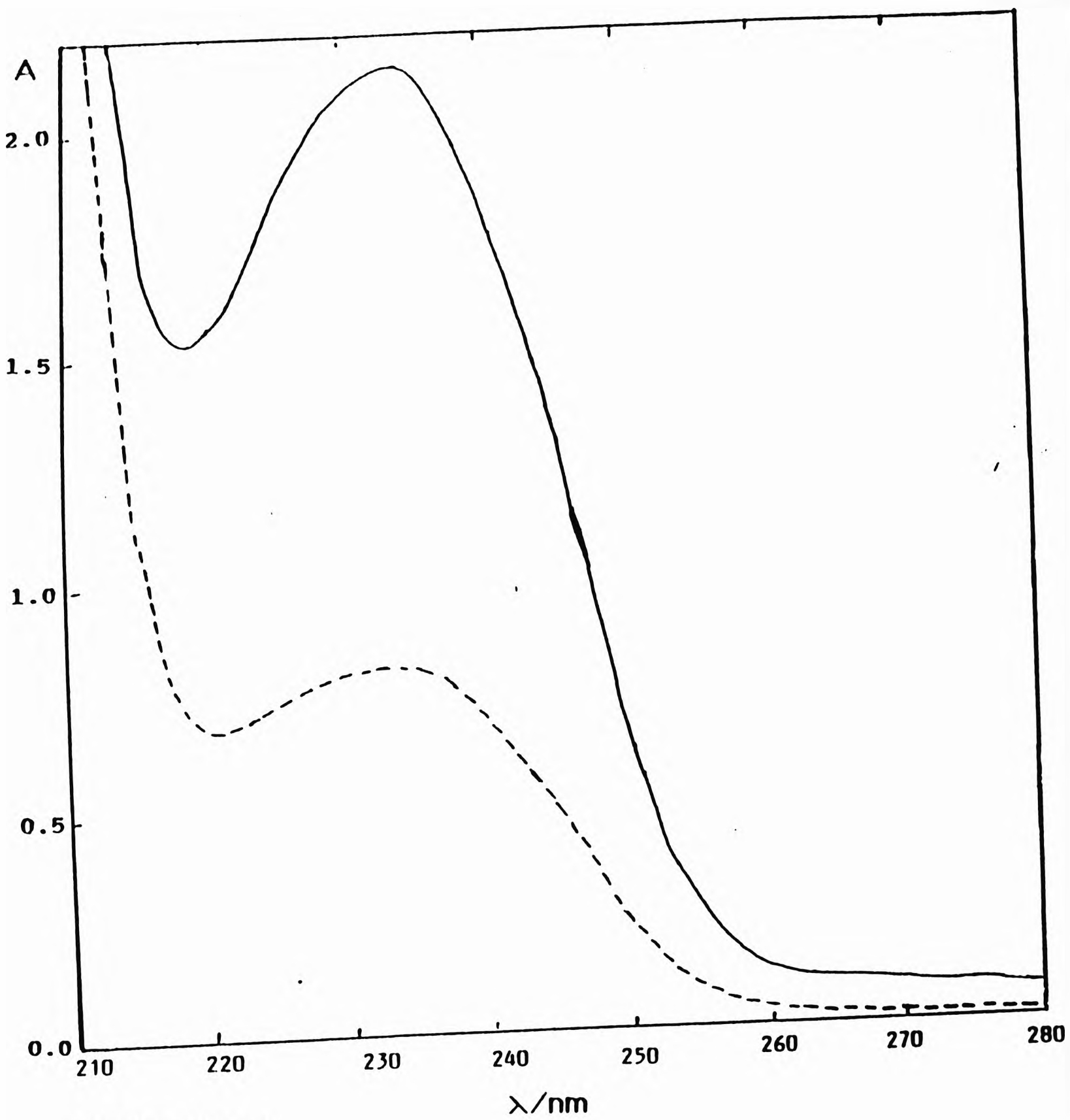

FIGURE 4.2 (a1)

Zero-order electronic absorption spectra of cyclohexane-reconstituted lipid/chloroform extracts of methyl linoleate obtained subsequent to autoxidation in air at ambient temperature (-----), or exposure to a catalytic Fe(II)/EDTA/H_2O_2 (—) system.

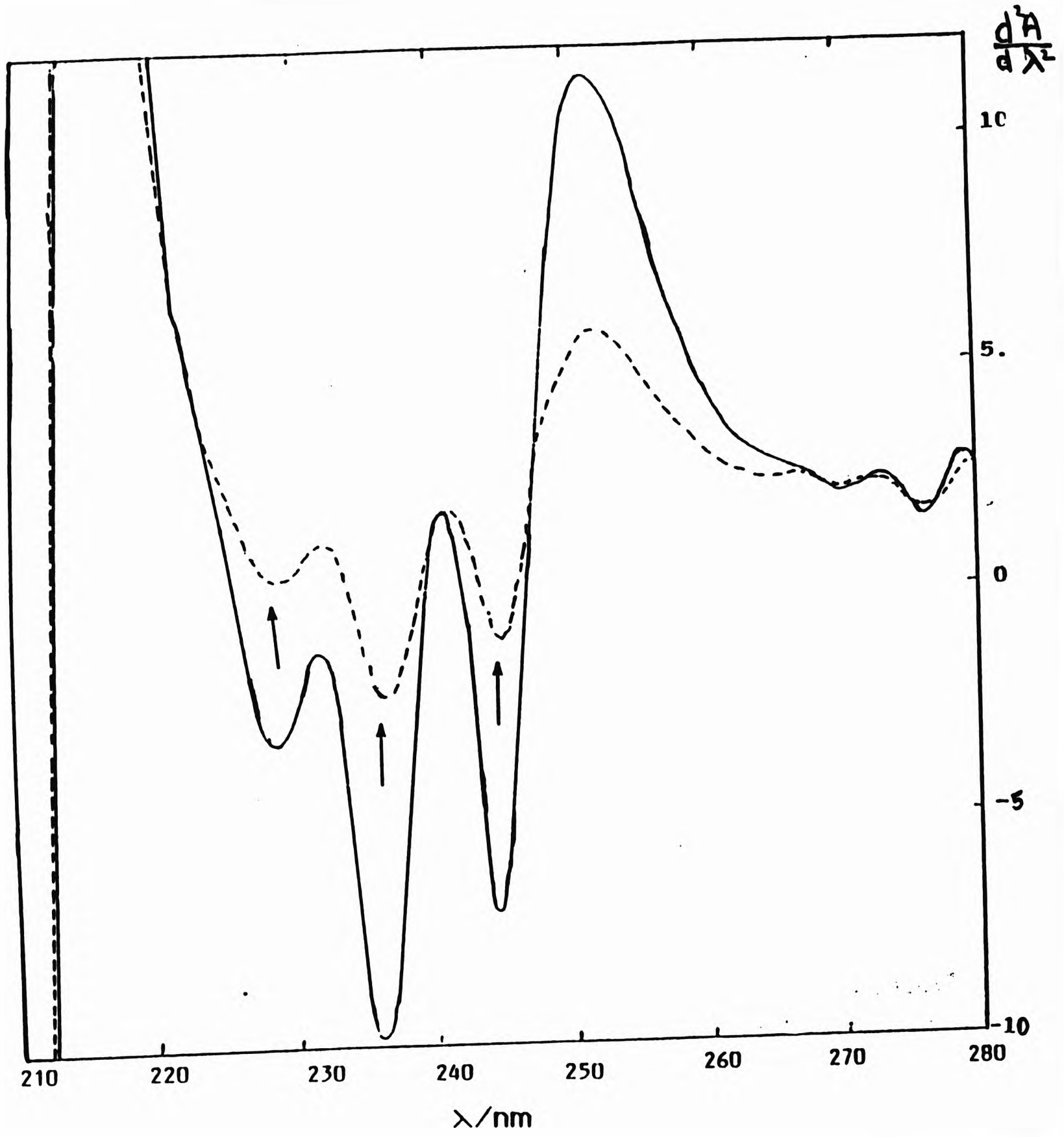

FIGURE 4.2 (a2)

Second derivative (2D) electronic absorption spectra of cyclohexane-reconstituted lipid/chloroform extracts of methyl linoleate obtained subsequent to autoxidation in air at ambient temperature (-----), or exposure to a catalytic Fe(II)/EDTA/H_2O_2 (—) system.

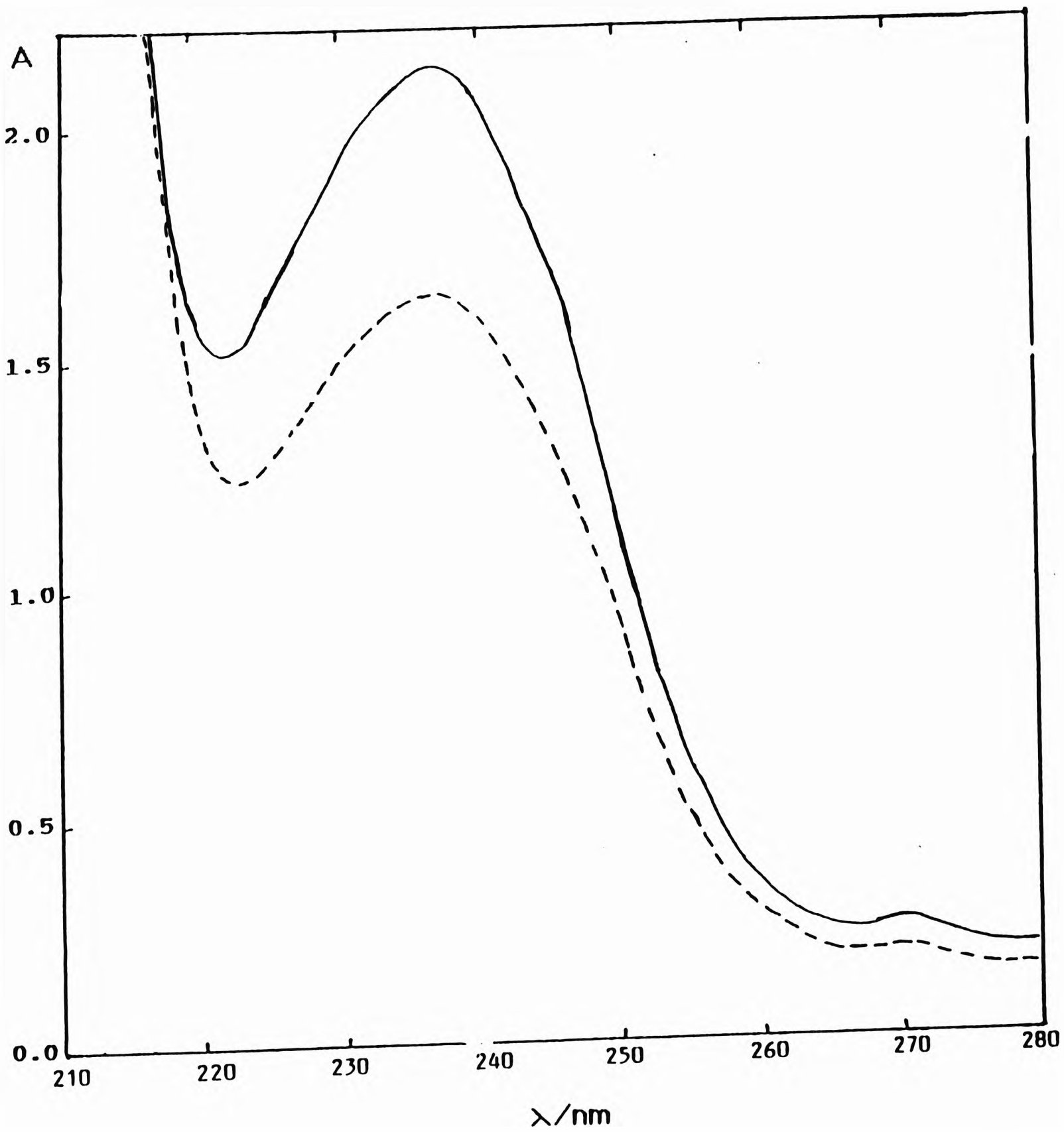

FIGURE 4.2 (b1)

Zero-order electronic absorption spectra of cyclohexane-reconstituted lipid/chloroform extracts of methyl linolenate obtained subsequent to autoxidation in air at ambient temperature (-----), or exposure to a catalytic Fe(II)/EDTA/H_2O_2 (———) system.

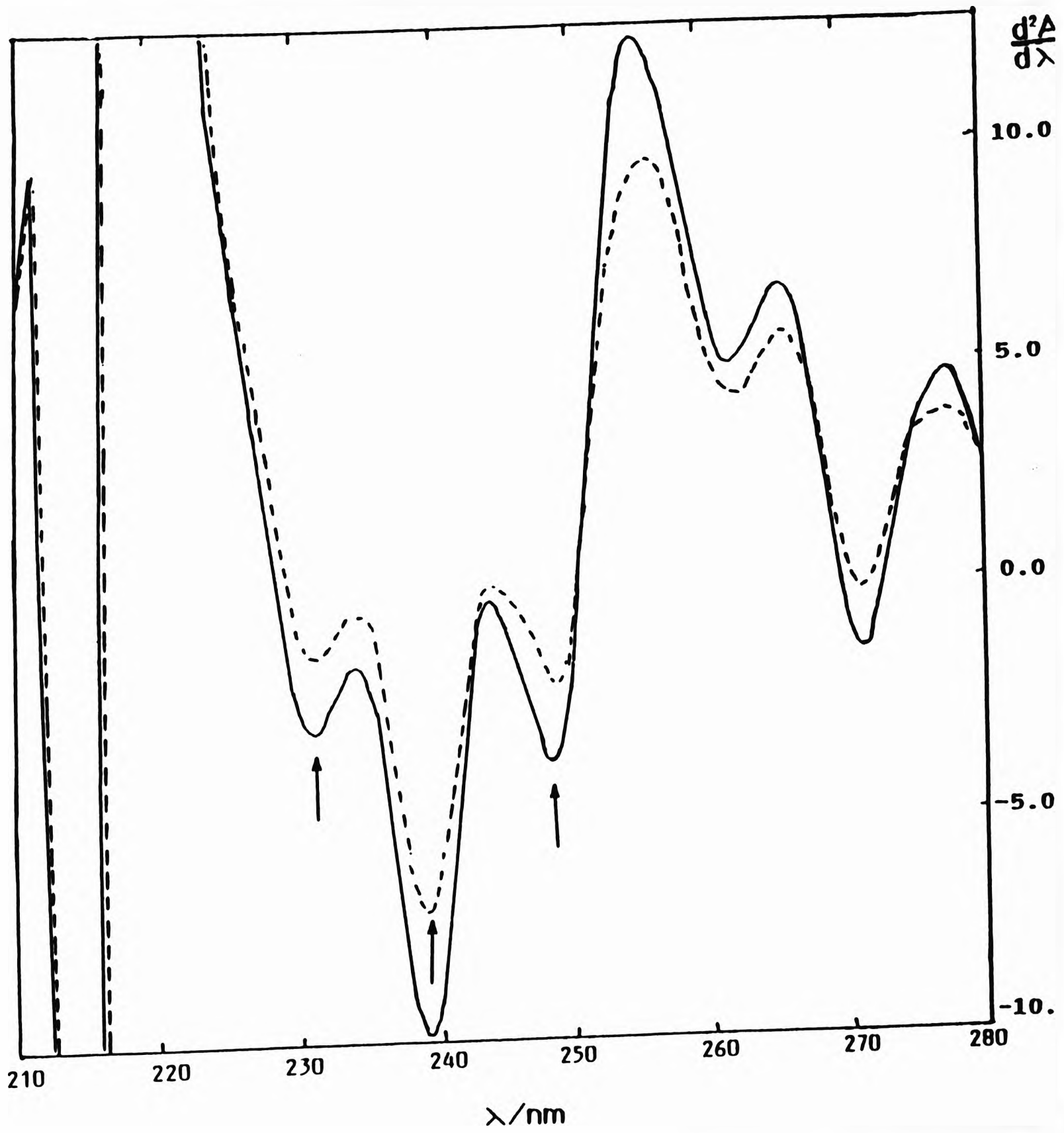

FIGURE 4.2 (b2)

Second derivative (2D) electronic absorption spectra of cyclohexane-reconstituted lipid/chloroform extracts of methyl linolenate obtained subsequent to autoxidation in air at ambient temperature (-----), or exposure to a catalytic Fe(II)/EDTA/H_2O_2 (—) system.

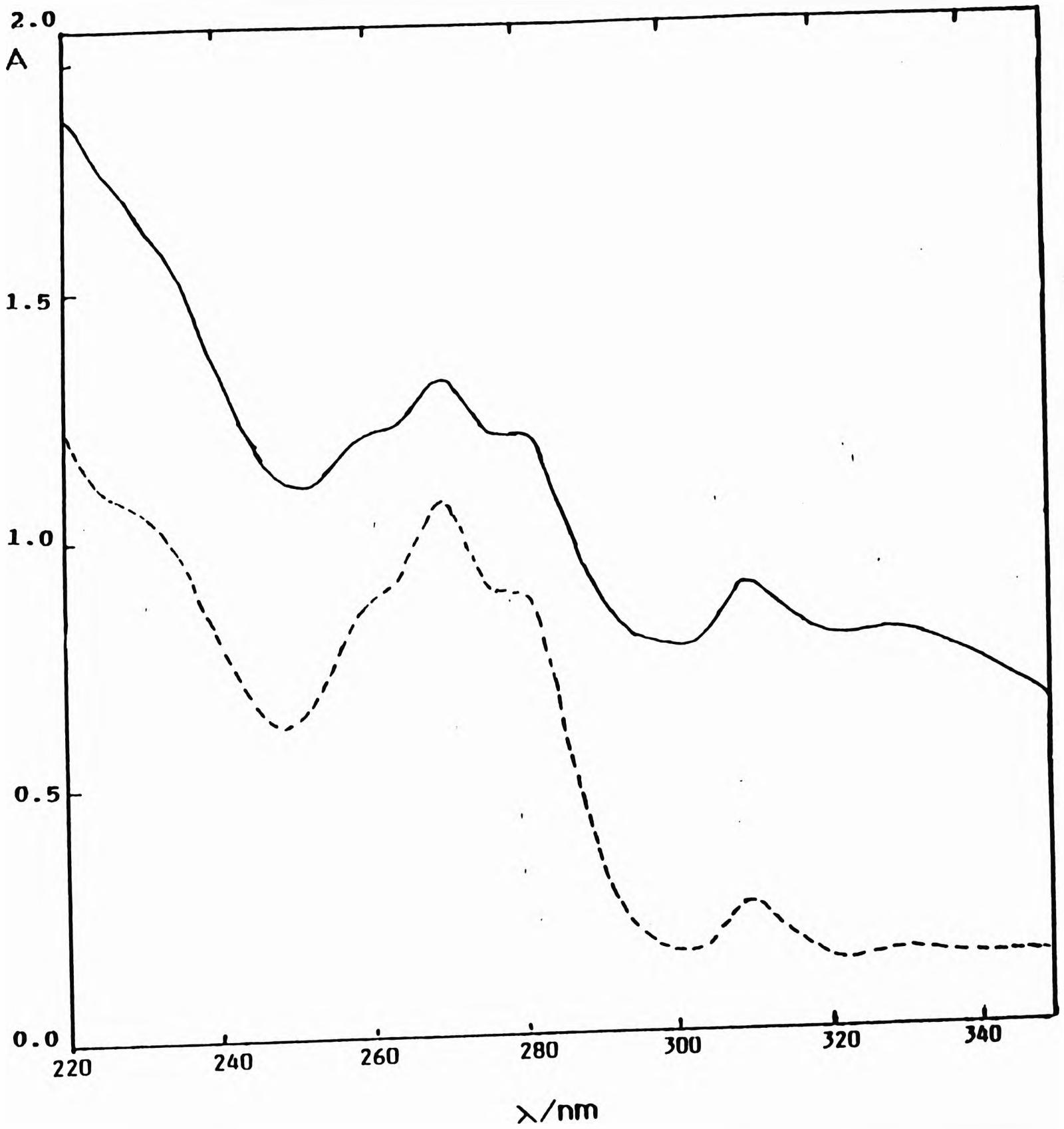

FIGURE 4.3 (a)

Zero-order electronic absorption spectra of methyl linoleate obtained subsequent to reduction with $NaBH_4$ followed by dehydration with alcoholic H_2SO_4 obtained subsequent to autoxidation in air at ambient temperature ((-----) or exposure to a catalytic Fe(II)/EDTA/H_2O_2 (—) system.

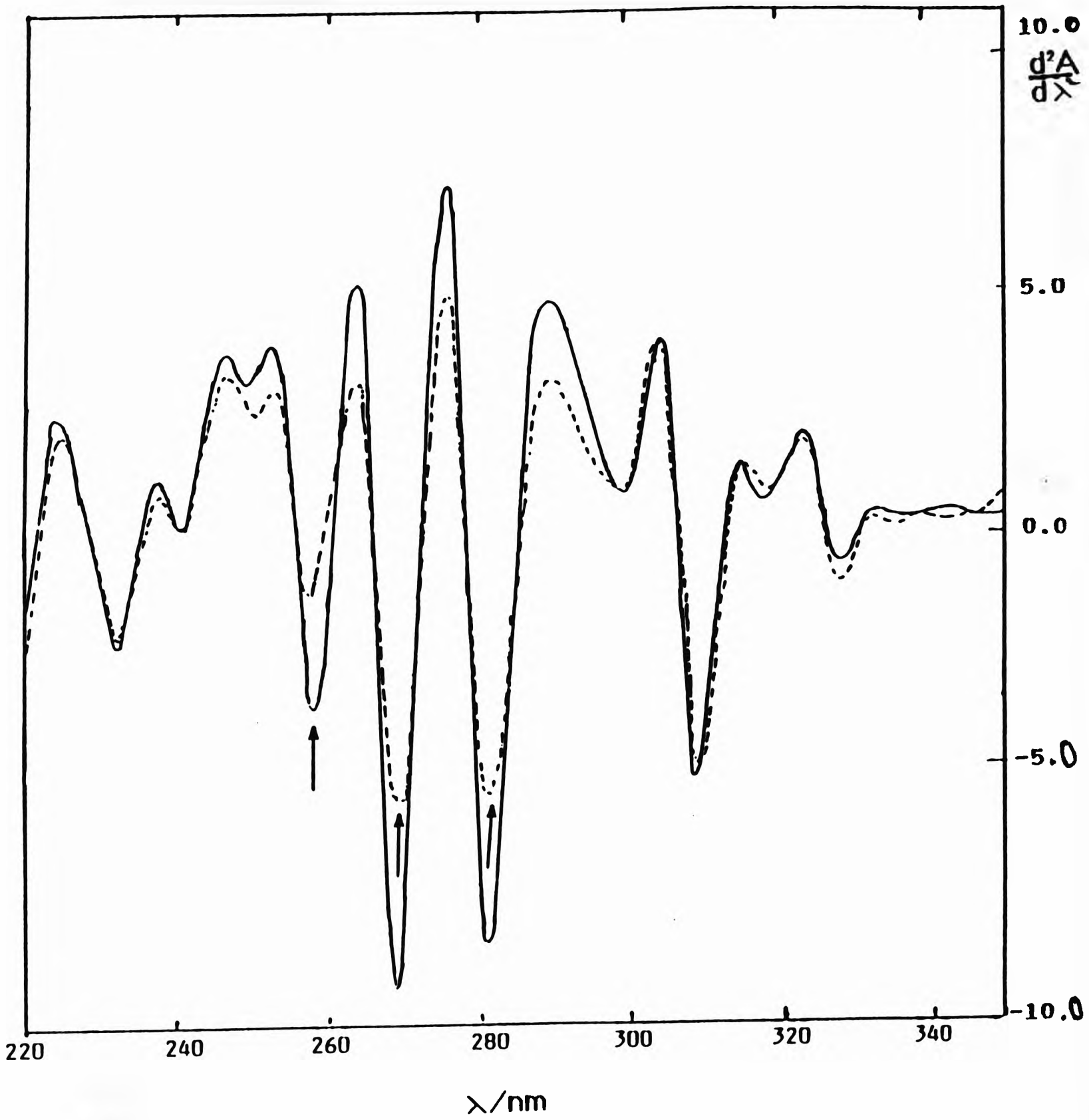

FIGURE 4.3 (b)

Second derivative (2D) electronic absorption spectra of methyl linoleate obtained subsequent to reduction with $NaBH_4$ followed by dehydration with alcoholic H_2SO_4 obtained subsequent to autoxidation in air at ambient temperature ((-----) or exposure to a catalytic Fe(II)/EDTA/H_2O_2 (—) system.

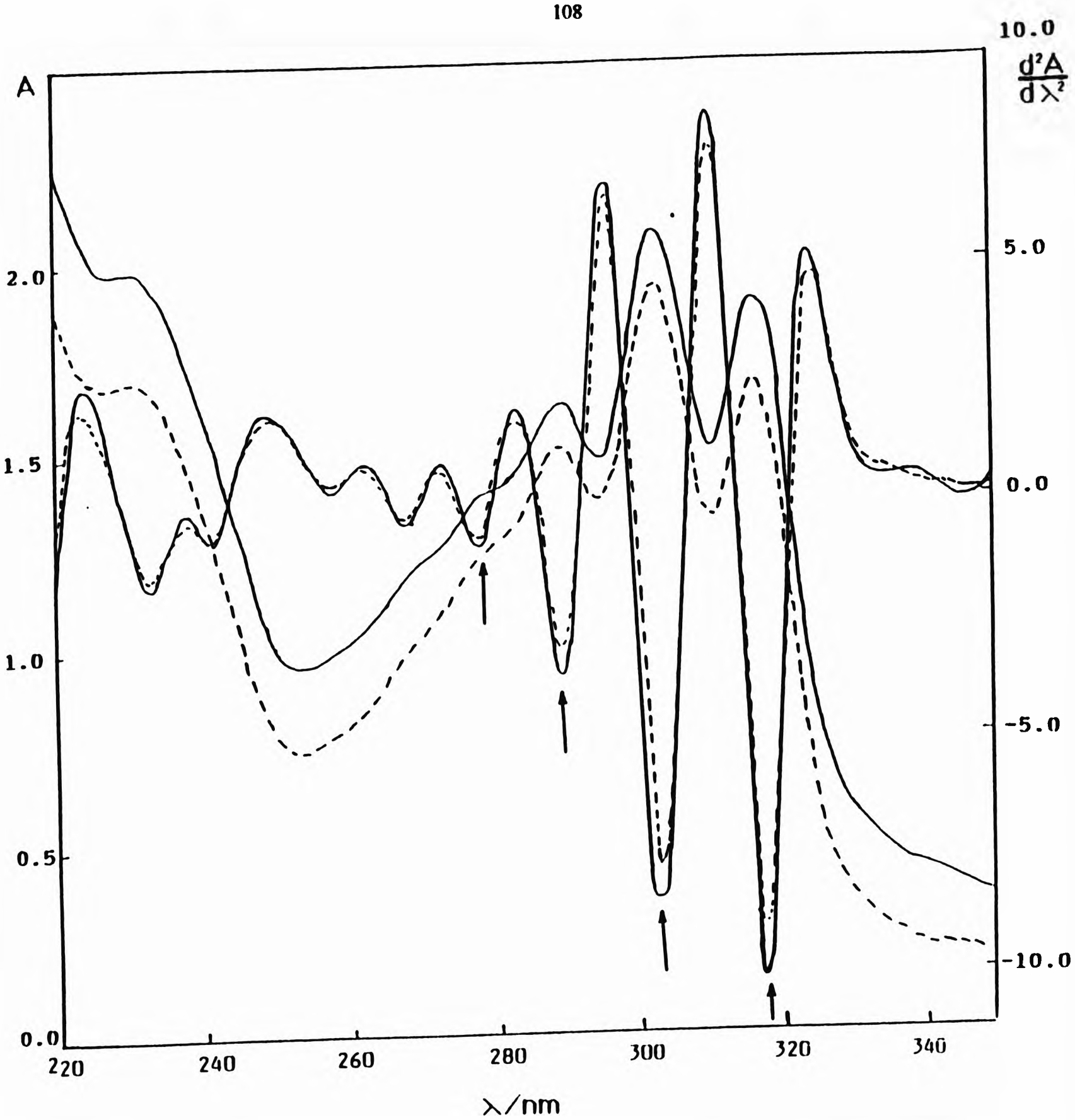

FIGURE 4.4

Zero-order and corresponding second derivative (2D) electronic absorption spectra of methyl linolenate obtained subsequent to reduction with $NaBH_4$ followed by dehydration with alcoholic H_2SO_4 obtained subsequent to autoxidation in air at ambient temperature (----) or exposure to a catalytic Fe(II)/EDTA/H_2O_2 (——) system.

4.2.2 Application of reduction/dehydration procedure to the analysis of inflammatory synovial fluid samples

Figure 4.5 shows typical examples of zero-order and corresponding 2D absorption spectra of $NaBH_4$-reduced/H_2SO_4-dehydrated samples of ethanol-reconstituted lipid/chloroform extracts of rheumatoid synovial fluid. The overlapping absorption bands observed in the 220-350 nm region of the zero-order spectra are clearly resolved in the corresponding 2D spectra. The 2D spectra of synovial fluid extracts contain signals (minima) located at 261, 269 and 279 nm (figure 4.5) which are characteristic of triene-containing chromophores (as illustrated for methyl linoleate in Figure 4.3) and are present in all spectra obtained from a series of 8 different synovial fluid samples studied. However, although these spectra contained a signal at 290.5 nm, the peroxidised linolenate-derived conjugated tetraene signal located at 318 nm was of only weak intensity and that at 303 nm was not detectable at all, indicating that there is little or no peroxidised linolenate in human knee-joint synovial fluid.

Treatment of rheumatoid synovial fluid samples with the catalytic Fe(II)/EDTA/H_2O_2 system gave rise to a marked increase in absorbance in the 220-350 nm region of the spectrum as shown in Figure 4.5. However, due to interferences from the Fe(II)/EDTA/H_2O_2 system-dependent increase in intensity of several alternative overlapping 2D signals present in the spectrum, the only detectable increase in magnitude of the peroxidised linoleate-derived triene signals is that at 269 nm.

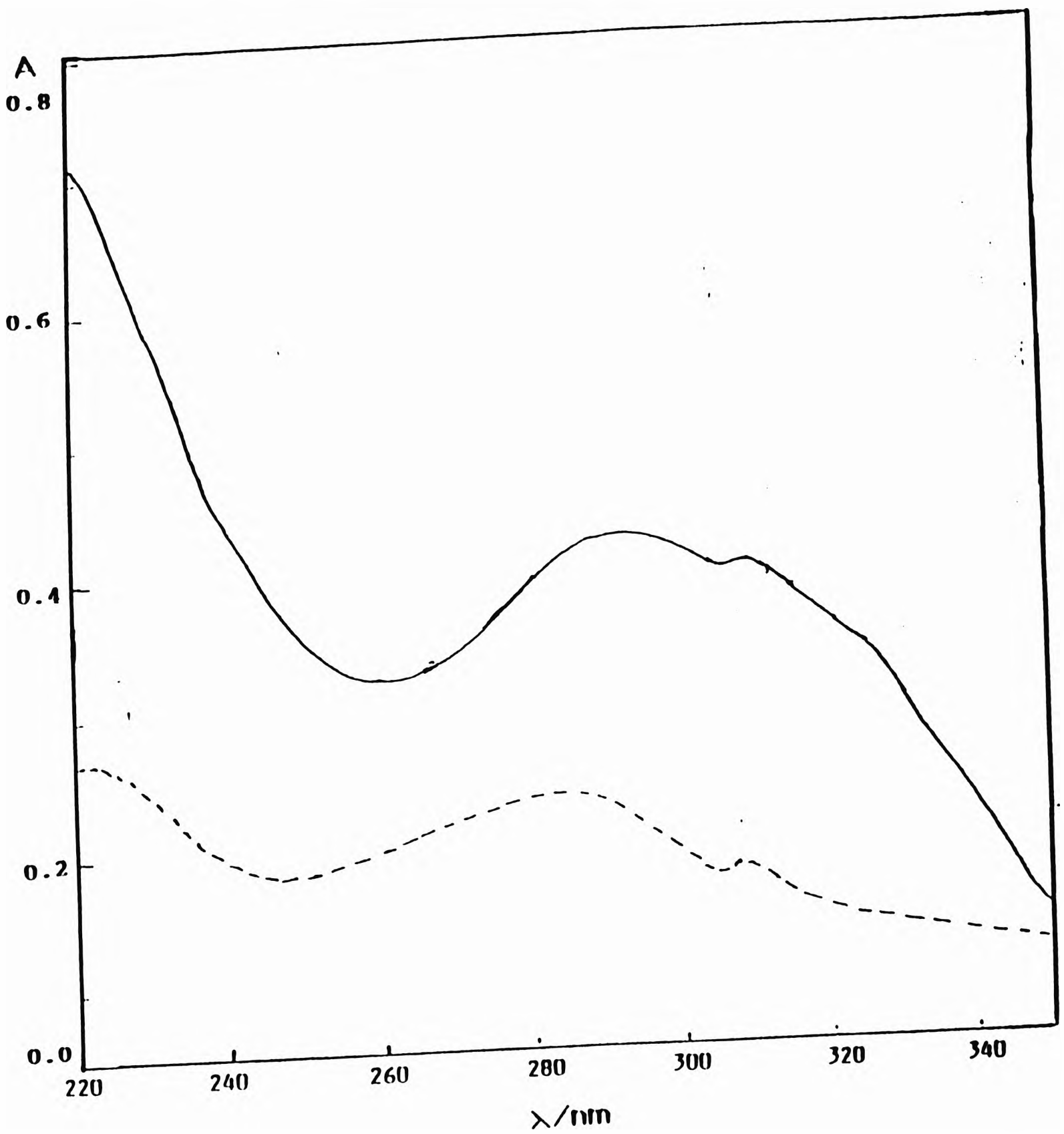

FIGURE 4.5 (a)

Zero-order electronic absorption spectra of synovial fluid after being subjected to reduction with $NaBH_4$ followed by dehydration with alcoholic H_2SO_4 (-----), or exposure to a catalytic Fe(II)/EDTA/H_2O_2 (—) system.

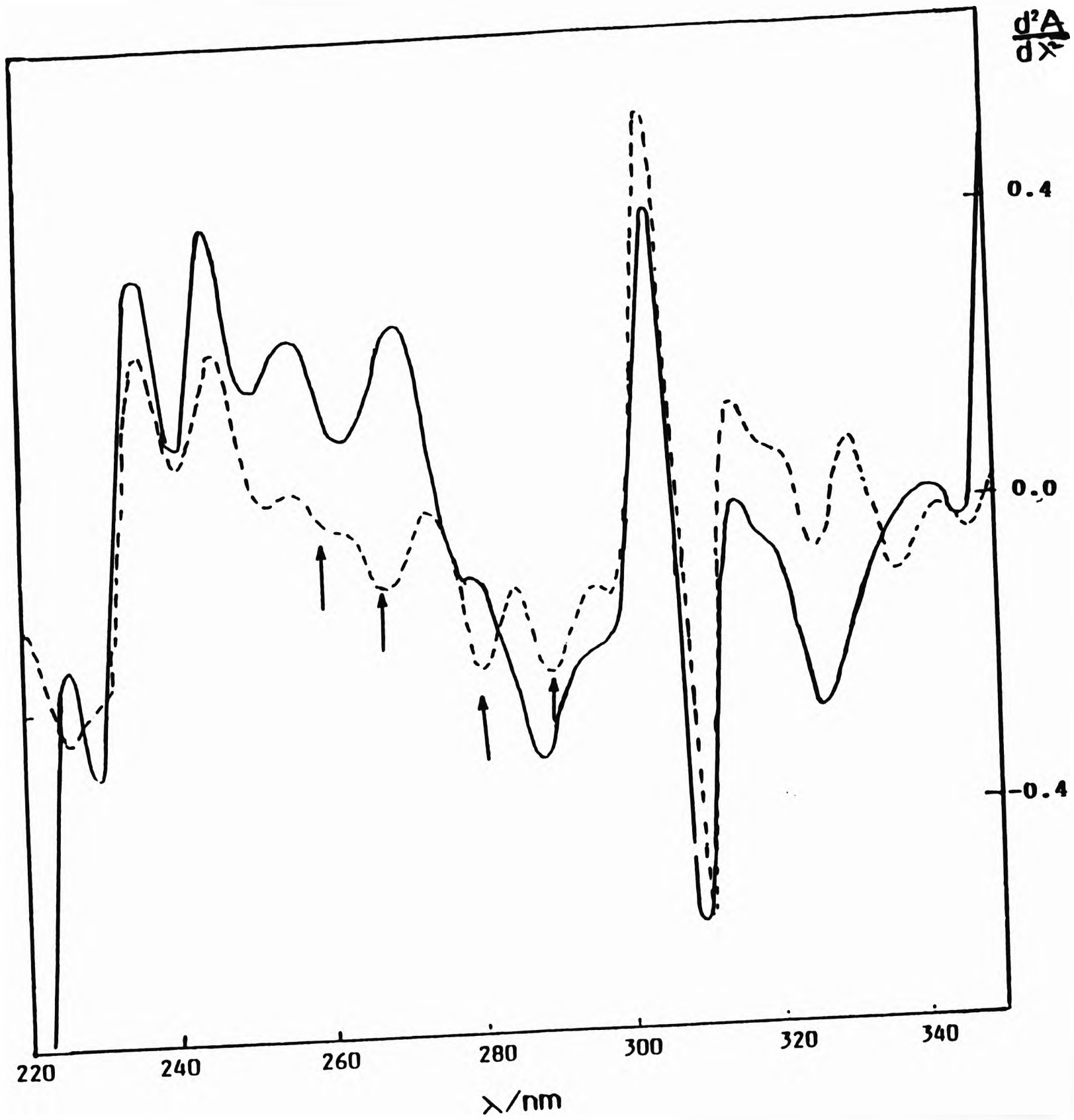

FIGURE 4.5 (b)

Second derivative (2D) electronic absorption spectra of synovial fluid after being subjected to reduction with $NaBH_4$ followed by dehydration with alcoholic H_2SO_4 (-----), or exposure to a catalytic Fe(II)/EDTA/H_2O_2 (—) system.

4.2.3 Prostaglandin E_2

A typical 2D-absorption spectra of prostaglandin E_2 after being subjected to the reduction./dehydration procedure described above is shown in figure 4.6. The 2D spectra of PGE_2 contains weak signals (minima) located at 260, 268, 273 and 282 nm, which are characteristic of triene species. This pattern was also observed in both control and peroxidised human colonic biopsies (Table 4.2). However, the magnitude of the intensity of signals for minima at 284 nm (0.0025, n=2) and at 273 nm (0.001, n=2) was less for PGE_2, than for those from colon biopsy samples (284 nm : 0.0062 $\pm$ 0.00098], mean $\pm$ standard deviation ; n=14). At 275 nm, these values were 0.0029 $\pm$ 0.00061, n=14.

4.2.4 *In vitro* peroxidation of colorectal biopsies.

Figure 4.7 shows a typical 2D absorption spectra obtained from paired human colon tissue samples of control patients (a) before and (b) after peroxidation with the Fe(II)/EDTA/H_2O_2 system. Figure 4.8(a) shows a typical 2D spectrum of a sample of human colon tissue obtained from a patient with ulcerative colitis which was processed with the reduction/dehydrating procedure, conducted immediately subsequent to thawing at ambient temperature. Figure 4.8(b) represents a 2D spectrum of a sample from the same paired biopsy sample which was incubated with the Fe(II)/EDTA/H_2O_2 system before being reduced and dehydrated in the above manner. In comparison to control peroxidised linoleic and linolenic acid, the colonic biopsy spectra appeared to have extra minima in the region detecting triene species (Table 4.2). Moreover, the magnitude of the minimum located at 281 nm (0.061 $\pm$ 0.0006, n=3) for control peroxidised linoleate is approximately the same as the minimum at 268 nm (0.065 $\pm$ 0.0021, n=3), whereas the magnitude of the minimum, for colonic biopsy samples at 284 nm (0.0064 $\pm$ 0.00098, n=14) was consistently greater than that at 274 nm (0.0029 $\pm$ 0.00061, n=14). Overall, there was no significant difference in the amounts of conjugated trienes and tetraenes detected with or without peroxidation induced by the Fe(II)EDTA/H_2O_2 system. This may be attributable to interferences arising from the

peroxidising system-dependent increase in the intensity of several alternative overlapping 2D signals present in the spectrum.

Figure 4.8 shows typical 2D absorption spectra obtained from paired human colon tissue samples of patients with inactive ulcerative colitis (a) before and (b) after peroxidation with the Fe(II)/EDTA/H_2O_2 system. Figure 4.8(a) shows a 2D spectrum of a sample from a patient with ulcerative colitis which was processed by the reduction/dehydration procedure. Figure 4.8(b) shows a 2D spectrum of a sample from the same paired biopsy sample which was incubated with the Fe(II)/EDTA/H_2O_2 system before being reduced and dehydrated in the manner described.

The peak identification and intensity of minima for colitis tissue samples were very similar to that of control colon samples (Figure 4.7) when compared to peroxidised linoleic and linolenic acids. The only significant difference observed between ulcerative colitis samples (Figure 4.8) and that of control biopsy (Figure 4.7) is that the signals in the tetraene regions (i.e. 303 and 317 nm) increased in the samples which were incubated with the ·OH radical generating system (iron/EDTA/H_2O_2). These results demonstrate the increased production of tetraene products (attributable to the peroxidation of linolenate) which may be ascribable to the faster peroxidation rate of the more unsaturated fatty acid.

4.2.5 Recovery experiment (linoleic or linolenic acid)

Figure 4.9 shows the results of recovery experiments in which peroxidised linoleic acid was added to biopsy samples which were processed as described above for the tissue samples. Figure 4.9(a) represents the result obtained with linoleic acid alone (Table 4.2). Figure 4.9(b) shows a virtually identical spectrum obtained with linoleic acid when added to a typical colon tissue sample.

Figure 4.10 shows the results of a recovery experiment in which peroxidised linolenic acid was added to biopsy samples processed as described above for the tissue samples. Figure 4.10(a) represents a spectrum obtained with linolenic acid alone (Table 4.2), whilst

Figure 4.10(b) shows results obtained with linolenic acid when added to a typical colon tissue sample.

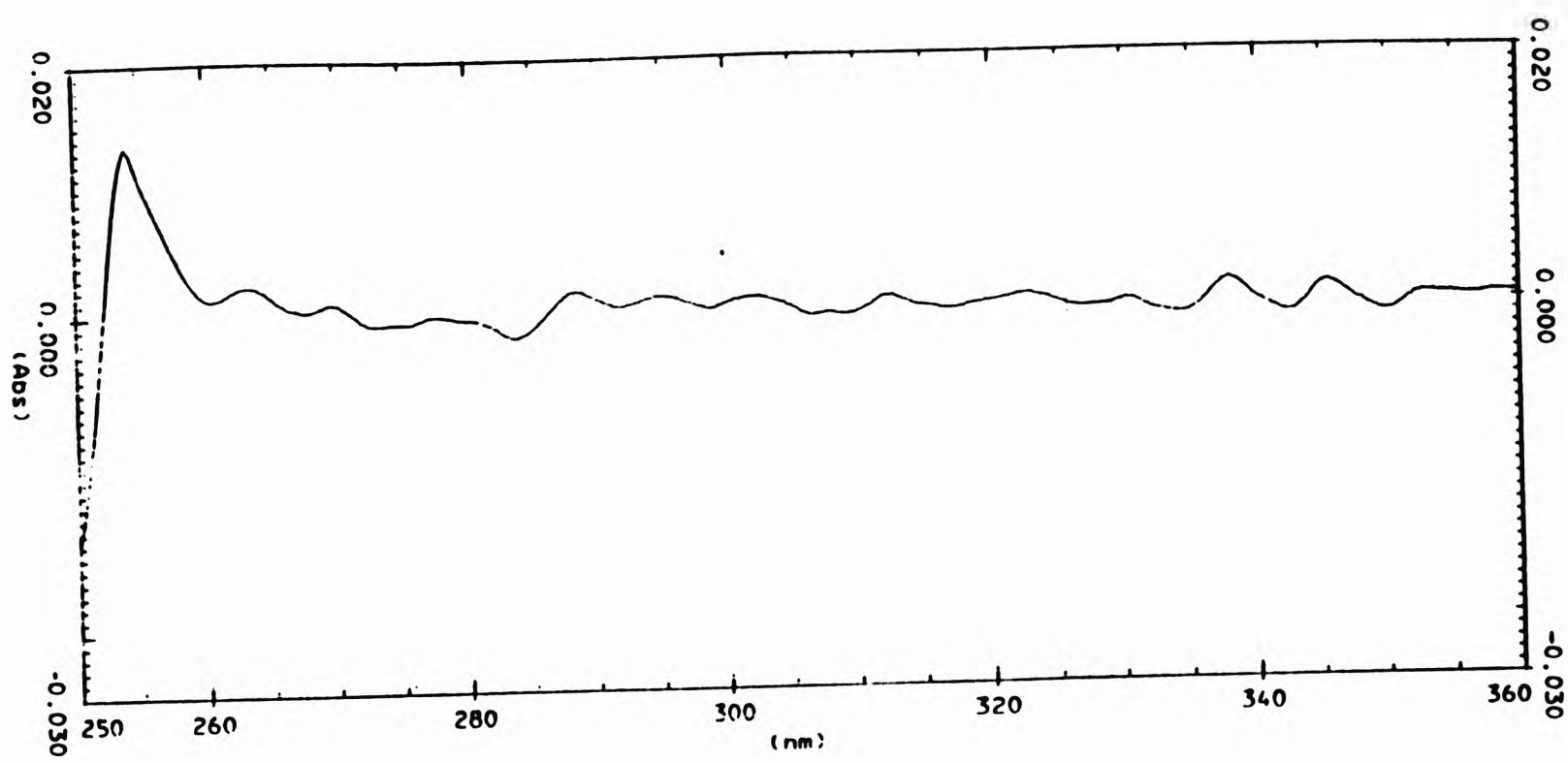

FIGURE 4.6

Second derivative electron spectra of PGE_2 obtained subsequent to reduction with $NaBH_4$ followed by dehydration with alcoholic H_2SO_4

a)

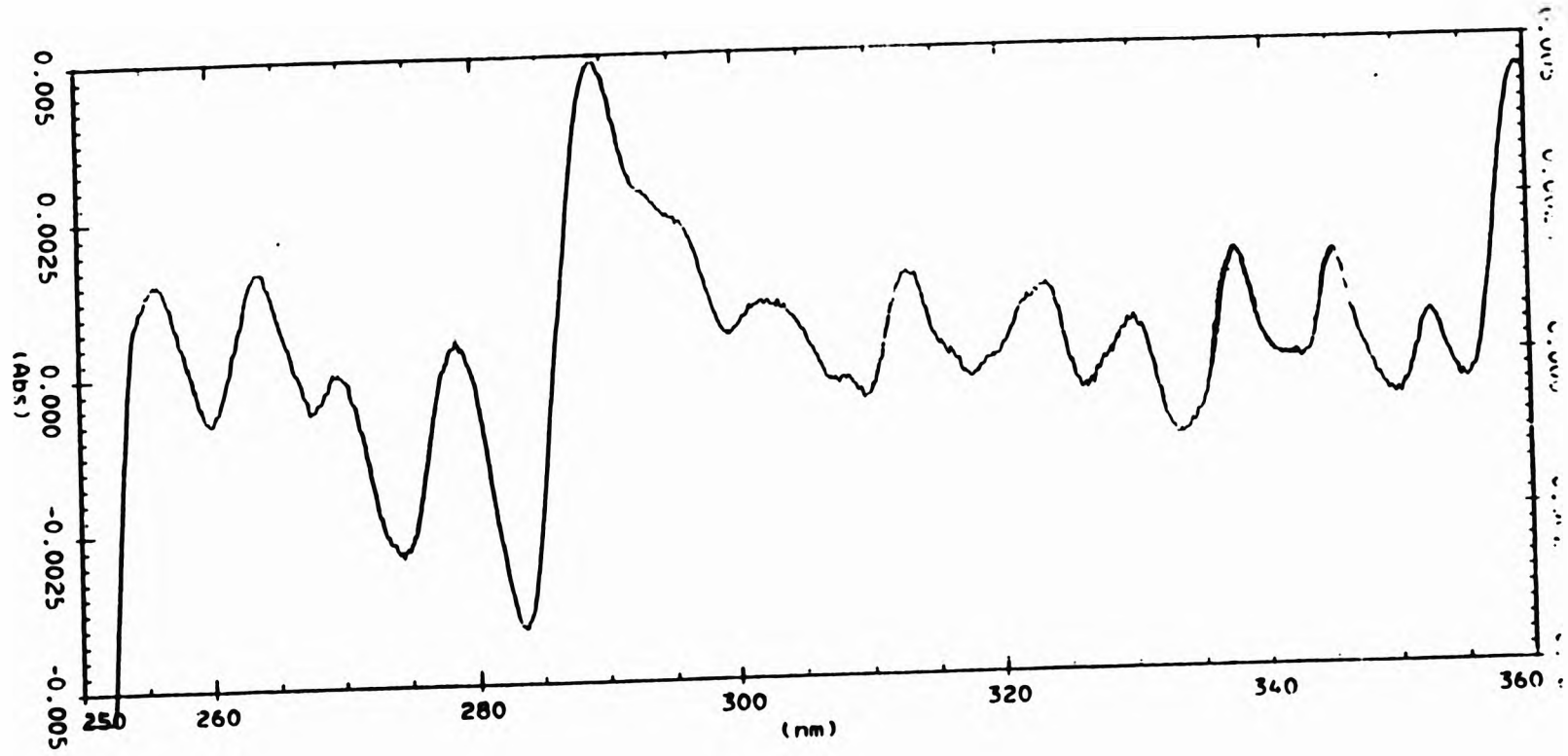

b)

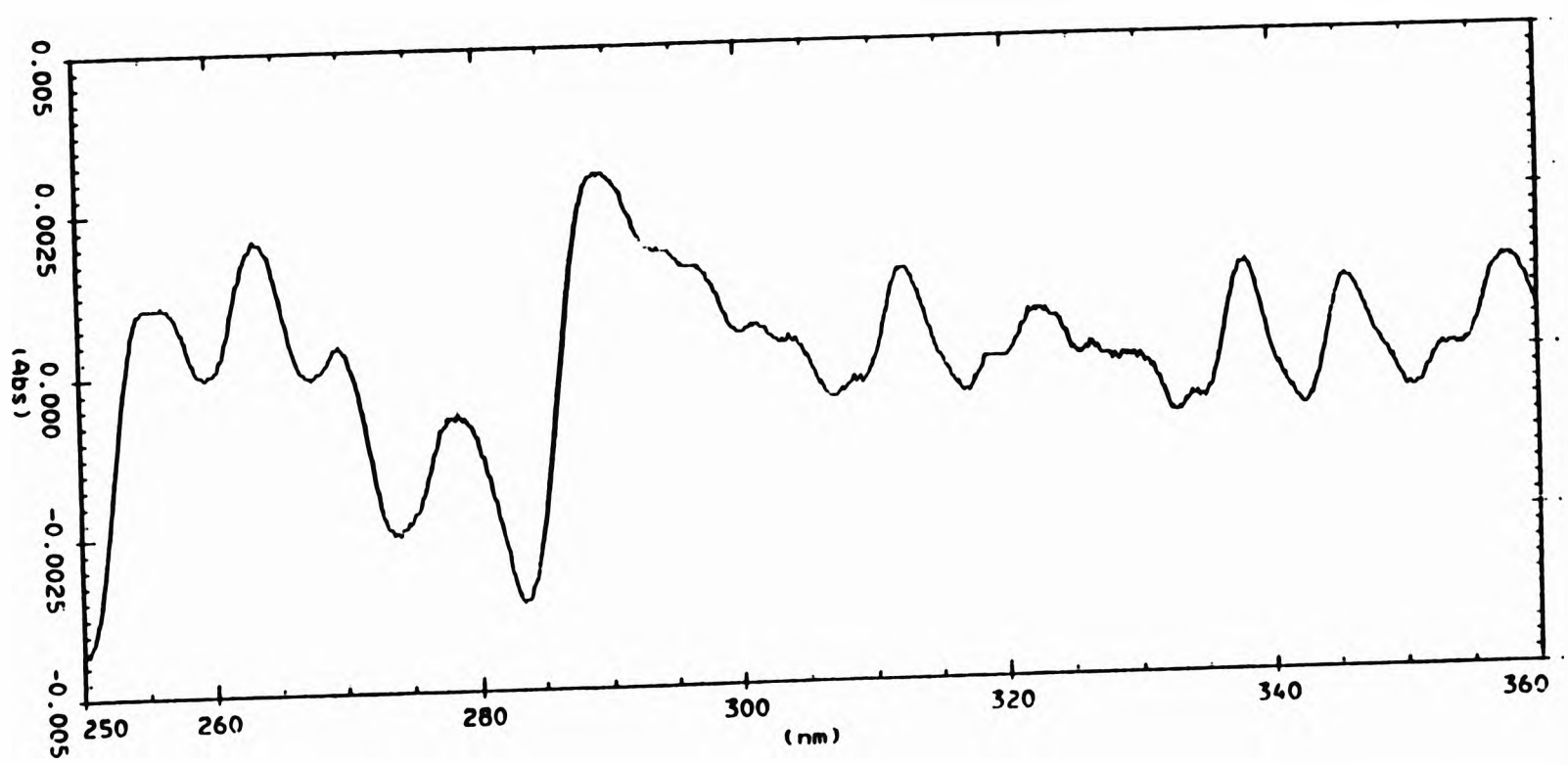

FIGURE 4.7

Second derivative absorption spectra obtained from paired human colon tissue sample of control patients which were processed with reducing/dehydrating procedure. a) shows the control sample which were processed immediately on thawing and, b) shows the sample which was incubated with the Fe(II)/EDTA/H_2O_2 system before being reduced and dehydrated.

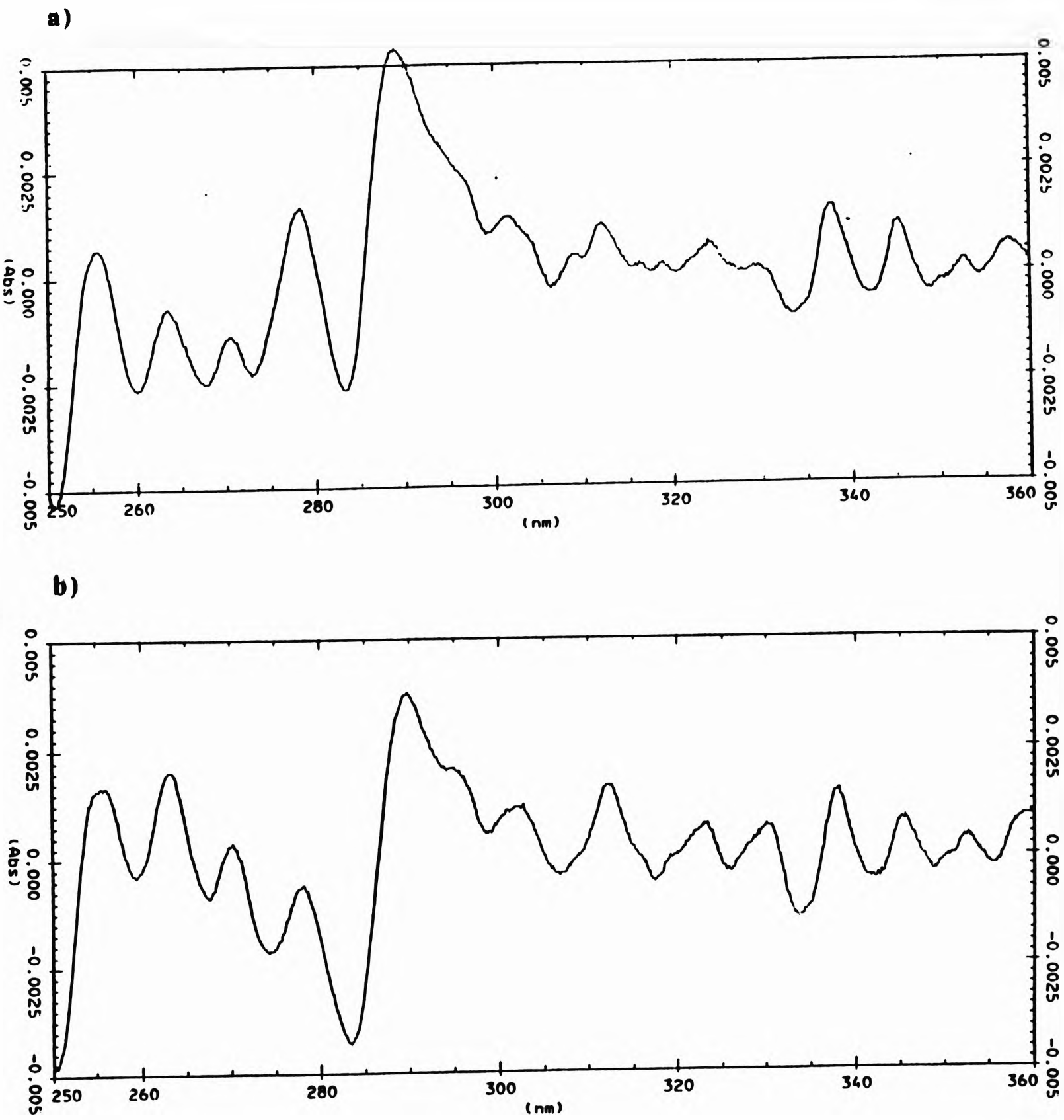

FIGURE 4.8

Second derivative absorption spectra obtained from paired human colon tissue sample of patients with ulcerative colitis which were processed with reducing/dehydrating procedure. a) shows the sample which were processed immediately on thawing and, b) shows the sample which was incubated with Fe(II)/EDTA/H_2O_2 system before being reduced and dehydrated

a)

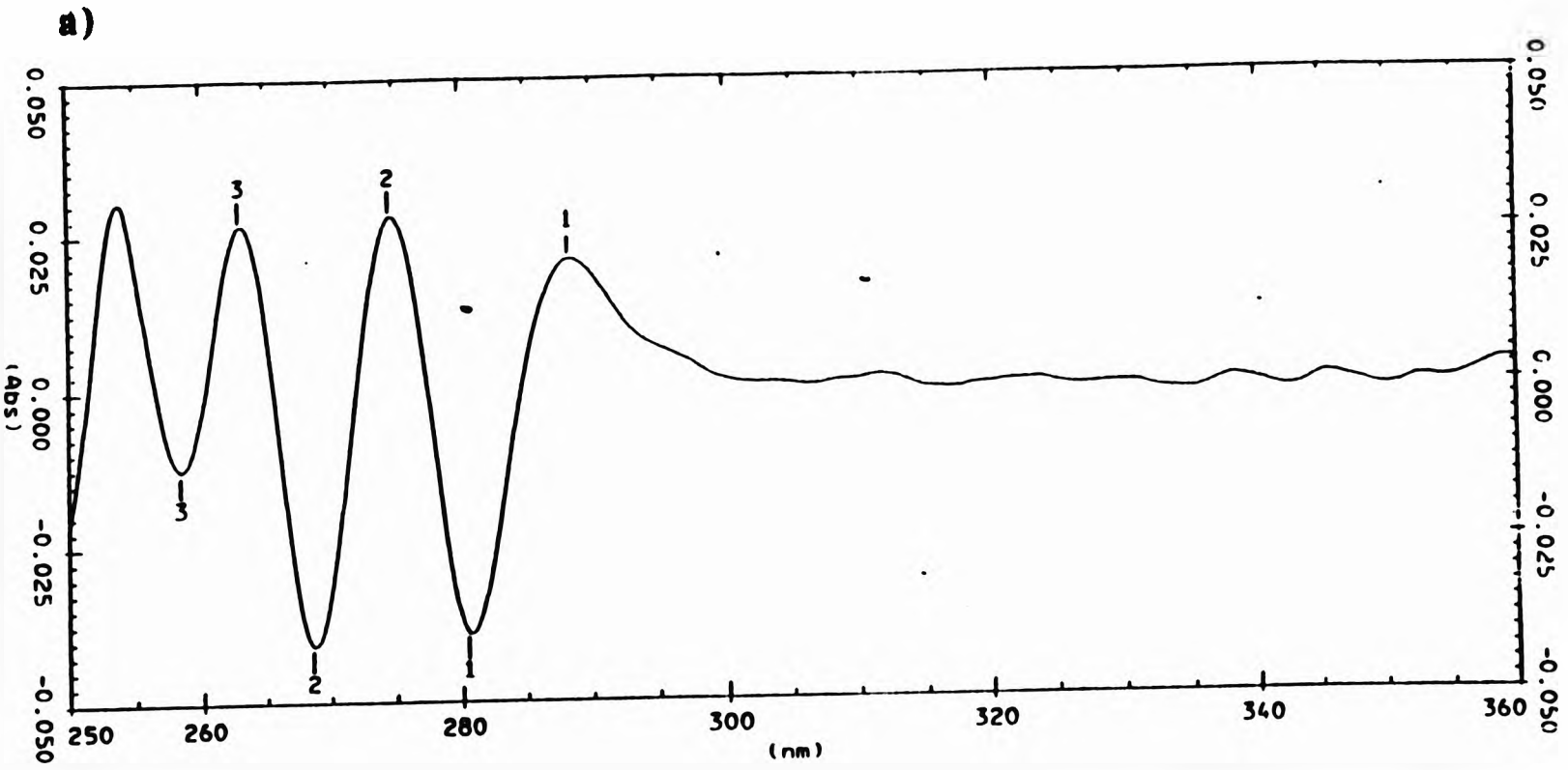

b)

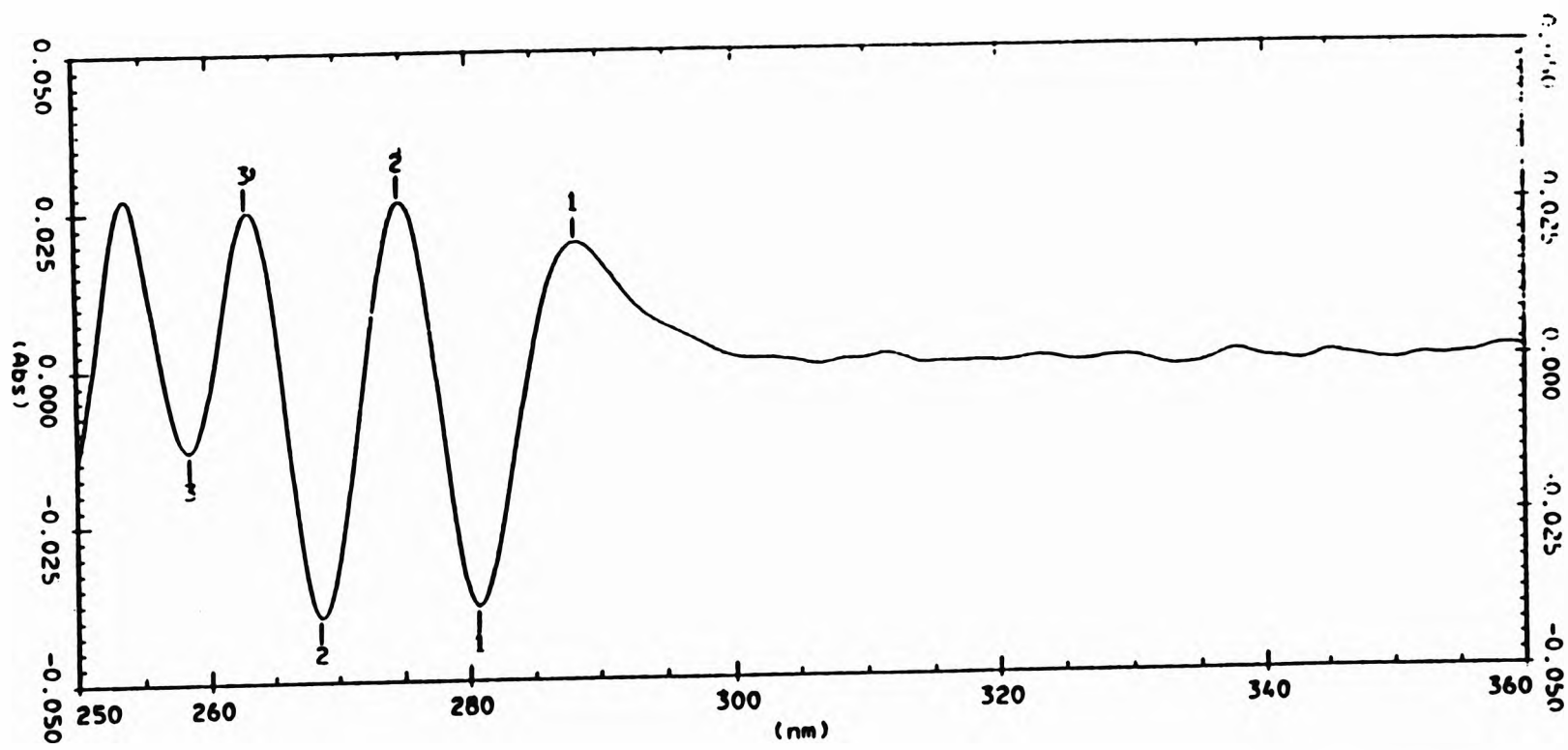

FIGURE 4.9

Second derivative spectra obtained from recovery experiment of linoleic acid after undergoing reduction/dehydration procedure from a) peroxidised linoleate and b) peroxidised linoleate added to colorectal biopsy and processed as described for tissue sample.

a)

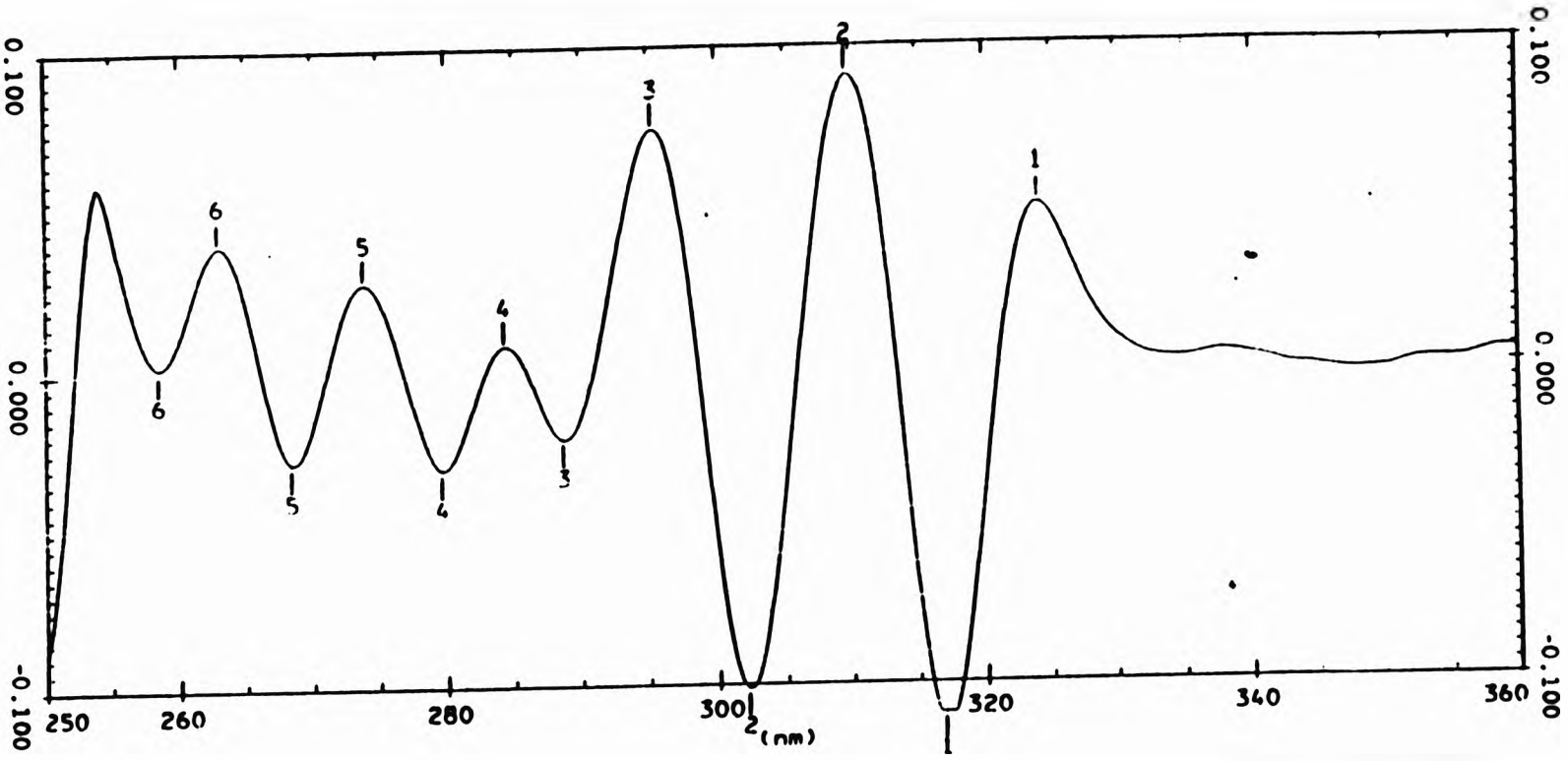

b)

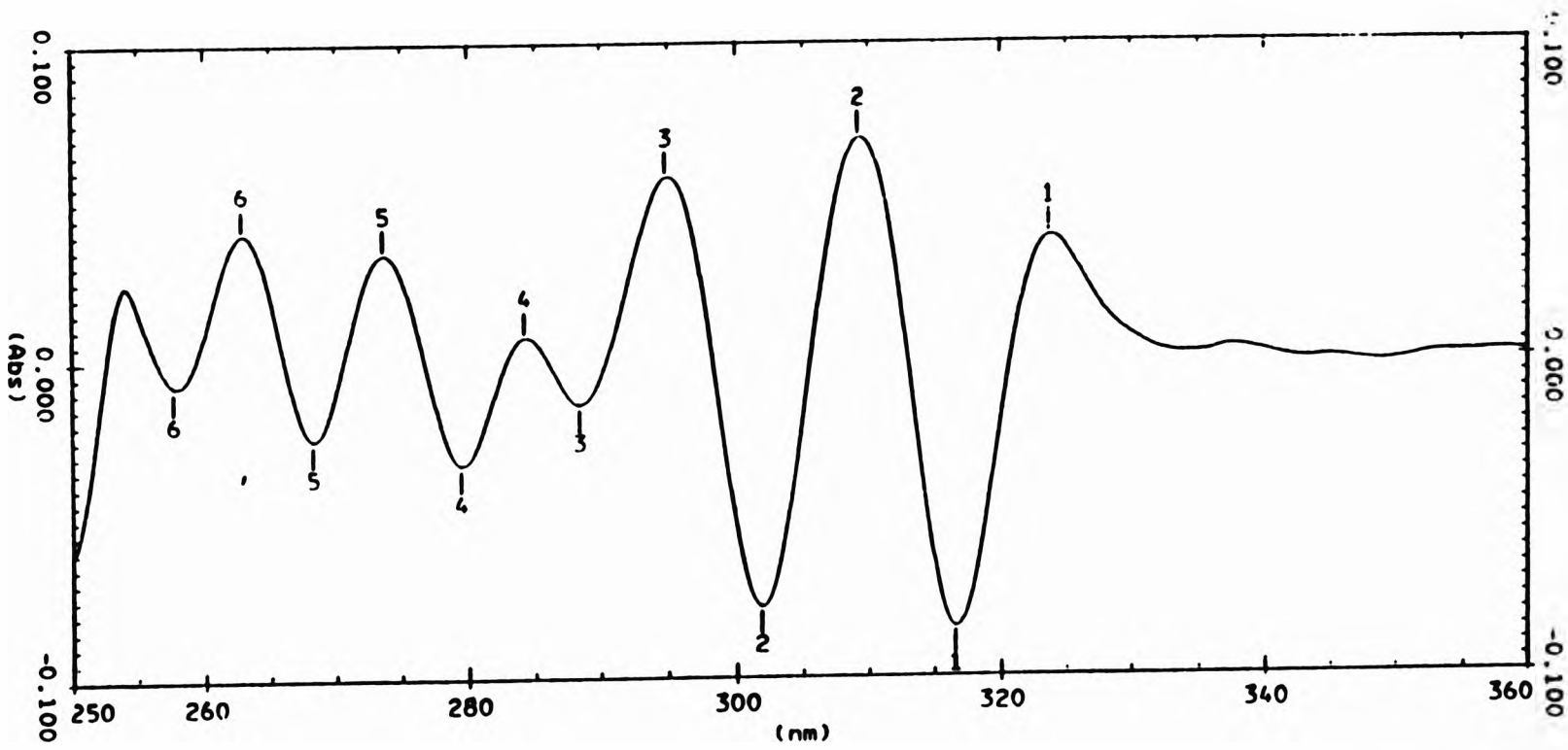

FIGURE 4.10

Second derivative spectra obtained from recovery experiment of linolenic acid after undergoing reduction/dehydration procedure from a) peroxidised linolenate and b) peroxidised linolenate added to colorectal biopsy and processed as described for tissue sample.

4.2.6 Peroxidation of colorectal biopsies from patients with ulcerative colitis

Figure 4.11 shows a typical 2D spectrum obtained from the colon tissue samples of 2 control patients, following derivatisation with the reduction/dehydration system. Figure 4.12 shows a 2D spectrum obtained from paired biopsies of the colorectal regions of 2 patients with active ulcerative colitis, subsequent to the reduction/dehydration procedure. For both control and active colitis patients, minima were observed at wavelengths suggestive of both triene and tetraene chromophores, but, as with the *in vitro* experiments with colorectal biopsies, 4 minima were seen in the region of the spectrum characteristic of peroxidised linoleate and linolenate (Table 4.2). Furthermore, as before the minima at 275 nm was less (108 ± 81, n=51) than that at 284 nm (376 ± 264, n=51). The major difference observed between the spectra of control and colitis patients was the variation in the relative amounts of triene and tetraene present. Figure 4.11 shows a control sample which appeared to predominately have triene chromophores after derivatisation, whereas Figure 4.12 shows a relative increase in the tetraene chromophore in patients with active ulcerative colitis.

Results are expressed as the absorbance change at a particular wavelength per gram weight of tissue. For each sample, the conjugated oxidation products (COP) ratio was also calculated as described by Fishwick and Swoboda[98]. This parameter is independent of the weight of the sample or the amount of lipid extracted and is an index of the proportions of the tetraene and triene chromophores present, (the ratio of absorbance change at 301 nm to that at 268 nm). For a pure triene the ratio is zero, and for a pure tetraene it is 2.8.

The coefficient of repeatability was calculated from 8 sets of results, where paired biopsies from the same patients underwent separate reduction/dehydration analyses. The coefficient of repeatibilities at 275 nm/g was 97.14 and at 305 nm/g was 116.12. For the COP, the coefficient of repeatability was 1.285.

Overall, there were no significant differences between control patients and those with ulcerative colitis in terms of the absorbance changes seen at 275 nm/g or at 305 nm/g. However, the COP was significantly greater in patients with ulcerative colitis (inactive UC :

mean 2.51, n = 25; active UC : 2.44, n = 9) compared with controls (1.59, n = 13) (ρ = 0.012, ANOVA on $\log_{10}$- transformed values). However, there was no significant difference between patients with active and inactive disease (Figure 4.13).

a)

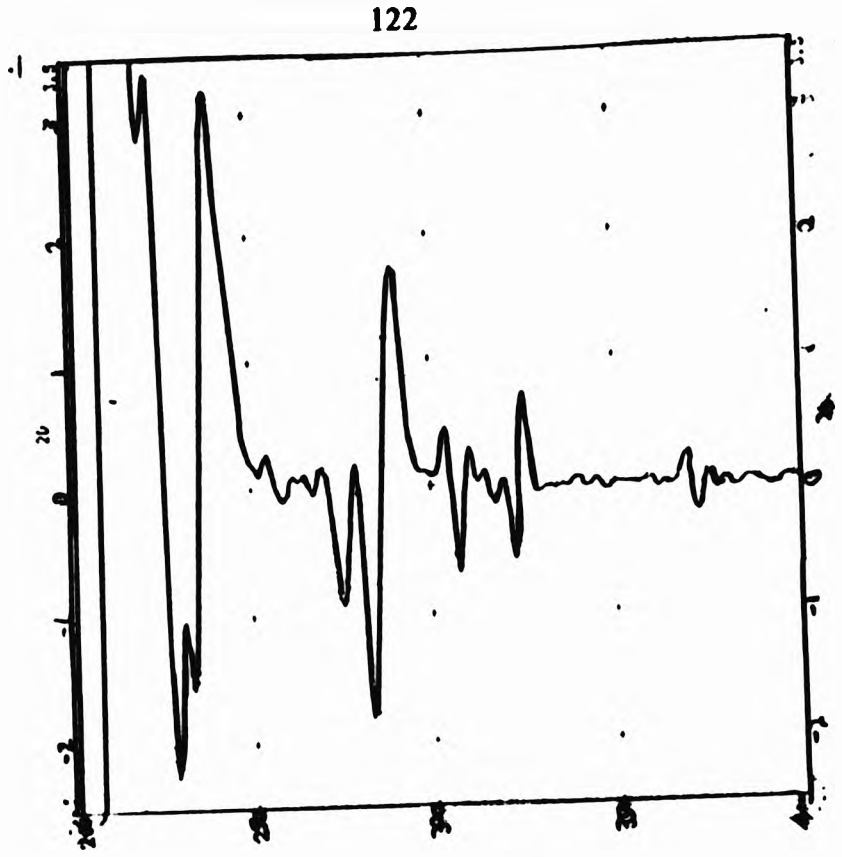

b)

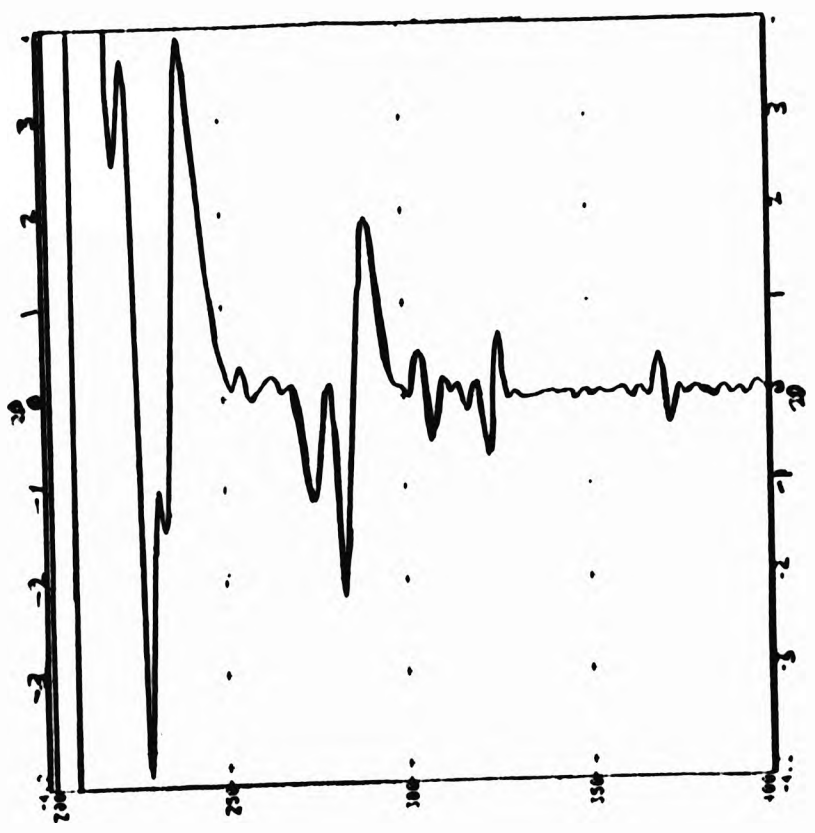

FIGURE 4.11

Second derivative electronic spectra obtained from colon tissue sample of 2 control patients after being treated with reduction/dehydration system.

a)

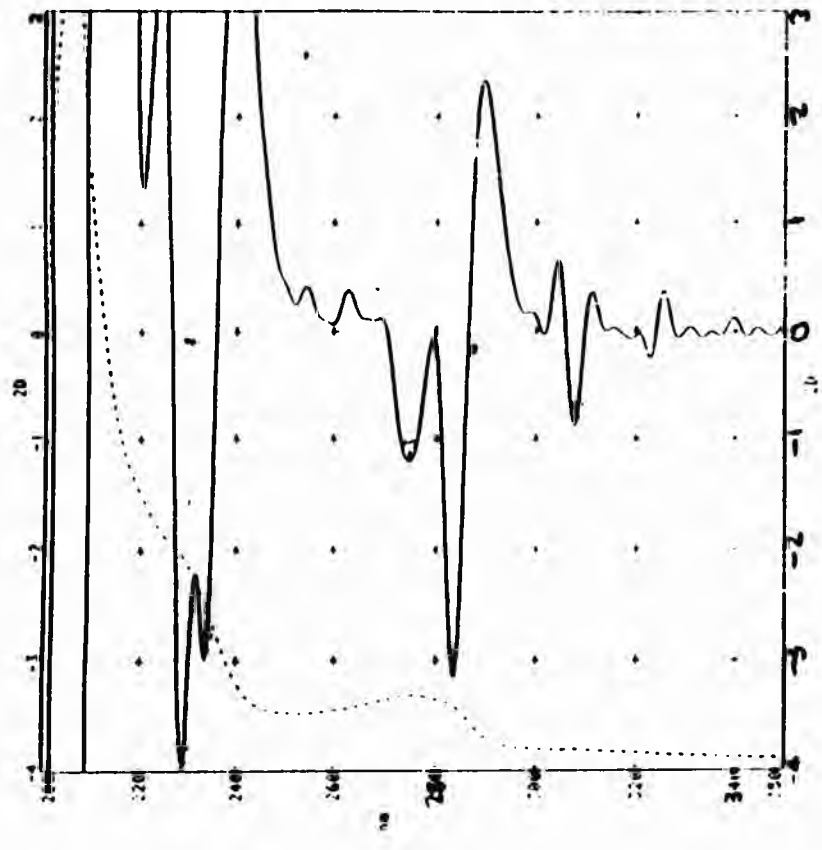

b)

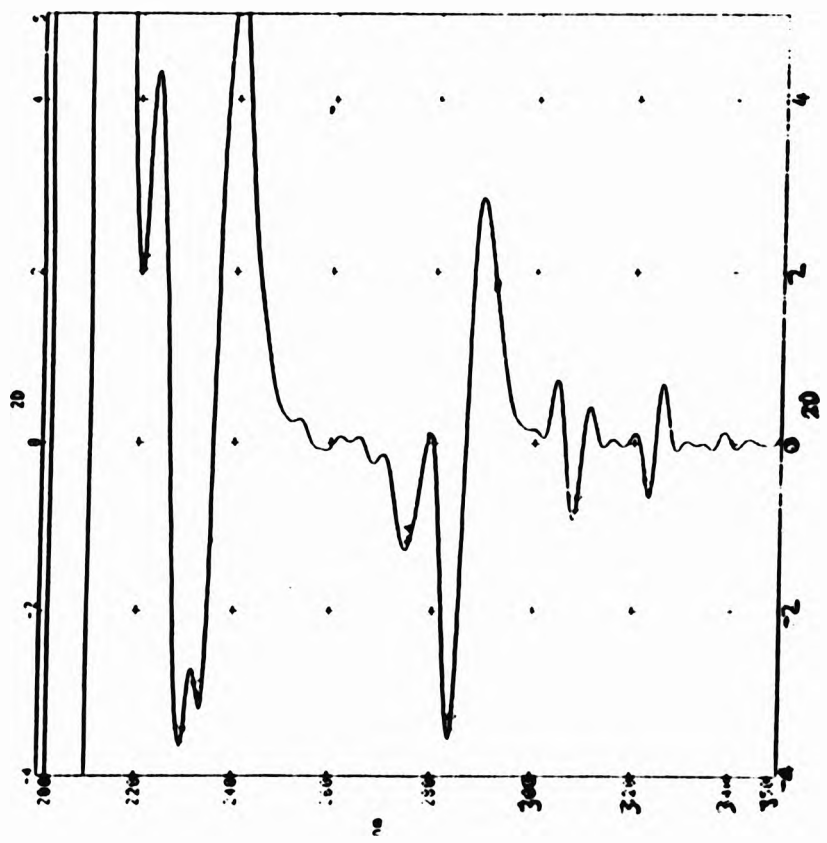

FIGURE 4.12

Second derivative electronic absorption spectra obtained from colon tissue sample of 2 patients with active ulcerative colitis after being treated with reduction/dehydration system.

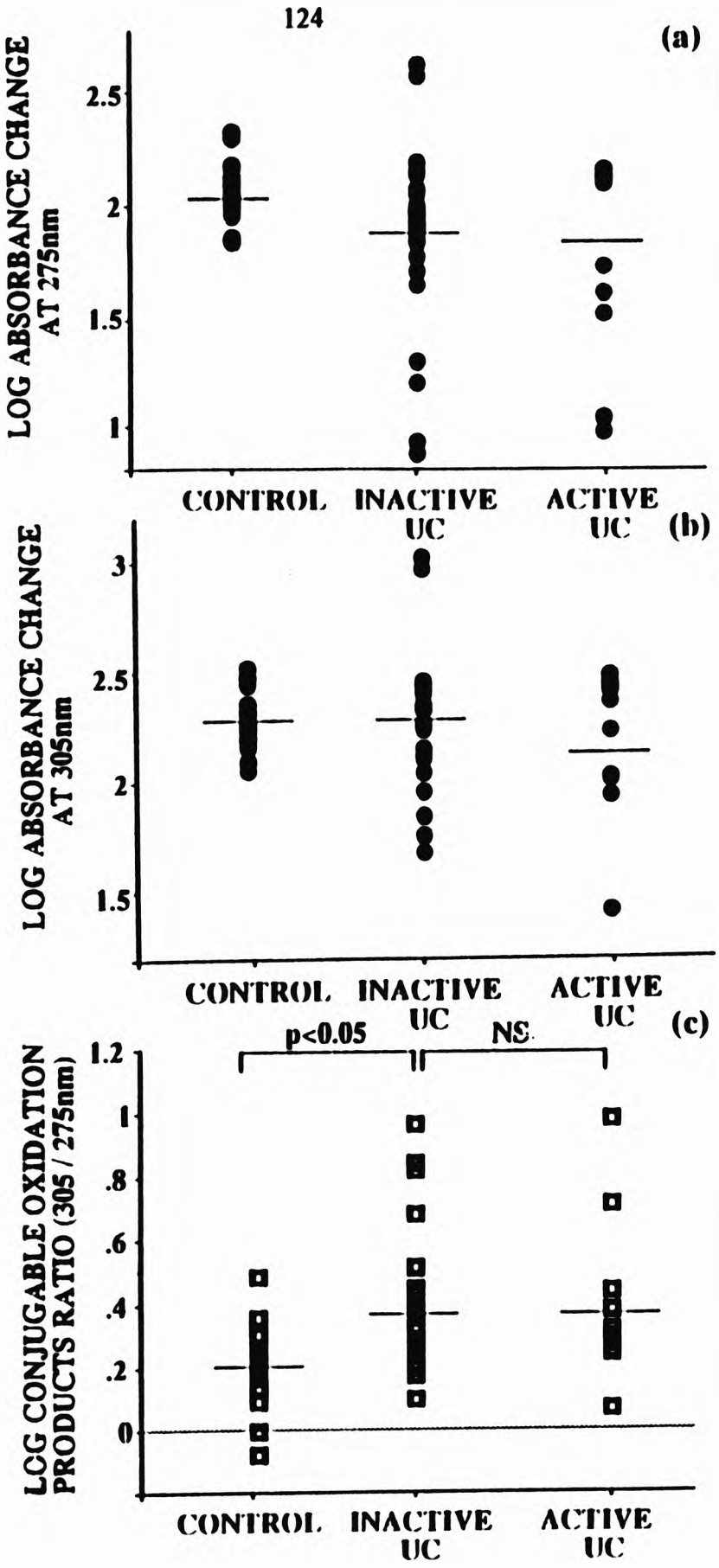

FIGURE 4.13

Graphical representation of the results obtained of lipid peroxidation in patients with ulcerative colitis disease. a) shows the results obtained at 275 nm (triene) and b) shows the results at 305 nm (tetraene) region. c) Shows the significant increases in the conjugable oxidation product (COP) ratio in ulcerative colitis. The bars shown in each spectrum indicate mean values.

4.3 Conclusion and Discussion

The two-step derivatisation of extracted lipid peroxidation products coupled with the employment of 2D spectrophotometry as described here permits an assessment of the molecular nature and extent of ROR-dependent oxidative damage to lipids in biological materials. The method can distinguish between different types of PUFA undergoing oxidative deterioration (e.g., dienoic linoleate or trienoic linolenate) and provides much useful information regarding the chemical nature of the secondary lipid peroxidation products. In view of the potentially large number of endogenous chloroform-extractable components present in biological samples, it is also important to note that the sharp 2D signals attributable to the triene and tetraene chromophores are readily detectable in regions of the spectrum which are relatively free from interfering signals.

These studies did not confirm those of Ahnfelt-Ronne *et al.*[94] who suggested an increase in lipid peroxidation associated with active disease. However, the results obtained have shown a relative increase in the amount of peroxidised trienes when expressed relative to that of dienes in patients with ulcerative colitis. This may simply reflect the increasing susceptibility of PUFAs to peroxidation with an increasing number of double bonds. The results obtained in the *in vitro* experiments presented here confirm that prostaglandins produce only minimal absorbance changes using this method which is designed to assay peroxidised linoleic and linolenic acid, and that these are less than those produced by rectal biopsies.

The spectra obtained from PUFA methyl esters differed slightly from those obtained using colorectal biopsies, this being mainly attributable to some interference in the tissue samples. This may be attributable to the large number of chloroform- extractable endogenous components other than conjugated lipid- derived species which may also be chemically modified by the employed derivatisation procedure. In colonic biopsy spectra, 4 minima were detected instead of usual 3 at wavelengths detecting trienes. Moreover, the magnitude of the minima at 275 and 284 nm had altered. In the control linoleic and linolenic

samples, the minima were approximately equal, whereas in the tissue samples the minima at 284 nm was consistently larger than that at 275 nm. This is probably attributable to interference, but the substance involved is, as yet, unknown. The difference in magnitude of minima observed in the assay may partly explain the difference between the results presented in this study and those of Ahnfelt-Ronne *et al.*[94]. It is also possible that the powerful oxidising system used may have resulted in the conversion of any linoleic or linolenic acids peroxides to corresponding aldehydic products.

Application of this analytical procedure to colon tissue samples obtained from patients with ulcerative colitis demonstrates that colonic biopsies contained peroxidation products that were largely derived from linoleate. However, smaller levels of linolenate-derived peroxidation products were also detectable, consistent with the findings reported by Nitisda *et. al.*[103].

This method is sensitive and therefore ideally suited to the quantification of conjugated hydroperoxydiene, hydroxydiene and oxodiene components derived from oxidative damage to different PUFAs present in biological materials. In principle, the method has the ability to assess the nature and extent of ROR-dependent oxidative damage to lipids in alternative inflammatory diseases. Moreover, its application to human colon tissue samples permits an investigation of the effects of RORS generation in inflammatory conditions such as Crohn's disease and ulcerative colitis.

CHAPTER 5

MOLECULAR NATURE OF NON-TRANSFERRIN-BOUND IRON IN SYNOVIAL FLUID FROM PATIENTS WITH INFLAMMATORY JOINT DISEASES: CHARACTERISATION BY PROTON NMR SPECTROSCOPY

5.1 Introduction.

5.1.1 Presence of bleomycin-detectable, non-transferrin-bound iron in synovial fluids from patients with inflammatory joint diseases.

In chapter 1 it was established that formation of ·OH and/or other highly reactive oxidants account for much of the damage done to biological molecules by increased generation of $O_2^{\cdot -}$ and H_2O_2. During phagocytosis, monocytes, neutrophils and macrophages all generate $O_2^{\cdot -}$ and H_2O_2. Formation of ·OH via an iron catalysed Haber-Weiss reaction requires the presence of a suitable metal-ion catalyst[114]. Many metal complexes that form the basis of metal-catalysed reactions are present *in vivo* and include simple complexes of iron salts with phosphate compounds, as well as non-haem-iron proteins. Both Fe(II) and Fe(III) salts are effective, as are haemoglobin and myoglobin. Ferritin catalyses the decomposition of hydroperoxide to an extent proportional to the amount of iron that it contains, However, transferrin and lactoferrin do not stimulate hydroperoxide decomposition until they are fully saturated (which does not occur *in vivo* except in cases of iron overload) and then they are only weakly effective[19].

Halliwell, Gutteridge and others have previously reported that the knee-joint synovial fluid of patients with rheumatoid arthritis and other inflammatory arthritis contains non-transferrin-bound iron, which appears to be present as low-molecular-mass, redox-active iron complexes[19,115,122]. The iron ions of such complexes may be supplied in the acidic environment of the inflamed rheumatoid joint by their reductant-and oxidant-mediated mobilisation from ferritin and haemoglobin respectively, the latter being released from erythrocytes which lyse during episodes of traumatic injury or haemorrage. This non-transferrin-bound iron can readily promote the generation of the highly toxic ·OH from superoxide anion and H_2O_2 which are released by polymorphonuclear leukocytes and macrophages during phagocytosis[105]. The highly reactive ·OH radical can attack a wide range of endogenous 'target' molecules such as lipids[106], proteins[107], ascorbate[108], and

carbohydrates[109] to produce 'unnatural' chemical species (i.e., those not usually formed by normal metabolic processes) that are detectable biomolecules present in inflammatory diseases by modern analytical techniques (chapter 3 & 4). These degradation products can themselves stimulate synovitis and progressive joint destruction[110,110].

Non-transferrin-bound iron ions capable of generating ·OH radical have been measured in inflammatory synovial fluid by the bleomycin assay[104,112], which detects iron ions available for complexation with the drug bleomycin. In the presence of oxygen and ascorbate, bleomycin-bound iron degrades DNA and release thiobarbituric acid (TBA)-reactive products (predominantly malondialdehyde), the concentrations of which (determined spectrophotometrically at 532 nm) are proportional to the amount of non-transferrin-bound or 'mal-placed' iron present. Recently, Gutteridge[121] has demonstrated that (1) approximately 40% of rheumatoid or osteoarthritic synovial fluid samples are capable of releasing iron from a protein component to bleomycin at pH value of <5.3, (2) such bleomycin-iron-positive synovial fluids have significantly lower transferrin levels than bleomycin-iron- negative fluids, (3), lactoferrin was undetectable in the bleomycin-iron-positive fluids but present in bleomycin-iron- negative samples and (4) in the presence of excess ascorbate, 'pure' iron-loaded (40%) transferrin can release iron in a bleomycin-detectable form throughout a pH range covering that of the synovial fluid of subjects with inflamed knees (i.e. <7.0). However, to date there have been no attempts to clarify the precise chemical nature of such iron. Since the chromatographic fractionation of biological fluids causes the degradation of proteins and release of metal-ions[113], further investigation of the chemical nature of non-protein-bound iron requires a methodology that involves minimal sample pre-treatment.

In this study Hahn spin-echo and single-pulse proton (^{1}H) NMR spectroscopy combined with the use of powerful iron(III) chelators (desferrioxamine and nitrilotriacetate), and the iron(III) binding protein apotransferrin, are employed to 'speciate' catalytic, low-

molecular-mass complexes of iron in inflammatory synovial fluid samples. In addition, the ability of increasing concentrations of added iron(III) (0.5 - 20 x 10^{-5} mol dm^{-3}) to cause further complexometric or oxidatively-mediated modifications in the ^{1}H NMR profile of synovial fluid are investigated.

5.2 Results

5.2.1 High resolution proton NMR spectra of synovial fluid from patients with inflammatory synovitis.

The Hahn spin-echo technique suppresses broad resonance's arising from macromolecules leaving an NMR spectrum that has well resolved resonance's arising from relatively mobile components. Figure 5.1 shows the low frequency (high field) region of 500 MHz proton Hahn spin-echo NMR spectra of paired synovial fluid and serum samples obtained from a subject with moderately severe rheumatoid arthritis. Notable differences between these spectra include:

(1) highly intense synovial fluid lactate -CH_3 and -CH group proton resonances located at 1.33 and 4.13 ppm respectively, reflecting a markedly elevated lactate concentration in these samples over that of paired sera,

(2) the relatively weak intensities of the synovial fluid glucose proton resonances (measured by integrating the α– and β-anomeric ^1H signals at 5.3 and 4.7 ppm respectively), which were ca. 20% less intense than those present in spectra of matched sera,

(3) the very weak intensities of synovial fluid triacylglycerol (TAG) acyl chain terminal-CH_3 and bulk $(-CH_2-)_n$ proton resonance's (representing a molecularly mobile, metabolizable fatty acid pool[123] associated with very-low-density-lipoprotein ((VLDL) and chylomicrons[124]), and an increased TAG -CH_3: $(-CH_2-)_n$ resonance intensity ratio indicating a reduced mean triglyceride chain length,

(4) the weak intensity or absence of the high-density-lipoprotein (HDL)- and low-density-lipoprotein (LDL)- associated fatty acid acyl chain terminal -CH_3 and the LDL fatty acid acyl chain bulk chain $(-CH_2-)_n$ signals from the synovial fluid spectrum, and

(5) the presence of resonance's attributable to the ketone bodies 3-D-hydroxybutyrates, acetone and acetoacetate in the synovial fluid spectrum (all of which were absent from that of the matched serum sample) suggesting an increased utilisation of fats for fuel in the inflamed joint.

All of these observations were reproducible in a total of five independent sets of paired synovial fluid and serum samples collected at the same time points from patients with rheumatoid arthritis. The substantially raised synovial fluid lactate levels (*c.a.* 5-12 x 10^{-3} mol dm^{-3}) and the diminished glucose concentrations are characteristic features of the hypoxic environment within the inflamed knee-joint and consequent anaerobic metabolism.

Figure 5.1(a)

Low frequency (high field) regions of the 500 MHz ^1H Hahn spin- echo NMR spectra of blood serum from a patient with rheumatoid arthritis at the same time-point. Typical spectra is shown.

Abbreviations: A, acetate-CH_3; Ala, Alanine-CH_3; BU, 3-D- hydroxybutyrate-CH_3; Cit, citrate-CH_2; Cn_1, creatinine N-CH_3; Cn_1, creatine N-CH_3; Cn_2, creatinine -CH_2-; Glc, glucose resonance's; Gln_1, and Gln_2, B- and T-CH_2 groups of glutamine respectively; Ile, isoleucine -CH_3; Lac -CH_3 and Lac -CH, lactate -CH_3 and -CH proton resonance's respectively; N-Ac-CH_3, N-acetyl- CH_3 groups of mobile portions of N-acetylated glycoproteins; - $N(CH_3)_3$, choline, betaine and carnitine -$N(CH_3)_3$ group resonance's overlying the broader signal attributable to the HDL- associated triacylglycerol choline head group; Chyl, VLDL TAG-CH_3 and Chyl, VLDL TAG-CH_2, terminal-CH_3 and chain (-CH_2-)$_n$ groups respectively of chylomicron- and VLDL-associated triacylglycerols; LDL, HDL TAG-CH_3, terminal-CH_3 group of LDL- and HDL-associated triacylglycerols; Suc, succinate-CH_2; Thr, threonine-CH_3; Val, valine-CH_3.

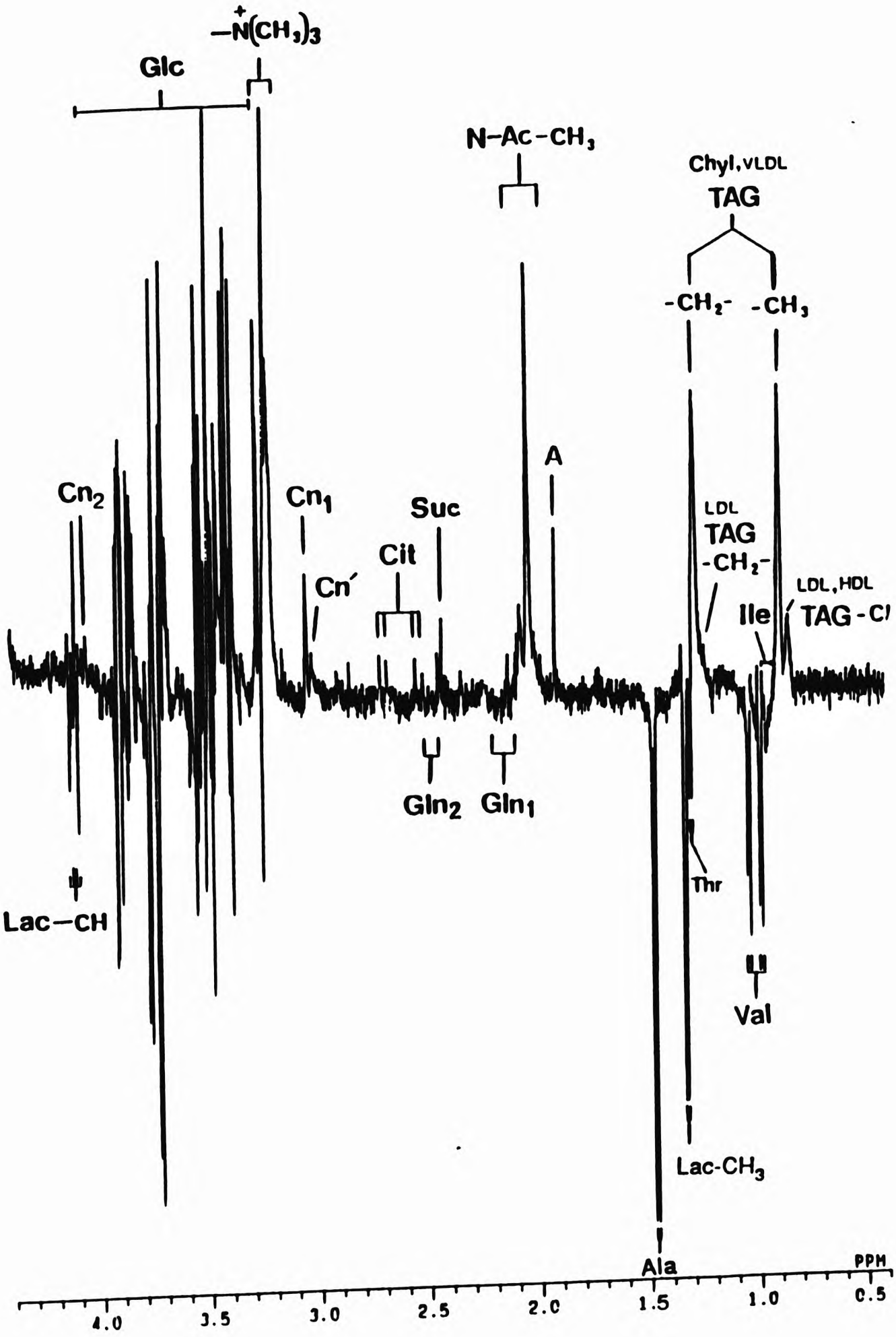
$-\overset{+}{N}(CH_3)_3$
Glc
N-Ac-CH_3
Chyl, VLDL
TAG
-CH_2-
-CH_3
A
Cn_2
Cn_1
Cn´
Suc
Cit
LDL
TAG
-CH_2-
LDL, HDL
TAG - Cl
Ile
Gln_2
Gln_1
Thr
Lac—CH
Val
Lac-CH_3
Ala
PPM
4.0
3.5
3.0
2.5
2.0
1.5
1.0
0.5

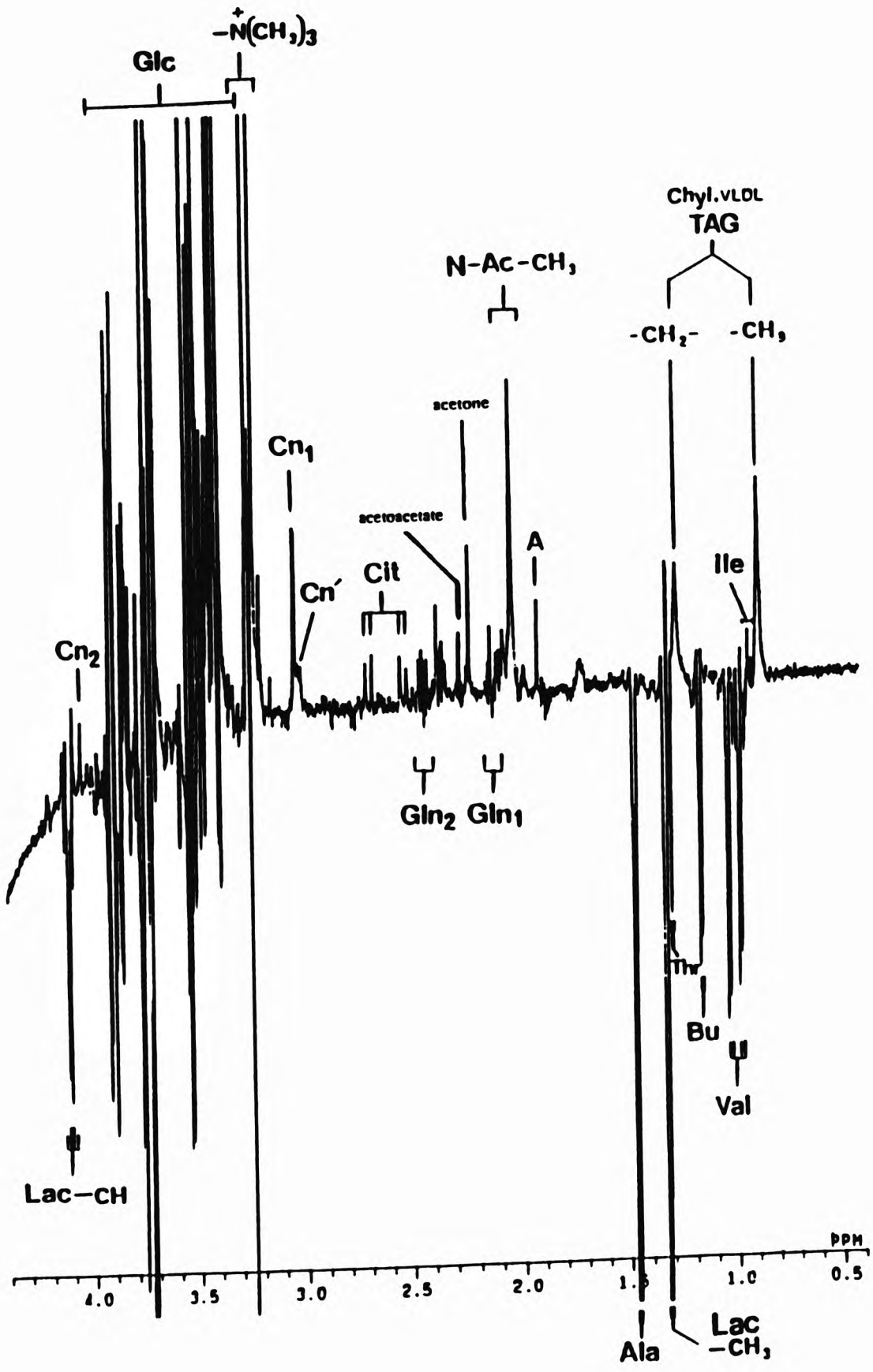

Figure 5.1(b)

Low frequency (high field) regions of the 500 MHz ^{1}H Hahn spin- echo NMR spectra of Knee-joint synovial fluid collected from a patient with rheumatoid arthritis at the same time-point. Typical spectra is shown.

Abbreviations: As in Figure 5.1(a)

5.2.2 Treatment of synovial fluid samples with iron(III)

Addition of increasing concentrations of Iron(III) ions (as aqueous $FeCl_3$) to samples of rheumatoid or osteoarthritic synovial fluid gave rise to a marked broadening of the characteristic AB coupling pattern of the citrate -CH_2- group resonance's (a shortening of their spin-spin relaxation time (T_2) so that they disappear from the spectrum), i.e. synovial fluid citrate chelates added iron (III) ions. Figure 5.2 displays typical results for samples of a) rheumatoid and b) osteoarthritic synovial fluid. Significant increases in the line-widths of the citrate resonance's were observed at added iron(III) concentrations of $<1.00 \times 10^{-5}$ mol dm^{-3}, and considerable broadening occurred at concentrations greater than 5.00×10^{-5} mol dm^{-3}. Indeed, for one of the samples investigated, treatment with 1.88×10^{-5} mol dm^{-3} iron(III) resulted in the complete removal of the citrate signals from its Hahn spin-echo spectrum. Similar broadening were observed in a total of seven different samples studied. A typical plot of the 'within sample' mean citrate peak line-width (i.e., the mean line-width of the four peaks comprising the citrate AB coupling pattern present in each spectrum) and associated standard errors verses added iron(III) concentration, corresponding to the NMR data given in Figure 5.2(b), is shown in Figure 5.2(c).

Intriguingly, in two of the synovial fluid samples investigated, treatment with increasing concentrations of Fe(III) gave rise to the curious production of a new resonance (an apparent triplet) located at 2.69 ppm in between the two higher frequency citrate peaks. This resonance was detectable at an added Fe(III) concentration of 5.00×10^{-5} mol dm^{-3}, and increased in intensity with higher concentrations. An example of the Fe(III)-dependent production of this signal in Hahn spin-echo NMR spectra of synovial fluid is also shown in Figure 5.2(b). This new resonance may be attribute to either a product derived from the iron(III)-mediated oxidation of a synovial fluid component, or alternatively, a species released from a protein binding-site, perhaps as a secondary consequence of iron(III) chelation.

Figure 5.3 exhibits the complete high field (0.00 - 4.40 ppm) regions of typical 500 MHz ^1H Hahn spin-echo NMR spectra of a typical osteoarthritic synovial fluid samples treated with increasing concentrations of iron(III). These spectra demonstrate that the resonance's of alternative potential endogenous iron(III)-chelators (e.g. 3-D-hydroxybutyrate, glutamine, lactate and amino acids such as alanine or valine) remain largely unaffected by added iron(III) concentrations as high as 1.00×10^{-4} mol dm^{-3}, and indicate that synovial fluid citrate is a highly selective ligand for low-molecular-mass (non-transferrin-bound) iron(III). Indeed, addition of 2.00×10^{-4} mol dm^{-3} Fe(III) did not cause any significant broadening in the resonance's of these alternative chelators However, it should be noted that for two of the samples investigated, one or more broad resonance's attributable to the chain $(-CH_2-)_n$ protons of the fatty acid component of very low density lipoproteins and/or chylomicrons became visible in the spectrum at an added iron(III) concentration of 1.00×10^{-5} mol dm^{-3} and increased in intensity with increasing iron concentration up to 1.00×10^{-4} mol dm^{-3} (an example of these modifications in the spectra is shown in Figure 5.3). These iron (III)-mediated changes in the synovial fluid ^1H NMR profile may be attributable to an influence of this redox-active metal ion on the mobility and/or particle packing of these triacylglycerol-containing macromolecules which may arise as a consequence of the susceptibility of their choline head groups to the electrostatic binding of negatively-charged iron(III) complexes[125], e.g. iron(III)-citrate chelates. However, treatment of synovial fluid samples with higher levels of added Fe(III) (>5.00×10^{-4} mol dm^{-3}) gave rise to a significant broadening of this TAG $(-CH_2-)_n$ signal in samples in which it was NMR detectable, suggesting that high concentrations of this transition metal ion decrease the T_2 value of the component(s) to which it is attributable. The line-width of the largely unresolved VLDL/chylomicron-associated TAG terminal-CH_3 group resonance's increased marginally following equilibration with $5.00 - 10.00 \times 10^{-5}$ mol dm^{-3} Fe(III), a typical sample giving values of 17.4 Hz prior to treatment and 20.1 Hz after at an added iron(III) concentration of 5.00×10^{-5} mol dm^{-3}. The $-N^+(CH_3)_3$ group singlet resonance of the molecularly mobile high density lipoprotein-associated phospholipid choline head group

located at 3.25 ppm was not affected by treatment with Fe(III) throughout the concentration range 1.00-10.00 x 10^{-5} mol dm^{-3}.

Subsequent treatment of these iron(III)-loaded synovial fluid samples with desferrioxamine (a linear trihydroxamic acid siderophore) had little or no effect on the spectra initially, but the citrate resonance became visible again following equilibration at ambient temperature for a period of 6 hr. (Figure 5.4) consistent with a slow transfer of iron(III) from citrate and the possible involvement of a polynuclear iron(III)-citrate species.

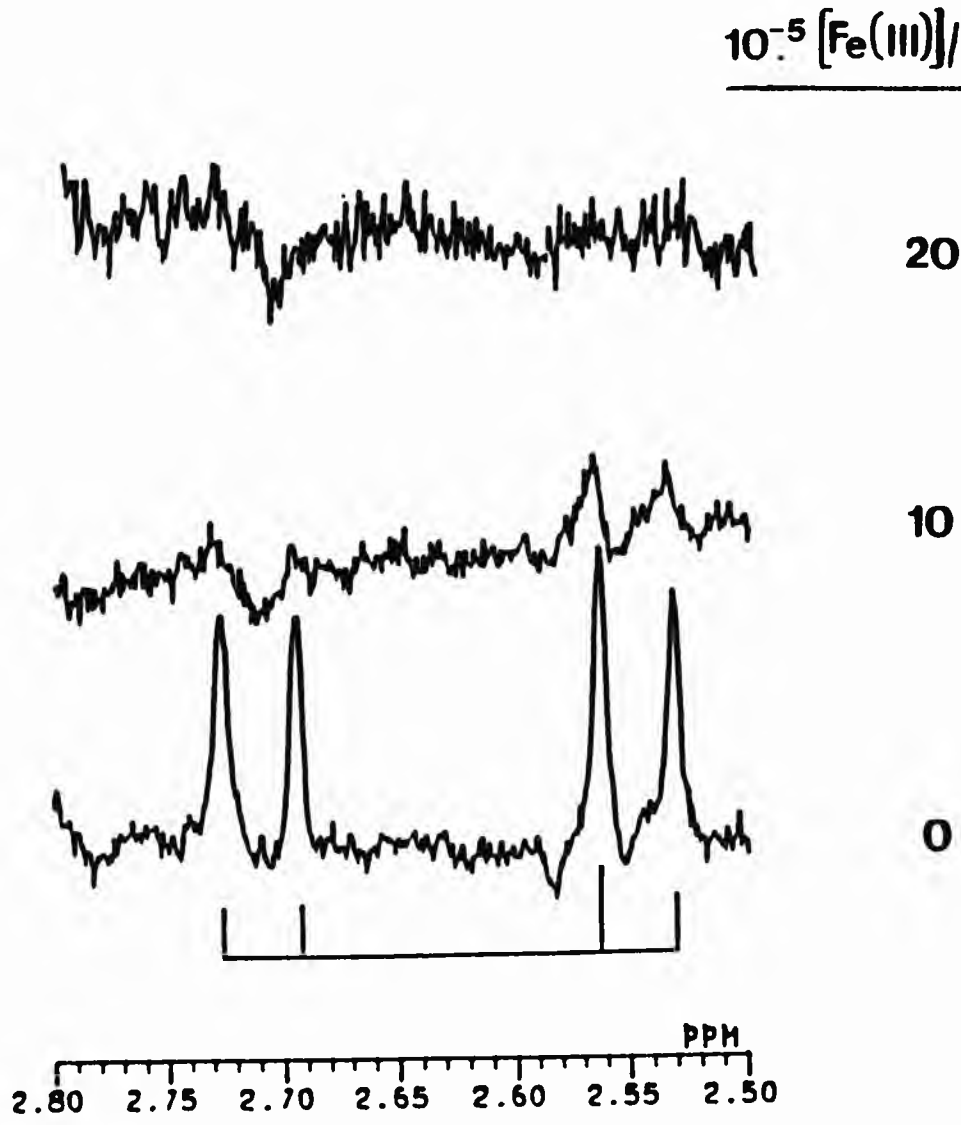

Figure 5.2(a)

2.50 - 2.80 ppm region of 500 MHz ^{1}H Hahn spin-echo spectra of a typical rheumatoid synovial fluid sample before and after equilibration with 1.00 and 2.00 x 10^{-4} mol dm^{-3} iron(III) (as $FeCl_3$)

Abbreviations: As in Figure 5.1(a)

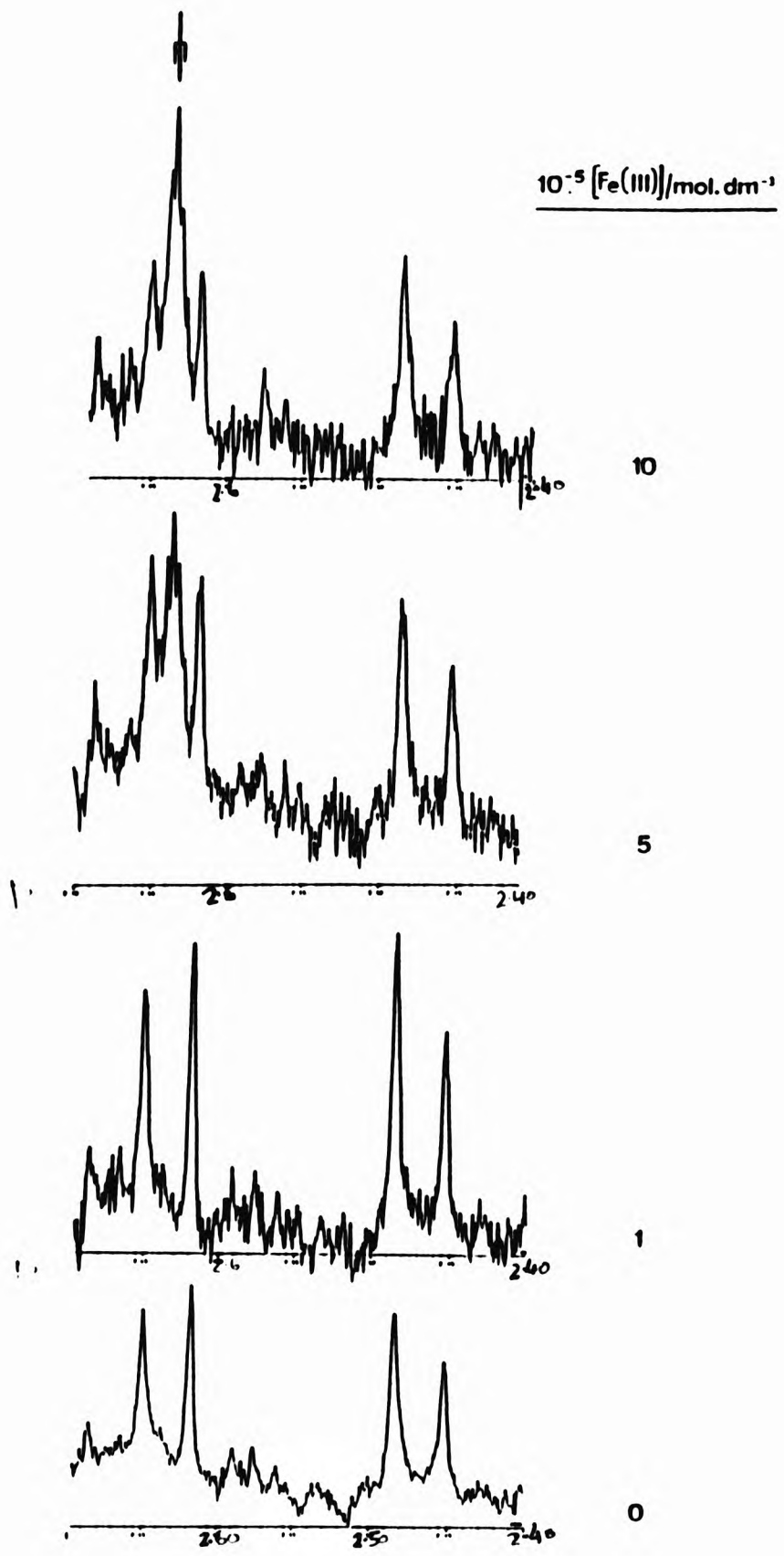

Figure 5.2(b)

2.40 - 2.70 ppm region of corresponding spectra of a typical osteoarthritic synovial fluid sample before and after equilibration with 0.10, 0.50 and 1.00 x 10^{-4} mol dm^{-3} iron(III).

Abbreviations: As in Figure 5.1(a)

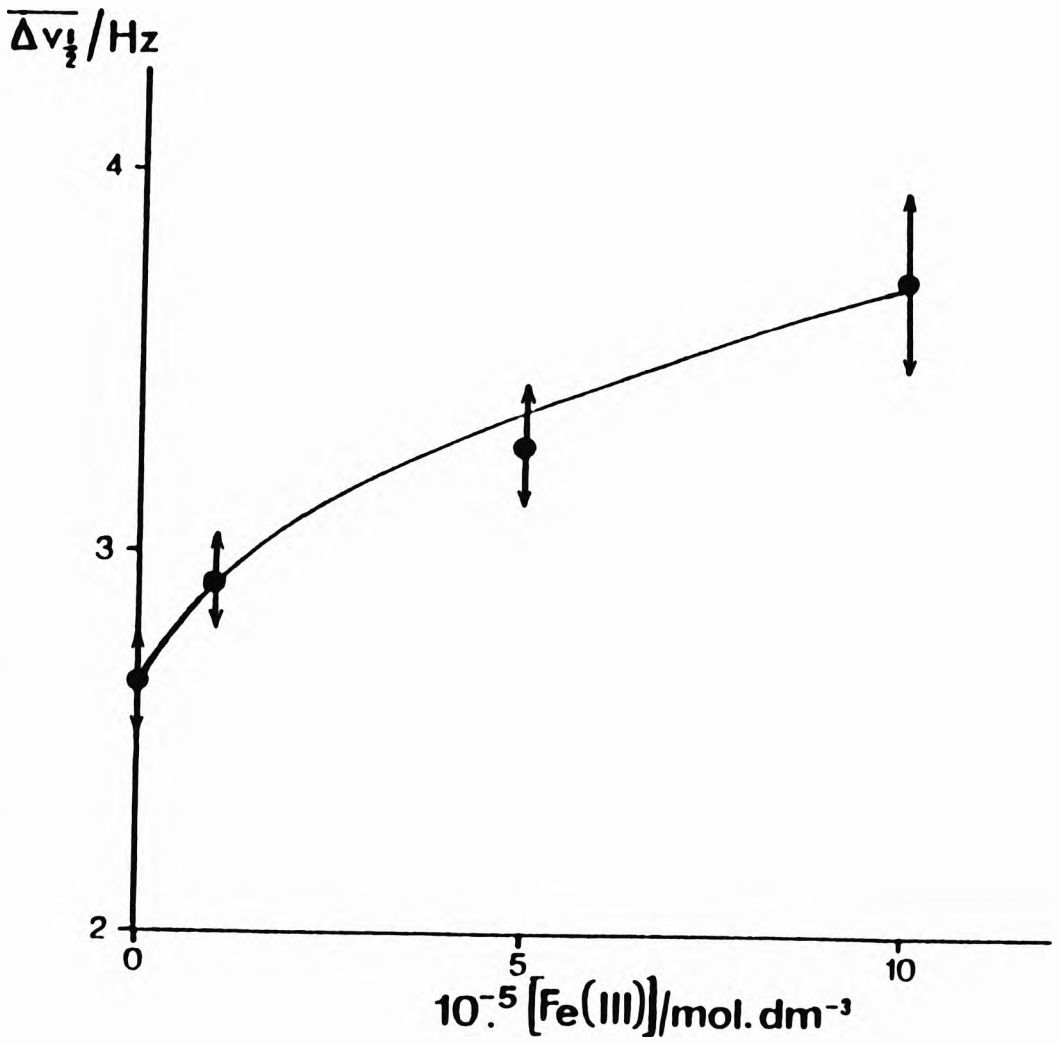

Figure 5.2(c)

Plot of the mean citrate resonance line-width ($\Delta v_{1/2}$) (with associated standard errors) versus added iron(III) concentration for the data of Figure 5.2(b).

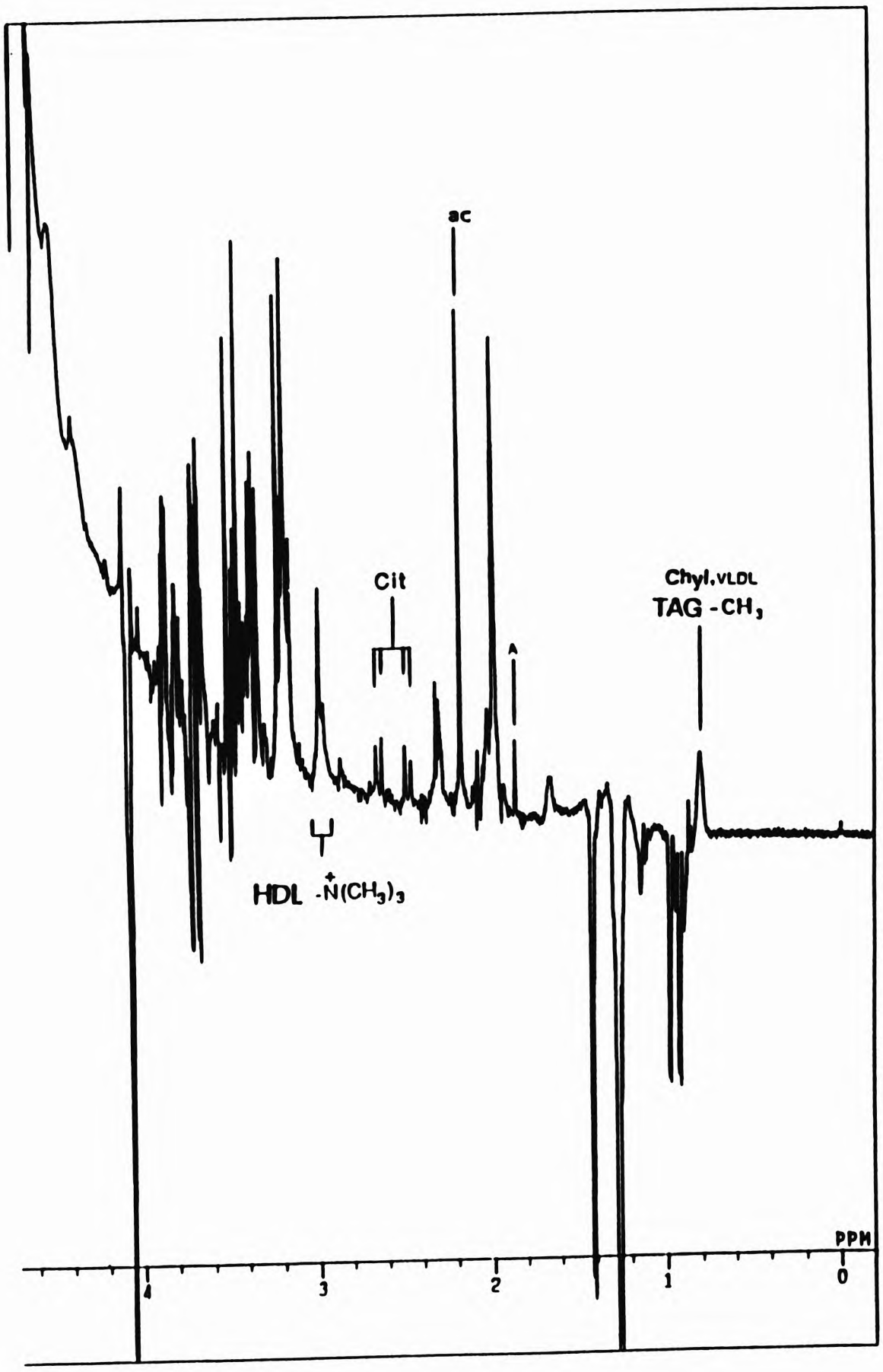

Figure 5.3(a)

Low frequency (0.00 - 4.40 ppm) region of the 500 MHz ^1H Hahn spin-echo spectra of typical osteoarthritic synovial fluid sample untreated with iron(III)

Abbreviations: as Figure 5.1(a).

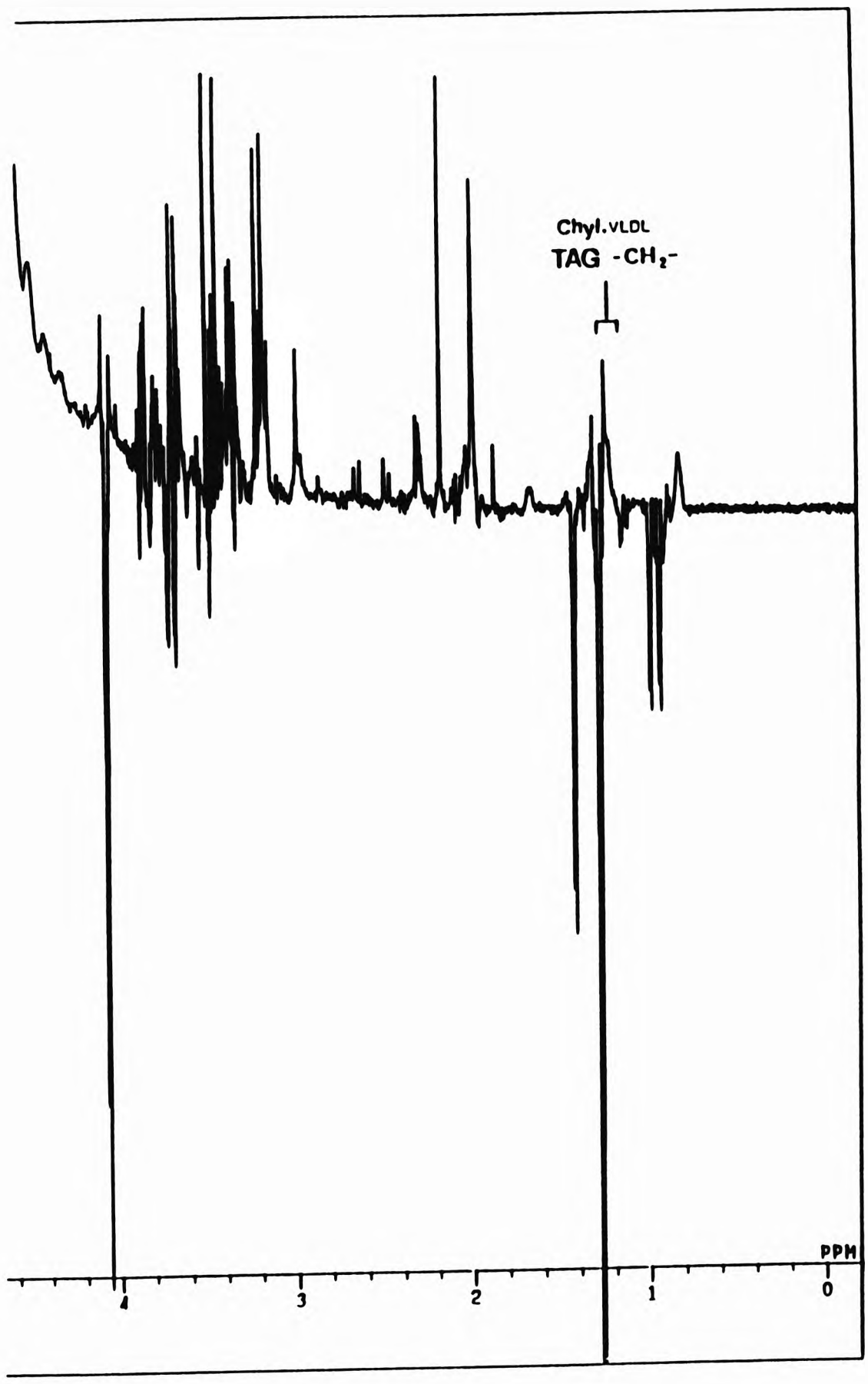

Figure 5.3(b)

Low frequency (0.00 - 4.40 ppm) region of the 500 MHz ^{1}H Hahn spin-echo spectra of typical osteoarthritic synovial fluid sample treated with 0.10×10^{-4} mol dm^{-3} iron(III) (as $FeCl_3$).

Abbreviations: as Figure 5.1(a).

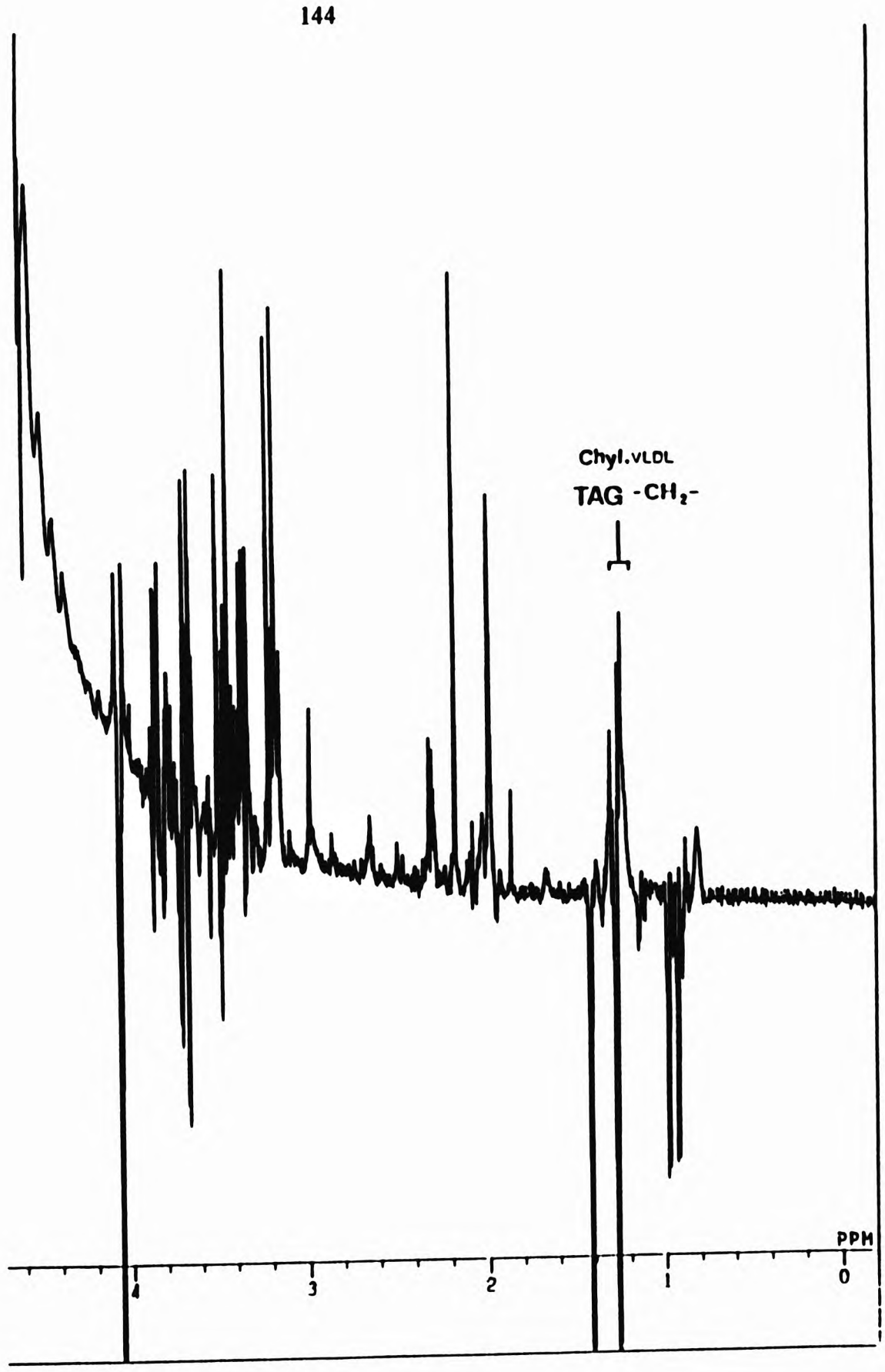

Figure 5.3(c)

Low frequency (0.00 - 4.40 ppm) region of the 500 MHz ^1H Hahn spin-echo spectra of typical osteoarthritic synovial fluid sample treated with 1.00×10^{-4} mol dm^{-3} iron(III) (as $FeCl_3$).

Abbreviations: as Figure 5.1(a).

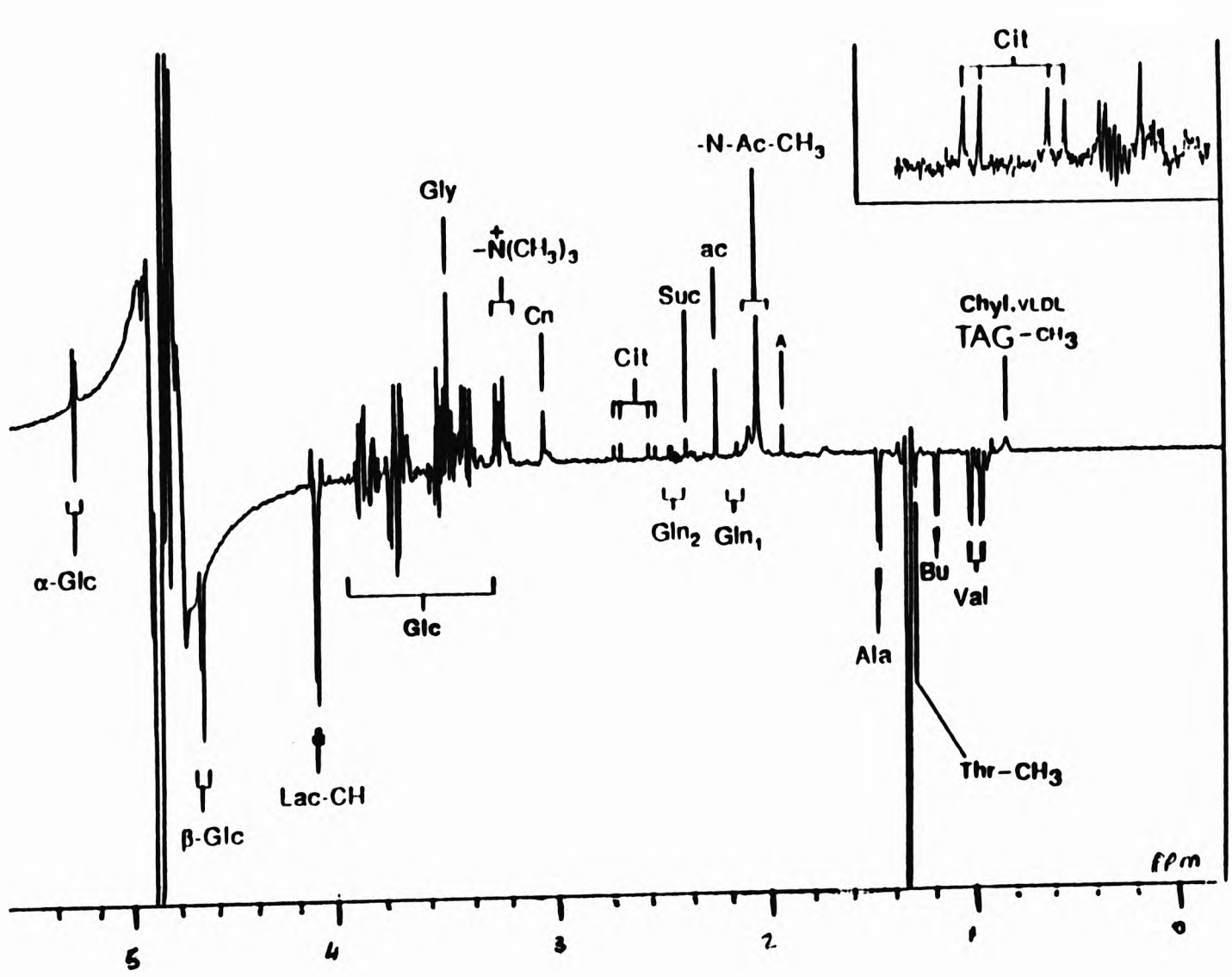

Figure 5.4(a)

Low frequency (0.00 - 5.50 ppm) regions of the 500 MHz ^1H Hahn spin-echo spectra of a rheumatoid synovial fluid sample before treatment with iron(III) and desferrioxamine. Insets: expanded 2.20 -3.00 ppm

Abbreviations: as Figure 5.1(a) with DFO, desferrioxamine resonance; A-Glc and B-Glc, α -and β-anomeric proton resonance's of glucose.

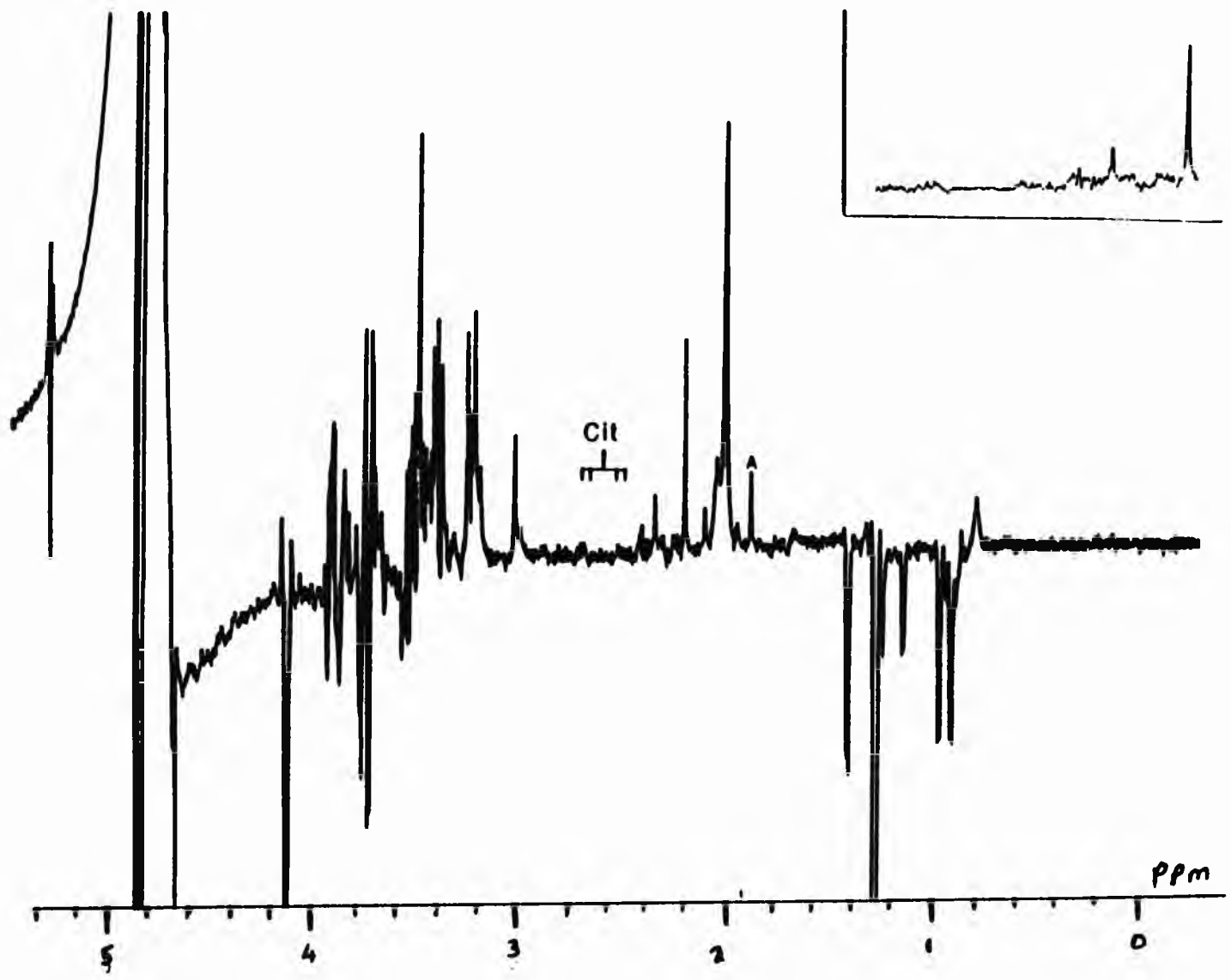

Figure 5.4(b)

Low frequency (0.00 - 5.50 ppm) regions of the 500 MHz ^1H Hahn spin-echo spectra of a rheumatoid synovial fluid sample after treatment with iron(III) and desferrioxamine.; after equilibration with 1.50×10^{-4} mol dm^{-3} iron(III) for 6 hr. at ambient temperature: Insets: expanded 2.20 -3.00 ppm.

Abbreviations: as Figure 5.1(a) with DFO, desferrioxamine resonance; A-Glc and B-Glc, α -and β-anomeric proton resonance's of glucose.

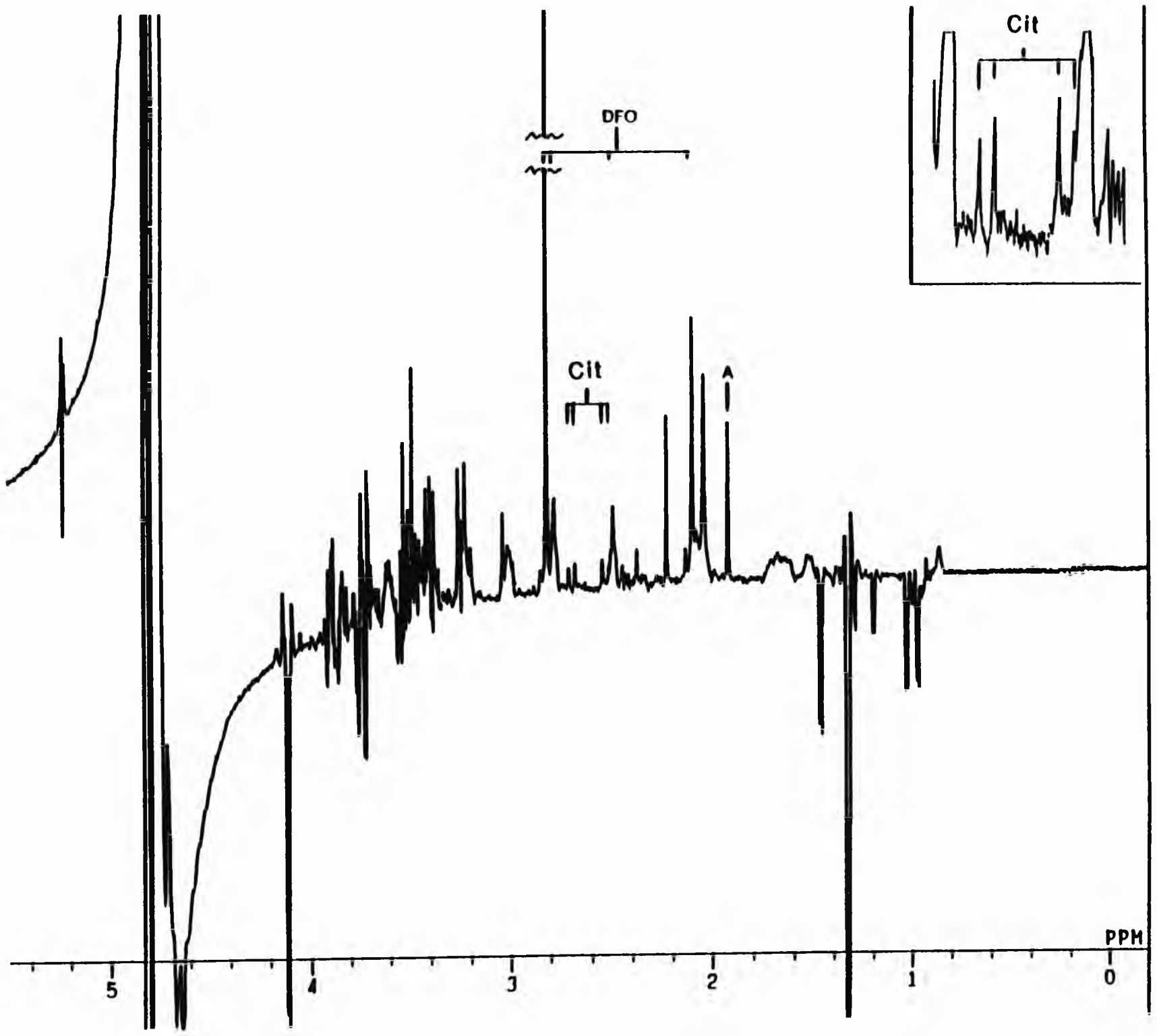

Figure 5.4(c)

Low frequency (0.00 - 5.50 ppm) regions of the 500 MHz ^{1}H Hahn spin-echo spectra of a rheumatoid synovial fluid sample after treatment with iron(III) and desferrioxamine.; after equilibration with 1.50×10^{-4} mol dm^{-3} iron(III) for 20 hr. at ambient temperature: Insets: expanded 2.40 -2.80 ppm.

Abbreviations: as Figure 5.1(a) with DFO, desferrioxamine resonance; A-Glc and B-Glc, α -and β-anomeric proton resonance's of glucose.

5.2.3 Treatment of synovial fluids with nitrilotriacetate and apotransferrin

Incubation of typical freshly obtained rheumatoid synovial fluid samples (n=4) with a high concentration of the disodium salt of nitrilotriacetic acid (4.10×10^{-2} mol dm^{-3}) for a period of 12 hr at ambient temperature gave rise to substantial increases in the intensities of the citrate proton resonance's (Figure 5.5(a) and (b)) with a corresponding decrease in the mean citrate resonance line-widths, typical values being 2.31 ± 0.12 Hz prior to equilibration, and 1.94 ± 0.05 Hz after. These modifications in ^1H Hahn spin-echo spectra (observed in three of the samples investigated) may arise from the ability of this chelator to remove any 'catalytic' iron present in these samples from citrate when present in a large excess. However, the magnitude of the nitrilotriacetate-mediated elevation in the citrate resonance intensities observed indicates that such modifications probably result from the displacement of citrate from protein binding-sites by the added reagent. Indeed, smaller increases in the intensities of the lactate and succinate signals were also observed subsequent to equilibration with nitrilotriacetate, phenomena which probably reflect the role of this anionic reagent in displacing these species from protein binding sites in addition to their potential abilities to chelate any non-transferrin-bound Fe(III) present (especially succinate). Although succinate, and, to a lesser extent, acetate and formate also have the ability to complex low-molecular-mass iron(III), the displacement of these species from positively- charged protein binding sites cannot be ruled out. Indeed, the thermodynamic equilibrium constants for the formation of Fe(III)- acetate complexes are very low[126].

Prolonged equilibration of apotransferrin (4.03 g dm^{-3}) with three separate fresh rheumatoid synovial fluid samples for a period of 12 hr. at ambient temperature gave rise to modifications in the intensities of the citrate $-CH_2-$ and acetate $-CH_3$ group resonance (Figure 5.6(a) and (b)). The influence of apotransferrin on the citrate signals (observed in two of the samples examined) may reflect the removal of Fe(III) from citrate. However, the marked rise in the acetate resonance intensity probably arises from the presence of this carboxylic acid anion as an impurity in the commercial sample of apotransferrin employed.

Further modifications in the synovial fluid spectra following equilibration with apotransferrin included the production of a series of 'unknown' new resonances in the 1.1 - 1.6 ppm chemical shift range (inverted doublets). The presence of the EDTA impurity in the apotransferrin sample employed in these experiments was also detectable in these apotransferrin-treated synovial fluid samples by the presence of a singlet resonance at 2.57 ppm attributable to the ethylene protons of its Ca^{2+} complex[123]. At physiological pH (7.4), the rate constant for the exchange of $HEDTA^{3-}$ (monoprotonated EDTA) with $[Ca(EDTA)]^{2-}$ has been estimated to be < 1 s^{-1}, i.e. slow exchange on the NMR time scale[127].

In contrast to the results obtained following incubation of this iron(III)-binding protein with knee-joint synovial fluid, pre-equilibration of a 1.56 x 10^{-3} mol dm^{-3} aqueous solution of trisodium citrate with 4.03 g dm^{-3} apotransferrin (final pH 7.00) at ambient temperature for 6 hr gave rise to a substantial increase in the mean citrate resonance line-width (from 1.33 + 0.03 to 4.93 + 0.25 Hz). However, subsequent titration of these citrate/apotransferrin mixtures with increasing concentrations of Fe(III) (3.50 and 8.00 x 10^{-5} mol dm^{-3}) did not further influence the mean citrate signal $\Delta v_{1/2}$ value (Table 5.1) indicating that this concentration of apotransferrin, equivalent to an iron (III) binding capacity of 1.00 x 10^{-4} mol dm^{-3}, preferably complexes iron(III) under these experimental conditions.

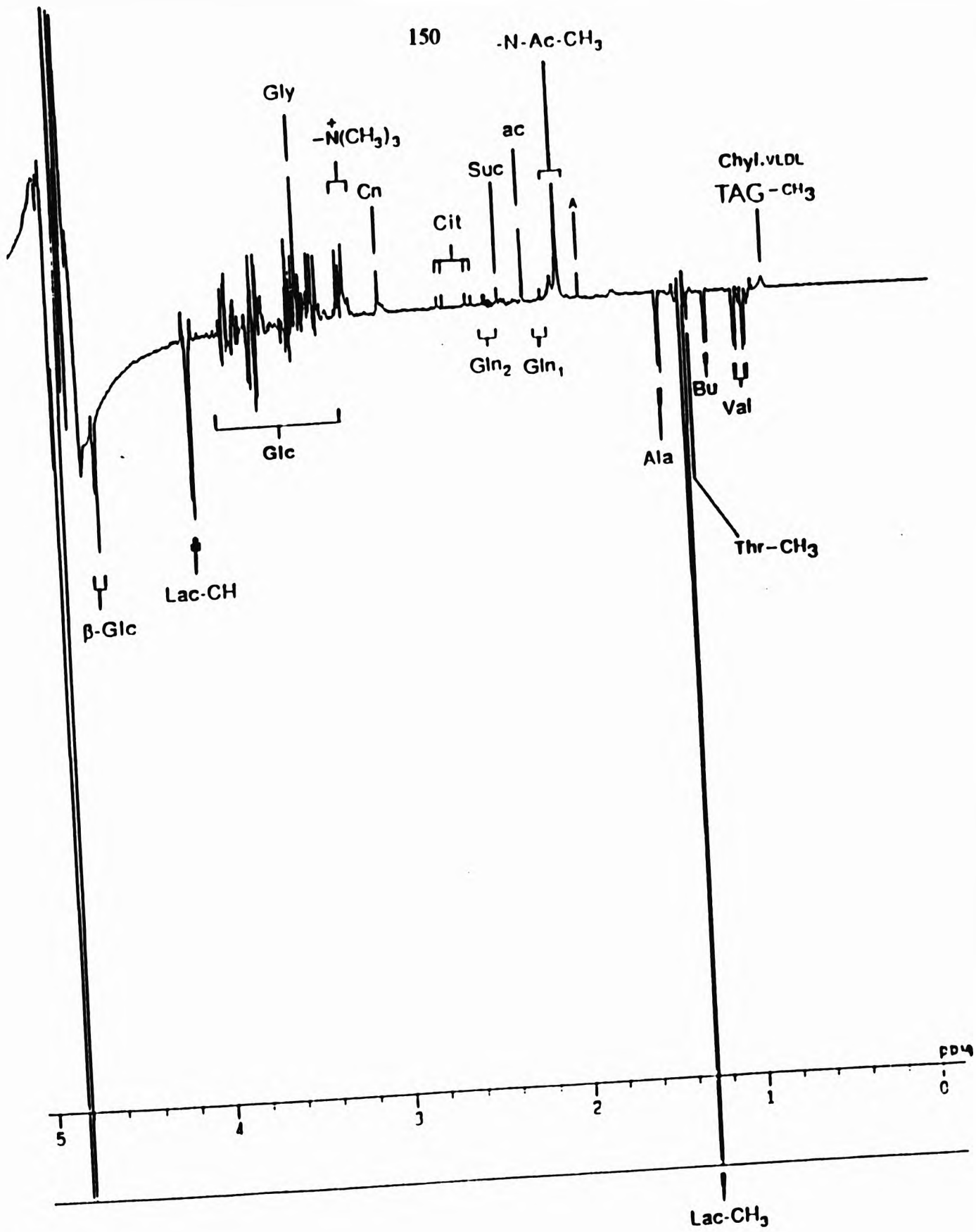

Figure 5.5(a)

Low frequency regions of 500 MHz ^1H Hahn spin-echo spectra of a rheumatoid synovial fluid sample prior to equilibration with nitrilotriacetate. Typical spectra is shown.

Abbreviations: as Figure 5.4(a) with NTA representing the nitrilotriacetate $-CH_2$ proton resonance.

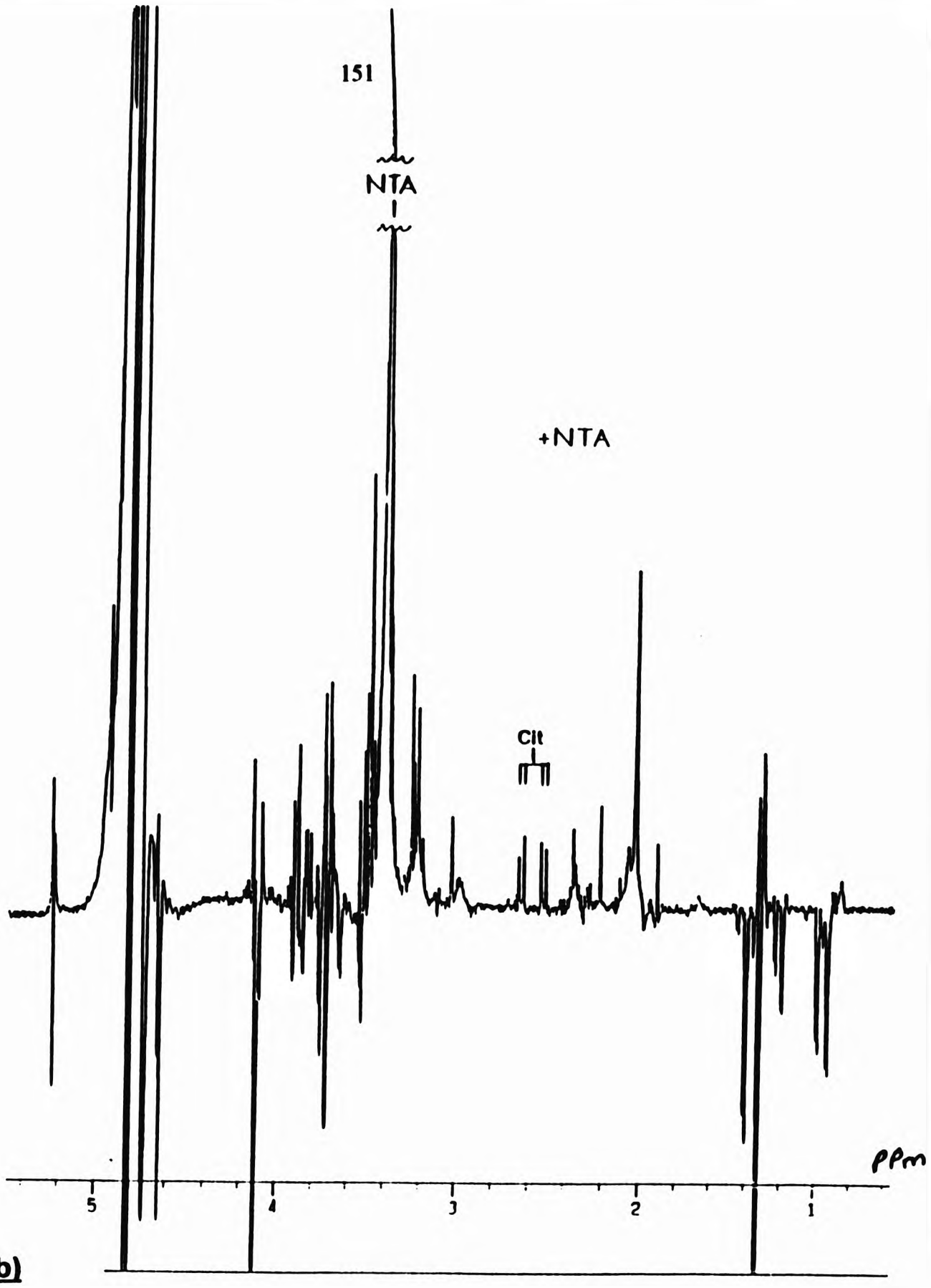

Figure 5.5(b)

Low frequency regions of 500 MHz ^1H Hahn spin-echo spectra of a rheumatoid synovial fluid sample subsequent to prolonged equilibration (12 hr) with 4.1×10^{-2} mol dm^{-3} nitrilotriacetate. Typical spectra is shown.

Abbreviations: as Figure 5.4(a) with NTA representing the nitrilotriacetate $-CH_2$ proton resonance.

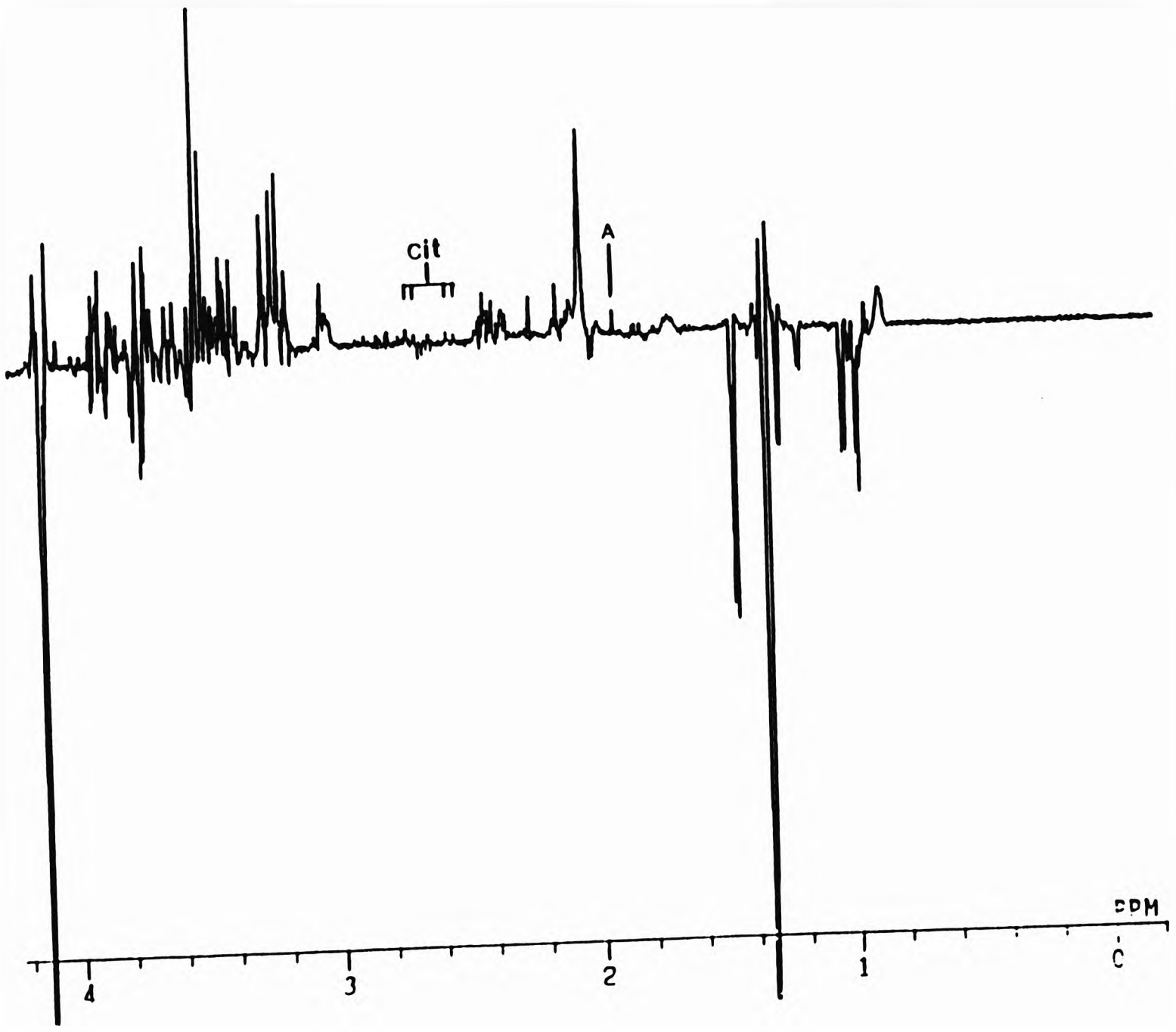

Figure 5.6(a)

Low frequency regions of 500 MHz ^1H Hahn spin-echo spectra of a separate rheumatoid synovial fluid sample prior to equilibration with apotransferrin. Typical spectra is shown.

Abbreviations: as Figure 5.4(a) with Ca^{2+}-EDTA representing that of the ethylenic protons of the calcium complex of EDTA.

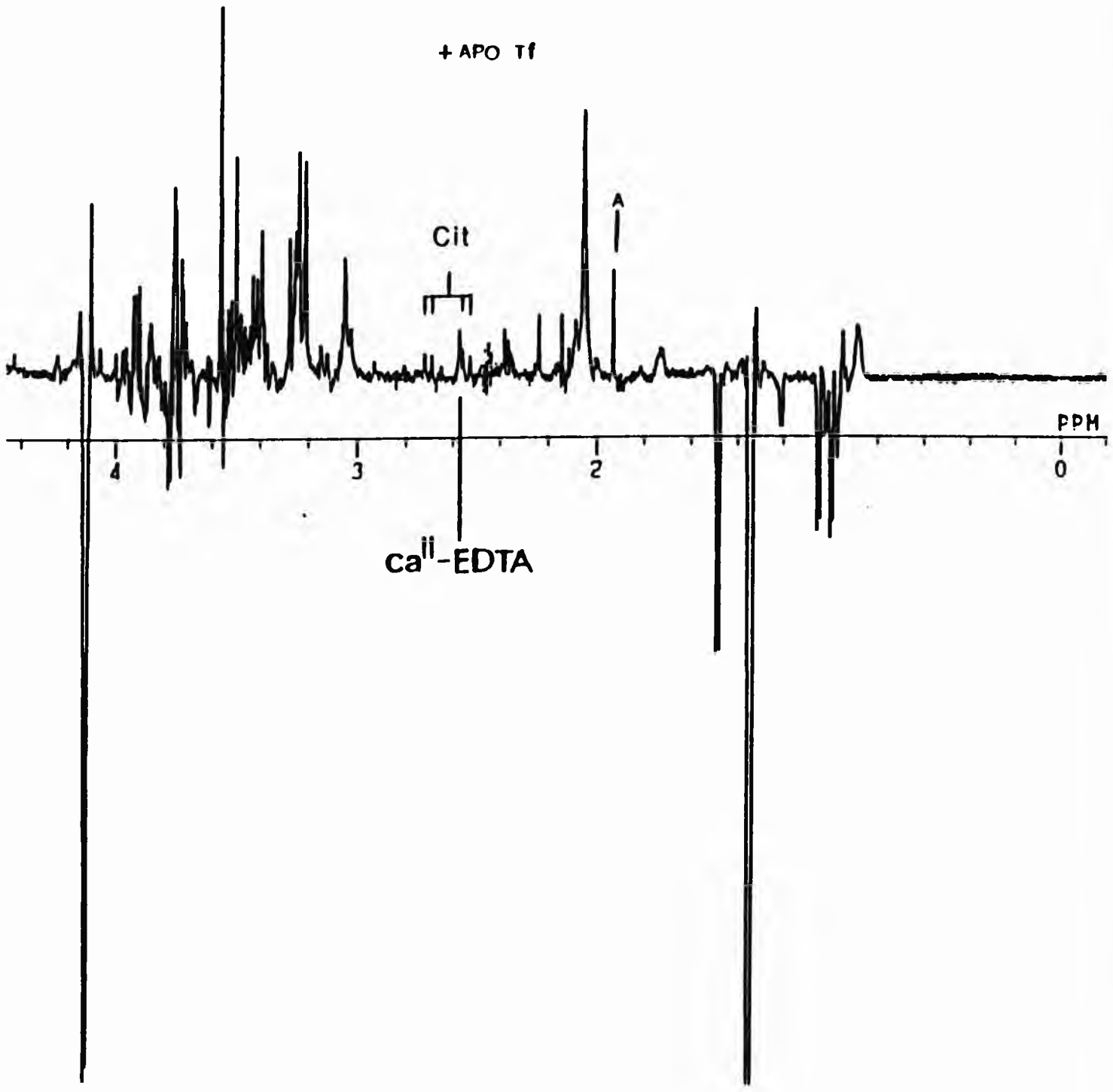

Figure 5.6(b)

Low frequency regions of 500 MHz ^1H Hahn spin-echo spectra of a rheumatoid synovial fluid sample subsequent to prolonged equilibration (12 hr) with 4.03 g dm^{-3} apotransferrin. Typical spectra is shown.

Abbreviations: as Figure 5.4(a) with Ca^{2+}-EDTA representing that of the ethylenic protons of the calcium complex of EDTA.

Sample	Line-widths($\Delta\nu_{1/2}$) of citrate resonance peaks (Hz)				$\overline{\Delta\nu_{1/2}}$(Hz)	Standard error
	1	2	3	4		
(a) 1.56 x 10^{-3} mol.dm^{-3} citrate	1.38	1.38	1.32	1.24	1.33	±0.03
(b) 1.56 x 10^{-3} mol.dm^{-3} citrate plus 4.03 g dm^{-3} apotransferrin	5.14	5.38	5.00	4.20	4.93	±0.25
(c) As (b), with 3.50 x 10^{-5} mol.dm^{-3} Fe(III)	5.15	5.16	5.10	4.78	5.04	±0.09
(d) As (b), with 8.00 x 10^{-5} mol.dm^{-3} Fe(III)	5.00	4.50	4.50	4.60	4.65	±0.14

Table 5.1

Line-widths of the citrate resonance peaks (with their mean values and associated standard errors) of 1.56 x 10^{-3} mol dm^{-3} aqueous solutions of trisodium citrate (pH 7.00) and the influence of 4.03 g dm^{-3} apotransferrin and, where indicated, 3.50 or 8.00 x 10^{-5} mol dm^{-3} iron(III) on these values. 1, 2, 3 and 4 refer to the peaks present in the characteristic AB coupling pattern of the citrate -CH_2- group resonances in order of decreasing frequency.

5.2.4 Kinetics of the transfer of iron(III) from citrate to desferrioxamine

Since the NMR experiments conducted demonstrated a slow rate of transfer of iron(III) from citrate to desferrioxamine at ambient temperature (Figure 5.4), the rate of the reaction of iron(III)-monocitrate with desferrioxamine was monitored by electronic absorption spectroscopy.

Figure 5.7 shows the spectral changes that occur with time following the addition of one molar equivalent of desferrioxamine methanesulphonate to an aqueous solution of iron(III)-monocitrate (4.20×10^{-4} mol dm^{-3}) containing 0.10 mol dm^{-3} sodium nitrate at pH 8.00 and 25.0°C. The slow increase in absorbance at 425 nm with increasing time is attributable decrease in absorbance in the ultraviolet and near-ultraviolet regions of the spectrum is ascribable to the decrease in iron(III)-monocitrate concentration (equation 5.4). The series of spectra generated contain a clear isobestic point at 342 nm. The reaction proceeds essentially to completion (>99%) but it is a very slow process, taking more than 2 hr for complete conversion to ferrioxamine under these experimental conditions. Hence this reaction has a significant kinetic barrier, consistent with the synovial fluid NMR experiments.

$$[Fe(Citrate\ H_{-1})]^{-} + H_4DFO \rightarrow [Fe(HDFO)] + [Citrate(OH)]^{3-} + 2H^{+} \qquad (5.4)$$

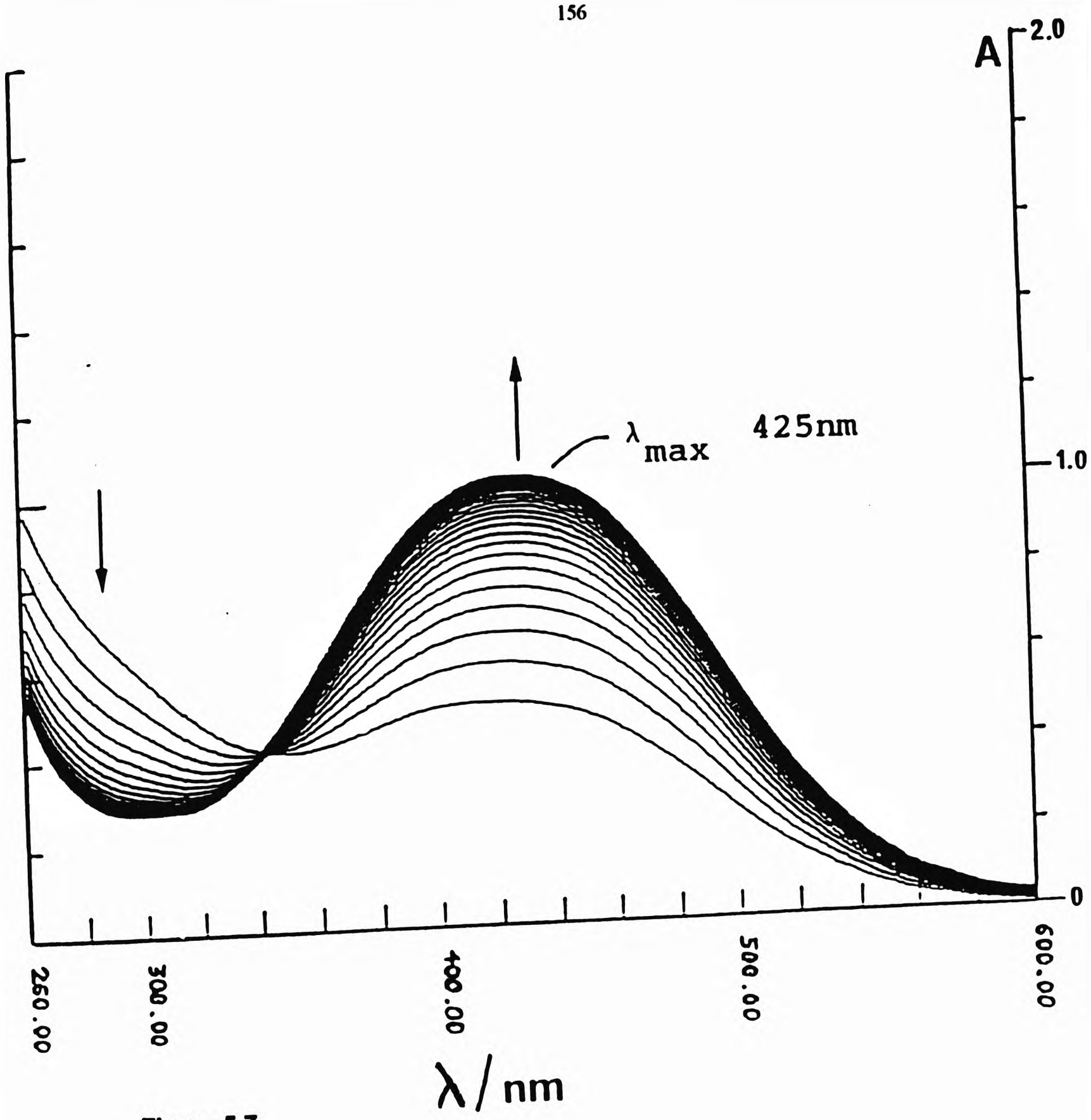

Figure 5.7

Electronic absorption spectra of a 4.20×10^{-4} mol dm^{-3} aqueous solution of iron(III)-monocitrate ($[Fe(III)(citrate\ H_{-1})]^-$) containing 0.10 mol dm^{-3} $NaNO_3$ at pH 8.00 and 25.0° C obtained at increasing time intervals subsequent to the addition of 1.00 molar equivalent of desferrioxamine. The first spectrum was recorded at 4.5 min following desferrioxamine addition, and subsequent spectra were recorded at 4.5 min intervals.

5.3 Conclusion and Discussion

The simultaneous study of the status of a wide range of molecularly mobile components present in knee-joint synovial fluid samples obtained from patients with inflammatory joint diseases by high field proton NMR spectroscopy, combined with the use of the powerful iron(III) chelators desferrioxamine and nitrilotriacetate, and the iron(III)-binding protein apotransferrin, provides evidence for the complexation of a significant fraction of low-molecular-mass (non-transferrin-bound) iron(III) ions by endogenous citrate.

Further evidence for the chelation of non-transferrin-bound iron ions by citrate in synovial fluid was provided by the observation that addition of iron(III) to the samples gave rise to a marked broadening of the citrate proton resonance's. In the light of the observations by Singh *et. al.*[129] concerning the molecular nature of non-transferrin-bound iron(III) in blood serum obtained from patients with iron-overloaded, the substantial increases in the citrate resonance line-widths observed here subsequent to the addition of very low concentrations of aqueous iron(III) ($\leq 1.00 \times 10^{-5}$ mol dm^{-3}) to synovial fluid indicate that iron(III) does not associate with synovial fluid proteins as polynuclear clusters. Such species would not exert a selective influence on the citrate proton resonances unless they also contained this physiological-available chelator in a form which rapidly exchanged between the 'free' and protein-bound iron(III)-cluster states on the NMR time scale. Moreover, the low concentrations of albumin present in rheumatoid synovial fluid (17.2 ± 6.3 g dm^{-3}) relative to those of rheumatoid or normal blood plasma (36.3 ± 7.9 and 50.3 ± 4.4 g dm^{-3} respectively)[130] will thermodynamically retard the formation of any albumin-associated multinuclear iron(III) clusters, facilitating chelation by the oxygen donor ligand citrate. Furthermore, the large excess of citrate concentration (ca. $0.5 - 4.5 \times 10^{-4}$ mol dm^{-3})[119] over that of any non-transferrin-bound iron(III) present in knee-joint synovial fluid will also suppress such polynuclear iron(III) complex formation.

Interestingly, Konopka and Neilands[131] recently observed that human serum and human serum albumin impede the transfer of iron(III) from transferrin to enterobactin and that albumin acts synergistically with other serum factors (e.g. transferrin) to limit iron supply to bacteria via a mechanism involving its ability to bind chelators capable of removing this metal ion from transferrin. The low concentrations of albumin in synovial fluid further contribute to the susceptibility of transferrin present in this biological fluid to release iron(III) to endogenous chelators such as citrate.

The above observations suggest that transferrin present in some synovial fluid samples is poorly receptive to the binding of added iron(III), a phenomenon consistent with previous suggestions that the physiochemical properties of transferrin in 'bleomycin- iron-positive' synovial fluid samples may differ from those of the protein present in 'bleomycin-iron-negative' fluids[122]. Similar considerations may also apply to synovial fluid lactoferrin. Based on the data of Gutteridge[122] which revealed that the mean rheumatoid synovial fluid transferrin concentration is 1.67 ± 0.31 g dm^{-3} and its mean percentage saturation with iron(III) is $26.3 \pm 11.7\%$, the estimated residual iron(III) binding capacity of these fluids is ca. 3×10^{-5} mol dm^{-3}, a value which markedly exceeds the minimum levels of added iron(III) required to give rise to detectable citrate resonance broadening.

It is also conceivable that transferrin in 'bleomycin-iron-positive' synovial fluid may contain some non-specifically associated polynuclear iron(III) complexes which are available to physiological chelators such as citrate. Indeed, Smit *et. al.*[132] have recently demonstrated that laboratory preparations of iron-loaded transferrin contains such protein-associated multinuclear species, the production of which can be avoided by careful laboratory manipulation and the monitoring of purification techniques.

The exchange of iron(III) from transferrin to various chelators has been shown to involve three salient features: (1), a conformational change in the ternary Fe(III)-Tf-CO_3^{2-} complex prior to attack by the chelator (Tf represents transferrin), (2), the generation of a

mixed ligand chelator-Fe(III)-Tf-CO_3^{2-} species, and (3), removal of iron(III) by the chelator. Indeed, Bates *et. al.*[133] have previously observed that at a ratio of citrate to transferrin-bound iron(III) of 9.1 x 10^{-2} mol dm^{-3} : 3.6 x 10^{-5} mol dm^{-3}, i.e., approximately 2,500:1, iron-loaded transferrin releases ca. 50% of its iron(III) to the chelator, a reaction complete within 2 hr at a temperature of 25°C. Moreover, the kinetics of the reverse reaction, i.e. transfer of iron(III) from citrate to apotransferrin are complicated by the polynuclear nature of the iron(III)-citrate complex which predominates at alkaline pH values[133]. At a citrate:iron(III) ratio of 1:1, the rate-limiting step involves the de-polymerisation of this complex to form a low-molecular-mass reactive species. At citrate : iron(III) ratios of >20:1, however, iron(III)-dicitrate complexes are formed which readily release iron(III) to transferrin. Although the 1:1 iron(III)-nitrilotriacetate complex reacts rapidly with apotransferrin at 25°C and a pH value of 7.5 , transfer of iron(III) from the multinuclear 1:1 Fe(III)-citrate complex to apotransferrin requires ca. 20 hr to reach equilibrium under these experimental conditions[133]. Any iron(III)-citrate complexes present in certain synovial fluid samples may be such polynuclear species with an associated slow rate of iron(III) transfer to transferrin.

Although relatively high levels of powerful endogenous chelators such as citrate may effect the release of thermodynamically significant levels of iron(III) from the protein, the high carbon dioxide tension of the synovial fluid of inflamed rheumatoid joints would be expected to enhance the level of transferrin iron saturation relative to that in corresponding serum or plasma samples, even in the acidotic environment therein. However, Bates *et. al.*[133] found that the rate of iron(III) transfer from a 1:1 iron(III)-citrate complex to transferrin was not appreciably influenced by increasing bicarbonate ion concentration from 10^{-3} to 10^{-1} mol dm^{-3}, an observation consistent with the slow, rate-determining dissociation of the polymeric species prior to iron(III) exchange. Interestingly, Reiter *et. al.*[134] have previously suggested that the high citrate concentration of colostral whey effectively competes with transferrin and lactoferrin for iron(III), facilitating the uptake of

this metal ion by bacteria. Suppression of bacteriostasis by citrate in this manner was reversible in the presence of physiologically-relevant levels bicarbonate. Hence the availability of iron-citrate chelates in certain samples of knee-joint synovial fluid poses some intriguing questions regarding the susceptibility of these fluids to bacterial infection.

The loss of CO_2 from biological fluids during storage subsequent to collection (which increases their pH values) presents some problems in that iron(III) may be released from transferrin to low-molecular-mass chelators during the gradual decline in the concentrations of synovial fluid HCO_3^-/CO_3^{2-} anions which readily stabilise the specific binding of Fe(III) to the protein.

Equilibration of rheumatoid or osteoarthritic synovial fluid samples with 4.10×10^{-2} mol dm^{-3} nitrilotriacetate gave rise to striking increases in the intensities of the citrate and formate proton resonance in Hahn spin-echo spectra of synovial fluid, with little or no rise in that of the acetate signal.

Moreover, prolonged incubation of synovial fluid samples with 4.03 g dm^{-3} apotransferrin resulted in signal sharpening of citrate, formate and acetate, observations that may provide further evidence for the role of these species in the complexation of non-transferrin-bound iron in synovial fluid. These observations are particularly intriguing in view of the ability of apotransferrin to cause substantial citrate resonance broadening in a simple chemical model system via protein binding equilibrium (Table 5.3), and further demonstrate that interactions between synovial fluid citrate, formate and acetate and anionic binding sites present on added apotransferrin do not occur in the samples investigated. These results are also likely to reflect the saturation of such apotransferrin binding sites by alternative metabolites present at higher concentrations, e.g. lactate, which has synovial fluid levels of up to 1.2×10^{-2} mol dm^{-3}.[135]

The binding of citrate to apotransferrin observed here in a chemical model system is not unexpected in view of the high affinity of this apoprotein for anionic species, e.g.

phosphate, sulphate and vanadate in addition to bicarbonate[135]. Titration of an aqueous solution of citrate with Fe(III) in the presence of apotransferrin did not give rise to any iron(III)-mediated increases in the line-widths of the citrate proton resonance, in marked contrast to the broadening observed in rheumatoid or osteoarthritic synovial fluid samples on treatment with low concentrations of iron(III).

Although levels of Hahn spin-echo NMR-detectable (i.e. non-protein-bound) citrate in samples of rheumatoid or osteoarthritic synovial fluid vary widely both between and within patients (ca. 0.5 - 4.5 x 10^{-4} mol dm^{-3})[49], this endogenous chelator is always present in large excess over the concentrations of non-transferrin-bound (bleomycin-detectable) iron. Under these conditions, and at neutral pH Martin[120] calculated that the predominant Fe(III)-citrate complex is iron(III)-monocitrate $[Fe(III)(citrate\ H_{-1})]^-$ with all three carboxylate groups and the hydroxyl group deprotonated. At lower pH values, however, the 1:2 $[Fe(III)(citrate)_2]^{5-}$ complex forms, and is 40% mol fraction of the total iron concentration at a pH value of 5 in an isolated aqueous iron(III)/citrate system.

The complexation of non-transferrin-bound iron by synovial fluid citrate is also consistent with alternative evidence. Iron(III)-citrate chelates can readily stimulate the adverse production of oxygen-derived free radical species, and are detectable by the bleomycin assay[121]. Moreover, the rate of transfer of iron(III) from synovial fluid onto desferrioxamine is a slow process, as is the rate of transfer of iron(III) onto this chelator from citrate (Figure 5.8).

Halliwell and Gutteridge[14] postulated that the presence of bleomycin-detectable iron in rheumatoid or osteoarthritic synovial fluid could be explained by its release from transferrin in a 'sealed-off' microenvironment existing between macrophages or other phagocytes and cell or cartilage surfaces, the pH of which can drop to a value of 5 or less, facilitating removal of iron from the protein. However, a recent study[117] has suggested that iron can be released from ferritin by physiological chelators such as citrate or acetate, and

since synovial fluid levels of ferritin are markedly elevated over those of corresponding plasma samples[137], this phenomenon could also give rise to low-molecular-mass iron chelates.

A further important source of low-molecular-mass iron complexes in synovial fluid is haemoglobin which can arise from the lysis of erythrocytes that can occur during periods of traumatic injury in the inflamed joint. Indeed, Puppo and Halliwell[138] have shown that the interaction of H_2O_2 with haemoglobin produce a highly reactive species resembling $^{\cdot}OH$ radical.

The modifications in the Hahn spin-echo NMR-detectable VLDL- and chlymicron-associated lipid acyl chain terminal-CH_3 and bulk $(-CH_2-)_n$ resonance's observed following the addition of increasing concentration of iron(III) to synovial fluid may arise by the interaction of Fe(III) ions with pre-formed lipid hydroperoxides (LOOH, derived from peroxidation of the PUFA components of these signals) to generate peroxyl radical (LOO) which can further promote the autocatalytic, self-perpetuating chain reaction of lipid peroxidation. Alternatively, reduction of some of the added Fe(III) to Fe(II) by endogenous electron donors present in synovial fluid (e.g., thiols, ascorbate) could also give rise to this process.

In conclusion, these results demonstrate the value of proton Hahn spin-echo NMR spectroscopy in studies involving the speciation of metal-ions in body fluids obtained from patients with inflammatory joint diseases, providing a broad 'picture' of abnormalities in metal-ion metabolism.

CHAPTER 6

THE ROLE OF N-ACETYLCYSTEINE IN PROTECTING SYNOVIAL FLUID BIOMOLECULES AGAINST RADIOLYTICALLY-MEDIATED OXIDATIVE DAMAGE: A HIGH FIELD NMR STUDY

6.1 INTRODUCTION

It has been known for over 40 years that certain thiols and disulphides exhibit a radioprotective ability if administered prior to exposure to sources of ionising radiation[141-143], a phenomenon which presents the possibility that such compounds are able to confer protection of living organisms against the low levels to which they are being continuously exposed. Thiols such as cysteamine may act in this capacity by playing a role in neutralising the toxic effects of hydroxyl radical (·OH) (equation 6.1) or, alternatively, by repairing damage to biomolecules oxidatively modified by ·OH radical (equation 6.2 and 6.3).

$$RSH + \cdot OH \rightarrow RS\cdot + H_2O \qquad (6.1)$$

$$RH + \cdot OH \rightarrow R\cdot + H_2O \qquad (6.2)$$

$$R\cdot + RSH \rightarrow RH + RS\cdot \qquad (6.3)$$

Further radiolytically-induced chemical modifications to thiols include the subsequent dimerisation to thiyl radicals (RS·) to form the corresponding disulphide[144] (RSSR) (equation 6.4) and interaction of RS· radicals with dioxygen to produce thiylperoxy radical species (equation 6.5) which has been demonstrated in pulse radiolysis experiments[145-147]. In addition, sulphenyl radicals (RSO·) are also generated in the presence of O_2[148]. Radical ion dimers ($RSSR^{\cdot -}$) can arise from the reaction of thiyl radicals with further thiol[149] (equation 6.6) or from the reduction of disulphides by radiolytically-generated aquated electrons ($e_{(aq.)}^-$) in systems depleted of O_2 (equation 6.7)[150].

$$2RS\cdot \rightarrow RSSR \qquad (6.4)$$

$$RS\cdot + O_2 \rightarrow RSO_2\cdot \qquad (6.5)$$

$$RS\cdot + RSH \rightarrow RSSR^{\cdot -} + H^+ \qquad (6.6)$$

$$e_{(aq.)}^- + RSSR \rightarrow RSSR^{\cdot -} \qquad (6.7)$$

However, Wefer and Sies[151] have presented evidence consistent with the oxidation of glutathione by superoxide anion ($O_2^{\cdot -}$) to its disulphide together with smaller quantities of sulphonate, a reaction which yields the aggressively-reactive singlet oxygen. Moreover, Aruoma *et. al.*[152] have proposed that in the presence of O_2, sulphur-containing radical species arising from the interaction of physiologically-generated oxidants with penicillamine can inactivate α_1-antiprotease.

The antioxidant actions of N-acetylcysteine in a wide range of experimental systems are now well established. Examples of its ability to suppress oxidative damage in biological systems include inhibition of endotoxin-induced lung damage[153], reduction of membrane damage by superoxide generating systems in porcine aortic endothelial cells[154], protection of animals against paracetamol hepototoxicity[155], alleviation of diquat toxicity to hepatocytes[156], and preventation of damage to human bronchial fibroblasts by tobacco smoke condenstates[157]. Indeed, N-acetylcysteine has been employed as an effective therapeutic agent for the treatment of a range of human respiratory diseases[158]. Postulated mechanisms of action for this thiol drug include its ability to: (1) increase intracellular concentrations of cysteine and hence gluthathione and (2) scavenge oxidants such as $O_2^{\cdot -}$, hydrogen peroxide (H_2O_2) and hypochlorous acid (HOCL)[157], the latter of which is generated by the myeloperoxidase (MPO)-H_2O_2-Cl^- system.

Arouma *et. al.*[159] have recently investigated the antioxidant action of N-acetylcysteine with respect to its reactions with ·OH radical, $O_2^{\cdot -}$, H_2O_2 and HOCl, and concluded that it reacts rapidly with ·OH radical (second-order rate constant, $k_2 = 1.36 \times 10^{10}$ mol^{-1} dm^3 s^{-1}), is a powerful scavenger of HOCl, but reacts very slowly with H_2O_2 (at 25°C and pH 7.4). No evidence for the reaction of N-acetylcysteine with O_2^- was obtained in these studies.

In view of the large amount of evidence available for the deleterious role of reactive oxygen-derived radical species in the pathogenesis of inflammatory joint diseases (reviewed

in chapter 1), it is conceivable that N-acetylcysteine may have a therapeutic role to play in such conditions by modulating oxidative damage to endogenous biomolecules arising from the action of such radicals *in vivo*. Indeed, the diminished antioxidant status of inflammatory synovial fluids renders biomolecules therein particularly susceptible to damage by biologically-generated oxidants.

In this study high field ^{1}H nuclear magnetic resonance (NMR) spectroscopy has been employed to assess the ability of N-acetylcysteine to suppress radiolytically-mediated oxidative modifications to biomolecules present in inflammatory human knee- joint synovial fluid *in vitro*. The action of the naturally-occurring amino acid cysteine in regulating such oxidative damage has also been investigated in this manner for purposes of comparison. Grootveld *et. al.*[23] have previously reported the application of high field proton (^{1}H) Hahn spin-echo NMR spectroscopy to the simultaneous detection of a variety of products derived from the reactions of radiolytically-generated reactive oxygen species (specifically $^{\cdot}OH$ radical) with components present in inflammatory knee-joint synovial fluid samples (e.g., low-molecular-mass oligosaccharides arising from hyaluronate fragmentation).

6.2 RESULTS

6.2.1 Gamma-radiolysis of Aqueous Thiol Solutions

400 MHz ^1H NMR spectra of control and gamma-irradiated (5.00 kGy) aqueous solutions of N-acetylcysteine demonstrated that N-acetylcystine was a major product derived from the attack of radiolytically-generated ·OH radical and, to a lesser extent, $O_2^{\cdot -}$ on the thiol. The ABX coupling system of this disulphide was readily detectable in spectra of gamma-irradiated samples (Figure 6.1). This product was not detectable in the solution of N-acetylsteine allowed to equilibrate at 4°C in the presence of atmospheric O_2 for 18 hr, indicating the high stability of this thiol under these conditions. A singlet resonance of low intensity located at 8.27 ppm was also present in spectra of gamma-irradiated N-acetylsteine solutions, a signal which is presumably attributable to an amide (-NH-CO-CH_3) proton present in an alternative radiolytic product. Moreover, a small quantity of acetate (singlet at 1.93 ppm) was generated from the radiolytic degradation of the -$NHCOCH_3$ functional group of the molecule, and a doublet centred at 1.41 ppm was present in spectra of gamma-irradiated samples, further indicating the diversity of radiolytic products arising from this thiol.

Gamma-radiolysis of aqueous cysteine solutions gave rise to cystine as the predominant radiolytic product. Its characteristic ABX coupling pattern was readily detectable in spectra of irradiated samples (Figure 6.2), and a reference spectrum of a solution of an authentic sample of L-cystine in ^2H_2O confirmed the identity of this product. In contrast to results obtained with N-acetylcysteine, incubation of aqueous solutions of cysteine in an O_2 atmosphere at 4°C for a period of 18 hr was found to produce a small amount of disulphide from the parent thiol, a product which presumably arises from its autoxidation via equation 6.10, followed by a combination of thiyl radicals generated to produce the corresponding disulphide (equation 6.4).

$$RS^- + O_2 \rightarrow RS\cdot + O_2^{\cdot -} \qquad (6.10)$$

After allowing for the small quantity of cystine already present in the control (unirradiated) cysteine solution, the intensity of the cystine-CH proton resonance relative to that of the remaining cysteine in gamma-irradiated solutions was 0.28 ± 0.03 (mean ± standard error, n=4), demonstrating a 22 ± 2% conversion of cysteine to its disulphide under these experimental conditions.

Hence, from these investigations it is clear that the major products derived from gamma-radiolysis of aqueous solutions of both N-acetylsteine and cysteine in this manner are the corresponding disulphides. The sulphonates of these thiols were not detected by ^{1}H NMR spectroscopy in these experiments.

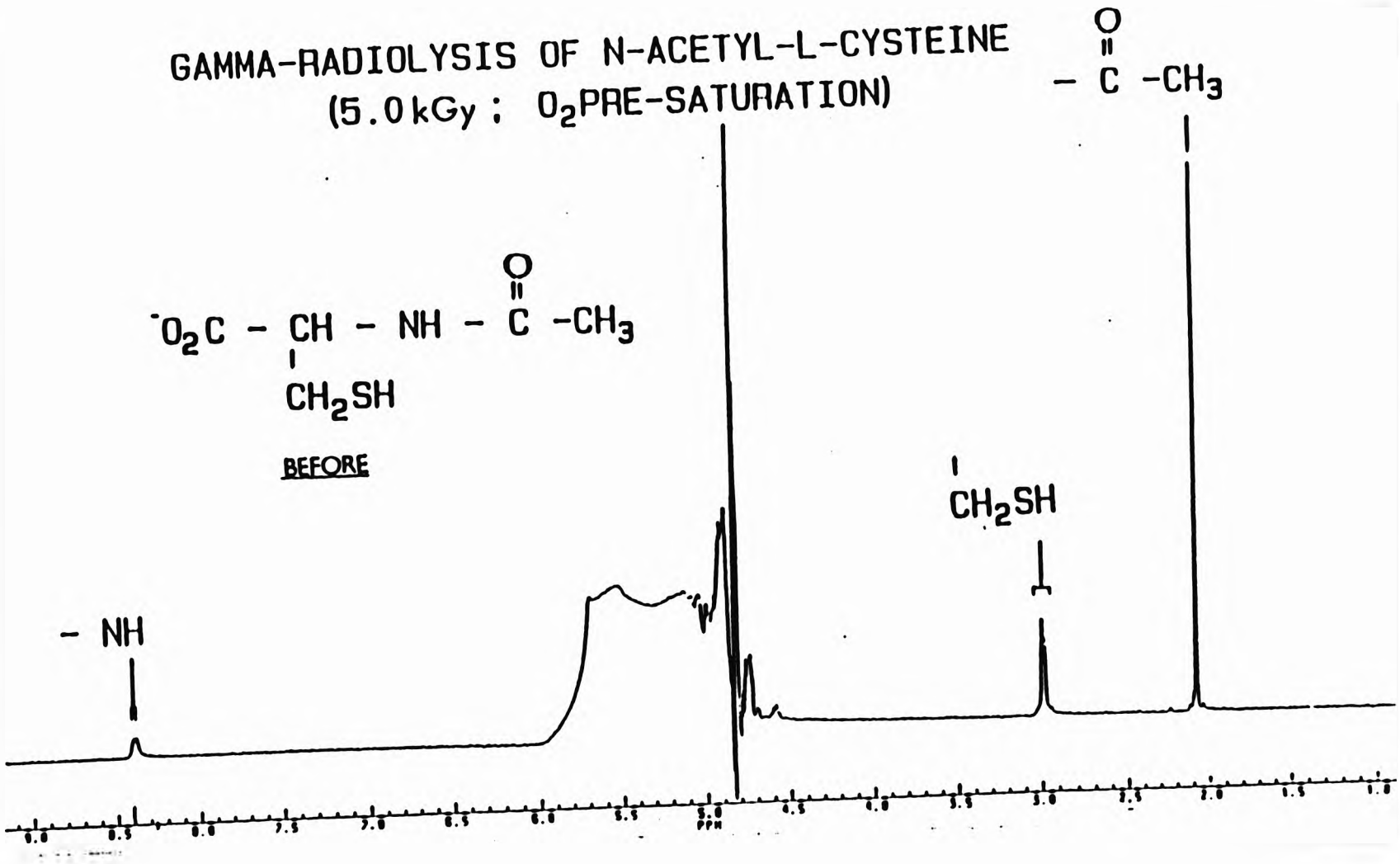

Figure 6.1(a)

400 MHz single-pulse ^1H NMR spectra of a 2.00×10^{-2} mol dm^{-3} aqueous solution of N-acetylcysteine containing 2.00×10^{-2} mol dm^{-3} phosphate buffer (pH 7.00) obtained before gamma-radiolysis.

Abbreviations : A, acetate-CH_3.

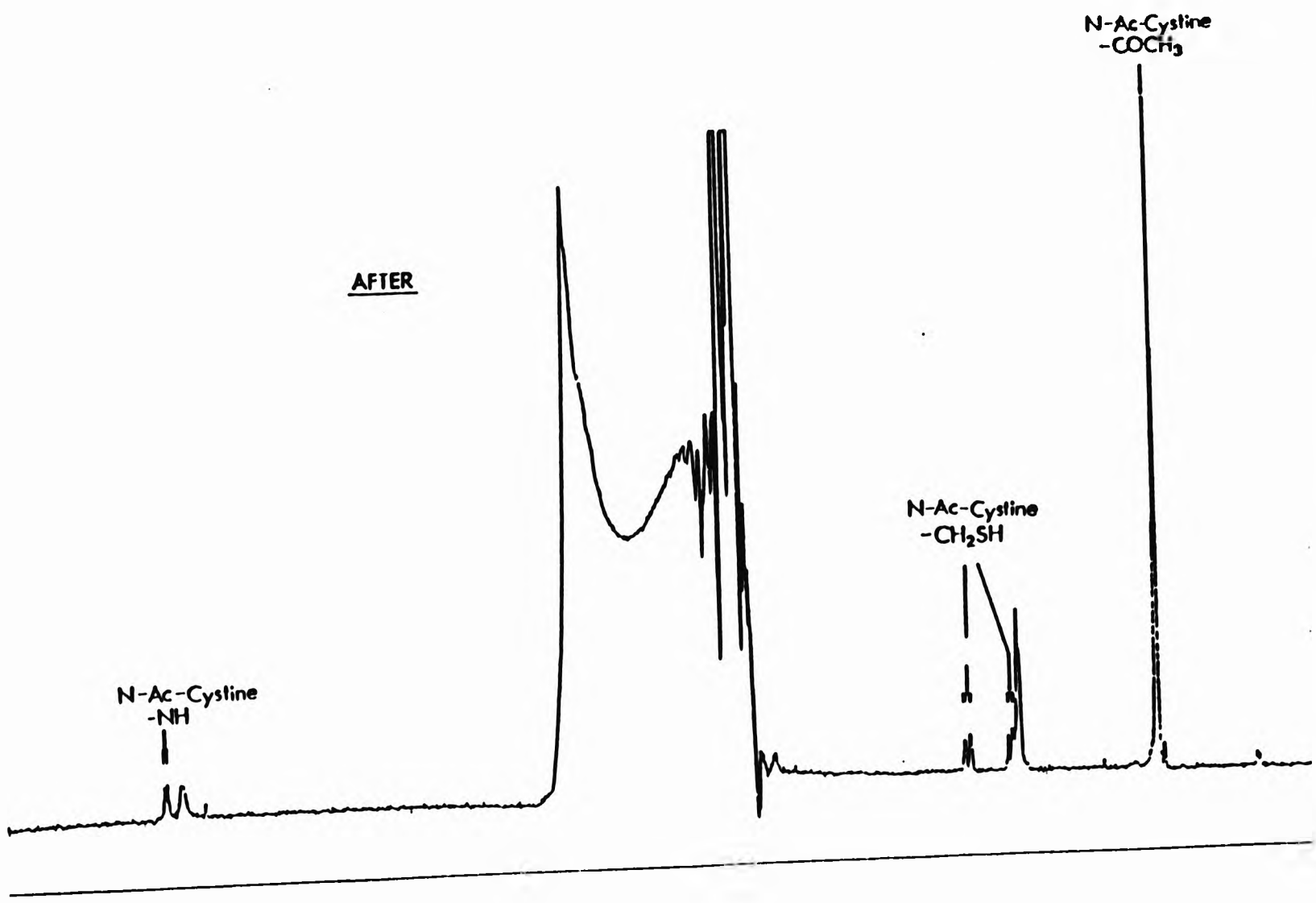

Figure 6.1(b)

400 MHz single-pulse ^1H NMR spectra of a 2.00×10^{-2} mol dm^{-3} aqueous solution of N-acetylcysteine containing 2.00×10^{-2} mol dm^{-3} phosphate buffer (pH 7.00) obtained after gamma-radiolysis at a dose level of 5.00 kGy.

Abbreviations : A, acetate-CH_3.

ABX COUPLING SYSTEM

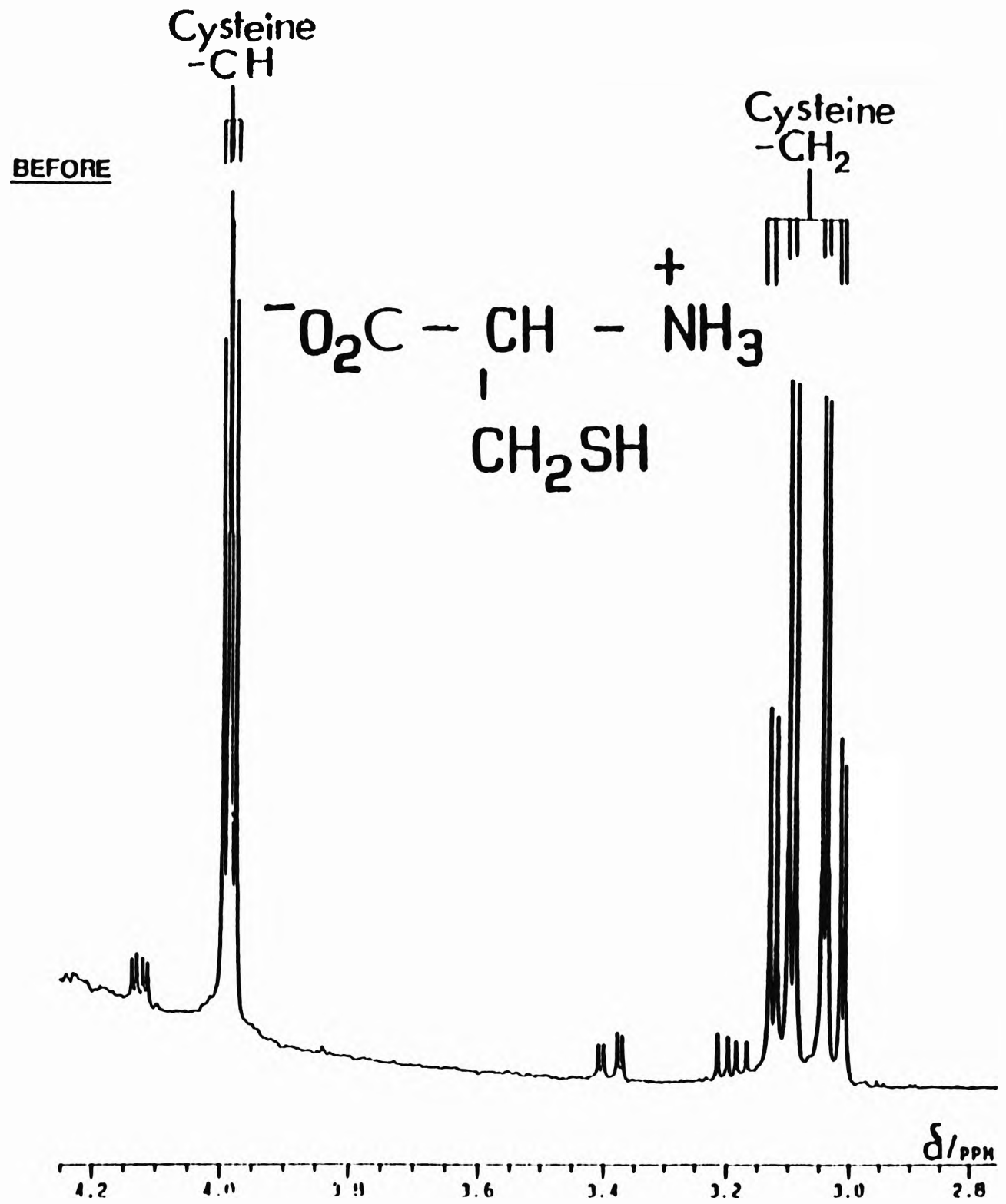

Figure 6.2(a)

500 MHz single-pulse ^1H NMR spectra of a 0.10 mol dm^{-3} aqueous solution of L-cysteine containing 2.00 x 10^{-2} mol dm^{-3} phosphate buffer (pH 7.00) obtained prior to gamma-radiolysis (5.00 kGy).

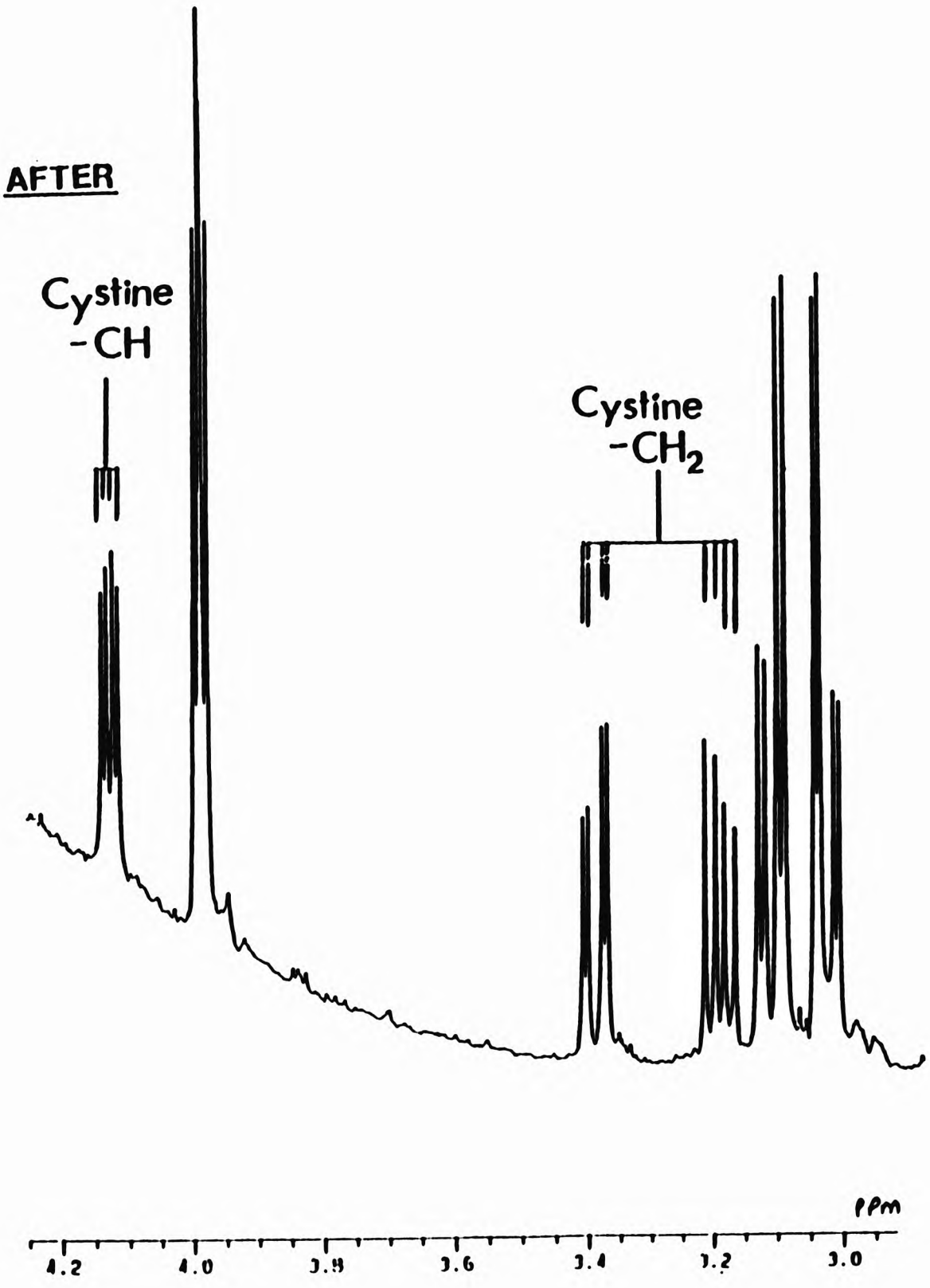

Figure 6.2(b)

500 MHz single-pulse ^{1}H NMR spectra of a 0.10 mol dm^{-3} aqueous solution of L-cysteine containing 2.00 x 10^{-2} mol dm^{-3} phosphate buffer (pH 7.00) obtained subsequent to gamma- radiolysis (5.00 kGy).

6.2.2 Radioprotective ability of N-acetylcysteine towards components present in inflammatory synovial fluids

As previously documented, modification in the high field region of ^1H Hahn spin-echo NMR spectra mediated by radiolytically-generated ·OH radical consisted of the production of an intense singlet resonance located at 2.032 ppm attributable to the N-acetyl-CH_3 group protons of low-molecular-mass N-acetylglucosamine-containing oligosaccharide fragments derived from depolymerisation of the glycosaminoglycan hyaluronate, together with the marked rise in the concentration of non-protein-bound acetate, the latter predominantly arising from the reaction of ·OH radical with the high levels of lactate present[163]. Smaller quantities of acetate are derived from the oxidative decarboxylation of pyruvate by radiolytically-generated H_2O_2 and/or further ·OH radical. In addition, a singlet resonance located at 2.74 ppm of unknown identity was also generated subsequent to gamma radiolysis.

The high field (aliphatic) region of typical ^1H Hahn spin- echo NMR spectra of control and gamma-irradiated (5.00 kGy) synovial fluid samples are shown in Figure 6.3.

Modifications in the low field (aromatic) region of these spectra arising from the potent oxidising actions of radiolytically-generated ·OH radical included the generation of (1) formate (singlet at 8.46 ppm) from carbohydrates in general (predominantly glucose), and (2) allantoin (singlet at 5.40 ppm) from urate (Figure 6.4), as previously reported[163].

Equilibration of synovial fluid samples with the 1.00 or 3.00 x 10^{-3} mol dm^{-3} N-acetyl-L-cysteine prior to gamma-radiolysis exerted a selective, concentration-dependent influence on the quantities of NMR-detectable radiolytic products generated. At an added N-acetylcysteine concentration of 1.00 x 10^{-3} mol dm^{-3}, the magnitudes of the allantoin-CH and formate-H signals were significantly diminished (Figure 6.4), whereas those of the acetate-CH_3 group and 2.74 ppm singlet resonance remained unaffected (Figure 6.3). On increasing the level of added N-acetylcysteine to 3.00 x 10^{-3} mol dm^{-3}, the intensity of the

allantoin-CH signal was not further reduced. However, the levels of NMR-detectable formate and acetate were elevated above those observed at an added N-acetylcysteine concentration of 1.00×10^{-3} mol dm^{-3}, the former to a value similar to that observed in gamma-irradiated samples that were not pre-equilibrated with the thiol.

In these experiments, the intensity of the singlet resonance attributable to the N-acetyl-CH_3 group protons of N-acetylglucosamine residue present in hyaluronate-derived oligosaccharide fragments was not accurately determined since it is located very close to those of the 5,5'-position N-acetylsugars of the molecularly mobile 'acute-phase' glycoprotein carbohydrate side-chains (predominantly those of α_1-acid glycoprotein), N-acetylcysteine and N-acetylcystine, the latter arising from radiolytic damage to the added thiol. However, the spectra obtained suggest that the amplitude of this oligosaccharide resonance, when normalised to that of the broader glyco protein signal centred slightly down field (δ=2.04 ppm), is reduced at an added N-acetylcysteine concentration of 3.00×10^{-3} mol dm^{-3}, suggesting a limited suppression of radiolytically-mediated hyaluronate depolymerisation by this radioprotectant.

The radiolytic product N-acetylcystine was simultaneously detectable in ^1H Hahn spin-echo NMR spectra of gamma-irradiated synovial fluid samples pre-treated with N-acetylcysteine, demonstrating the radioprotectant/antioxidant activity of this thiol when present in intact biofluids. A substantial elevation in the concentration of N-acetylcystine generated (measured by the intensity of its -$NHCOCH_3$ group proton resonance) was observed in gamma-irradiated synovial fluids on raising that of added N-acetylcysteine from 1.00 to 3.00×10^{-3} mol dm^{-3}. Normalisation of the intensity of the N-acetylcystine-$NHCOCH_3$ group signal to that of the alanine-CH_3 group revealed that the level of this radiolytic product generated increases by ca. 60% on elevating the added N-acetylcysteine concentration in this manner. The approximate relative intensity of the N-acetylcystine to N-acetylcysteine-$NHCOCH_3$ resonance was 0.6 at both concentrations of added N-acetylcysteine.

Further evidence for the radiolytically-mediated generation of N-acetylcystine from its thiol precursor was provided by the observation of its magnetically-unequivalent-CH_2-S-S-CH_2- proton resonances (part of its ABX coupling system) located at 3.08 and 3.29 ppm in these spectra at an added N-acetylcysteine concentration of 3.00×10^{-3} mol dm^{-3}. These signals were only barely detectable at an added N-acetylcysteine level of 1.00×10^{-3} mol dm^{-3}.

Each of the above observations were reproducible in a total of 5 different synovial fluid samples investigated.

Figure 6.3(a)

High field (aliphatic) region of 500 MHz ^1H Hahn spin-echo NMR spectra of a typical inflammatory synovial fluid sample; Typical spectra is shown.

Abbreviations: A, acetate-CH_3; Ac, acetone-CH_3; Ala, alanine-CH_3: APG-I and II; N-acetyl sugars present in the 5,5'- and 2,7- positions, respectively, of the molecularly-mobile carbohydrate side-chains of 'acute-phase' glycoproteins (predominantly α_1-acid glycoprotein); Bu, 3-D-hydroxybutyrate-CH_3; Cit, citrate-CH_2; Cn_1 and Cn_2, creatinine-N-CH_3 and -CH_2 groups respectively; Cn, creatine-N-CH_3; Glc, glucose carbohydrate ring proton resonance; Gln_1 and Gln_2, b- and -CH_2 groups of glutamine respectively; Gly, glycine-CH_2; HA-derived OS, N-acetyl-CH_3 groups of N-acetylglucosamine residues present in oligosaccharide fragments arising from the radiolytic depolymerisation of hyaluronate; Ile and b-Ile, isoleucine terminal-CH_3 and b-CH_3 groups respectively; Lac-CH_3 and Lac-CH, lactate-CH_3 and -CH groups; -$N(CH_3)_3$, - $N(CH_3)_3$ groups of betaine, carnitine and choline; TAG-CH_3 and TAG-CH_2-, acyl chain terminal-CH_3 and bulk (-CH_2-)$_n$ groups respectively of chylomicron- and very-low-density-lipoprotein (VLDL)-associated fatty acids (predominantly triacylglycerols); Thr, threonine-CH_3; Val, valine-CH_3. The asterisk in spectra (b), (c) and (d) denotes the radiolytically-generated 2.74 ppm singlet resonance.

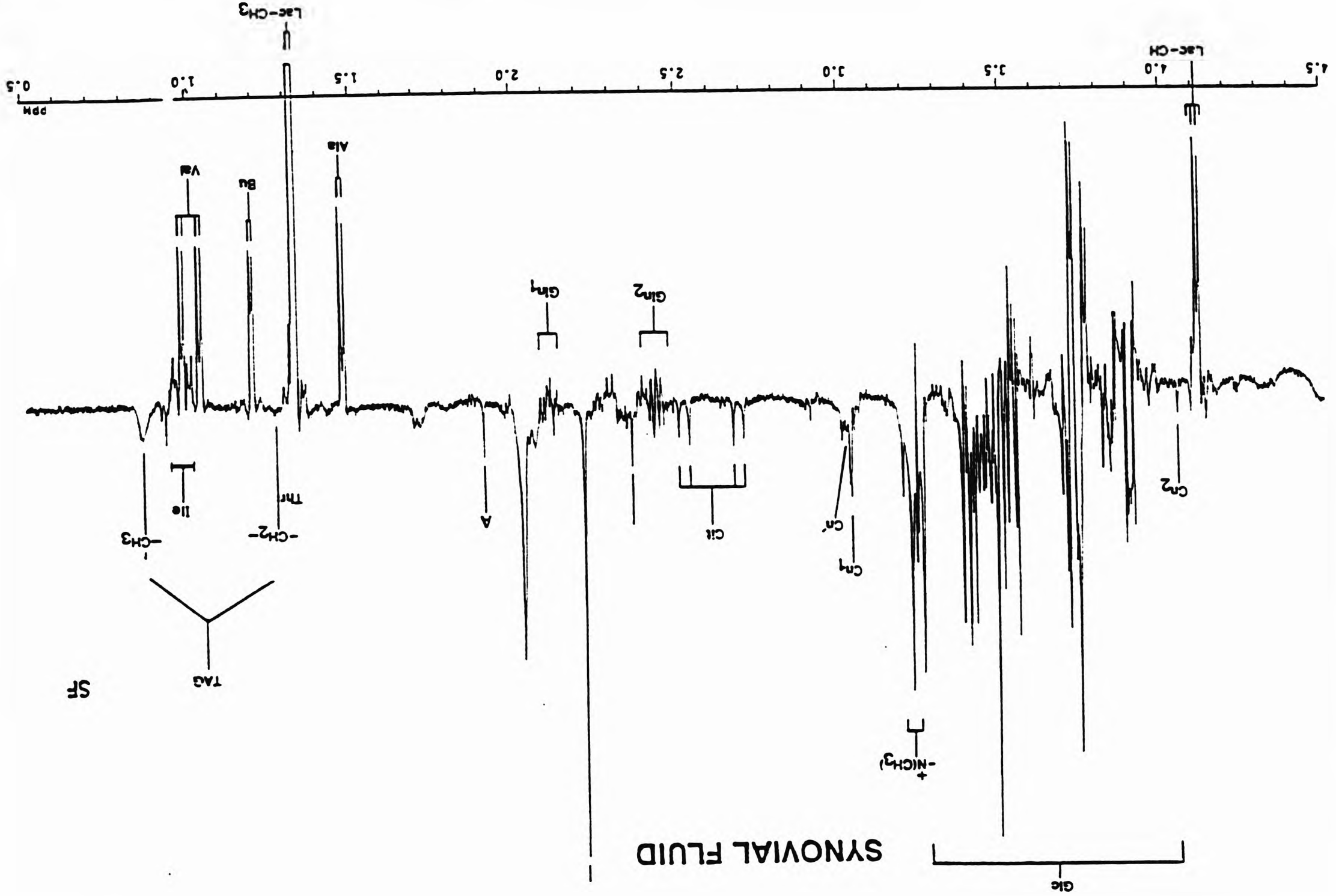
SYNOVIAL FLUID
SF
Glc
-N⁺(CH₃)₃
CH₃
CH₂
Cit
Cn'
Cn
Gln₂
Gln₁
A
-CH₂-
Thr
Ile
-CH₃
Bu
Val
Ala
Lac-CH
Lac-CH₃
TAG
ppm
4.5
4.0
3.5
3.0
2.5
2.0
1.5
1.0
0.5

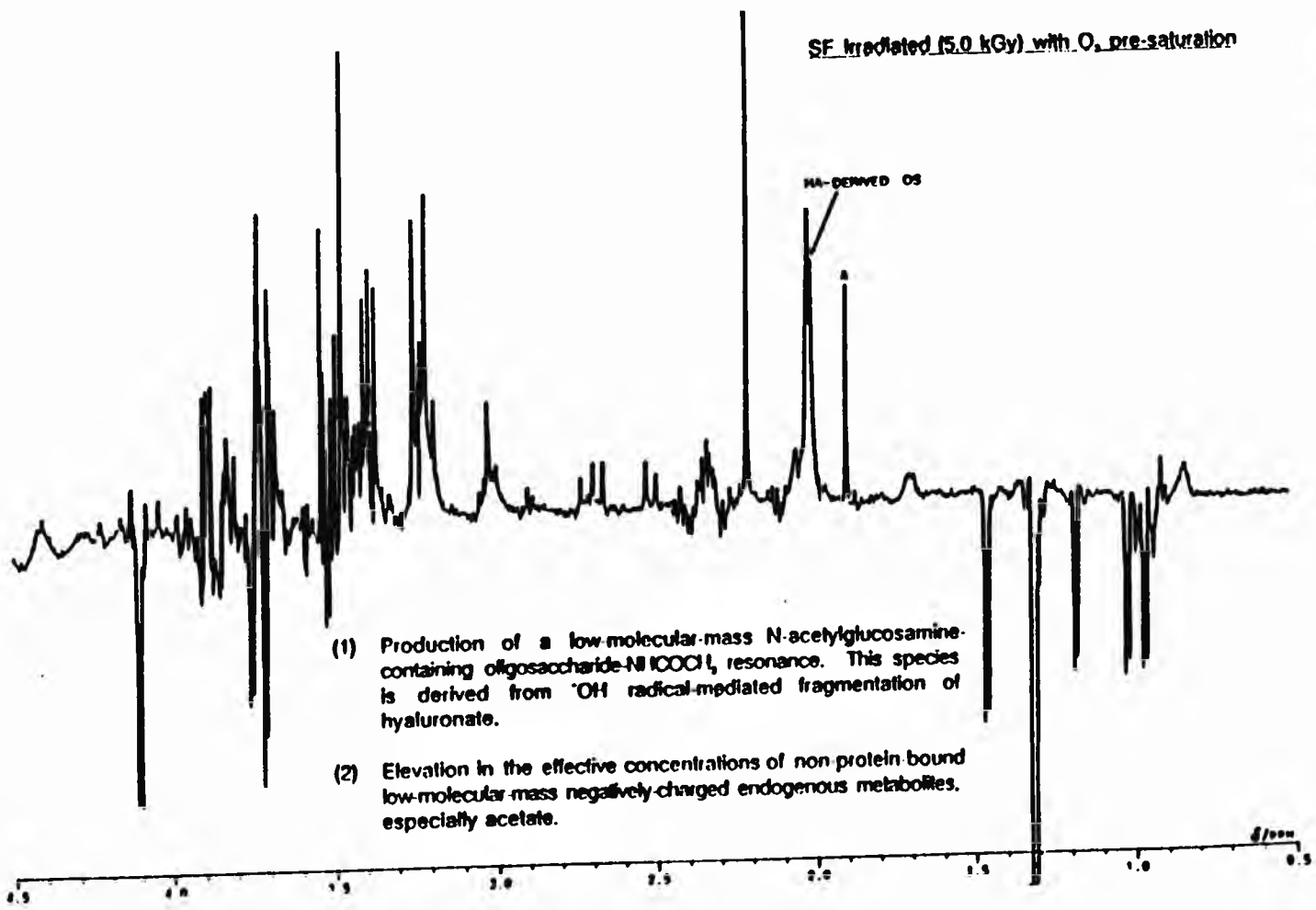

Figure 6.3(b)

High field (aliphatic) region of 500 MHz ^1H Hahn spin-echo NMR spectra of a typical inflammatory synovial fluid sample following gamma-radiolysis (5.00 kGy). Typical spectra is shown.

Abbreviations: as in Figure 6.3(a)

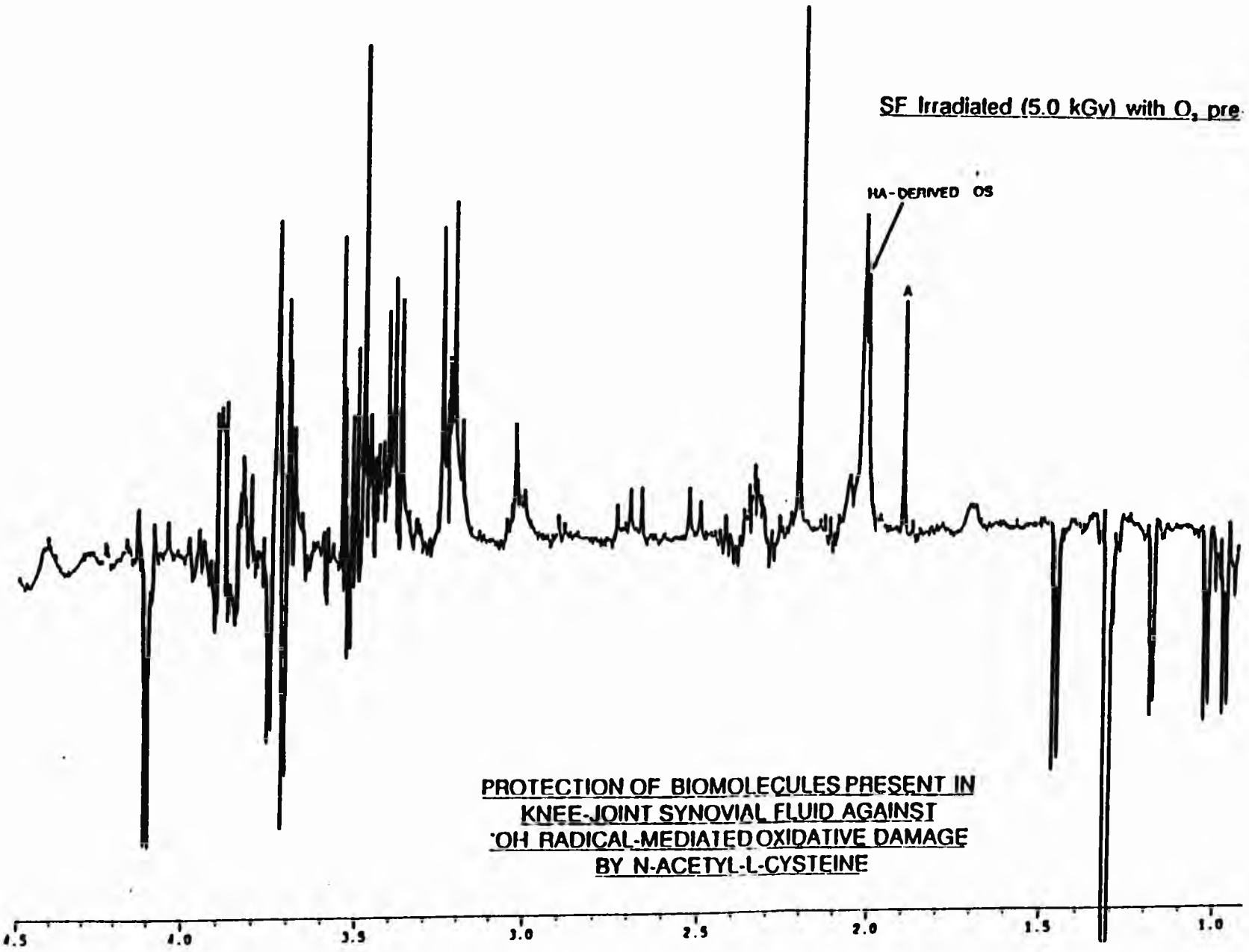

Figure 6.3(c)

High field (aliphatic) region of 500 MHz ^{1}H Hahn spin-echo NMR spectra of a typical inflammatory synovial fluid sample; following gamma-radiolysis (5.00 kGy); but treated with 1.00×10^{-3} mol dm^{-3} N-acetylcysteine prior to gamma-radiolysis. Typical spectra is shown.

Abbreviations: as in Figure 6.3(a)

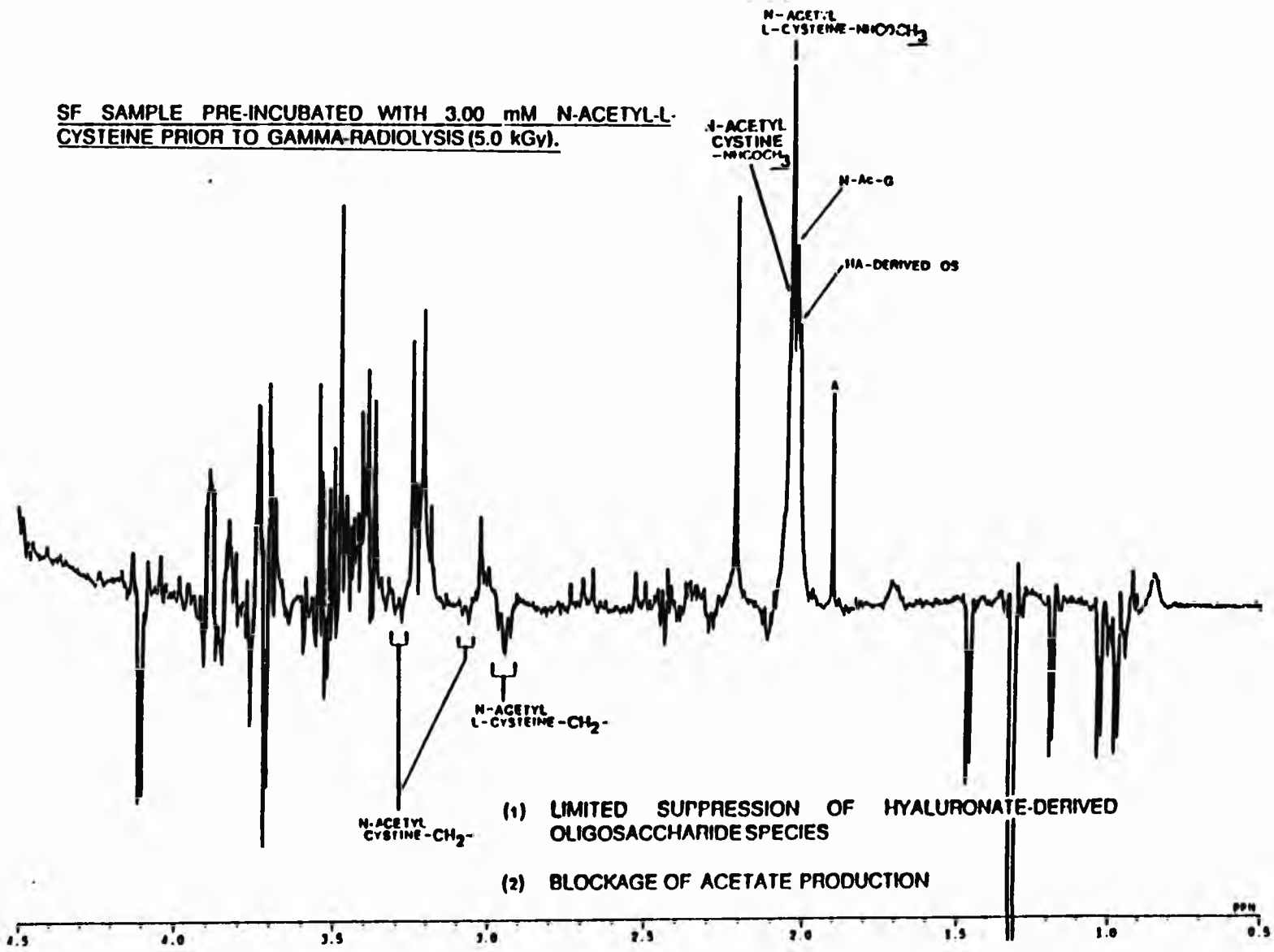

Figure 6.3(d)

High field (aliphatic) region of 500 MHz ^1H Hahn spin-echo NMR spectra of a typical inflammatory synovial fluid sample; but following gamma-radiolysis (5.00 kGy); but treated with 3.00×10^{-3} mol dm^{-3} N-acetylcysteine prior to gamma-radiolysis. Typical spectra is shown.

Abbreviations: As in Figure 6.3(a).

SYNOVIAL FLUID

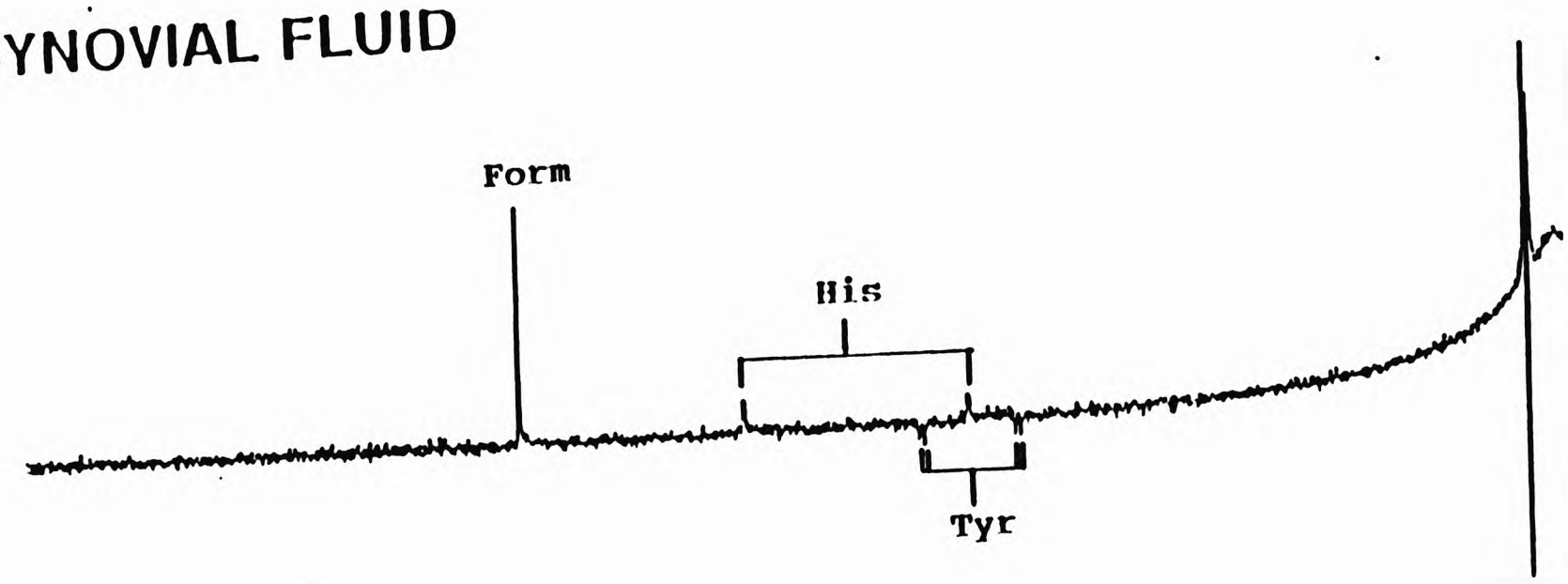

Figure 6.4(a)

Low field (aromatic) region of the 500 MHz ^1H Hahn spin-echo NMR spectra shown in Figure 6.3: of untreated (control) synovial fluid.

Abbreviations: At, allantoin-CH; Form, formate-H; α-GLC, α-glucose anomeric ring proton; His, histidine imidazole ring protons; Tyr, tyrosine aromatic ring protons.

SF Irradiated (5.0 kGy) with O_2 pre-saturation

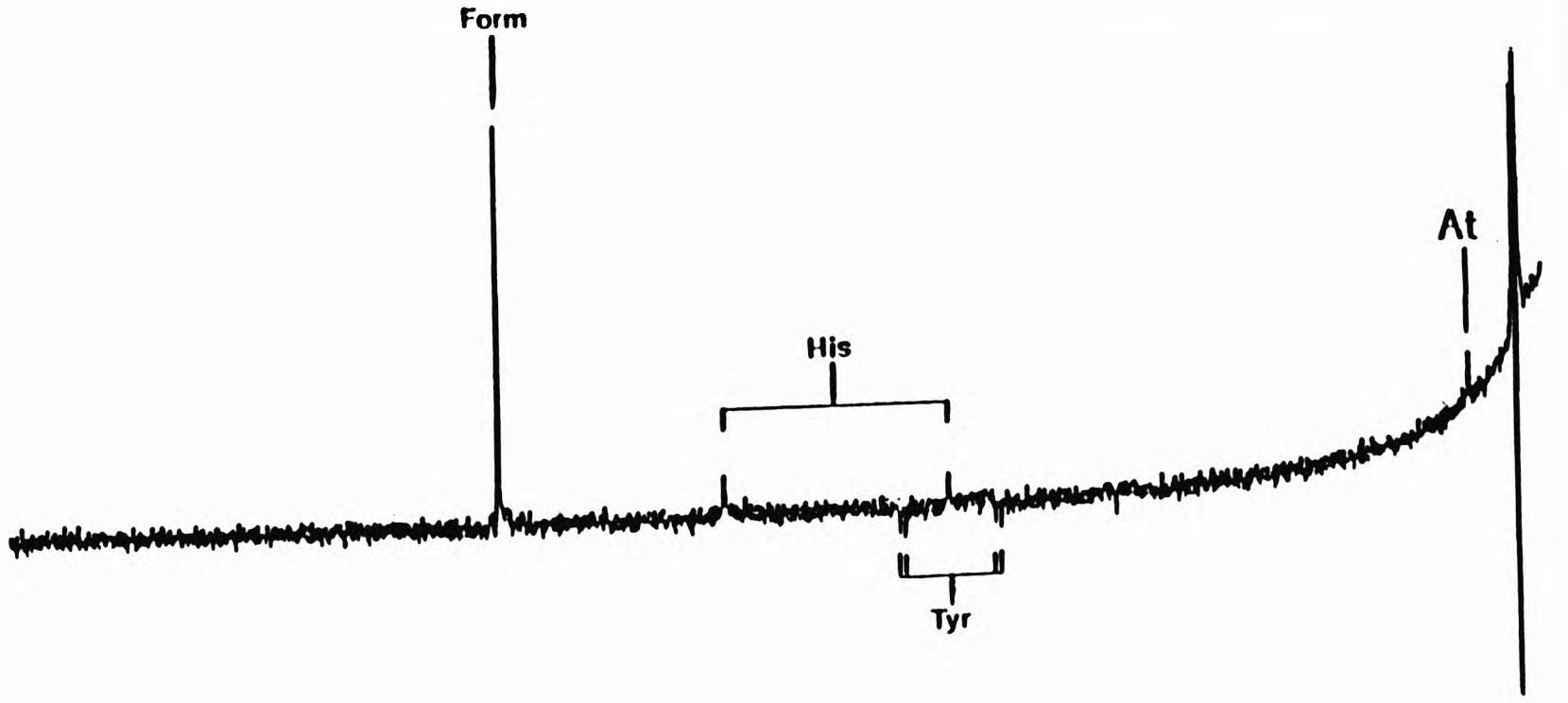

(1) Marked increases in the concentration of formate derived from reaction of ·OH radical with endogenous carbohydrate systems (predominantly glucose).

(2) Production of allantoin from attack of radiolytically-generated ·OH radical on urate

Figure 6.4(b)

Low field (aromatic) region of the 500 MHz ^1H Hahn spin-echo NMR spectra shown in Figure 6.3: of, untreated (control) synovial fluid but subsequent to gamma-radiolysis (5.00 kGy).

Abbreviations: At, allantoin-CH; Form, formate-H; α-GLC, α-glucose anomeric ring proton; His, histidine imidazole ring protons; Tyr, tyrosine aromatic ring protons.

PROTECTION OF BIOMOLECULES PRESENT IN KNEE-JOINT SYNOVIAL FLUID AGAINST $^{\bullet}OH$ RADICAL-MEDIATED OXIDATIVE DAMAGE BY N-ACETYL-L-CYSTEINE

SF Irradiated (5.0 kGy) with $O_2^{\bullet}$ pre-saturation

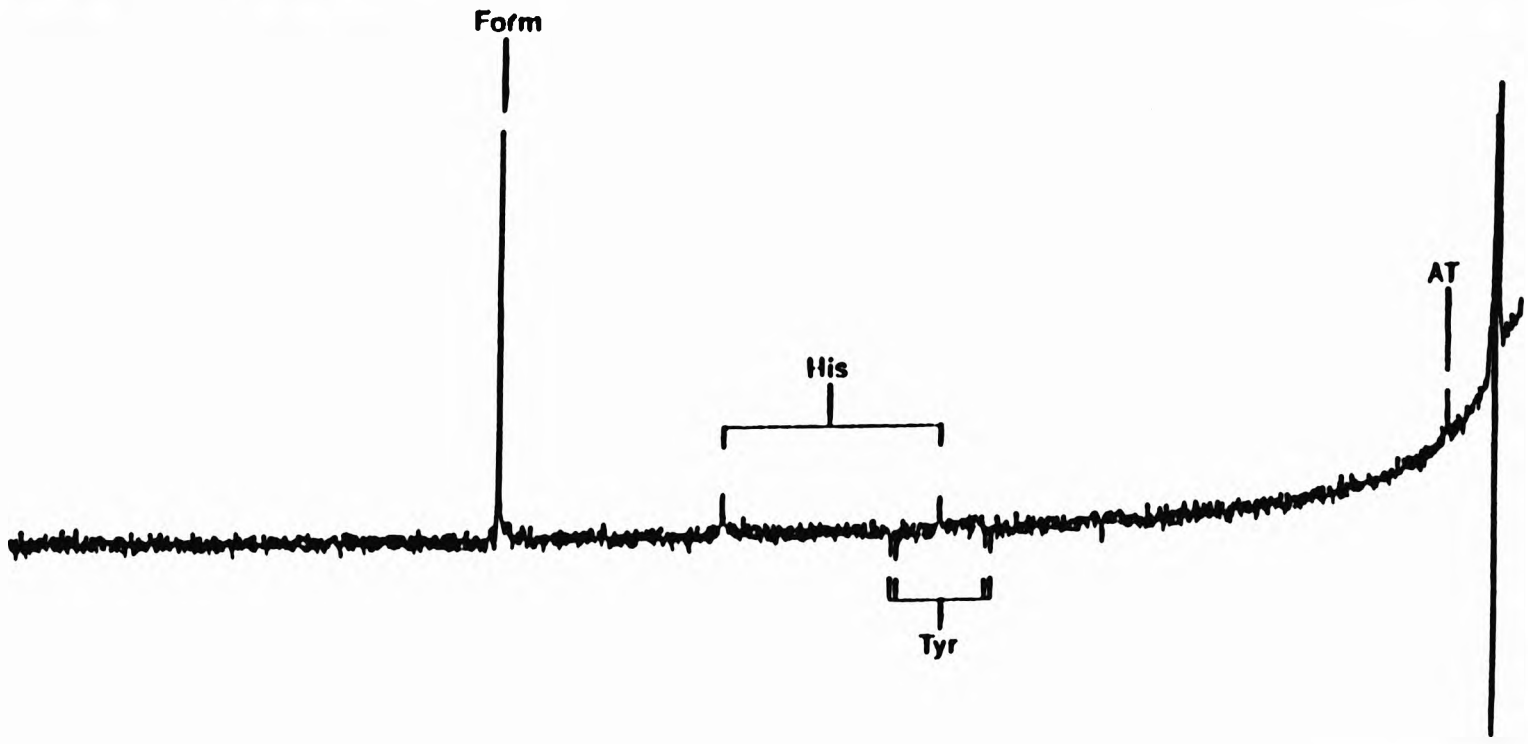

Figure 6.4(c)

Low field (aromatic) region of the 500 MHz ^1H Hahn spin-echo NMR spectra shown in Figure 6.3: of, untreated (control) synovial fluid; subsequent to gamma-radiolysis (5.00 kGy); but treated with 1.00×10^{-3} mol dm^{-3} N-acetylcysteine prior to gamma-radiolysis.

Abbreviations: At, allantoin-CH; Form, formate-H; α-GLC, α-glucose anomeric ring proton; His, histidine imidazole ring protons; Tyr, tyrosine aromatic ring protons.

SF SAMPLE PRE-INCUBATED WITH 3.00 mM N-ACETYL-L-CYSTEINE PRIOR TO GAMMA-RADIOLYSIS (5.0 kGy).

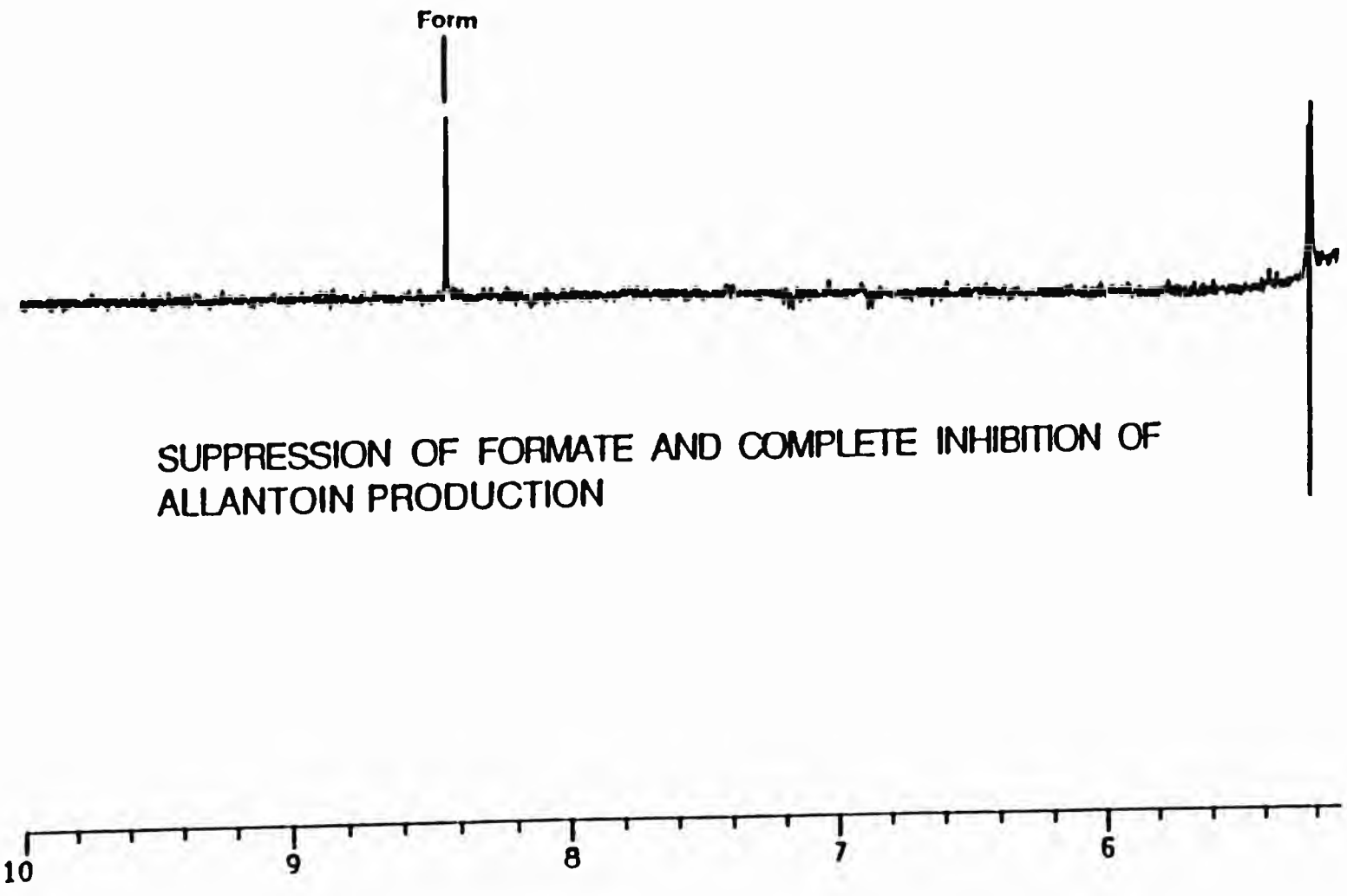

Figure 6.4(d)

Low field (aromatic) region of the 500 MHz ^1H Hahn spin-echo NMR spectra shown in Figure 6.3: of, untreated (control) synovial fluid subsequent to gamma-radiolysis (5.00 kGy), but treated with 3.00×10^{-3} mol dm^{-3} N-acetylcysteine prior to gamma-radiolysis.

Abbreviations: At, allantoin-CH; Form, formate-H; α-GLC, α-glucose anomeric ring proton; His, histidine imidazole ring protons; Tyr, tyrosine aromatic ring protons.

6.2.3 Capacity of exogenous cysteine to protect synovial fluid biomolecules against radiolytically-mediated oxidative damage.

High field ^{1}H NMR analysis demonstrated that equilibration of knee-joint synovial fluids with increasing concentrations of L-cysteine (1.00, 2.00 or 5.00 x 10^{-3} mol dm^{-3}) prior to gamma-irradiation treatment also gave rise to concentration-dependent modifications in the nature and extent of radiolytic damage to biomolecules therein (Figures 6.5 and 6.6).

In the high field region of the resulting Hahn spin-echo spectra, these modifications comprised (1) a minor suppression of acetate production from lactate, and subsequently pyruvate, at the highest concentration of added cysteine employed (5.00 x 10^{-3} mol dm^{-3}), and (2) a limited blockage of hyaluronate fragmentation throughout the whole added cysteine concentration range. However, as noted for N-acetylcysteine above, cysteine failed to exert an influence on the intensity of the 2.74 ppm singlet resonance.

Cysteine-induced modifications in the levels of radiolytic products detectable in the low field region of Hahn spin-echo spectra included a substantial reduction in the concentration of allantoin arising from oxidative damage to urate. Indeed, this radiolytic product was completely undetectable at an added cysteine concentration of 5.00 x 10^{-3} mol dm^{-3}. Although a limited inhibition of the level of formate generation was observed at an added concentration of 2.00 x 10^{-3} mol dm^{-3}, a marked rise in the intensity of its 8.46 ppm resonance was noted at a cysteine concentration of 5.00 x 10^{-3} mol dm^{-3}. This observation may reflect the ability of cysteine, and/or its major radiolytic product cystine, to displace this anionic metabolite from positively-charged protein binding-sites (e.g. lysine or argine residues) at the highest level of added thiol. Previous ^{1}H NMR investigations have established that a pool of 'NMR-invisible', protein-bound anionic metabolites such as lactate can be mobilised from these macromolecular binding-sites by the addition of high levels of ammonium chloride ($\geq$ 0.5 mol dm^{-3}) to biofluids[164].

Although cysteine itself was readily detectable in ^{1}H Hahn spin-echo spectra of synovial fluid at the lowest concentration added (1.00×10^{-3} mol dm^{-3}), overlap with the resonances of endogenous metabolites such as glucose prevented the detection of the cystine -CH and $-CH_2$ group signals.

The above modifications in ^{1}H Hahn spin-echo NMR spectra of gamma-irradiated synovial fluids arising from their pre-treatment with 1.00, 2.00 or 5.00×10^{-3} mol dm^{-3} cysteine were observed in all 5 samples investigated.

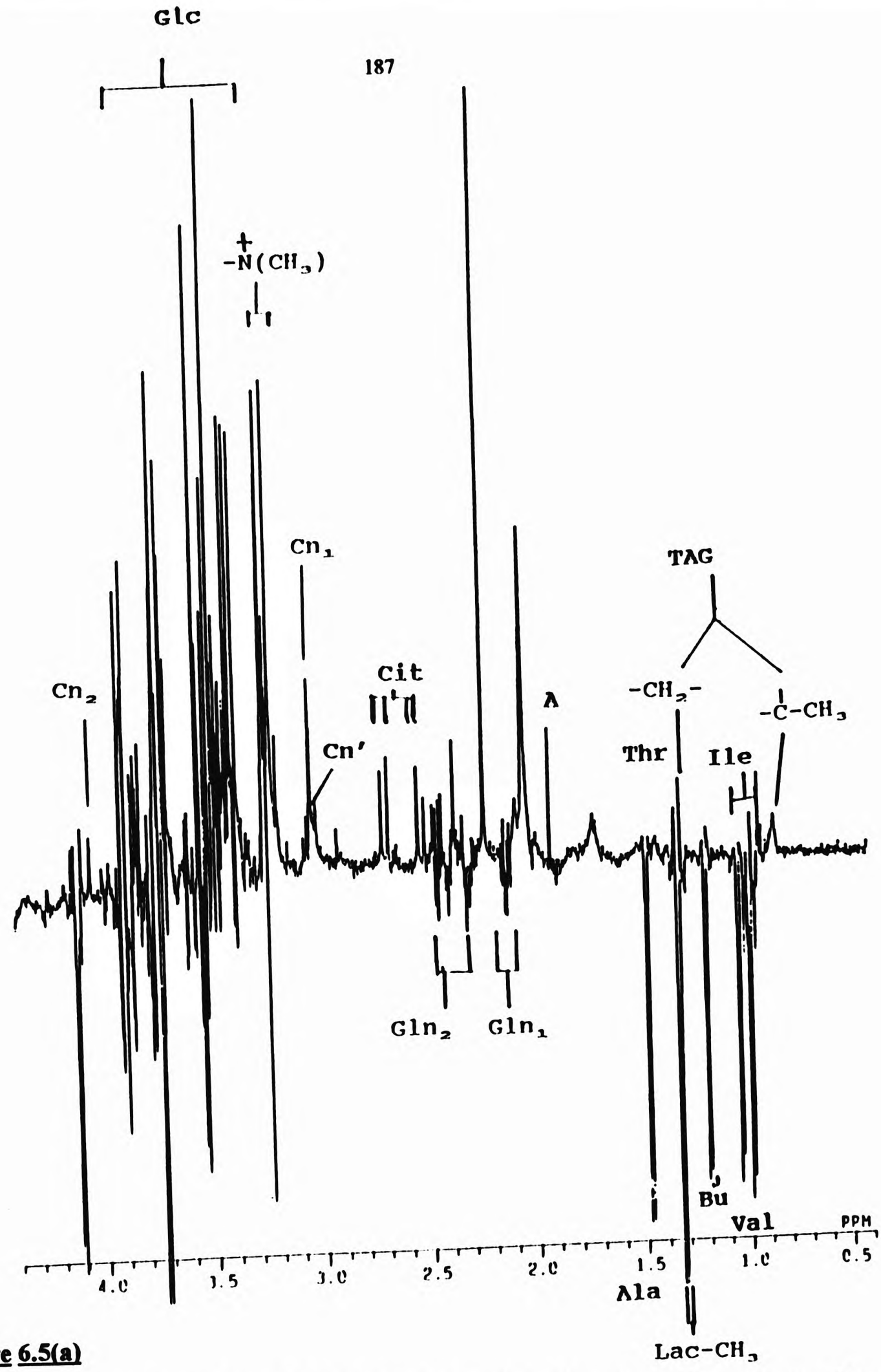

Figure 6.5(a)

High field (aliphatic) region of 500 MHz ^1H Hahn spin-echo NMR spectra of a inflammatory synovial fluid prior to gamma-radiolysis. Typical spectra is shown.

Abbreviations: as Figure 6.3(a).

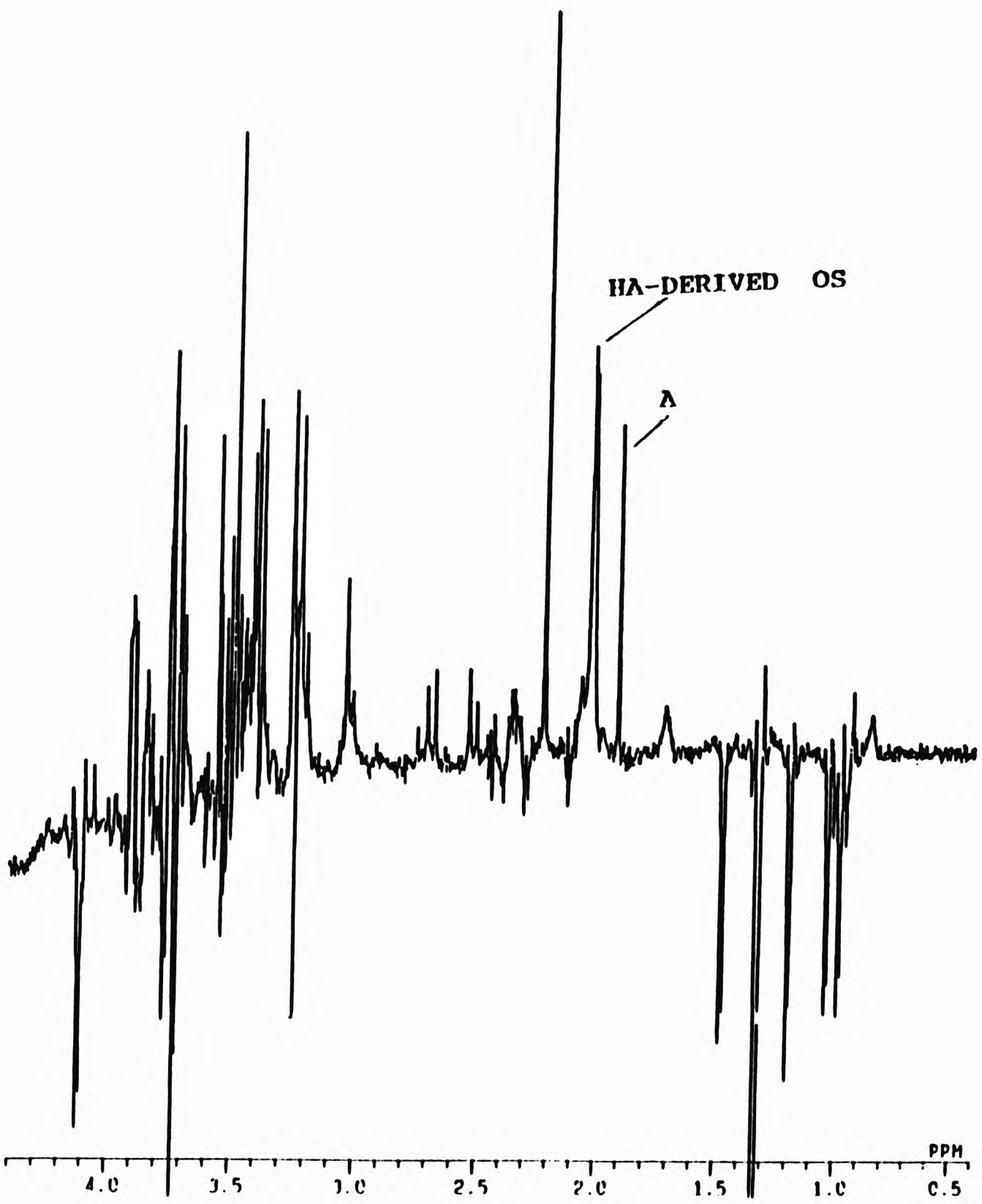

Figure 6.5(b)

High field (aliphatic) region of 500 MHz ^{1}H Hahn spin-echo NMR spectra of a inflammatory synovial fluid following gamma-radiolysis (5.00 kGy). Typical spectra is shown.

Abbreviations: as Figure 6.3(a).

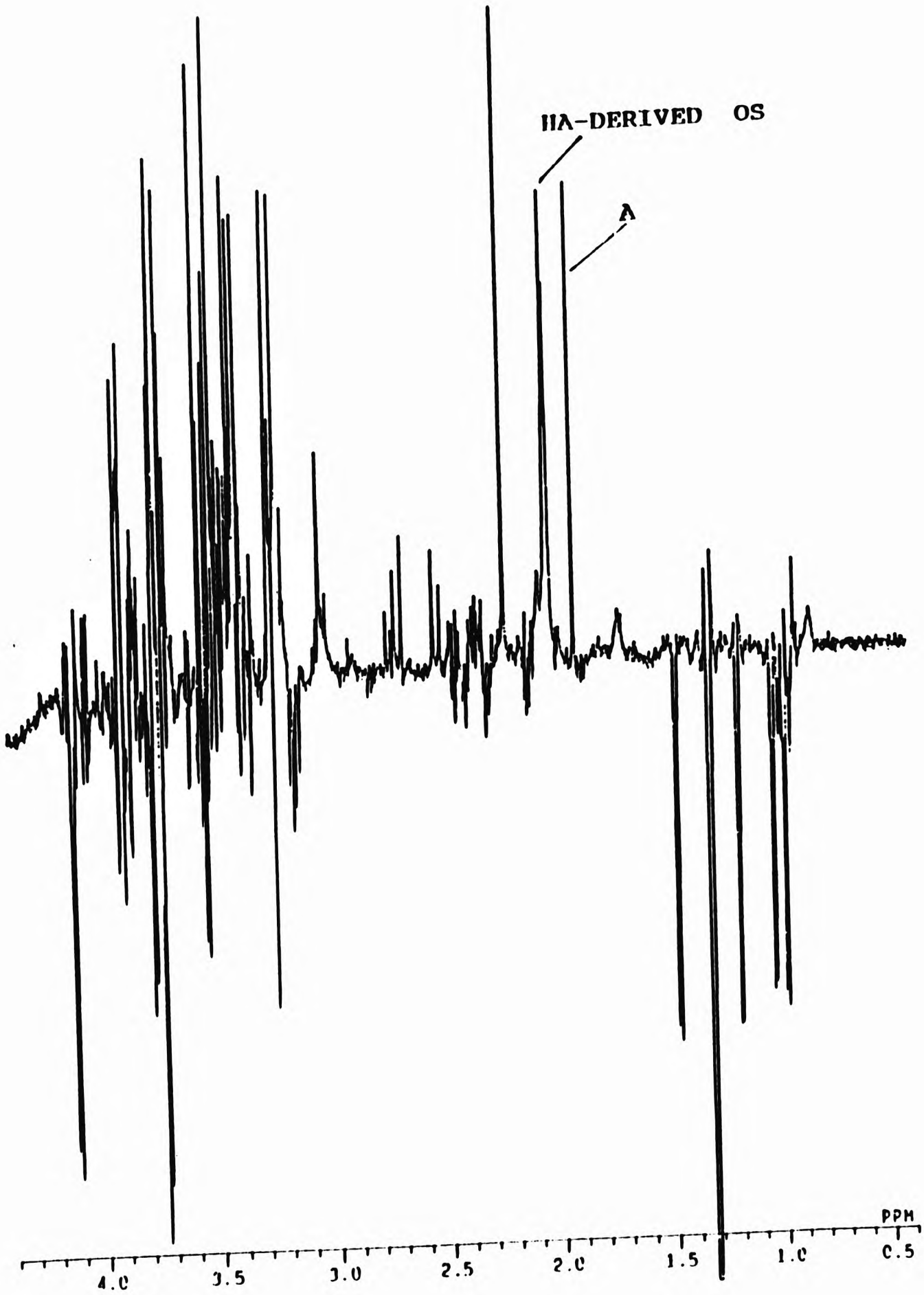

Figure 6.5(c)

High field (aliphatic) region of 500 MHz ^{1}H Hahn spin-echo NMR spectra of a inflammatory synovial fluid, following gamma-radiolysis (5.00 kGy), but treated with 1.00 x 10^{-3} mol dm^{-3} cysteine prior to gamma-radiolysis. Typical spectra is shown.

Abbreviations: as Figure 6.3(a).

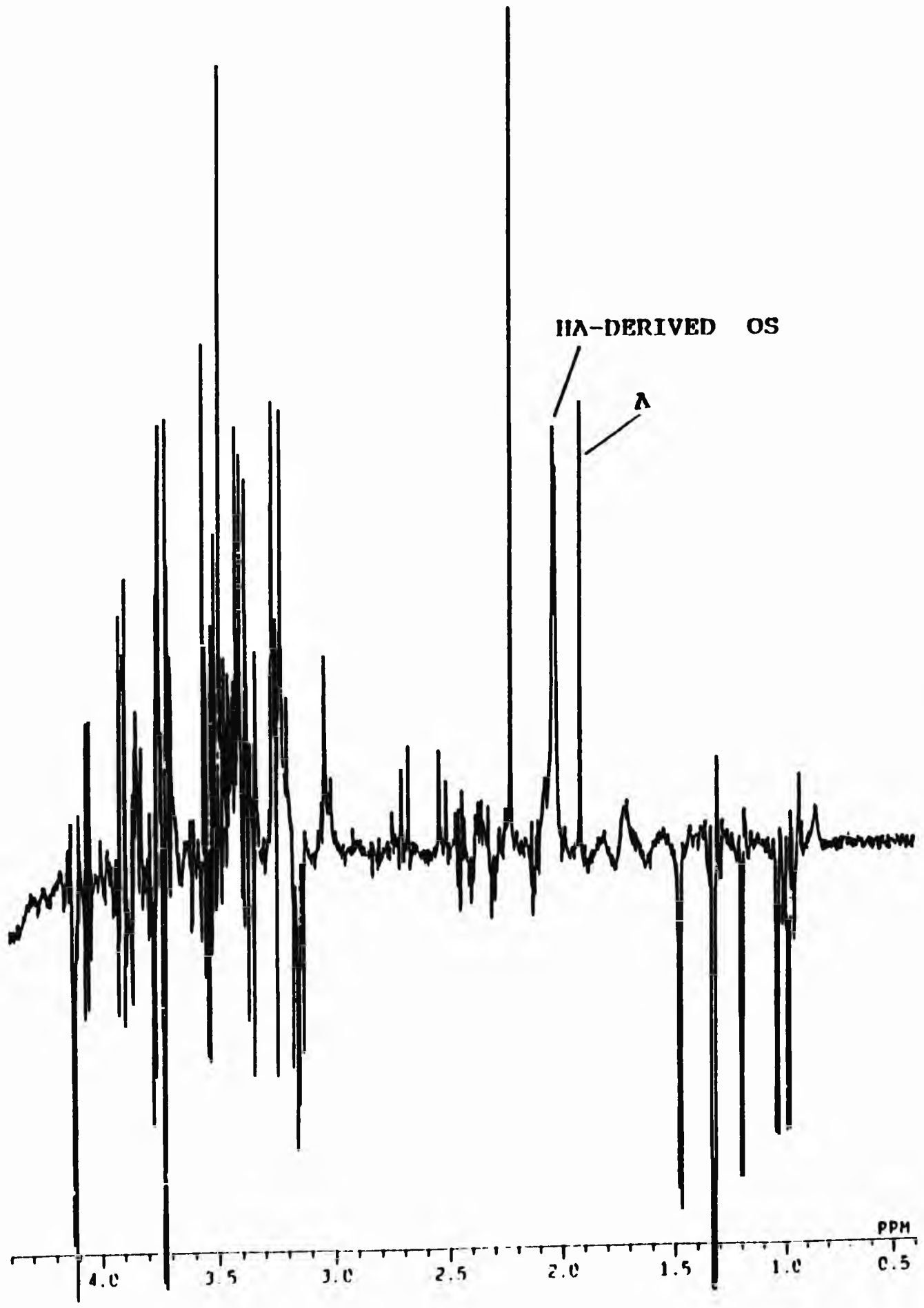

Figure 6.5(d)

High field (aliphatic) region of 500 MHz ^{1}H Hahn spin-echo NMR spectra of a inflammatory synovial fluid following gamma-radiolysis (5.00 kGy); but treated with 5.00 x 10^{-3} mol dm^{-3} cysteine prior to gamma-radiolysis. Typical spectra are shown.

Abbreviations: as Figure 6.3(a).

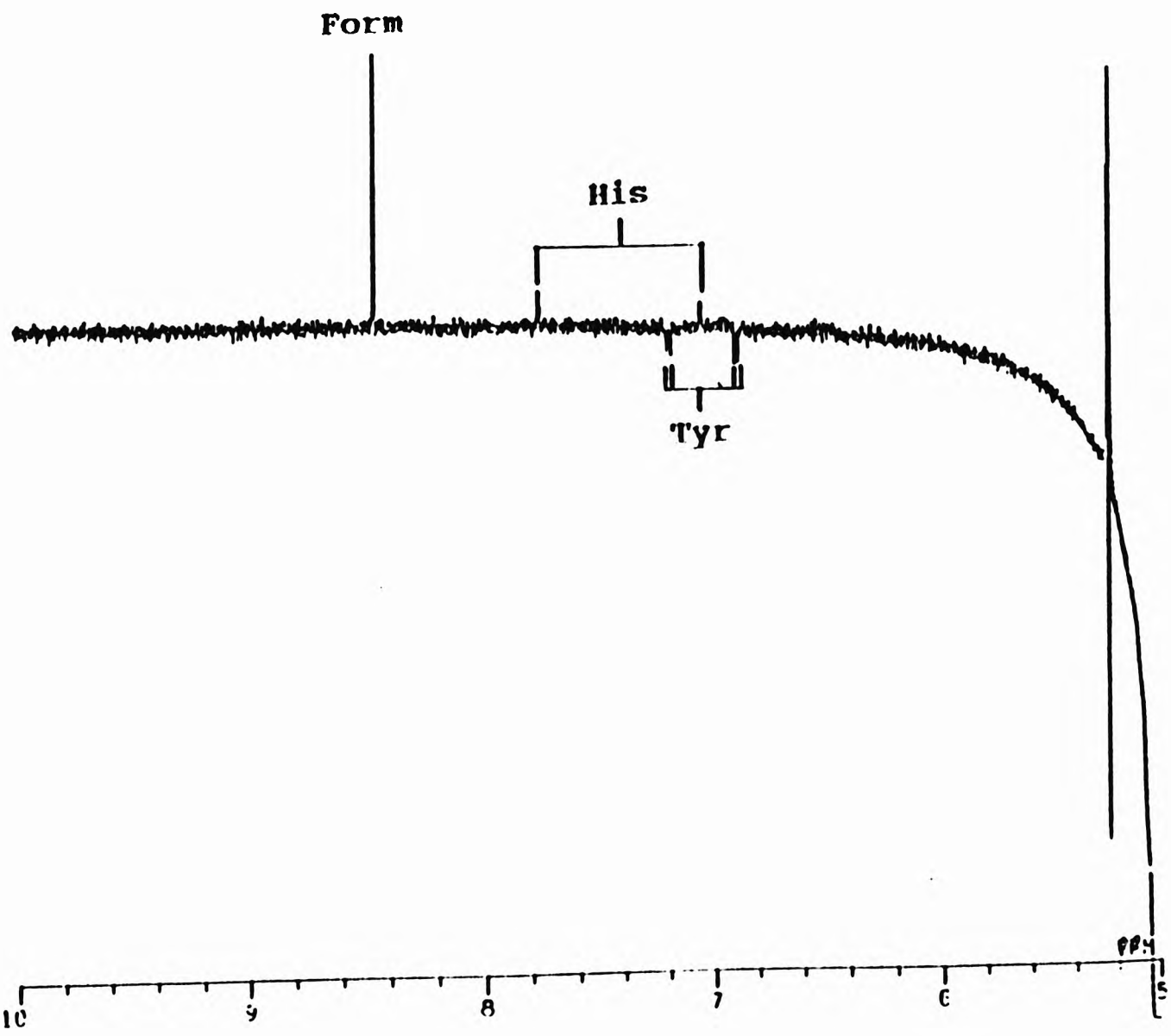

Figure 6.6(a)

Low field (aromatic) region of the 500 MHz ^1H Hahn spin-echo NMR spectra shown in Figure 5: a, untreated (control) synovial fluid.

Abbreviation: as Figure 6.4.

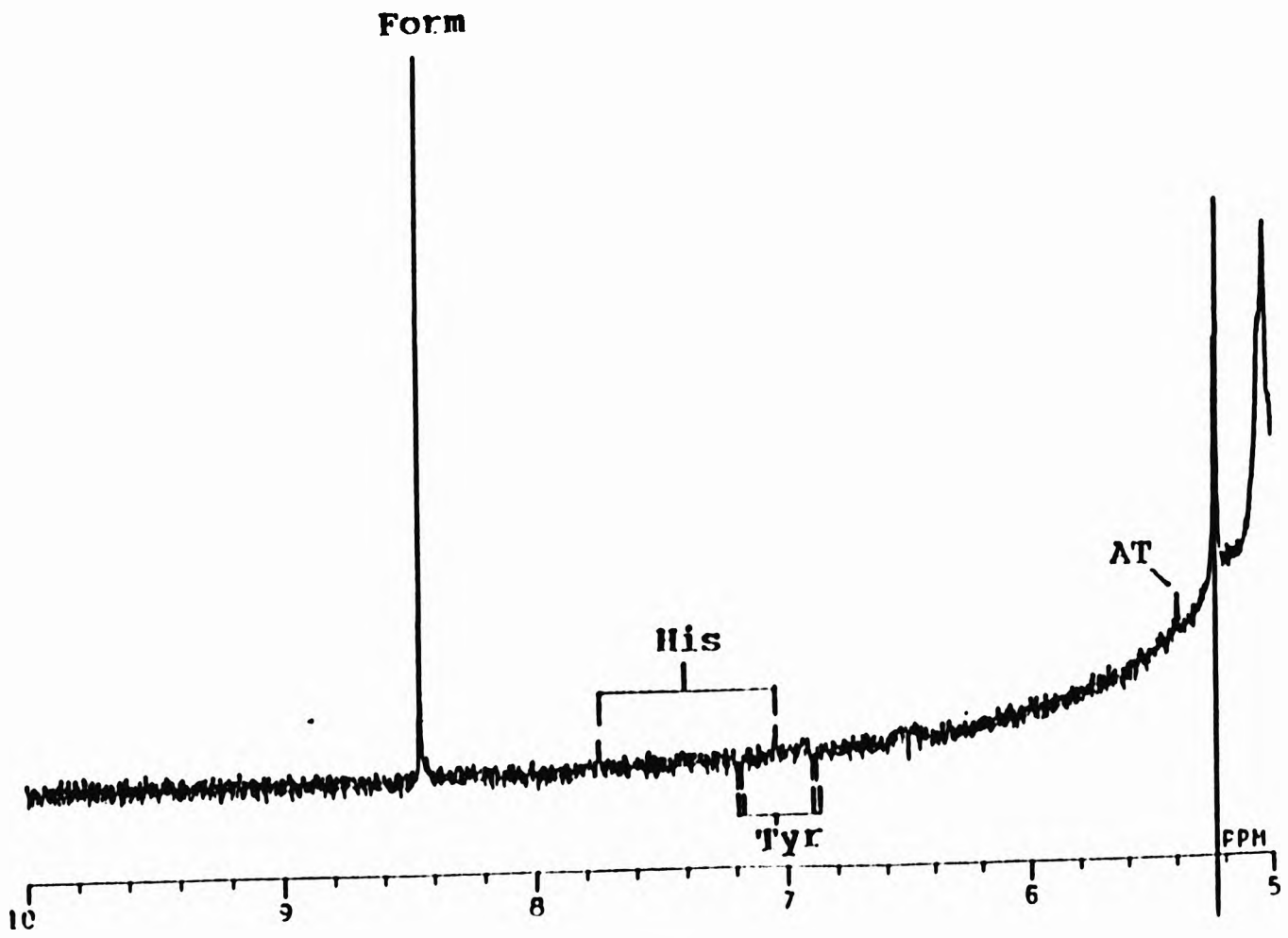

Figure 6.6(b)

Low field (aromatic) region of the 500 MHz ^{1}H Hahn spin-echo NMR spectra shown in Figure 5: a, untreated (control) synovial fluid subsequent to gamma-radiolysis (5.00 kGy).

Abbreviation: as Figure 6.4.

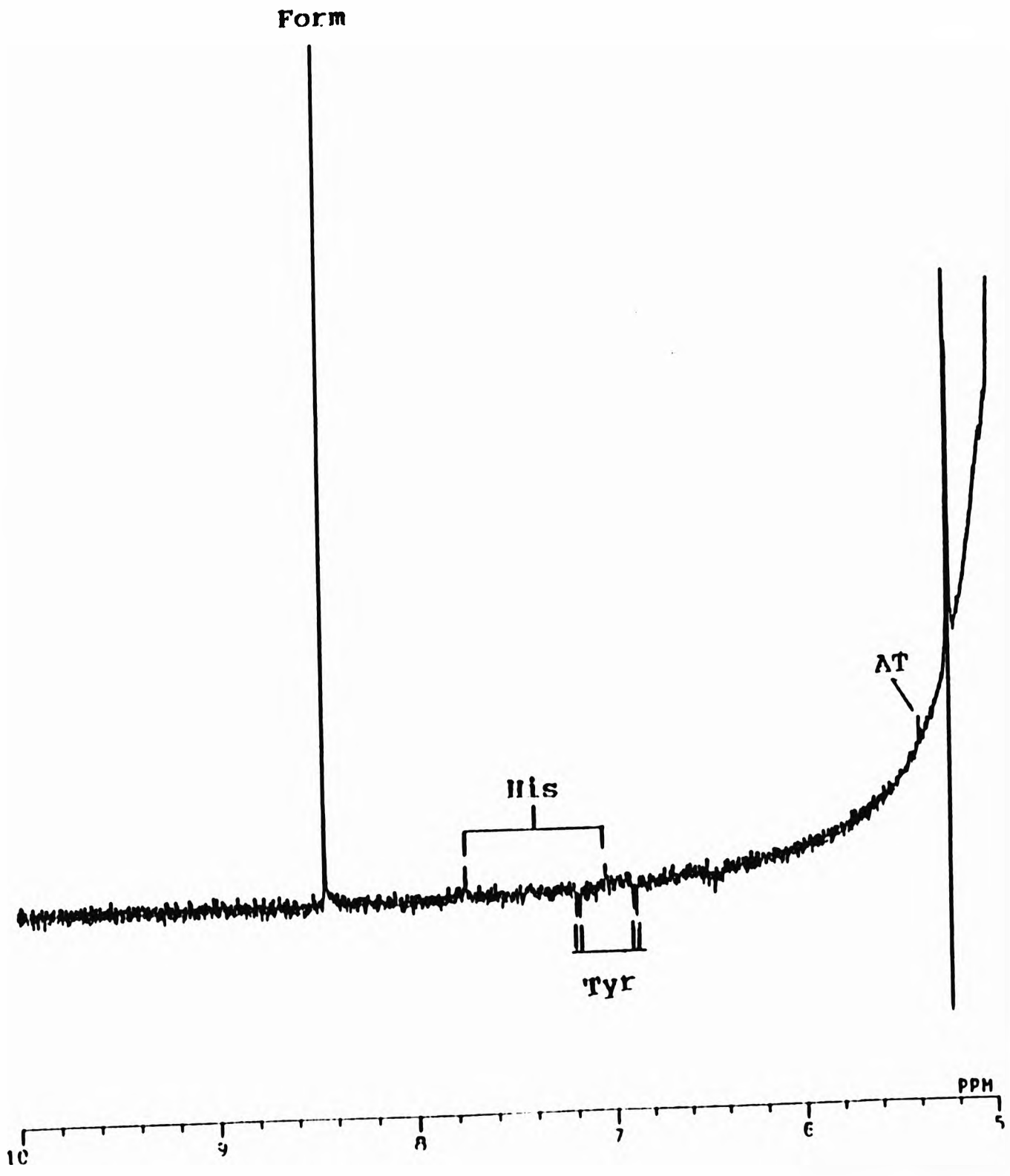

Figure 6.6(c)

Low field (aromatic) region of the 500 MHz ^{1}H Hahn spin-echo NMR spectra shown in Figure 5: a, untreated (control) synovial fluid subsequent to gamma-radiolysis (5.00 kGy) but treated with 1.00×10^{-3} mol dm^{-3} cysteine prior to gamma-radiolysis.

Abbreviation: as Figure 6.4.

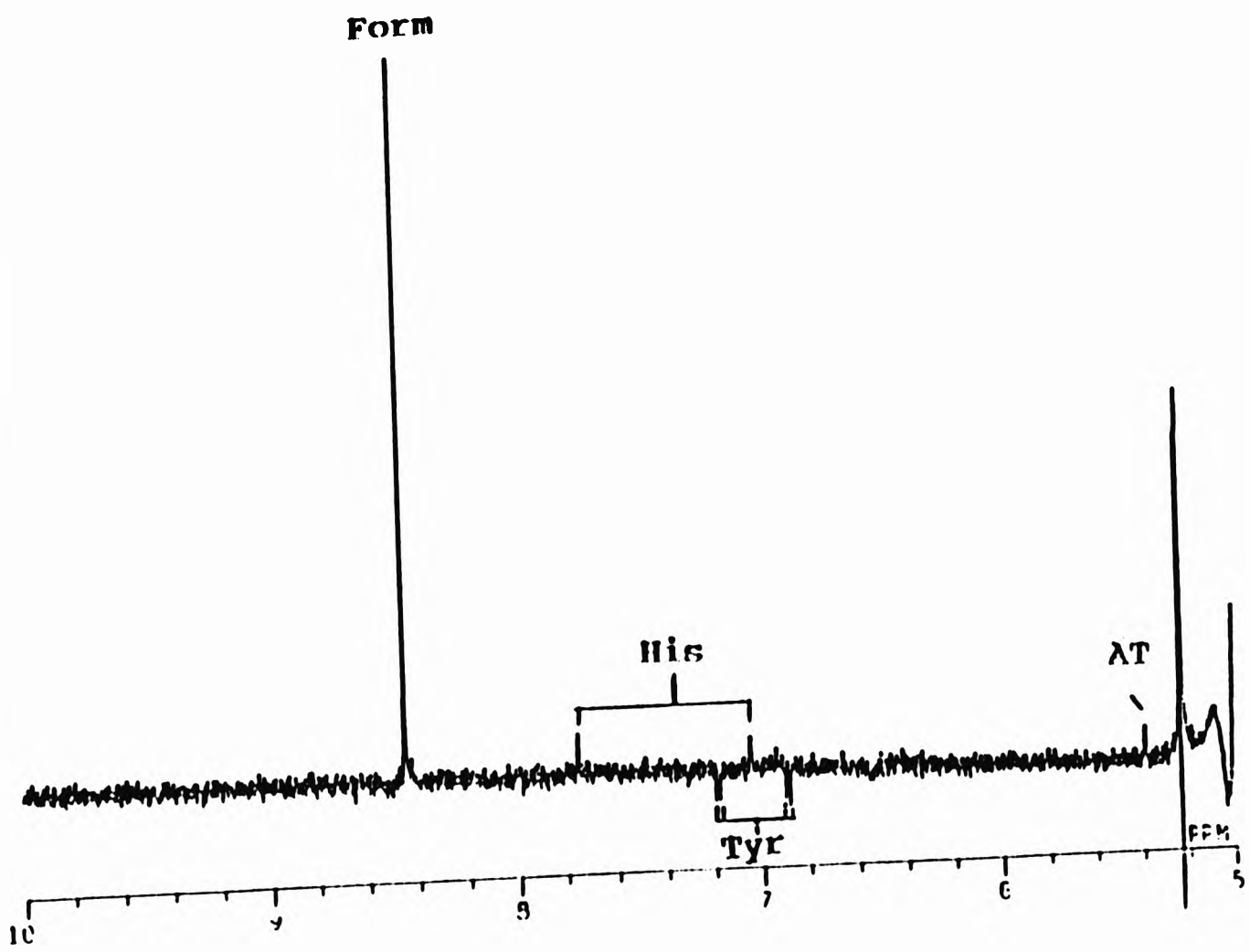

Figure 6.6(d)

Low field (aromatic) region of the 500 MHz ^{1}H Hahn spin-echo NMR spectra shown in Figure 5: a, untreated (control) synovial fluid, subsequent to gamma-radiolysis (5.00 kGy) but treated with 5.00×10^{-2} mol dm^{-3} cysteine prior to gamma-radiolysis.

Abbreviation: as Figure 6.4

6.3 Conclusion and Discussion

The multicomponent analytical ability of high field ^1H NMR spectroscopy offers major advantages over alternative analytical techniques in that it permits the rapid, simultaneous study of the status and levels of a wide range of metabolites present in biological samples and generally requires no knowledge of sample composition prior to analysis. As detailed in this investigation, the technique is readily applicable to the facile detection and quantification of a variety of products derived from radiolytically-mediated oxidative damage to biomolecules present in intact human body fluids, and allows both qualitative and quantitative assessments of the ability of radioprotectant and/or antioxidant agents to suppress such damage. Indeed, a rapid characterisation of the molecular nature of products arising from the interaction of radiolytically-generated oxygen radicals with exogenous antioxidants whilst present in whole biological fluids is also achievable, e.g. detection of N-acetylcystine proton resonances in ^1H Hahn spin-echo spectra of knee-joint synovial fluids containing added N-acetylcysteine.

The substantial reduction in the intensity of the allantoin-CH group singlet resonance observed on pre-equilibration of samples with N-actylcysteine demonstrates that this thiol drug offers protection of synovial fluid urate against oxidative damage induced by the actions of radiolytically-generated ·OH radical. However, only limited protection of hyaluronate against ·OH radical-mediated fragmentation was observed, consistent with the suggested autocatalytic nature of this reaction[165]. Although N-acetylcysteine suppresses the generation of formate (arising from radiolytic damage to synovial fluid carbohydrates) at an added concentration of 1.00×10^{-3} mol dm^{-3}, the level of this product in gamma-irradiated synovial fluids returns to a value close to its control value on raising the concentration of this added thiol to 3.00×10^{-3} mol dm^{-3}. This observation is probably attributable to the displacement of this anionic component from positively-charged protein binding-sites by the high level of added N-acetylcysteine. However, sulphur-containing radicals arising from the attack of radiolytically-generated ·OH radical on N-acetylcysteine may also play a role in

influencing levels of molecularly-mobile, NMR-detectable formate. The thiol cysteine exerted a similar concentration-dependent influence on the level of formate detectable in ^1H Hahn spin-echo spectra of gamma-irradiated synovial fluids.

The radiolytically-mediated elevation in synovial fluid acetate concentration observed at an added N-acetylcysteine concentration of 3.00×10^{-3} mol dm^{-3} is explicable by its generation from the attack of ·OH radical on N-acetylcysteine itself and/or its mobilisation from positively-charged protein binding sites as discussed for formate above. This increase in acetate concentration at high levels of added thiol was not observed when cysteine was employed as an ·OH radical scavenging radioprotectant, consistent with its direct radiolytically-mediated production from the N-acetyl-CH_3 group of N-acetylcysteine whilst present in intact synovial fluids. The role of N-acetylcysteine derived oxysulphur radicals in contributing towards radiolytic damage in this system is unclear at present, but Arouma *et. al.*[152] detected only a very small decrease in the ability of this agent to protect α_1-antiprotease against damage induced by radiolytically-generated ·OH radical on changing the irradiation atmosphere from pure N_2O to 80% (v/v) N_2O/20% (v/v) O_2.

The radioprotective capacity of exogenous cysteine was similarly characterised by a substantial inhibition of radiolytically-mediated allantoin generation from urate (a complete suppression occurring at an added concentration of 5.00×10^{-3} mol dm^{-3}), a limited reduction in the level of low-molecular-mass oligosaccharide species arising from the radiolytic fragmentation of hyaluronate, and a decrease in the concentration of formate generated at an added cysteine concentration of 2.00×10^{-3} mol dm^{-3}. A marginal reduction in the intensity of the acetate-CH_3 group signal at an added cysteine concentration of 5.00×10^{-3} mol dm^{-3} was also noted.

In conclusion, the experiments performed here provide much useful information regarding the particular biofluid components for which exogenous thiols such as N-acetylcysteine offer protection against radiolytic damage. Such information is also of much

physiological and clinical significance in view of the adverse toxicological properties associated with radiolytic products derived from various biomolecules[163], e.g.formate arising from radiolytic damage to carbohydrates. The technique employed here is equally applicable to investigations of the precise molecular mechanisms underlying the radioprotectant and/or antioxidant actions of alternative therapeutic agents such as non-steroidal anti-inflammatory drugs (NSAIDs).

CHAPTER 7

DISCUSSION AND CONCLUSION

7.1 Diene Conjugate Method

Previous work has established the existence of a pathophysiological environment within the inflamed human joint, capable of sustaining a hypoxic-reperfusion event. The most promising techniques used for the assessment of RORS activity in patients with inflammatory synovitis are the identification of intermediates in and so-called 'end-products' of the process of lipid peroxidation. Lipid peroxidation is a RORS-mediated process that leads to cell membrane damage, resulting in cellular dysfunction or death. It is initiated by the more potent radicals such as alkoxyl radicals (RO·), peroxyl radicals (ROO·), and the hydroxyl radical (OH·). This leads to an autocatalytic, self- perpetuating process and because of its autocatalytic nature, only a small quantity of OH· radical or other RORS is required to trigger the process, thereby facilitating the application of analytical methods of lowered sensitivity in the assessment of RORS generation. Generation of superoxide radicals, (by any source), in the presence of iron ions can lead to formation of OH· by Fenton chemistry and subsequent initiation of lipid peroxidation. Such 'catalytic' iron in human synovial fluid has been detected and shown to initiate lipid peroxidation within the joint.

Identification of one or more of the end products resulting from the RORS-initiated peroxidation process was utilized to form the basis of a method for the assessment of RORS-production in the inflamed joint. A procedure for the assessment of the early stages of the lipid peroxidation process is the detection of conjugated dienes and diene hydroperoxides. These species, and the conjugated keto-dienes arising from their degradation, exhibit UV absorbance at various wavelengths in the range 230- 270 nm.

In this project, a procedure is developed for the assessment of conjugated dienes in synovial fluid which involves the resolution and identification of different isomeric classes of conjugated lipid hydroperoxide species using second-derivative (2D) spectrophotometry. Direct measurement of absorbance at a specified wavelength in the 230-270nm range largely reflects the variable concentrations of two or more classes of conjugated diene species, with overlapping absorption maxima centered in this region of the spectrum. This problem was

overcome by monitoring minima present in the corresponding 2D spectra of the extracts. This methodology has previously been employed to monitor the time-dependent production of cis,trans and trans,trans diene conjugate of microsomal polyunsaturated fatty acids after exposure of rats to carbon tetrachloride[51]. Previous studies using chemical model systems have established that autoxidation of linoleic or arachidonic acid results in the production of cis,trans and trans,trans conjugated diene hydroperoxides that absorb light at 236 and 232.5 nm, respectively.

An alternative procedure is based on the observation that several of these end-product aldehydes, especially malondialdehyde (MDA), react with TBA under acidic conditions to produce a pink-colored chromogen that absorbs light strongly at a wavelength of 532nm, enabling a simple spectrophotometric measurement of lipid peroxidation. Although this technique has a somewhat limited specificity, it has been widely employed as a marker for RORS-mediated oxidative damage to lipids in a wide variety of biological samples. An improved methodology for the assessment of TBA-reactive material in synovial fluid was also achieved by the application of 2D spectrophotometry, which served to resolve the overlapping absorption maxima in the 450-700 nm region of the visible spectrum.

Measurement of conjugate dienes and TBA-reactive substances in synovial fluid was used as an index of lipid peroxidation in tissues within the inflamed knee and thus was used to investigate the effect of joint exercise on lipid peroxidation. Pilot studies assessing the novel use of 2D spectrophotometric analysis as a means of detecting lipid peroxidation were performed. This technique is rapid, sensitive and relatively free from a many of bioavailable interferences as previously discussed.

To understand these results fully, the theory behind hypoxic reperfusion event needs to be considered. It is well documented that there are several physiological and biochemical features present in the inflamed rheumatoid joint that provide a potential environment for hypoxic reperfusion injury[29-31]. In RA during exercise there is a temporary occlusion of the synovial capillary bed giving rise to a transient hypoxia enviroment[31]. Subsequent to exercise reperfusion occurs. Upon reperfusion, generation of O_2 is dramatically increased

when the oxygen supply is restored. $O_2^{\cdot -}$ is then converted simultanously to H_2O_2 by the enzyme SOD. Ischaemia also releases iron from its storage protein, ferritin, and this release of iron together with the generation of $O_2^{\cdot -}$ and H_2O_2 leads to the production of $^{\cdot}OH$ radical via the Fenton reaction[29]. It has been speculated that transferrin in inflammatory synovial fluid of lowered pH value does not retain its iron as avidly as that of normal serum, and that 'free' iron can participate in Fenton type reaction[11].

The studies in general shows that the magnitude of the 2D signals increased, indicating an increase in the concentration of conjugated diene species culminating from the generation of RORS (i.e. $^{\cdot}OH$ radical) in the inflamed rheumatoid joint during hypoxic reperfusion injury. There is generally an increase in intensity of signals followed by decrease with time. The greatest increase appears to take place during 4-6 min. post-exercise time period, a possible consequence of relative slow, autocatalytic nature of lipid peroxidation process. The decrease after 6 min. period (post-exercise) may be attributed to the fact that although conjugated lipid hydroperoxide is relatively stable at biologically relavent temperatures, their degradation to a wide variety of further lipid peroxidation 'end-products' is catalysed by traces of redox-active transition metal-ions. The secondary and tertiary end-products include saturated and unsaturated aldehydes, di- and epoxyaldehyde, lactones, furans, ketones, oxo- and hydroxyacids and saturated and unsaturated hydrocarbons[56]. The unexercised patients, however, exhibited no corresponding time-dependant change.

These effect of isometric exercise on levels of synovial fluid conjugated dienes was not so clear-cut. There was no statistically significant difference between pre-exercise and post-exercise levels at any time points, but there was a trend for levels to increase in the exercised group at 2 and 6 min post-exercise. A possible reason is likely to be attributable to the inherent lack of selectivity associated with this assay system. The 2D spectrophotometric conjugated diene lipid hydroperoxide assay shows that both isometric quadriceps contraction and 300 yds walking provoke qualitative change in both the zero-order and 2D spectra of a significant proporation of the patients, changes that were not observed in the unexercised patients. These observations suggest that a trend of elevated conjugated dienes seen in the

conventional spectrophotometric assessment of conjugated dienes, was indeed a real phenomenon.

The study shows that isometric quadriceps exercise of inflamed joint produces significantly elevated levels of TBA-reactive substances in synovial fluid, when compared to pre-exercise values, at all the post-exercise time point studied. In the unexercised patients, there was no such increase observed. The 2D spectrophotometric TBA-reactive assay on patients exercised by walking only, show a change in both the zero-order and 2D spectra in a significant proportion of the exercised patients. The greatest increase appears to take place during the 6-8 min. post-exercise time period, a possible consequence of the relatively slow, autocatalytic nature of the lipid peroxidation process. However, unlike the diene conjugate (where the intensity of diene conjugate produced decreased with time, possibly due to conversion to secondary and tertiary 'end- products') the intensities of TBA-reactive substance remains elavated. A possible consequence of no further end-products formed after this stage.These changes were not observed in the unexercised patients.

Taken together this series of experiments shows that exercise of an inflamed joint either by isometric quadriceps contraction or walking promotes lipid peroxidation within the joint.

7.2 Further Extension to Diene Conjugate Method

A method for determining the cis,trans- and trans,trans- conjugated hydroperoxydienes, hydroxydienes and conjugated oxodienes arising from their degradation is described. However, this method is somewhat limited in the information it provides. For example, it does not distinguish between the different types of unsaturated fatty acid ungergoing oxidation. Also, it is important to note that greater than 90% of conjugated diene species in freshly obtained human body fluids or tissue is accounted for by the presence of a single non-peroxidised fatty acid residue, octadeca-9 cis,11 trans-dienoic acid which is a simple isomer of linoleic acid.

The diene conjugate method was therefore further developed, which involved the conversion of conjugated hydroperoxydienes and the compounds derived from them, oxodienes and hydroxydienes, to strongly chromophoric conjugated triene and tetraene species. The transformation is conducted in two steps involving (1) reduction of these conjugated species with sodium borohydride and (2) dehydration of the resulting hydroxydienes with alcoholic sulphuric acid. The chromophore(s) produced are measured by absorbanceby measurement in the ultra-violet or near ultra-violet region of the spectrum using 2D spectrophotometry.

This procedure has been applied to assess the nature and extent of oxidative deterioration of PUFA's in (1) Knee joint synovial fluid obtained from subjects with inflammatory joint diseases and (2) human colon tissue obtained from patients with ulcerative colitis. The time this novel procedure was developed, IBD was the research topic discussed at the London Hospital and it was appropriate that this assay should be applied to the assessment of ROR-mediated oxidative damage to PUFAs in sample of human colon tissue from patients with ulcerative colitis.

To date, the only measurement performed on rectal biopsy sample was that by Ahnfelt-Ronne *et. al.*[94] They demonstrated an increase in lipid peroxidation in patients with active disease in human colonic samples, which returned to control levels after treatment. However, the technique used was the TBA test, which is a non-specific assay subject to

major interferences. This technique was used to re-evaluate the findings Ahnfelt-Ronne *et. al*.[94] which demonstrated increased lipid peroxidation in colorectal mucosal biopsies from IBD patients.

These studies did not confirm those of Ahnfelt-Ronne *et. al*[94]., however, the results obtained have shown a relative increase in the amount of peroxidised trienes when expressed relative to that of dienes in patients with ulcerative colitis. Application of this analytical procedure to colon tissue samples obtained from patients with ulcerative colitis demonstrated that colonic biopsies contained peroxidation that were largely derived from linoleate. However smaller levels of linolenate-derived peroxidation products were also detected, consistent with the findings reported by Nitisda *et. al*[103]. RORS-mediated oxidative damage to PUFA's in rheumatoid synovial fluid sample appear to be exclusively attributable to the peroxidation of linoleate, with no detectable linolenate-derived peroxidation products present.

7.3 Determination of Molecular Nature of Non-Transferrin-Bound Iron in Inflammatory Synovial Fluid by NMR Spectroscopy.

The presence of non-transferrin-bound iron in inflammatory synovial fluid, which appears to be present as low-molecular- mass, redox-active iron complexes has been well documented. The iron ions for such complexes are supplied in the acidotic environment of the inflamed rheumatoid joint by oxidant-mediated mobilisation from ferritin and haemoglobin. This non-transferrin- bound iron can readily promote the generation of the highly toxic ·OH from $O_2^{\cdot -}$ and H_2O_2. The highly reactive ·OH radical can attack a wide range of endogenous 'target' molecules such as lipids, proteins, ascorbate, and carbohydrate to produce 'unnatural' chemical species.

Non-transferrin-bound iron ions capable of generating the ·OH radical have been measured in inflammatory synovial fluid by the bleomycin assay. However, to date there have been no attempts to clarify the precise chemical nature of such iron. In this study Hahn spin-echo and single-pulse proton (^1H) nuclear magnetic resonance (NMR) spectroscopy combined with the use of the powerful iron(III) chelatore (desferrioxamine and nitrilotriacetate), and the iron(III) binding protein apotransferrinis employed to 'speciate' catalytic, low-molecular- mass complexes of iron in Knee-joint synovial fluid obtained from patients with inflammatory joint diseases. In addition, the ability of increasing concentrations of added iron(III) to cause further complexometric or oxidatively-mediated modifications in the ^1H NMR profile of synovial fluid is investigated.

The simultaneous study of the status of a wide range of molecularly mobile components present in Knee-joint synovial fluid samples obtained from patients with inflammatory synovial fluid by NMR spectroscopy provides evidence for the complexation of a significant fraction of low-molecular-mass (non-transferrin- bound) ions by citrate. In approximately 35% of fresh synovial fluid samples investigated, there are small, but reproducible modifications in the citrate proton resonances when the small quantities of this 'bleomycin-detectable' catalytic iron are transferred from this tetradentate endogenous chelator to desferrioxamine following prolonged incubation. Further evidence for the chelation of non-transferrin-bound iron ions by citrate in synovial fluid was provided by the

observation that addition of iron(III) to the sample gave rise to a marked broadening of the citrate proton resonances.

Proton Hahn spin-echo NMR spectroscopy is a tool that can be used in studies involving the speciation of metal-ion in body fluids obtained from patients with inflammatory joint diseases, providing a broad 'picture' of abnormalities in metal-ion metabolism.

7.4 The Role of N-acetylcysteine in Protecting Synovial Fluid Biomolecules against Radiolytically-Mediated Oxidative Damage by NMR Spectroscopy

Hahn spin-echo NMR spectroscopy technique is further exploited, to evaluate the abilities of antioxidant drugs N- acetylcysteine and exogenous cysteine to protect metabolites present in intact inflammatory synovial fluid samples against oxidative damage arising from gamma-radiolysis (5.00 KGy) in the presence of atmospheric O_2. It has ben known for over 40 years that certain thiols and disulphides exhibit a radioprotective ability if administered prior to exposure to sources of ionising radiation, a phenomenon which presents the possibility that such compounds are able to confer protection of living organisms against the low levels to which they are being continuously exposed.

The antioxidant actions of N-acetylcysteine in a wide range of experimental systems are now well established. Postulated mechanisms of action for this thiol drug include its ability to (1) increase intracellular concentrations of cysteine and hence glutathione and (2) scavenge oxidants such as $O_2^{\cdot -}$, H_2O_2 and HOCl.

In view of the large amount of evidence available for the deleterious role of RORS in the pathogenesis of inflammatory joint diseases (reviewed earlear), it is conceivable that N-acetylcysteine may have a therapeutic role to play here by modulating oxidative damage to endogenous biomolecules arising from the actions of such radicals in vivo. Indeed, the diminished antioxidant status of inflammatory synovial fluids renders biomolecules therein particularly susceptible to damage by biologically-generated oxidants.

In this study, high field ^1H NMR spectroscopy to assess the ability of N-acetylcysteine to suppress radiolytically-mediated oxidative modifications to biomolecules present in inflammatory human Knee-joint synovial fluid in vitro is employed. The action of the naturally-occuring amino acid cysteine in regulating such oxidative damage was also been investigated in this manner for purpose of comparison.

The experiment performed here provide much useful information regarding the particular biofluid components for which exogenous thiols such as N-acetylcysteine offer protection against radiolytic damage. Although oxidation of urate to allantoin by radiolytically-generated $^{\cdot}OH$ radical was readily circumventable by pre-treatment of synovial

fluid with N- acetylcysteine or cysteine, both thiols offered only a limited protective capacity with respect to hyaluronate depolymerisation and the production of formate from carbohydrates in general. Radiolytic products generated from the added thiols (predominantly their corresponding disulphides) were simultaneously detectable in ^{1}H Hahn spin-echo spectra of gamma- irradiated synovial fluid, permitting an evaluation of the radioprotective capacity of these agents. Such information is also of much physiological and clinical significance in view of the adverse toxicological properties associated with radiolytic products derived from various biomolecules, e.g. formate arising from radiolytic damage to carbohydrates. The technique employed here is equally applicable to investigation of the precise molecular mechanisms underlying the radioprotectant and/or antioxidant actions of alternative therapeutic agents such as non-steroidal anti-inflammatory drugs (NSAIDs).

REFERENCES

REFERENCES

1. Halliwell,B. and Gutteridge,J.M.C.. The importance of free radicals and catalytic metal ions in human diseases. *Molec. Aspects. Med. 1985; 8: 89-93.*

2. Blake,D.R., Merry,P., Unsworth,J., Kidd,B.L., Outhwaite,J.M., Ballard,R., Morris,C.J., Gray,L. and Lunec,J.. Hypoxic reperfusion injury in the inflamed human joint. *Lancet 1989; i: 289-293.*

3. Halliwell,B. and Grootveld,M.. The measurement of free radical reactions in humans. *FEBS Lett. 1987; 213(1): 9-14.*

4. Cross,C.E.. Oxygen radicals and human disease. *Ann. Int. Med. 1987; 107: 526-545.*

5. McCord,J.M. and Fridovich,I.. The reduction of cytochrome *c* by milk xanthine oxidase. *J. Biol. Chem. 1968; 243: 5753-60.*

6. Braganza,J.M., Wickens,D.G., Cawood,P. and Dormandy,T.L.. Lipid peroxidation (free radical-oxidation) products in bile from patients with pancreatic diseases. *Lancet 1983; 2: 375.*

7. McCord, J.M., Free radicals and inflammations protection of synovial fluid by SOD. *Science*. 1974; **185** : 529-531.

8. Halliwell,B. and Gutteridge,J.M.C.. Free radicals in biology and medicine. *Oxford University press, Oxford, 2nd edition (1989).*

9. Slater,T.F.. Free radical in tissue injury. *Biochem. J. 1984; 222: 1-15.*

10. Blake,D.R., Lunec,J., Brailsford,S., Winyard,P., Bacon,P.A. in : Decker,.L., Scott,J.T. eds. Oxygen free radicals and inflammatory joint disease. *Persp. in Rheum. 1984; Curr. Med. Lit. London 19-33.*

11. Blake,D.R., Allen,R.E. and Lunec,J.. Free radicals in biological system - a review orientated to inflammatory process. *British Medical Bulletin 1987; 43(2): 371-385.*

12. Blake,D.R., Lunec,J., Winyard,P., Brailsford,S., in: Moll, J.M.H., Sturrock,R.D. eds. Iron, Free radicals and Chronic Inflammation. *Recent advances in Rheumatology 4, Edinburgh : Churchill Livingstone 1986; 21-36.*

13. Walling,C in : Kingmason,H.S. and Morrison,M. eds. Oxidase and related redox system. *Pergamon press, Oxford 1982; 85-97.*

14. Cochrane,C.G..Mechanisms of oxidant injury of cells. *Mol. Asoects Med. 1991;* **12(2):** 137-147.

15. MelloFilho,A.C., Hoffmann,M.E. and Meneghini,R.. Cell killing and DNA damage by hydrogen peroxide are mediated by intracellular iron. *Biochem. J. 1984; 218: 273-275.*

16. Lunec,J., Halloran,S.P., White,A.G. and Dormandy,T.L.. Free-radical oxidation (Peroxidation) products in serum and synovial fluid in rheumatoid arthritis. *J. Rheumatol. 1981; **8(2):** 223-245.*

17. Halliwell,B. and Gutteridge,J.M.C.. Oxygen toxicity, oxygen radicals, transition metals and disease. *Biochem J. 1984; **219:** 1-14.*

18. Sinclair,A.J., Barnett,A.H. and Lunec,J.. Free radicals and antioxidant systems in health and disease. *Brit. J. Hosp. Med. 1990; **43:** 333-344.*

19. Halliwell,B. and Gutteridge,J.M.C.. Free Radicals in Biology and Medicine. *Clarendon press. Oxford, England (1985).*

20. McCord,J.M.. Oxygen-derived free radicals in post ischemic tissue injury. *New Eng. J. Med. 1985; **312(3):** 159-163.*

21. Pearson,A.M., Gray,J., Wolzak,A.M. and Herenstein,N.A.. Safety implication of oxidised lipids in muscle foods. *Food Technology 1983; 121-129.*

22. Hershko,C., Graham,G., Bates,G.W. and Rachmilewitz,E.A.. Non-specific serum iron in thalassaimia: an abnormal serum ion fraction of potential toxicity. *Br. J. Haematology 1978; **40:** 255-263.*

23. Bowman,W.C. and Rand,M.J.. Textbook of pharmacology. *Blackwell scientific publication 1984; 13.32-13.34.*

24. Auroma,O.I. and Halliwell,B.. Superoxide-dependent and ascorbate-dependent formation of hydroxyl radicals from hydrogen peroxide in the presence of iron: are lactoferrin and transferrin promoters of hydroxyl-radical generation? *Biochem J. 1987; **241:** 273-278.*

25. Halliwell,B., Gutteridge,J.M.C. and Blake,D.R.. Metal ions and oxygen radical reactions in human inflammatory joint disease. *Philos. Trans. R. Soc., Lond. (Biol) 1985; **311:** 659-671.*

26. Gutteridge,J.M.C.. Iron promoters of the Fenton reaction and lipid peroxidation can be released from haemoglobin by peroxides. *FEBS Lett. 1986; **201:** 291-5.*

27. Grootveld,M., Nazhat,N.B., Patel,I.Y. and Blake,D.R.. Free radical biochemistry and rheumatoid arthritis. *Curr. Med. Lit - Rheumatology 1992; **9(1):** 75.*

28. Merry,P., Grootveld,M. and Blake,D.R.. Free radicals and hypoxic reperfusion injury. A mechanism producing persistent synovitis ARC topical review 1990; No.15 Scott,T., Jayson,M., Moll,J. and Isenberg (Eds.).

29. Woodruff,T., Blake,D.R., Freeman,J., Andrews,F.J., Salt,P. and Lunec,J.. Is chronic synovitis an example of reperfusion injury? *Ann. Rheum. Dis. 1986; **45:** 608-611.*

30. Blake,D.R., Unsworth,J., Outhwaite,J.M., Morris,C.J., Merry,P., Kidd,B.L., Ballard,R., Gray,L. and Lunec,J.. Hypoxic-reperfusion injury in the inflamed human joint. *Lancet 1989; **1:** 289-293.*

31. Unsworth,J., Outhwaithe,.M., Blake,D.R., Morris,C., Freeman,J. and Lunec,J.. Dynamic studies of the relationship between intra-articular pressure, synovial fluid oxygen tension, and lipid peroxidation in the inflamed knee: an example of reperfusion injury. *Ann. Clin. Biochem. 1988; **25:** 8s-11s.*

32. Jayson,M.I.V., Dixon,A.S.T.J.. Intra-articular pressure in rheumatoid arthritis of the knee. II Effect of intra-articular pressure on blood circulation to the synovium. *Ann. Rheum. Dis. 1970; **29:** 266-268.*

33. Sinclair,A.J., Barnett,A.H. and Lunec,J.. Free radicals and antioxidant systems in health and disease. *Brit. J. Hosp. Med. 1990; **43:** 334-344.*

34. Freeman,B.A., Turren,J.F., Mirzu,Z., Gapo,J.D. and Young,S.L.. Modulation of oxidant lung injury by using liposome-entrapped superoxide dismutase and catalase. *Fed. Proc. 1985; **44:** 2591-2595.*

35. Greenwald,R.A. and Moy,W.W.. Effect of oxygen free radicals on hyalyronic acid. *Arthritis and Rheumatism 1980; **23:** 455-463.*

36. Halliwell,B. and Grootveld,M.. The measurement of free radical reaction in humans - Some thoughts for the future. *FEBS lett. 1987; **213(1):** 9-14.*

37. Williams,D.H. and Fleming,I.. Spectroscopic methods in organic chemistry. *McGraw Hill book company (U.K.) ltd 1980; 74-99.*

38. Atkins,P.W.. Physical Chemistry. *Oxford University press 1984; 603-610 & 630-650.*

39. Banwell,C.N.. Fundamentals of molecular spectroscopy. *McGraw Hill book company (U.K.) ltd 1983; 250-260.*

40. O'Haver,T.C.. Derivative and wavelength modulation spectrometry. *Anal. chem. 1979; **51(1):** 91a-100a.*

41. Bell,J.D., Brown,J.C.C., Nicholson,J.K. and Sadler,P.J.. Assignment of resonances for 'acute-phase' glycoproteins in high resolution proton NMR spectra of human blood plasma. *FEBS Lett. 1987; **215(2):** 311-315.*

42. Nicholson,J.K., O'Flyn,M.P., Sadler,P.J., Macleod,A.F., Juul,S.M. and Sonksen,P.H.. Proton-nuclear-magnetic-resonance studies of serum, plasma and urine from fasting normal and diabetic subjects. *Biochem J. 1984; **217:** 365-375.*

43. Brown,F.F., Campbell,I.D. and Kuchel,P.W.. Human erythrocyte metabolism studies by ^{1}H spin echo NMR. *FEBS lett. 1977; **82(1):** 12-16.*

44. Campbell,I.D., Dobson,C.M., Williams,R.J.P. and Wright,P.E.. Pulse methods for the simplification of proton NMR spectra. *FEBS lett. 1975; **57(1):** 96-99.*

45. Hahn,E.L.. Spin echoes. *Phys. Rev. 1950; **80:** 580-594.*

46. Rabenstein,D.L. and Nakashima,T.T.. Spin-echo Fourier transform nuclear magnetic spectroscopy. *Anal. Chem. 1979; **51(14):** 1465a.*

47. Daniels,P.A., Williams,R.J.P. and Wright,P.E.. Nuclear magnetic resonance studies of the adrenal gland and some other organs. *Nature 1976; **261:** 321-325.*

48. Stocks,J., Gutteridge,J.M.C., Sharp,R.J. and Dormandy,T.L.. The inhibition of lipid autoxidation by human serum and its relation to serum proteins and α-tocopherol. *Clin. Sci. Mol. Med. 1974; **47:** 223-233.*

49. Cristie,W.W.. *Lipid analysis - 2nd ed. Pergammon press, Oxford (1973).*

50. deMann,J.M.. *Principle of food chemistry, Westport,.T. 1976; 60.*

51. Jellum,E.. Profiling of human body fluids in healthy and diseased states using gas chromatography and mass spectrometry, with special reference to organic acids. *J. chrom. 1977; **143:** 427-462.*

52. Heininger,J., Muhte,E., Pahle,J. and Jellum,E.. Capillary column gas chromatography - Mass spectrometry in studies on rheumatoid arthritis. *J. chrom. 1978; **158:** 297-304.*

53. Brook,J.B., Kellogg,D.S., Alley,C.C., Short,H.B., Hendsfield,H.H. and Huff,B.J.. Gas chromatography as a potential means of diagnosing arthritis. I. Differentiation between staphylococcal, streptococcal, Gonococcal and traumatic arthritis. *Infect. Dis. 1974; **129:** 660-668.*

54. Porter,N.A., Weber,B.A., Weenan,H. and Khan,J.A.. Autoxidation of polyunsaturated lipids. Factors controlling the stereochemistry of product hydroperoxides. *J. Am. Chem. Soc. 1980; **102:** 5597-5601.*

55. O'Brien,P.J.. Intracellular mechanisms for the decomposition of lipid peroxide. Decomposition of a lipid peroxide by metal ions, haem compounds and nucleophiles. *Can. J. Biochem. 1969; **47:** 485.*

56. Esterbaurer,H. in: Poli,G., Cheeseman,K.H., Dianzani,M.V., Slater,T.F. eds. Lipid peroxidation products: formation, chemical properties, and biological activities. *Free Radical in Liver Injury, Oxford: IRL Press 1985; 29-47.*

57. Merry,P., Grootveld,M., Patel,I.Y., Kidd,B.L., Ballard,R. and Blake,D.R.. The application of second-derivative ultraviolet absorption spectroscopy to analyse lipid peroxidation product in inflammatory synovitis. *Brit. J. Rheum. 1989;* ***28(1):*** *74.*

58. DiLuzio,N.R. and Horman,A.D.. The effect of ethanol and carbon tetrachloride administration on hepatic lipid-soluble antioxidants. *Exp. Mol. Pathol. 1969;* ***11:*** *38-52.*

59. Cawood,P., Wickens,D.J., Iverson,S.A., Braganza,J.M. and Dormandy,T.L.. The nature of diene conjugation in human serum, bile and duodenal juice. *FEBS Lett. 1983;* ***162(2):*** *239-243.*

60. Iverson,S.A., Cawood,P. and Dormandy,T.L.. A method for the measurement of a diene-conjugated derivative of linoleic acid, 18:2 (9,11), in serum phopholipids, and possible origins. *Ann. Clin. Biochem. 1985;* ***22:*** *137-140.*

61. Corongiu,F.P., Poly,G., Dianzani,M.U., Cheeseman,K.H. and Slater,T.F.. Lipid peroxidation and molecular damage to polyunsaturated fatty acids in rat liver. Recognition of two classes of hydroperoxides formed under conditions *in vivo. Chem. Biol. Interactions 1986;* ***59:*** *147-155.*

62. Porter,N.A., Wolf,R.A., Yabro,E.M. and Weenan,H.. The autoxidation of arachidonic acid: formation of the proposed SRS-A intermediate. *Biochem. Biophys. Res. Commun. 1979;* ***89:*** *1058-1064.*

63. Chan,H.W.S. and Lewett,G.. Autoxidation of methyl linoleate. Separation and analysis of isomeric mixtures of methyl linoleate hydroperoxides and methyl hydroxy linileates. *Lipids 1977;* ***12:*** *99.*

64. Gutteridge,J.M.C. and Tickner,T.R.. The thiobarbituric acid-reactivity of bile pigments. *Biochem. Med. 1978;* ***19:*** *127-132.*

65. Khayat,A. and Schwall,D.. Lipid oxidation in seafood. *Food Technology, 1983; 130.*

66. Pearson,A.M., Gray,J., Wolzak,A.M. and Herenstein,N.A.. Safety implication of oxidised lipids in muscle foods. *Food Technology 1983; 121-129.*

67. Nair,V. and Turner,G.A.. The thiobarbituric acid test for lipid peroxidation : structure of the adduct with malondialdehyde. *Lipids 1984;* ***19:*** *10.*

68. Dahle,L.K., Hill,E.G. and Hollman,R.T.. The thiobarbituric acid reaction autoxidation of polyunsaturated fatty methyl esters. *Arch. Biochem. Biophys. 1962;* ***98:*** *253-261.*

69. Grootveld,M., Merry,P., Patel,I.Y., Kidd,B.L., Winyard,P.G. and Blake,D.R.. A specific second-derivative method for the determination of malondialdehyde in inflammatory synovitis. *Brit. J. Rheum. 1989;* ***28(2):*** *49.*

70. IUPAC, Standard Methods for the analysis of Fats and Derivatives, (paquot,c.,Ed.) IUPAC, App. Chem. Div. Commission on Oils, Fats and Derivatives, (1979) 6th. Edn..

71. Iversen,S.A., Cawood,P., Madigan,M.J., Lawson,A.M. and Dormandy,T.L.. Identification of a diene conjugated component of human lipid as octadeca-9,11-dienoic acid. *FEBS Lett. 1984;* ***171(2):*** *320-324.*

72. Satoh,K.. Serum lipid peroxide in cerebrovascular disorders determined by a new colorimetric method. *Clin. Chim. Acta. 1978* ***90:*** *37-43.*

73. Yagi,K. in Yagi,K.(ed.). Lipid Peroxidation in Biology and Medicine. *Academic Press. London 1982; 223-242.*

74. Kibrick,A.C., Safier,L.B. and Skipp,J..Evidnce of fatty acid peroxides in normal blood and tissues of man and animal. *Proc. Soc. Exp. Biol. Med. 1959;* ***101:*** 137-139.

75. Baugartner,W.A., Baker,N., Hill,V.A. and Wright,E.T.. Novel interference in thiobarbituric acid assay for lipid peroxidation. *Lipids* 1975; **10:** 309-311.

76. Grootveld,M. and Jain,R.. Methods for the detection of irradiated foodstuffs: Aromatic hydroxylation and degradation of polyunsaturated fatty acids. *Radiat. Phys. and Chem.* 1989; **34(6):** 925-934.

77. Morelli,B.. Determination of iron(III) and copper(II) by zeroth, first and second derivative spectrophotometry with 2-thiobarbituric acid (4,6-Dihydroxy-2-mercaptopyrimidine) as reagent. *Analyst 1983*; **108:** 870-879.

78. Shimizu,T., Kundo,K. and Hayaish,O.. Role of protsaglandin endoperoxides in serum thiobarbituric acid reaction. *Arch. Biochem. Biophys.* 1981; **206:** 271.

79. Coxon,D.T., Price,K.R. and Chan,H.W.E.. Formation, isolation and structure determination of methyl linolenate diperoxide. *Chem. Phys. Lipids* 1981; **28:** 365-378.

80. Bird,R.P., Hung,S.S., Hadley,M. and Draper,H.H.. Determination of malondialdehyde in biological materials by high-pressure liquid chromatography. *Anal. Biochem.* 1983; **128:** 240-244.

81. Gilbert,H.S., Stump,D.D. and Roh,S.F.. A method to correct for errors caused by generation of interfering compounds during erythrocyte lipid peroxidation. *Anal. Biochem.* 1984; **137:** 282-286.

82. Marcuse,R. and Johansson,L..Studies on TBA test for rancidity grading, -2. TBA reactivity of different alsehyde classes. *J. Am. Oil Chem. Soc.* 1973; **50:** 387.

83. Mookherjee,B.D., Deck,R.E. and Chang,S.S.. Relationship between monocarbonyl compounds and flavour of potato chips. *J. Agric. Food Chem.* 1965; **13:** 131.

84. Podolsky,D.K.. Inflammatory bowel disease. *N. Engl. J. Med* 1991; **325(13):** 928-937.

85. Podolsky,D.K.. Inflammatory bowel disease. *N. Engl. J. Med* 1991; **325(14):** 1008-1016.

86. Rampton,D.S. and Hawkey,C.J.. Prostaglandins and ulcerative colitis. *Gut* 1984; **25(12):** 1399-1413.

87. Verspaget,H.W., Aparico-Pages,M.N., Verner,S., Edelbroek,P.M., Hafkenscheid,J.C., Crama-Bohbouth,G.E., Pena,A.S., Waterman,I.T. and Lamers,C.B.. Influence of sulphasalazine and mesalazine on cellular and biochemical oxygen metabolite reduction. Effects on *in vivo* administration and an *in vitro* analysis. *Scand. J. Gastroenterol.* 1991; **26(7):** 779-786.

88. Yamada,T., Volkmer,C. and Grisham,M.. The effects of sulphasalazine metabolites on haemoglobin-catalysed lipid peroxidation. *Free Radic. Biol. Med.* 1991: **10(1):** 41-49.

89. Williams,A..Macrophage activity in Inflammatory Bowel Disease. *Gut.* 1990; **31(4):**481.

90. Fernandez-Barnare,F., Minorgan,M.D., Estern,M., Cabre,E., Lachica,M., Abadlacra,A., Humbert,P., Boix,J. and Gassull,M.A.. Seum, zinc, copper and selenium levels in inflammatoy bowel disease - Effect of total internal nutrition on trace-element status. *Am. J. Gastro., 1990.* **85(12).** 1548-1589.

91. Baker,S.S. and Cohen,H.J.. Altered oxidative metabolism in selenium-deficient rat granulocytes. *J. Immunol.* 1983; **130:** 2856-2860.

92. Maulder,C.J., Rondas,A.A., Wiitkin,E.H. and Tytgart,G.N.. Topical corticosteroid in inflammatory bowel disease . *Neth. J. Med.* 1989; **35(1):** 527-534.

93. Weber,G.F., Maertens,P., Meng,X.Z. and Pippenger,C.E.. Glutathione peroxidase deficiency and childhood seizure. *Lancet* 1991; **337(8755)**: 1443-4.

94. Ahnfelt-Ronne,I., Nielsen,O.H., Christensen,A., Langholz,E., Binder,V. and Riis.P.. Clinical evidence supporting the radical scavenger mechanism of 5-aminosalicylic acid. *Gastroenterology* 1990; **98(1):** 1162-1169.

95. Cawood.P., Whickens,D.G., Iversen,S.A., Braganza,J.M. and Dormandy,T.L.. The nature of diene conjugation in human serum, bile and duodenal juice. *FEBS letter* 1983; **162(2):** 239-243.

96. Fairbank,J., Ridgway,L., Griffin,J., Wickens,D., Singer,A. and Dormandy,T.L.. Octadeca-9-11-dienoic acid in diagnosis of cervical intraepithelial neoplasia. *The Lancet* 1988; 329.

97. Dormandy,T.L.. Dogma disputed - In praise of lipid peroxidation. *The Lancet* 1988; 1126-1128.

98. Fishwick,M.J. and Swoboda,P.. Measurement of oxidation of polyunsaturated fatty acids by spectrophotometric assay of conjugated derivatives. *J. Sc. Fd. Agric.* 1977; **28:** 387-393.

99. Frankel,E.N., Evans,C.D., McConnel,D.G., Selke,E. and Dutton,H.J.. Autoxidation of methyl linolenate, isolation and characterisation of hydroperoxides. *Org. Chem.* 1961; **26:** 4663.

100. Patel,I.Y., Grootveld,M., Simmonds,N., Rampton,D.S. and Blake,D.R.. Assessment of reactive oxygen radical-dependent peroxidation of PUFA's in biological materials by 2D absorption spectrophotometry. *Free Rad. Res. Commn.* (1993) in press.

101. Greenwald,R.A. and Moy,W.W.. Effect of oxygen free radicals on hyaluronic acid. *Arthritis and rheumatism* 1980; **23:** 455-463.

102. Lanacher,H.B.S. and Gunstone,F.D..The base-catalysed rearrangement of vernolic and other epoxy esters: The partial synthesis of methyl coriolate, methyl dimorphecolate and some conjugated polyenoic esters by a possible biosynthetic route. *Chem. Phys. Lipids* 1969; **3:** 191-202.

103. Nitishda.T., Miwa,H., Shigematsu,A., Yamamoto,M., Iiaa,M. and Fujishima,M.. Increased arachidonic composition of phospholipids in colonic mucosa from patients with active ulcerative colitis. *Gut* 1987; **28:** 1002-1007.

104. Rowley,D., Gutteridge,J.M.C., Blake,D.R., Farr,M. and Halliwell,B.. Lipid peroxidation in rheumatoid arthritis: thiobarbituric acid reactive material and catalytic iron salts in synovial fluid from rheumatoid arthritis patients. *Clin. Sci.* 1984; **66:** 691-695.

105. Halliwell,B.. Superoxide-dependent formation of hydroxyl radicals in the presence of iron chelates. *FEBS Lett.* 1978; **92:** 321-326.

106. Merry,P., Grootveld,M., Lunec,J. and Blake,D.R.. Oxidative damage to lipids within the inflamed human joint provides evidence of radical-mediated hypoxic-reperfusion injury. *Am. J. Clin. Nutr.* 1991; **53:** 362s-369s.

107. Lunec,J., Blake,D.R., McCleary,S.J., Brailsford,S. and Bacon,P.A.. Self-perpetuating mechanisms of immunoglobin G aggregation in rheumatoid inflammation. *J. Clin. Invest.* 1985; **76:** 2084-2090.

108. Lunec,J. and Blake,D.R.. The determination of dehydroascorbic acid and ascorbic acid in the serum and synovial fluid of patients with rheumatoid arthritis (RA). *Free Rad. Res. Commun.* 1986; **1:** 31-41.

109. Grootveld,M., Henderson,E.B., Farrell,A., Blake,D.R., Parkes,H.G. and Haycock,P.. Oxidative damage to hyaluronate and glucose in synovial fluid during exercise of the inflamed rheumatoid joint. *Biochem. J.* 1991; **273:** 459-467.

110. Lunec,J., Wakefield,A., Brailsford,S. and Blake,D.R.. In: Rice-Evans, C (Ed.) 'Free radicals, cell damage and disease.' 1986; pp 241-261: London: Riche lieu Press.

111. Merry,P., Winyard,P.G., Morris,C.J., Grootveld,M. and Blake,D.R..Oxygen free radicals, inflammation, and synovitis: the current status. *Ann. Rheum. Dis.* 1989; **48:** 864-870.

112. Gutteridge,J.M.C., Rowley,D.A. and Halliwell,B.. Superoxide-dependent formation of hydroxyl radicals and lipid peroxidation in the presence of iron salts. *Biochem. J.* 1982; **206:** 605-609.

113. Gutteridge,J.M.C., Winyard,P.G., Blake,D.R., Lunec,J., Brailsford,S. and Halliwell,B.. The behaviour of caeruloplasmin in stored human extracellular fluids in relation to ferroxidase II activity, lipid peroxidation and phenanthroline, detectable copper. *Biochem. J.* 1985; **230:** 517-523.

114. Spiro,T.G., Pape,L. and Saltman,P.. The hydrolytic polymerization of ferric citrate. *J. Am. Chem. Soc.* 1967; **89:** 5555-5558.

115. Blake,D.R., Hall,N.D., Bacon,P.A., Dieppe,P.A., Halliwell,B. and Gutteridge,J.M.C.. The effects of a specific iron chelating agent on animal models of inflammation. *Ann. Rheum. Dis.* 1983; **42:** 89-93.

116. Halliwell,B. and Gutteridge,J.M.C.. The importance of free radicals and catalytic metal ions in human diseases. *Mol. Aspects Med.* 1985; **8:** 89-193.

117. O'Connell,M.J., Ward,R.J., Baum,H. and Peters,T.J.. Iron release from haemosidiren and ferritin by therapeutic and physiological chelators. *Biochem. J.* 1989; **260:** 903-907.

118. Grootveld,M., Bell,J.D., Halliwell,B., Auroma,O.I., Bomford,A. and Sadler,P.J.. Non-transferrin-bound iron in plasma or serum from patients with idiopathic hemochromatosis. *J. Biol. Chem.* 1989; **264(8):** 4417-4422.

119. Grootveld,M. and Blake,D.R. Unpublished data.

120. Martin,R.B.. Citrate binding of Al^{3+} and Fe^{3+}. *J. Inorg. Biochem.* 1986; **28:** 181-187.

121. Gutteridge,J.M.C. and Hou,Y.. Iron complexes and their reactivity in the bleomycin assay radical-promoting loosely-bound iron. *Free Rad. Res. Commun.* 1986; **2:** 143-151.

122. Gutteridge,J.M.C.. Bleomycin-detectable iron in Knee-joint synovial fluid from arthritic patients and its relationship to the extracellular antioxidant activities of caeruloplasmin, transferrin and lactoferrin. *Biochem. J.* 1987; **245:** 415-421.

123. Nicholson,J.K., Buckingham,M.J. and Sadler,P.J.. High resolution ^1H NMR studies of vertebrate blood and plasma. *Biochem. J.* 1983; **211:** 605-615.

124. Bell,J.D., Sadler,P.J., Macleod,A.F., Turner,P.R. and LaVille,A.. ^1H NMR studies of human blood plasma. Assignment of resonances for lipoprotein. *FEBS Lett.* 1987; **219(1):** 239-243.

125. Hauser,H.. Lipid-protein interaction in porcine high-density (HDL_3) lipoprotein. *FEBS Lett.* 1975; **60:** 71-75.

126. Dawson,R.M.C., Elliot,D.C., Elliot,W.I. and Jones,K.M.. *Data for Biochemical Research* 1986; p411: Clarendon press, Oxford.

127. Bryson,A. and Fletcher,I.S.. Ligand exchange kinetics in the calcium-EDTA system. *Aust. J. Chem.* 1970; **23:** 1095-1110.

128. Grootveld,M., Patel,I.Y. and Blake,D.R.. Unpublished data.

129. Singh,S., Hider,R.C. and Porter,J.B.. A direct method for quantification of non-transferrin-bound iron. *Anal. Biochem.* 1990; **186:** 320-323.

130. Gutteridge,J.M.C.. Antioxidant properties of the protein caeruloplasmin in albumin and transferrin. A study of their activity in serum and synovial fluid from patients with rheumatoid arthritis. *Biochem. Biophys. Acta.* 1986; **869:** 119-127.

131. Konopka,K. and Neilands,J.B.. Effects of serum albumin on siderophere-mediated utilization of transferrin iron. *Biochemistry* 1984; **23:** 2122-2127.

132. Smit,S., Leijnse,B. and Van der Kraan,A.M..Polynuclear iron compounds in human transferrin preparations *J. Inorg. Biochem.* 1981; **15:** 329-328.

133. Bates,G.W., Billups,C. And Saltman,P.. The kinetics and mechanisms of iron(III) exchange between chelates and transferrin. *J. Biol. Chem.* 1967; **242(12):** 2816-2821.

134. Reiter,B., Brock,J.H. and Steel,E.D.. The bacteriostatic effects of lactoferrin on a serum susceptible and serum resistable strain E. Coli. *Immunology* 1975; **28:** 83-95.

135. Grootveld,M., Whelan,M., Farrell,A., Smith,E., Henderson,E. and Blake,D.R..Modifications in the metabolic profile of synovial sluid (SF) from pateints with inflammatory synovitis by excersice of the inflamed joint: A proton NMR study. *Brit. J. Rheum*. 1990; **30(A2):** 39.

136. Harris,W.R.. Thermodynamics of anion binding to human serum transferrin. *Biochemistry* 1985; **24:** 7412-7418.

137. Blake,D.R., Bacon,P.A., Eastham,E.J. and Brigham,K.. Synovial fluid ferritin in rheumatoid arthritis. *Br. Med. J.* 1980; **281:** 715-716.

138. Puppo,A. and Halliwell,B.. Formation of hydroxyl radical from hydrogen peroxide in the presence of iron. *Biochem. J.* 1988; **249:** 185-190.

139. El-Hazmi,M.A.F., Al-Ballaa,S.R., Warsy,A.S., Al-Arfaj,H., Al-Sughair,S. and Al-Dalaan,A.N..Transferrin C subtypes in pateints with rheumatoid arthiritis. *Br. J. Rheum.* 1991; **30:** 21-23.

140. Beckman,L., Beckman,G., Cedergren,B., Goransson,K., Hallqvist,E.B. and Sikstrom,C..Transferrin C subtypes and occupational photodermatosis of the face. *Hum. Hered*. 1985; **35:** 89-94.

141. Mundy,R.L., Heiffer,M.H. and Leifleit,H.C.. Blood and urine mercapto and disulphide levels after large doses of B-mercaptoethylamine (MEA) or cystamine. *Radiat. Res.* 1961; **14:** 421.

142. Vergroessen,A.J., Budke,L. and Cohen,J.A.. Factors influencing the radioprotection of tissue culture cells by sulphudryl compounds. *Nature (Lond.)* 1964; **204:** 206.

143. Jellum,E.. The role of cystamine-nucleic acid interactions in protection against x-ray-induced damage of DNA. *Int. J. Radiat. Biol*. 1966; **10:** 577.

144. Kosower,N.S. and Kosower,N.S.. The glutathione status of cells. *Int. Rev. Cytol.* 1978; **54:** 109.

145. Schafer,K., Bonifacic,M., Bahnemann,D. and Asmus,K.D.. Addition of oxygen to organic sulphur radicals. *J. Phys. Chem*. 1978; **82:** 2777.

146. Al-Thannon,A.A., Barton,J.P., Packer,J.E., Sims,R.J., Trumbore,C.N. and Winchester,R.V.. Radiolysis of aqueous solutions of cysteine in the presence of oxygen. *Int. J. Radiat. Phys. Chem*. 1974; **6:** 233.

147. Quintiliane,M., Badiello,R., Tamba,M., Esfandi,A. and Gorin,G.. Radiolysis of glutathione in oxygen-containing solutions of pH 7. *Int. J. Radiat. Biol.* 1977; **32:** 195.

148. Asmus,K.D.. Sulphur-centred free radicals. In: Radioprotectors and Anti carcinogens. Slater,T.F. (Ed.) 1983; pp. 23-42. Academic Press, London.

149. Adams,G.E., McNaughton,G.S. and Micheal,B.D.. In: The chemistry of ionisation and excitation. Johnson,G.R.A. and Scholes,G. (Eds.) 1967; pp. 281-283. Taylor and Francis, London.

150. Hoffman,M.Z. and Hayon,E.J.. Pulse radiolysis of sulphydryl compounds in aqueous solution. *J. Phys. Chem.* 1973; **77:** 990.

151. Wefer,H. and Sies,H.. Oxidation of glutathione by the superoxide radical to the disulphide and the sulphonate yielding singlet oxygen. *Eur. J. Biochem.* 1983; **137:** 29.

152. Auroma,O.I., Halliwell,B., Butler,J. and Hoey,B.M.. Apparent inactivation of α^1-antiproteinase by sulphur-containing radicals derived from penicillamine. *Biochem. Pharmacol.* 1989; **38(24):** 4353.

153. Gernard,G.R., Lucht,W.D., Niedermeyer,M.E., Snapper,J.R., Ogletree,M.L. and Brigham,K.L.. Effect of N-acetylcysteine on the pulmonary response to endotoxin in the awake sheep and upon *in vitro* granulocyte function. *J. Clin. Invest.* 1984; **73:** 1772.

154. Junod,A.F., Jornot,L. and Grichting,G.. Comparative study on the selenium-and N-acetylcysteine-related effects on the toxic actions of hyperoxia, parquet and the enzyme reaction hypoxanthine-xanthine oxidase in cultured endothelial cells. *Agents Actions* 1987; **22:** 177.

155. Miners,J.O., Drew,R and Birkett,D.J.. Mechanism of action of paracetamol protective agents in mice *in vivo*. *Biochem. Pharmacol.* 1984; **33:** 1995.

156. Cotgreave,I.A., Sandy,M.S., Berggren,M. Moldeus,P.W. and Smith,M.T.. N-acetylcysteine and glutathione-dependent protective effect of PZ51 (Ebselen) against diquat-induced cytotoxicity in isolated hepatocytes. *Biochem. Pharmacol.* 1987; **36:** 2899.

157. Moldeus,P., Cotgreave,I.A. and Berggren,M.. Lung protection by a thiol-containing antioxidant: N-acetylcysteine. *Respiration* 1986; **50(Suppl.1):** 31.

158. Ziment,I.. Acetylcysteine: a drug with an interesting past and fascinating future. *Respiration* 1986; **50(Suppl.1):** 26.

159. Aruoma,O.I., Halliwell,B., Hoey,B.M. and Butler,J.. The antioxidant action of N-acetylcysteine: its reaction with hydrogen peroxide, hydroxyl radical, superoxide and hypocholorous acid. *Free Rad. Biol. Med.* 1989; **6:** 593.

160. Merry,P., Grootveld,M. and Blake,D.R.. Free radicals and hypoxic reperfusion injury. A mechanism producing persistent synovitis. *ARC topical review* 1990; No.15 Scott,T., Jayson,M., Moll,J. and Isenberg (Eds.).

161. Grootveld,M., Nazhat,N.B., Patel,I.Y. and Blake,D.R.. Free radical biochemistry in rheumatoid arthritis. *Current Med. Lit.-Rheumatology* (1992); **9(1):** 75.

162. Henderson,E.B., Winyard,P.G., Grootveld,M.C. and Blake,D.R.. Pathophysiology of reperfusion injury in human joints. In: Pathophysiology of reperfusion injury. (1993); pp 429-470: Das,D.K. (Eds.), *Boca Raton*: CRC Press.

163. Grootveld,M., Herz,H., Haywood,R., Hawkes,G.E., Naughton,D., Perere,A., Knappitt,J., Blake,D.R. and Claxson,A.W.D.. Multicomponent analysis of radiolytic product in human body fluids using high field proton nuclear magnetic resonance (NMR) spectroscopy. *Radiat. Phys. Chem.* 1993; (in press).

164. Bell,J.D., Brown,J.C.C., Kubal,G. and Sadler,P.J.. NMR-invisible lactate in blood plasma. *FEBS Lett.* 1988; **235:** 81.

165. McNeil,J.D., Wiebkin,O.W., Betts,W.H. and Cleland,L.G.. Depolymerisation products of hyaluronic acid after exposure to oxygen-derived free radicals. *Ann. Rheum. Dis.* 1985; **44:** 780.

DX

189635